

INFORMATION TO USERS

This manuscript has been reproduced from the microfilm master. UMI films the text directly from the original or copy submitted. Thus, some thesis and dissertation copies are in typewriter face, while others may be from any type of computer printer.

The quality of this reproduction is dependent upon the quality of the copy submitted. Broken or indistinct print, colored or poor quality illustrations and photographs, print bleedthrough, substandard margins, and improper alignment can adversely affect reproduction.

In the unlikely event that the author did not send UMI a complete manuscript and there are missing pages, these will be noted. Also, if unauthorized copyright material had to be removed, a note will indicate the deletion.

Oversize materials (e.g., maps, drawings, charts) are reproduced by sectioning the original, beginning at the upper left-hand corner and continuing from left to right in equal sections with small overlaps.

Photographs included in the original manuscript have been reproduced xerographically in this copy. Higher quality 6" x 9" black and white photographic prints are available for any photographs or illustrations appearing in this copy for an additional charge. Contact UMI directly to order.

ProQuest Information and Learning
300 North Zeeb Road, Ann Arbor, MI 48106-1346 USA
800-521-0600

UMI[®]

UNIVERSITY OF ALBERTA

Design, Synthesis and Evaluation of High
Affinity Oligosaccharide Ligands

By

Rodney A. Gagné



A thesis submitted to the Faculty of Graduate Studies and Research in partial
fulfillment of the requirements for the degree of Doctor of Philosophy

DEPARTMENT OF CHEMISTRY

Edmonton, Alberta

Spring 2000



National Library
of Canada

Acquisitions and
Bibliographic Services

395 Wellington Street
Ottawa ON K1A 0N4
Canada

Bibliothèque nationale
du Canada

Acquisitions et
services bibliographiques

395, rue Wellington
Ottawa ON K1A 0N4
Canada

Your file *Votre référence*

Our file *Notre référence*

The author has granted a non-exclusive licence allowing the National Library of Canada to reproduce, loan, distribute or sell copies of this thesis in microform, paper or electronic formats.

The author retains ownership of the copyright in this thesis. Neither the thesis nor substantial extracts from it may be printed or otherwise reproduced without the author's permission.

L'auteur a accordé une licence non exclusive permettant à la Bibliothèque nationale du Canada de reproduire, prêter, distribuer ou vendre des copies de cette thèse sous la forme de microfiche/film, de reproduction sur papier ou sur format électronique.

L'auteur conserve la propriété du droit d'auteur qui protège cette thèse. Ni la thèse ni des extraits substantiels de celle-ci ne doivent être imprimés ou autrement reproduits sans son autorisation.

0-612-59963-9

Canada

UNIVERSITY OF ALBERTA
LIBRARY RELEASE FORM

NAME OF AUTHOR: Rodney A. Gagné

TITLE OF THESIS: Design, Synthesis and Evaluation of
High Affinity Oligosaccharide Ligands.

DEGREE: Doctor of Philosophy

YEAR THIS DEGREE GRANTED: 2000

Permission is hereby granted to the University of Alberta Library to reproduce single copies of this thesis and to lend or sell such copies for private, scholarly or scientific research purposes only.

The author reserves all other publication rights and all other rights in association with the copyright in the thesis, and except as hereinbefore provided, neither the thesis nor any substantial portion thereof may be printed or otherwise reproduced in any material form whatever without the author's prior written permission.



PERMANENT ADDRESS:

#106, 10335 - 117 Street

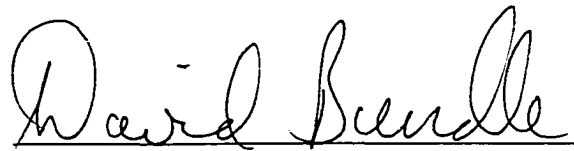
Edmonton, Alberta

CANADA T5K 1X9

March 10, 2000

UNIVERSITY OF ALBERTA
FACULTY OF GRADUATE STUDIES AND RESEARCH

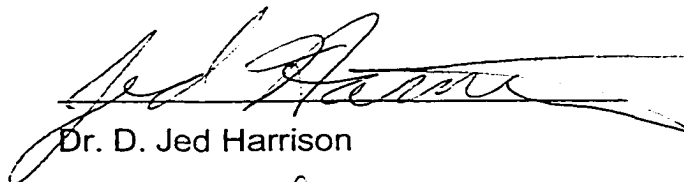
The undersigned certify that they have read, and recommended to the Faculty of Graduate Studies and Research for acceptance, a thesis entitled **Design, Synthesis and Evaluation of High Affinity Oligosaccharide Ligands** by **Rodney A. Gagné** in partial fulfillment of the requirements for the degree of **Doctor of Philosophy**.



Dr. David R. Bundle (Supervisor)



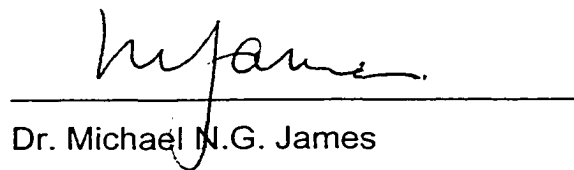
Dr. Derrick L.J. Clive (Chair)



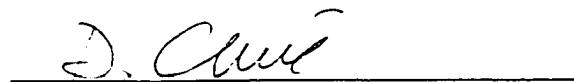
Dr. D. Jed Harrison



Dr. Rik R. Tykwinski



Dr. Michael N.G. James



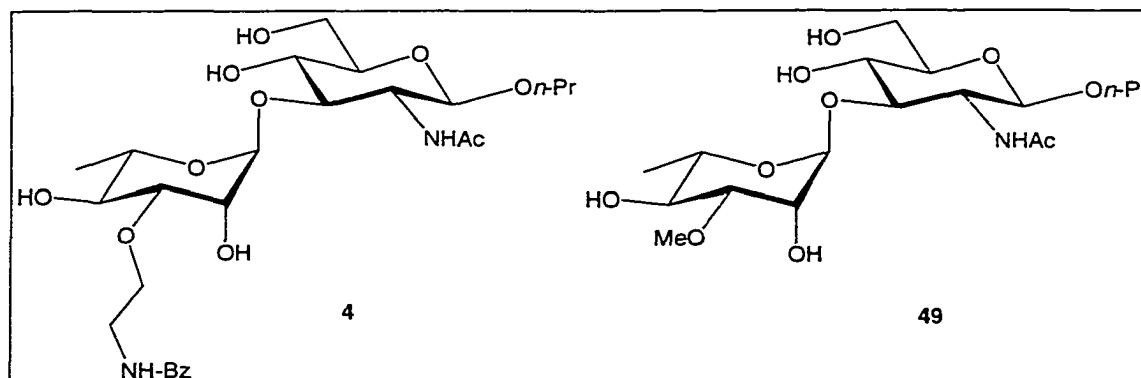
Dr. T. Bruce Grindley (External Examiner)

Dated: March 6th, 2000

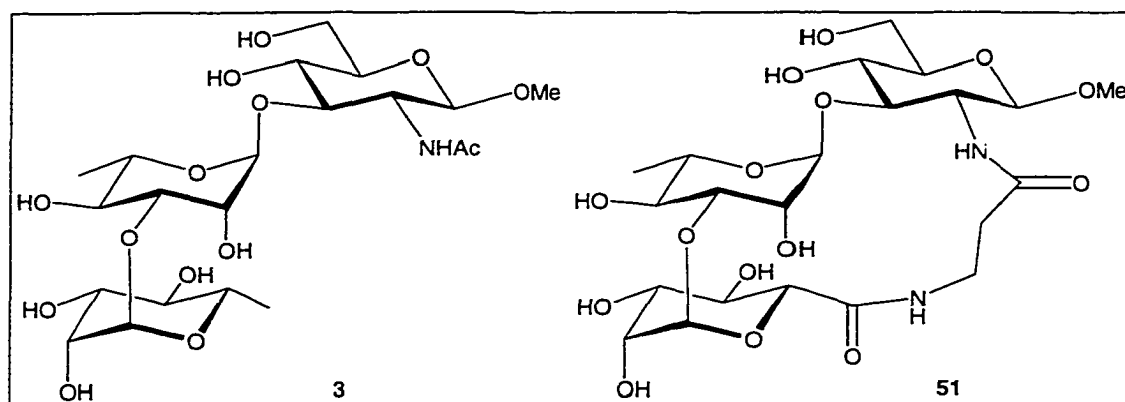
Abstract

A monoclonal antibody, SYA/J6, that was produced against the lipopolysaccharide layer of variant Y *Shigella flexneri* was used as a model to investigate carbohydrate – protein interactions. Crystal structures of this protein and bound ligands, that showed the position of the trisaccharide Rha-Rha-GlcNAc, enabled the use of two different strategies to design tighter binding, low molecular weight ligands.

The first strategy involved the addition of novel contacts, such as putative hydrogen bond and hydrophobic residues, to the core disaccharide epitope *via* a two-carbon linker arm. The synthesis of seven test ligands was carried out and it was found using a solid phase competitive assay that three of the ligands had higher affinities to the protein than the native disaccharide **49**. The best inhibitor, **4**, had an association constant that was 50 times better than **49**, but an order of magnitude less than the native trisaccharide **3**.



The second strategy involved the addition of intramolecular constraints to the native trisaccharide structure to decrease its flexibility in solution. The synthesis of three tethered trisaccharides was accomplished. Results from a solid phase assay indicated that one of the ligands, **51**, was a better inhibitor than **3** by a factor of three. Microcalorimetry measurements provided a more accurate factor of twenty for this ligand. It was found that both the enthalpy and entropy of binding were improved with this design strategy, relative to **3**.



To account for the improvement in binding seen in biological assays, minimum energy calculations using the AMBER_PLUS forcefield were performed. The results indicated that **51** adopted a conformation that was similar to **3** in solution. Both **3** and **51** showed good overlap with the bound ligand in the crystal structures. Molecular dynamics simulations revealed that this ligand was more rigid in solution than **3**. Distances obtained from nOe enhancements substantiated the results of molecular modeling.

Acknowledgements

I would like to thank my supervisor, Dr. David R. Bundle for his expert guidance, generosity, superior knowledge, and patience, especially in the last stages of my degree. The education that I received from him in chemistry and biology will certainly prove to be an asset to my career.

I was fortunate enough to work in a group filled with excellent chemists during my degree and their help and camaraderie will always be remembered. I would like to thank all of the members of the group over the years including: Todd Lowary, Ramon Alibes, Jeff Zhang, Pavel Kitov, Chang-Chun Ling, Shah Nilar, Shirley Wacowich-Sgarbi, Lina Setti, Carol Zheng, Michael Warwas, Mary Chervenak, Bernd Becker, Mark Nitz, Dale Cameron, Elena Kitova, Ping Zhang, Henry Yu, Lesley Liu, Amanda Seago, and last (but not least) Joanna Sadowska.

I was also lucky enough to have expert NMR and scientific guidance from Albin Otter and the excellent organizational skills of Lynne Lechelt will never be forgotten.

A big thank you to the "HUB Mall Gang" - Suzanne Hof, Steve Trepanier, Amanda Seago, Ali Mukherjee, Bernd Becker, and Henry Yu who managed to tolerate me for a number of years. I will miss you guys. The "Poker Boys" - Steve Trepanier, Paul Tiede, and Darren "Grandma" Mayhew also hold a place in my heart along with my fellow Solvent members: Vince Yeh, Don Coltart, Paul Tiede, and Mike Ferguson.

Away from work, I was always glad I was part of the U of A Dance Club that allowed me to meet good friends like Rob Carr and Ilene Hermann among others.

I'd like to thank my family - Mom, Marcel, Christina, Tom, Dad, and Grace for all of their love and support over the years. It was difficult to be away from Chris and Tom during the last few years and it'll even be more difficult to be away from Mom and Marcel over the coming years. Thanks to the Folinsbee's - Peggy, John, Marya, Tristen, and Bob for treating me like a friend and one of the family.

Finally, I'd like to give a big thank you and hug to the love of my life, Kaila, who came into my life over a year ago and made it the best one of my life so far. Her intelligence, enthusiasm, and companionship made me feel good about myself and gave me the courage to try new things. I'm eternally grateful for all of the big and little things she has done for me and I hope that the years to come will be as wonderful as the last.

Table of Contents

Title	Page
Ch. 1 Introduction	1
A) Carbohydrate – Binding Proteins	1
a. Definition of the Binding Constant	3
B) Use of Antibodies in Protein – Carbohydrate Studies	6
a. Production of Antibodies for Structural Studies	6
b. Hybridoma Myeloma Technique	7
c. Protein Crystallography	8
C) Description of System Used in the Project	8
a. Antibody Structure	9
b. Crystal Structure of SYA/J6 Antibody	10
c. Description of Binding Site Observed in the Crystal Structure	12
D) Thermodynamics of Carbohydrate – Antibody Interactions	15
a. Free Energy of Binding	15
b. Enthalpy Terms	17
c. Hydrogen Bonding	18
d. Hydrophobic Interactions	19

Title	Page
e. Summary of the Factors Involved in the Binding of Carbohydrate Ligands to the SYA/J6 Antibody	20
f. The Enthalpic Role of Water	22
g. Entropy Terms	23
h. Flexibility	23
E) Scope of Project	26
Ch. 2 Synthesis of Oligosaccharides with Improved Contacts With the SYA/J6 Antibody	28
A) Ligand Design	28
B) Synthetic Strategy	31
a. Choice of Anomeric Leaving Group	31
b. Method of Attachment of Linker Arm	36
c. Choice of Protecting Groups	38
d. Retrosynthetic Analyses of Ligands	39
C) Syntheses of Ligands	41
I. Synthetic Ligands of Type I Modification	41
a. Introduction of the Cyanomethyl Group	41
b. Preparation of the Glycosyl Donors (20), (21), and (22)	42
c. Preparation of the Glycosyl Acceptor (26)	46
d. Preparation of the Protected Disaccharides (27), (28), and (29)	47

Title	Page
e. Syntheses of Test Compounds (4), (5), and (6)	49
II. Synthetic Ligands of Type II Modification	51
a. Synthesis of the Glycosyl Acceptor (39) with an Ethylene - Spaced Azide	51
b. Preparation of the Rhamnose Donor (43)	53
c. Synthesis of the Disaccharide (46) with an Ethylene - Spaced Amine	55
d. Syntheses of Test Compounds (7), (8), (9), and (10)	56
III. Synthesis of the 3'-O-Methyl Native Disaccharide (49)	58
a. Preparation of the Native Disaccharide Mimic	58
Ch. 3 The Design and Synthesis of Constrained Trisaccharide Ligands	60
A) Ligand Design	60
B) Retrosynthetic Analysis of the Proposed Ligands	65
C) Synthesis of Ligands	69
I. Synthesis of Lactams (50) and (51)	69
a. Synthesis of the Rhamnose C ring of the Trisaccharide Structure	69
b. Synthesis of the Glucosamine D ring of the Trisaccharide Structure	71

Title	Page
c. Synthesis of the L-Mannose B ring of the Core Trisaccharide	72
d. Assembly of the Trisaccharide Unit	73
e. Partial Deprotection of the Core Trisaccharide	74
f. Synthesis and Deprotection of the Lactam (50)	77
g. Synthesis and Deprotection of the Lactam (51)	80
II. Synthesis of Cyclic Carbamate (52)	83
III. Synthesis of the Native Trisaccharide Comparison Ligand (83)	86
a. Preparation of the Native Trisaccharide Mimic	86
Ch. 4 Evaluation of the Biological Activities of the Synthetic Ligands	88
A) Solid Phase Binding Assay	88
a. IC ₅₀ Values for Synthetic Disaccharides (4), (5), and (6)	92
b. IC ₅₀ Values for Synthetic Disaccharides (7), (8), (9), and (10)	94
c. Inhibition Constants for Constrained Trisaccharides (50), (51), and (52)	96
B) Micro-Calorimetry Data for the Tightest-Binding Ligand, (51)	99
a. Microcalorimetry Data for (3) and (51)	99
b. Interpretation and Comparison of Results	103

Title	Page
Ch. 5 A Comparison of the Solution Conformation and Flexibility of the Native Trisaccharide (3) and (51)	104
A) Introduction	105
B) Conformation and Flexibility of the Native Trisaccharide	107
a. Potential Energy Minimization Studies	107
b. Molecular Dynamics	108
C) Conformation and Flexibility of the Tethered Trisaccharide (51)	111
a. Potential Energy Minimization Studies	111
b. Structure of the Ligand	113
c. Suggestions for the Improvement of the Enthalpy Term	114
d. Molecular Dynamics	116
e. Summary of the Origin of the Favourable Thermodynamics	121
D) NMR Studies on the Native and Tethered Trisaccharides	122
a. Comparison of Interproton Distances Found in Modeling with NMR-Based Experiments for the Native Trisaccharide (3)	122
b. A Comparison of Inter-Proton Distances Found in Modeling with NMR for the Tethered Trisaccharide (51)	126
Ch. 6 Conclusion	129

Title	Page
Ch. 7 Experimental	133
Ch. 8 Bibliography	200

List of Figures

Figure	Title	Page
Figure 1	General Structure of an IgG Antibody	10
Figure 2	Ligands Co-Crystallized with the Fab of SYA/J6	11
Figure 3	Illustration of the BCD Trisaccharide in the Binding Site of the SYA/J6 Antibody	13
Figure 4	The Hydrogen Bond Scheme and Distances for the Complex Between the ABCDA' Pentasaccharide (1) and the SYA/J6 Fab	14
Figure 5	The Hydrogen Bond Map for the Complex Between the Monodeoxy BCD Trisaccharide (2) and the SYA/J6 Fab as Observed in the Crystal Structure	14
Figure 6	The Differences in the Free Energy ($\Delta\Delta G$) of Binding Between the Native and Modified Trisaccharides	21
Figure 7	Definition of the Φ and Ψ Torsional Angles and Their Signs	24
Figure 8	Introduction of New Contacts on the Rhamnose C Ring	28
Figure 9	Introduction of New Contacts on the Glucosamine D Ring	30
Figure 10	Proposed Ligands	31
Figure 11	Anomeric Leaving Groups	32
Figure 12	General Classes of Glycosylation Reactions	33
Figure 13	Structural Types in Hexopyranosides	35
Figure 14	Introduction of an ethylene-spaced amine	37
Figure 15	Retrosynthetic Analysis of Compounds of Type I	40
Figure 16	Retrosynthetic Analysis of Compounds of Type II	41
Figure 17	Synthesis of the Nitrile (16)	43
Figure 18	Syntheses of the Donors (20), (21), and (22)	45
Figure 19	Preparation of the Acceptor (26)	46
Figure 20	Syntheses of the Disaccharides (27), (28), and (29)	48

Figure	Title	Page
Figure 21	Syntheses of the Test Compounds (4), (5), and (6)	50
Figure 22	Synthesis of the Acceptor Molecule (39)	52
Figure 23	Preparation of the Donor (43)	54
Figure 24	Synthesis of the Deprotected Disaccharide (46)	56
Figure 25	Syntheses of Test Compounds (7), (8), (9) and (10)	57
Figure 26	Preparation of the Disaccharide (49)	59
Figure 27	An Example of Improved Affinity <i>via</i> the Introduction of Constraints	61
Figure 28	Examples of Constrained Ligands	62
Figure 29	Proximity of Linkage Sites	63
Figure 30	Possible Tethers	64
Figure 31	Proposed Ligands	65
Figure 32	Retrosynthetic Analysis of the Lactam (75)	67
Figure 33	Retrosynthetic Analysis of the Core Trisaccharide	68
Figure 34	Synthesis of Rhamnose Donor (58)	70
Figure 35	Synthesis of Glucosamine Acceptor (61)	71
Figure 36	Synthesis of L-Mannose Donor (67)	73
Figure 37	Assembly of the Core Trisaccharide	75
Figure 38	Partial Deprotection of the Core Trisaccharide	76
Figure 39	Synthesis of the Carboxylic Acid (74)	78
Figure 40	Synthesis and Deprotection of the Lactam (50)	79
Figure 41	Synthesis of the Carboxylic Acid (77)	81
Figure 42	Synthesis and Deprotection of the Lactam (51)	82
Figure 43	Synthesis of the Carbonate (80)	84
Figure 44	Synthesis and Deprotection of the Cyclic Carbamate (52)	85
Figure 45	Synthesis and Deprotection of the Trisaccharide (83)	87
Figure 46	ELISA Protocol for the Evaluation of the Binding Affinity of the Synthetic Ligands	91

Figure	Title	Page
Figure 47	Competitive Inhibition Data For (4), (5), and (6)	92
Figure 48	Test Compounds (4), (5), and (6)	93
Figure 49	Competitive Inhibition Data For (7), (8), (9), and (10)	95
Figure 50	Test Compounds (7), (8), (9), and (10)	96
Figure 51	Competitive Inhibition Data for (50), (51), (52) and (83)	97
Figure 52	Test Compounds (50), (51), (52), and (83)	98
Figure 53	Calorimetry Data for the Tethered Trisaccharide (51)	101
Figure 54	Calorimetry Data for the Native Trisaccharide (3)	102
Figure 55	Definition of the Torsional Angles Φ_1 , Ψ_1 , Φ_2 , and Ψ_2	106
Figure 56	MD Simulations: Φ_1 vs. Time (left) and Ψ_1 vs. Time (right) for the Native Trisaccharide (3)	109
Figure 57	MD Simulations: Φ_2 vs. Time (left) and Ψ_2 vs. Time (right) for the Native Trisaccharide (3)	109
Figure 58	MD Simulations: Ψ_1 vs. Φ_1 (left) and Ψ_2 vs. Φ_2 (right) for the Native Trisaccharide (3)	110
Figure 59	Superimposition of the Native and Tethered Trisaccharides (3) and (51)	112
Figure 60	Structure of (51) in Solution	113
Figure 61	Chemical Shift vs. Temperature for the Amide Protons in (51)	116
Figure 62	MD Simulations: Φ_1 vs. Time (left) and Ψ_1 vs. Time (right) for the Tethered Trisaccharide (51)	118
Figure 63	MD Simulations: Φ_2 vs. Time (left) and Ψ_2 vs. Time (right) for the Tethered Trisaccharide (51)	118
Figure 64	MD Simulations: Ψ_1 vs. Φ_1 (left) and Ψ_2 vs. Φ_2 (right) for the Tethered Trisaccharide (51)	119
Figure 65	Definition of the Torsional Angles φ and ω	120

Figure	Title	Page
Figure 66	MD Simulations: ω <i>vs.</i> Time (left) and φ <i>vs.</i> Time (right) for the Tethered Trisaccharide (51)	121
Figure 67	Selected Proton Assignments for the Native Trisaccharide (3)	123
Figure 68	MD Simulations: H-1'' \rightarrow H-3' distance <i>vs.</i> time (left) and H-1' \rightarrow H-3 distance <i>vs.</i> time (right) for the Native Trisaccharide (3)	124
Figure 69	Selected Proton Assignments for the Tethered Trisaccharide, (51)	126
Figure 70	One Possible Extension of this Project	131

List of Tables

Table	Title	Page
Table 1	Examples of Developed Carbohydrate Drugs	4
Table 2	Thermodynamic Parameters for the Binding of the Native Trisaccharide (3) to SYA/J6 Antibody at 25°C	26
Table 3	IC ₅₀ Values for (4), (5), and (6)	93
Table 4	Estimated IC ₅₀ Values for (7), (8), (9), (10)	95
Table 5	IC ₅₀ Values for (50), (51), (52), (83)	97
Table 6	Calorimetry Results and Literature Values	103
Table 7	Computed $\Phi_1, \Psi_1, \Phi_2,$ and Ψ_2 Angles for the Native Trisaccharide (3)	108
Table 8	$\Phi_1, \Psi_1, \Phi_2,$ and Ψ_2 Angles of the Native and Tethered Trisaccharides (3) and (51)	111
Table 9	Inter-Proton Distances for Selective Correlations Calculated from Crystallography, Molecular Dynamics, and NMR for the Native Trisaccharide (3)	125
Table 10	Inter-Proton Distances for Selective Correlations Calculated from Molecular Dynamics and NMR for the Tethered Trisaccharide (51)	127
Table 11	Inter-Proton Distances for Correlations Across the Glycosidic Linkages for the Trisaccharides (3) and (51)	128

Abbreviations

Ac	acetyl
Ala	alanine
All	allyl
AMBER	assisted model building with energy refinement
Arg	arginine
Bn	benzyl
<i>t</i> -Boc	<i>t</i> -butoxycarbonyl
<i>t</i> -Bu	<i>t</i> -butyl
Bz	benzoyl
2D	two dimensional
DCM	dichloromethane
DDQ	2,3-dichloro-5,6-dicyano-1,4-benzoquinone
DMAP	4-dimethylaminopyridine
DMF	<i>N,N</i> -dimethylformamide
DMTST	dimethyl(methylthio)sulfonium triflate
EIA	enzyme immunosorbent assay
ES HRMS	electrospray high resolution mass spectrometry
Et	ethyl
EXSIDE	excitation-sculptured indirect-detection
Fab	antigen-binding fragment
Fmoc	9-fluorenylmethoxycarbonyl
GCOSY	gradient coupling correlated spectroscopy
Glc	glucose
GlcNAc	<i>N</i> -acetylglucosamine, 2-acetamido-2-deoxy- <i>D</i> -glucose
GlcNPhth	<i>N</i> -phthaloylglucosamine, 2-deoxy-2-phthalimido- <i>D</i> -glucose
Glu	glutamic acid
Gly	glycine

His	histidine
HMQC	heteronuclear multiple quantum coherence
HOBt	1-hydroxybenzotriazole
HPLC	high pressure liquid chromatography
HRP	horseradish peroxidase
IC ₅₀	inhibitor concentration required to give 50% inhibition
IUPAC	International Union of Pure and Applied Chemistry
Man	mannose
MD	molecular dynamics
Me	methyl
M.S.	molecular sieves
Ms	methanesulphonyl
NEM	<i>N</i> -ethylmorpholine
NIS	<i>N</i> -iodosuccinamide
<i>n</i> -Pr	<i>n</i> -propyl
PBS	phosphate buffer saline
PBST	phosphate buffer saline containing Tween 20
Ph	phenyl
Phe	phenylalanine
PhthN	phthalimido
ppm	parts per million
Pyr	pyridine
ROE	rotating-frame nuclear Overhauser effect
R _f	retention factor
Rha	L-rhamnose, 6-deoxy-L-mannose
S _N 2	bimolecular nucleophilic substitution
TBAF	tetrabutylammonium fluoride
TBDPS	<i>t</i> -butyldiphenylsilyl
TBTU	2-(1H-benzotriazole-1-yl)-1,1,3,3,-tetramethyluronium tetrafluoroborate

TEA	triethylamine
TEMPO	2,2,6,6-tetramethyl-1-piperidinyloxy, free radical
Tf	trifluoromethanesulphonate
THF	tetrahydrofuran
Thr	threonine
TLC	thin layer chromatography
TMB	3,3',5,5'-tetramethylbenzidine
T-ROESY	transverse rotating-frame Overhauser effect spectroscopy
Trp	tryptophan
Tyr	tyrosine
UV	ultraviolet

Chapter 1

Introduction

The study of the ways in which carbohydrates bind to their protein receptors is an important and challenging multidisciplinary field of research prominent in “glycobiology”.¹ Since these studies began over a century ago when Emil Fischer stated, “... I would like to say that the enzyme and the glucoside have to fit each other like a lock and key,” proteins that recognize and bind carbohydrates have been studied and divided into two groups.² Group I proteins tend to accommodate monosaccharides in deep cavities.³ For example, proteins that transport sugars across cell membranes are associated with this class of proteins. Group II proteins usually fit larger sugars (oligosaccharides) in shallower binding sites. Enzymes, lectins, and antibodies belong to the latter group of proteins and are prominent in the literature of biochemical research.⁴

A) Carbohydrate – Binding Proteins

Enzymes such as glycosyltransferases and glycosidases recognize a variety of carbohydrates and have been the subject of many reviews.⁵ These enzymes are

involved in co- and post-translational modifications of glycoproteins in the endoplasmic reticulum and Golgi apparatus of cells. The discovery of the mechanisms by which these proteins function and their isolation have enabled chemists to synthesize complex oligosaccharides in high yield without the need for protecting group manipulations.⁶ These enzymes can catalyze stereoselective reactions in the building of larger carbohydrates.

Lectins are carbohydrate-binding proteins or glycoproteins of non-immune origin that are found in most plants, animals, and microorganisms.⁷ They recognize carbohydrate structures, but exhibit no enzymatic activity towards them. In mammals, they are thought to direct certain cell-cell interactions.⁸ One application of the research done on lectins is in the area of diagnostics. They have been used to probe the carbohydrate structures on the surface of cells. A number of assays have been developed whereby lectins adhere to the surfaces of cells that contain the specific carbohydrate that they recognize.

Like lectins, antibodies have been used to probe cellular recognition events.⁹ Antibody molecules are the active agents of the host immune response against foreign substances. These molecules recognize carbohydrate antigens on the surface of foreign cells. A wide body of research has been reported in the last two decades that presents information on antibody – carbohydrate systems.¹⁰ An excellent application of antibody research is the development of vaccines.

Recently, it has been said that, "Vaccines are arguably the greatest achievement of modern medicine".¹¹ Traditional vaccinations involve the introduction of either

killed or weakened pathogens into the blood stream of patients. However, these inoculations are very costly to prepare and are not applicable to many lethal diseases like AIDS, herpes, malaria, bacterial infections, and hepatitis C. In addition, immuno-compromised patients are susceptible to full-blown illness from them. Due to the drawbacks of whole-organism vaccines, there remains a need for small molecule, synthetic alternatives.

Carbohydrate – binding enzymes, lectins, and antibodies have been targets of ligand design in order to obtain viable synthetic carbohydrate – based therapeutics over the last two decades.^{12,13,14,15} As a result of this research, a number of carbohydrate-based vaccines and therapeutics have been developed recently in the literature (Table 1) and have been reviewed by Hindsgaul and McAuliffe in 1997.¹⁶

a. Definition of the Binding Constant

The strength of binding between a carbohydrate and its protein receptor can be characterized quantitatively by an equilibrium constant sometimes referred to as a binding constant.¹⁷ It is conventional to use a dissociation constant, K_D , defined as $K_D = [\text{Carb}][\text{Prot}]/[\text{Carb}\bullet\text{Prot}]$ for the most simple case of a bimolecular carbohydrate – protein interaction where Carb, Prot, and Carb•Prot represent the carbohydrate ligand, protein receptor, and carbohydrate-protein complex respectively (equation 1). The association constant, K_A , is the inverse of K_D .



Table 1: Examples of Developed Carbohydrate Drugs

Substance	Target	Company	Status
Cylexin	Reperfusion injury	Cytel	Phase II
Theratope	Cancer	Biomira	Phase II/III
NCCG	Cancer	IGG International	Pre-clinical
Hyaluronic acid	Cancer	Hyal Pharmaceuticals	Pre-clinical
SR90107	Thrombosis	Sanofi/Organon	Phase I
Acarbose	Diabetes	Bayer AG	Released
AO-128	Diabetes	Takeda/Abbot	Released
NE-0080	Stomach ulcers	Neose Technologies	Phase II
SYNSORB Pk	Haemorrhagic colitis	SYNSORB Biotech	Phase III
GG-167	Influenza	Glaxo Wellcome	Phase II
MDL-24,574A	HIV/AIDS	Searle & Co	Phase II
Acemannan	Infection healing	Carrington Labs	Released
Betafectin	Post-surgical infection	Alpha-Beta Tech	Phase III
Topiramate	Epilepsy	Johnson & Johnson	Released
Ganglioside GM ₁	Parkinson's disease	Fidia Pharmaceuticals	Phase I

Most oligosaccharides that are recognized by enzymes, lectins, and antibodies only bind to their protein receptors with weak dissociation constants in the millimolar to micromolar range.¹⁸ In general, nature uses the result of avidity in cell-cell recognition to circumvent this low affinity. Avidity refers to the association constant of a polyvalent interaction.¹⁹ It has been shown in many cases that

polyvalent binding results in very tight binding between receptors and ligands even though individual association constants may be small. Hence, many carbohydrate-binding proteins such as antibodies and lectins have two or more binding sites on one molecule.

The association constant of an individual carbohydrate – protein interaction must be significantly improved in order to design small ligands as potential drug candidates. In addition, if a natural substrate is to be inhibited, the avidity of the system must also be overcome. Therefore, individual interactions should be in the nanomolar range.²⁰ Many carbohydrate ligand designs have failed to reach this quantity.

Another roadblock for chemists in ligand design is the difficulty of carbohydrate synthesis.²¹ Unlike other biopolymers, oligosaccharides are usually branched. In addition, monosaccharide molecules are attached at a stereogenic centre, the anomeric centre, which can have two different conformations, α and β . In contrast, three amino acids can be assembled into only six tripeptides. Three different monosaccharides can produce up to 1056 different trisaccharides.²² Therefore, all of the hydroxyl groups not involved in polymerization need to be selectively protected which results in a large number of synthetic steps in the chemical assembly of oligomers. Finally, glycosidic bond formation to link sugar building blocks together does not generally proceed in high yield and usually results in mixtures of α - and β -anomers.

It has been stated by Hindsgaul and others that the production of an 'average' trisaccharide requires 21 weeks of chemical synthesis time for an experienced individual and about \$4000-5000 worth of chemicals and solvents.²¹ Therefore, there is a need for the design of small molecular weight carbohydrates that bind tightly to their receptors. Advances in the field of glycobiology have provided model systems to study carbohydrate – protein interactions to enable this possibility.

B) Use of Antibodies in Protein – Carbohydrate Studies

One recognition system that has emerged during studies on carbohydrate – protein interactions is the antibody – carbohydrate antigen binding system. Beginning in the 1970's, when a number of pure antibodies was isolated, and continuing in the 1980's when the first crystal structures of antibodies containing bound ligands were resolved, this area of research has been of great importance in ligand design.^{23,24} These antibodies have been the focus of multidisciplinary research involving biophysical techniques such as protein crystallography, chemical mapping, and NMR spectroscopy.

a. Production of Antibodies for Structural Studies

Pure antibodies of significant quantity need to be available in order to study antibody – antigen interactions. A heterogeneous supply of antibody in blood

serum was the common source of antibody in the early work in antibody research.²⁵ Since then, large quantities of uniform antibodies that only bind to one type of antigen, called monoclonal antibodies, have been obtained using the hybridoma myeloma technique.²⁶

b. Hybridoma Myeloma Technique

To generate large quantities of uniform antibody, BALB/c mice were immunized with phenol-killed bacterial cells. The mice produced a number of antibody molecules in their spleen against this foreign invader. The spleen cells were then placed into microtiter wells and assayed to determine which cells are specific to the polysaccharide of interest. The active spleen cells were then fused with melanoma cells to produce cells known as hybridomas. The hybridomas containing the antibody of interest were then injected back into the mice and a tumour ensued. The fluid that formed in the tumour was rich in monoclonal antibody that could be isolated and purified.

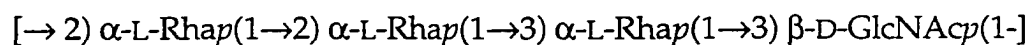
Since this development in the 1970's by Milstein, Bundle and others have used this technique to produce a number of monoclonal antibodies for structural study in order to investigate the features of carbohydrate – protein interactions that were important for specificity and affinity.²⁷

c. Protein Crystallography

The preferred method of three-dimensional structure determination is protein crystallography.² If an antibody could be co-crystallized with a bound ligand, the amount of information that can be obtained from a solved crystal structure is large. Not only can the details of the protein and its active site be discovered—the residues that are the basis of the interaction with the guest molecule can be assigned. This, in turn, can shed light onto which functional groups can be modified to obtain higher binding ligands. This is the concept behind a model system. One example of a model system is the antibody SYA/J6 that is specific to the lipopolysaccharide that is present on the cell surface of variant Y *Shigella flexneri*, a Gram negative bacterium, which is the subject of the present study.^{28,29}

C) Description of System Used in the Project

The monoclonal antibody SYA/J6 has been produced by the hybridoma myeloma technique in mice against segments of the cell wall of a *Shigella* bacterium. The carbohydrate antigen that is recognized by this antibody is a linear polysaccharide composed of repeating units of an ABCD tetrasaccharide:³⁰



A

B

C

D

a. Antibody Structure

The monoclonal antibody SYA/J6 belongs to the IgG class of antibody. The general structure of antibodies is shown in Figure 1 and consists of a symmetrical monomer of two light chains (L) and two heavy chains (H) that are covalently attached by disulphide bonds.³¹ The light chain consists of two domains, one variable (V_L) and one constant (C_L), whereas the heavy chain consists of four domains, one variable (V_H) and three constant domains (C_{H1} , C_{H2} , and C_{H3}). The term “variable” refers to an amino acid sequence that is specific for the particular antibody, whereas “constant” refers to amino acid sequences that are the same for all antibodies of that family.

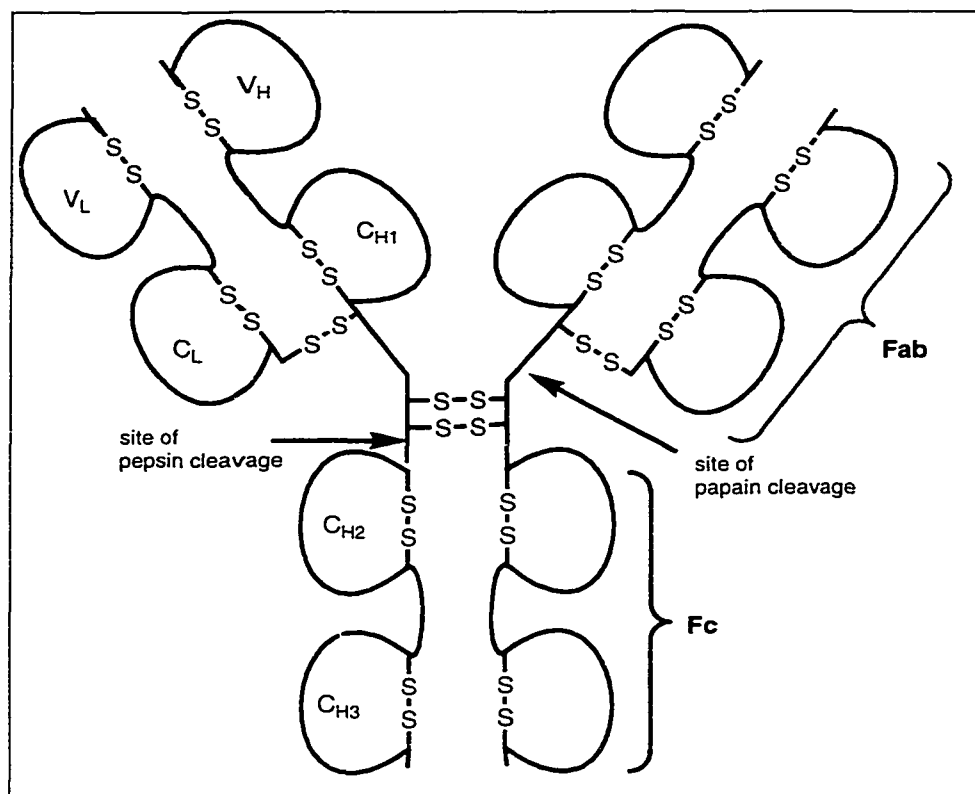
There are two types of light chains (λ and κ) and five types of heavy chains (μ , γ , α , ϵ , and δ) which define the five major classes of immunoglobulins (Ig): IgM, IgG, IgA, IgE, and IgD, respectively. Mouse and human serum contains mostly IgG antibodies.

Two constant domains, C_{H2} and C_{H3} , make up the Fc fragment. This section can be used to purify the antibody using affinity chromatography because this region can bind to proteins immobilized on solid supports. For example, the SYA/J6 antibody was purified by an elution through a Protein A agarose affinity column.²⁷

The rest of the molecule consists of two arms of the two light chain domains and the two remaining heavy chain domains. These fragments, called the **Fab** regions, contain two recognition units, called the binding sites, that bind to antigens

at the outermost variable domains in grooves or pockets that are formed at the *N*-termini between the heavy and light chain variable loops.

Figure 1: General Structure of an IgG Antibody

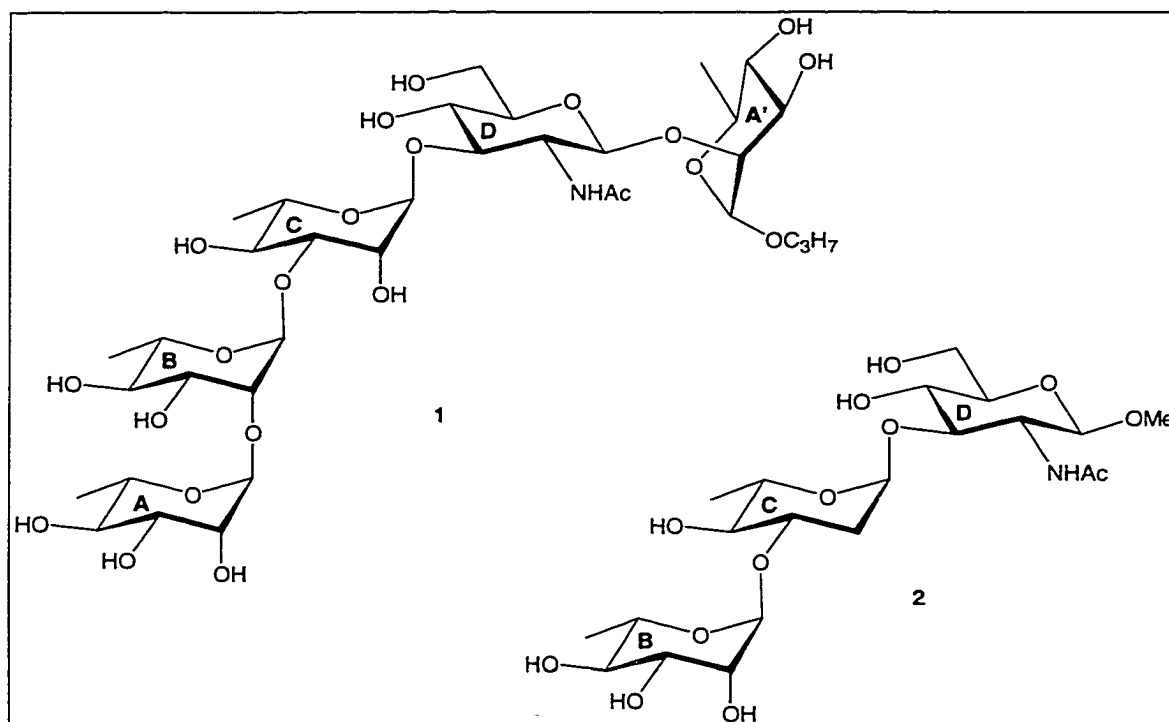


b. Crystal Structure of SYA/J6 Antibody

A papain digestion of the antibody provided the **Fab** region after purification.³² Crystals of this fragment were obtained through precipitation with 2-methyl-2,4-pentanediol. A crystal structure was obtained using X-ray diffraction data at 2.5 Å

resolution and placed in the Protein Data Bank.³³ Two other crystal structures were obtained with bound ligands by co-crystallizing in a 1 : 10 **Fab** : sugar solution. The ligands were the ABCDA' pentasaccharide **1** and the modified BCD trisaccharide **2** that had a deoxygenation at the 2 position of the C ring.^{34,35}

Figure 2: Ligands Co-Crystallized with the Fab of SYA/J6



It has been shown that the recognition element in the binding site in carbohydrate – binding antibodies is limited to two or three sugar residues called the epitope that is part of a larger antigenic determinant.³⁶ In the case of SYA/J6, the two

crystal structures of the **Fab** fragments with bound ligands show that the CD disaccharide α -L-Rhap(1 \rightarrow 3) β -D-GlcNAc ρ is buried deep in the binding site.

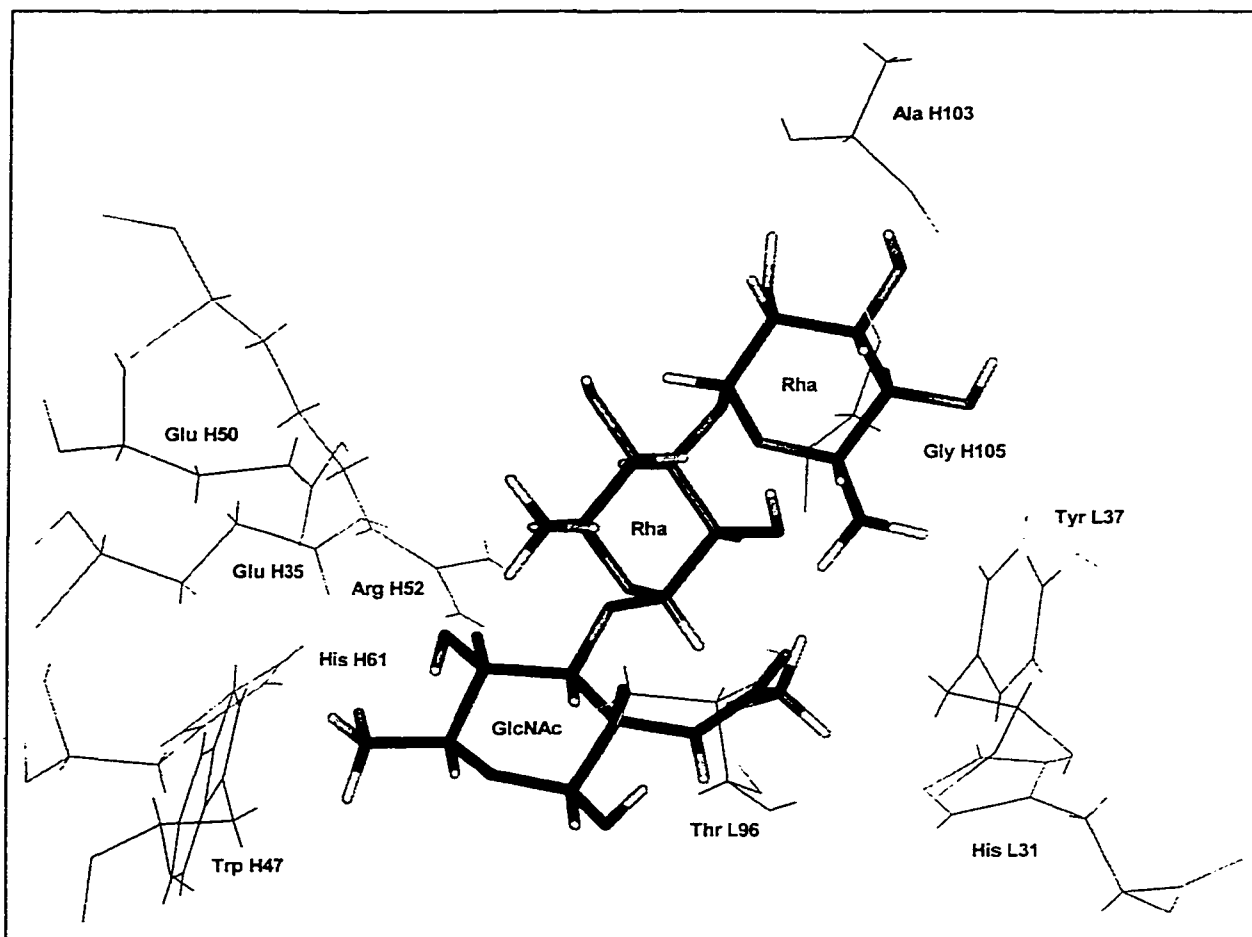
c. Description of Binding Site Observed in the Crystal Structure

To observe the important contacts between the sugar and antibody and to determine the conformation of the bound sugar, the crystal structures of the antibody complexed with the two ligands was used. In the crystal structure obtained from the Protein Data Bank for the ABCDA' pentasaccharide **1** bound to the **Fab** domain, the coordinates of the two flanking hexose residues, A and A', were not present; only the BCD trisaccharide coordinates were present. In addition, the O-6 of the glucosamine D ring was absent. Although the reason of the lack of electron density for these residues is unknown, the explanation is that these residues are mobile and not involved in interactions between the sugar and protein.³⁷

A backside view of the complex is shown in Figure 3. The view of the carbohydrate and the amino acid residues that contact the bound sugar is from the middle of the protein and looks out to bulk solvent.

The plausible hydrogen bond network in the complex for both bound ligands, **1** and **2**, is shown in Figures 4 and 5. The hydrogen bonds that are listed are based on interatomic O \rightarrow O and N \rightarrow O distances in the crystal structure. Hydrogen bonds are assumed between heavy atoms that are closer than 3.5 Å apart.

**Figure 3: Illustration of the BCD Trisaccharide
in the Binding Site of the SYA/J6 Antibody***



* The view is from the base of the active site to the outside of the complex.

Figure 4: The Hydrogen Bond Scheme and Distances for the Complex Between the ABCDA' Pentasaccharide (1) and the SYA/J6 Fab

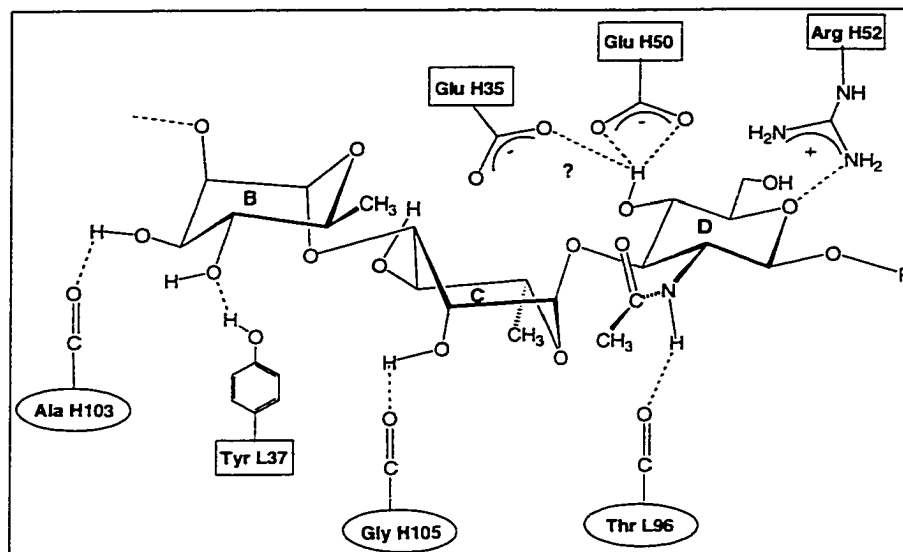
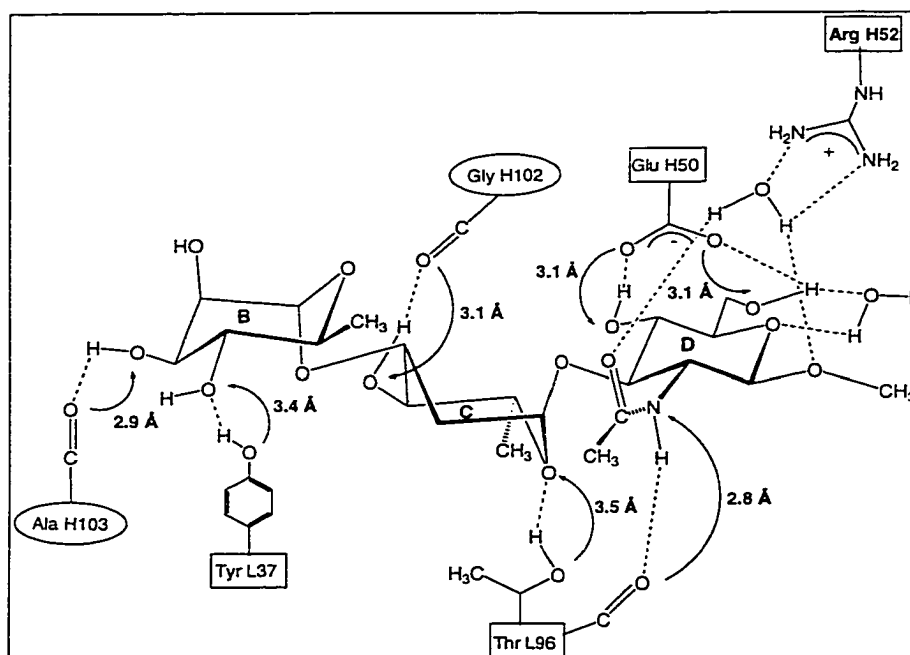


Figure 5: The Hydrogen Bond Map for the Complex Between the Monodeoxy BCD Trisaccharide (2) and the SYA/J6 Fab as Observed in the Crystal Structure



The crystal structure of the modified BCD trisaccharide bound in the Fab fragment of SYA/J6 showed more detail than for the ABCDA' pentasaccharide 1 because the modified trisaccharide had a higher association constant than the pentasaccharide and was situated closer to the protein.³⁸ More details of the hydrogen bond network were seen in this structure, including the hydrogen bonding involving two water molecules near the reducing end of the molecule. However, the two structures are in general agreement with regard to the main hydrogen bonds that hold the ligands in place.

D) Thermodynamics of Carbohydrate – Antibody Interactions

Due to the advances made in the last three decades of the 20th century in carbohydrate synthesis, biological assay techniques, NMR spectroscopy and protein crystallography, researchers have been able to investigate and summarize the factors that are responsible for the formation and stability of carbohydrate-protein complexes.⁴

a. Free Energy of Binding

In principle, the association constant, K_A , should be relatively easy to measure but, in practice, convenient methods for its accurate measurement are somewhat limited.

A number of biological assay techniques have been developed to quantify the dissociation constant.⁹ The most common assays are solid phase enzyme and radioimmunoassays (EIA and RIA) which are both convenient and rapid. The assays can be accomplished in the direct detection mode by coating plastic microtiter plates with an antibody and allowing them to stand with an antigen that is covalently linked to a number of enzymes which produce signals for detection.³⁹ These assays can also be performed in the indirect mode by coating the plate with antigen and allowing the antibody to stick to the antigens on the plate and then adding a signal molecule that binds to the antibody. The amount of signal that arises from these assays is directly proportional to the strength of the antibody – antigen interaction.

The binding constant, K_D , can be used to calculate the free energy of binding (ΔG) according to equation 2 where R is the universal gas constant and T is the temperature of the system.¹⁷ Both the free energy and the dissociation constant give a quantitative measure of the strength of binding between a ligand and its receptor.

$$\Delta G = -RT \ln K_D \quad (2)$$

The free energy of binding has both an enthalpic (ΔH) and entropic (ΔS) component and is summarized in equation 3.

$$\Delta G = \Delta H - T\Delta S \quad (3)$$

It is beneficial to know the enthalpy and entropy to obtain a detailed thermodynamic understanding of the interactions and forces responsible for complex formation. This information can be obtained by a van't Hoff analysis of the temperature dependency of the dissociation constants obtained from solid phase assay techniques.⁴⁰ Unfortunately, these measurements are very time-consuming and have been shown to be inaccurate.

With the advent of a powerful solution-phase technique called microcalorimetry, the binding constant, free energy, enthalpy, stoichiometry, and entropy can be obtained in a single experiment, provided a significant amount of protein/antibody is available. Due to the availability of sensitive, commercial microcalorimeters, several groups have used this technique to obtain thermodynamic details for the associations between carbohydrates and proteins. The new generations of microcalorimeters operate under computer control with specialized software for data acquisition and processing.⁴¹

b. Enthalpy Terms

The enthalpy term in equation 3 is comprised of two major components- ΔH_{bind} and ΔH_{conf} .⁴² The first term, ΔH_{bind} refers to the favourable van der Waals, electrostatic and hydrogen bond contributions that occur in the system upon binding. The second term, ΔH_{conf} is the unfavourable change in conformational energy required in

the bound state. It is synonymous with the strain energy of the system and is unavoidable.

c. Hydrogen Bonding

Many designs of tighter binding ligands have involved increasing the number of hydrogen bonds between the ligand and protein in order to increase the favourable ΔH_{bind} term.⁴³ Although there is a general increase in binding when more hydrogen bonds are introduced to the system, there are many examples of tight-binding ligands that are not involved in hydrogen bonding.⁴⁴ For example, only a few hydrogen bonds form between an antibody and a steroid. The binding of these ligands arises from nonpolar interactions.⁴⁵

Generally, sugar hydroxyl groups that are buried in a protein site need to be paired to hydrogen-bonding residues on the protein surface or bound water molecules.⁴ The hydrogen bonds between sugar and protein may be cooperative or bidentate hydrogen bonds.

Cooperative bonds follow the scheme: $\text{NH} \rightarrow \text{OH} \rightarrow \text{O}$ where NH and O represent the donor and acceptor groups of a protein that originate mostly from polar side chains on asparagine, aspartic acid, glutamine, glutamic acid, and arginine residues or the protein backbone and OH corresponds to a carbohydrate hydroxyl group.² Occasionally, hydroxyl side chains on serine, threonine, or tyrosine serve as hydrogen bonding residues. In the binding of the carbohydrate antigen to the

SYA/J6 antibody, Glu H50, Glu H35, and Tyr L37 are involved in cooperative hydrogen bonds to the sugar. The decrease in activity of synthetic ligands lacking the hydroxyl partners of the aforementioned residues substantiates the presence of important hydrogen bonds.⁴⁶

Bidentate hydrogen bonds can form between vicinal equatorial or axial – equatorial hydroxyl groups on the sugar ring and the polar side chains listed above. Bidentate hydrogen bonds involving adjacent axial hydroxyl groups on the sugar have not been observed. For the SYA/J6 antibody, Arg H52 is involved in a bidentate hydrogen bond with the 6 position and ring oxygen of the glucosamine D ring.

d. Hydrophobic Effects

Some ligand designs have involved increasing lipophilic contacts between protein and ligand.⁴⁴ Generally, binding affinity is proportional to lipophilic contacts, but there are many examples of ligands with high binding affinity to proteins that contain no lipophilic contact surfaces. One example is the strong affinity of the sulphate ligand to the sulphate binding protein, even though the sulphate ligand contains no lipophilic surface area.⁴⁷

In carbohydrate – binding sites, there are usually aromatic residues that stack against the sugar residues.² These stacking forces contribute to the stability and specificity of sugar – protein complexes through discrimination against epimers.

Although oligosaccharides possess many polar groups, a large proportion of the surface is non-polar. Due to the formation of glycosidic bonds and hydrogen bonds between sugar residues, polysaccharides have significant lipophilic surfaces that need to be paired with non-polar surfaces in the binding site to stabilize the complex.

e. Summary of the Factors Involved in the Binding of Carbohydrate Ligands to SYA/J6 Antibody

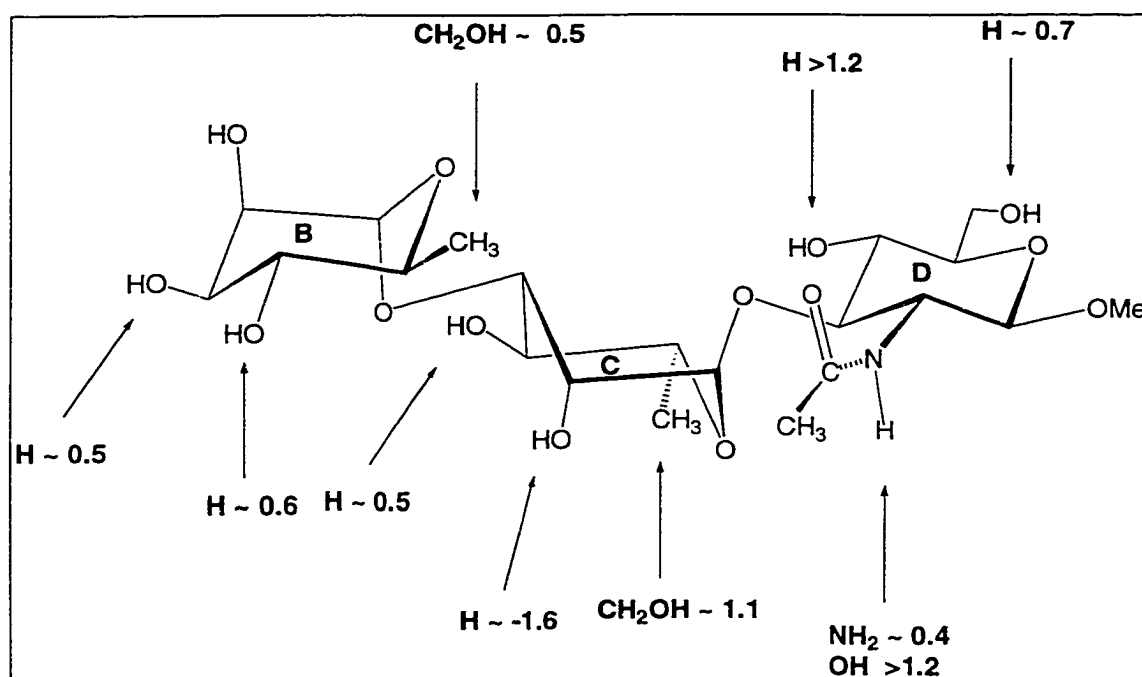
Previous literature on this system has discussed the substitution effects on the trisaccharide which are illustrated in Figure 6.⁴⁸ Free energy differences (kcal/mol) that are positive indicate weaker binding. It has been shown that the substitution of the hydroxyl groups on the 4 and 6 positions of the glucosamine D ring with hydrogen resulted in a dramatic reduction of free energy, suggesting that these groups are essential elements in the hydrogen bond scheme. Modifications to the acetamido group on the D ring also resulted in substantially weaker binding.⁴⁹

In contrast, deoxygenation of the 2 position of the C ring results in a large gain of free energy, suggesting an unfavourable hydrophobic clash between the hydroxyl group and the protein backbone.³⁵ The observation of the close proximity of the nonpolar side chains of Tyr L37 and Trp H47 to this position suggests that these are the residues responsible for the hydrophobic clash with the sugar upon binding. The incorporation of a polar group to the 6 position of the buried rhamnose C ring

also resulted in a hydrophilic-hydrophobic clash. It can be inferred that this region of the active site is very hydrophobic in nature.

Modifications on the rhamnose B ring appear to have negligible effects on the binding of the sugar to antibody, suggesting that this residue is not completely buried in the active site of the antibody.

Figure 6: The Differences in the Free Energy ($\Delta\Delta G$) of Binding Between the Native and Modified Trisaccharides*



* Positive differences indicate weaker binding. Negative values indicate that the ligand with that modification binds more tightly to the antibody.

f. The Enthalpic Role of Water

There has been considerable debate in the last few years about the origin of the enthalpy term.⁵⁰ Most researchers believe the major contributor to the enthalpy of binding comes from solute – solute attractive interactions between a sugar and its receptor. Lemieux and Toone have separately shown that reorganization of water molecules contributes significantly to the enthalpy of binding. It is suggested that water molecules directly adjacent to the amphiphilic surfaces possess high energy because they cannot satisfy all of their hydrogen bonding potential. The return of these molecules to bulk solvent following complex formation results in a favourable enthalpic contribution. Water molecules displaced from the binding site also likely provide some favourable entropic contribution but the former enthalpic contribution seems to be much larger.

Lemieux has used molecular modeling to show that the surfaces of the protein and carbohydrate are covered with mostly disordered water.⁵¹ To do this, he and co-workers constructed an active site surrounded by 250 water molecules. At thermal equilibrium, the calculated water-to-water interaction energies strengthen with increasing distance from the receptor site. They concluded that many water molecules are perturbed over the receptor surfaces and that the alleviation of this perturbation provides a significant contribution to the enthalpy of binding.

Toone has performed calorimetry experiments in light and heavy water to verify Lemieux's findings.⁵² He and co-workers found that the enthalpy term for a

number of different protein-ligand interactions decreased when the associations took place in heavy water rather than in light water. Assuming that all of the other binding factors such as conformations remained the same, the difference was due to solvent effects. They then concluded that the reorganization of water comprised 25 to 100% of the observed enthalpy of binding for protein – ligand interactions.

For various reasons such as protein solubility and recoverability, none of these solvent studies have been performed with the SYA/J6 antibody.

g. Entropy Terms

The free energy of binding also depends on the entropy of binding as shown in equation 3. The entropy term is comprised of three components: $\Delta S_{rot+trans}$, ΔS_{flex} and ΔS_{solv} .⁵³ The unfavourable loss of rotational and translational entropy, $\Delta S_{rot+trans}$ upon binding is an intrinsic quantity that occurs in every molecular association. The final entropy term, ΔS_{solv} is the favourable or unfavourable change in entropy for the release of solvent molecules during a binding event.⁵⁴ It can be positive or negative depending on the features of the individual complex formation.

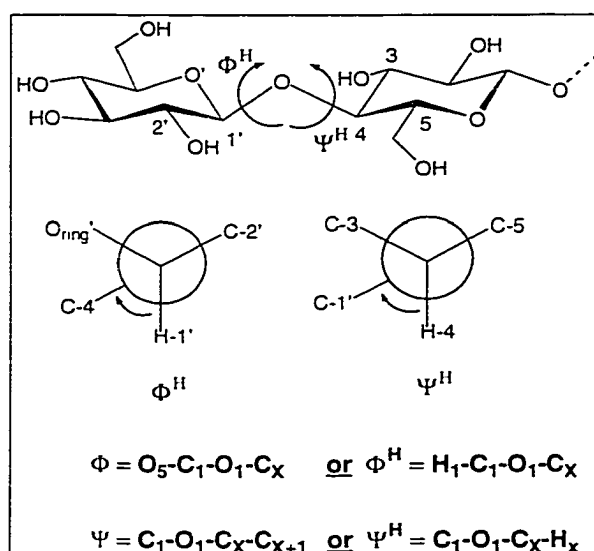
h. Flexibility

The loss of flexibility of the system during a binding event inherently gives rise to the second unfavourable entropy term, ΔS_{flex} . It was originally thought that the

major contributor of this term was due to the loss of conformational freedom in the protein upon binding the ligand.⁵⁵

More recently, it has been postulated that one major source of unfavourable entropy comes from the loss of conformational freedom in the carbohydrate ligand upon binding.⁵⁶ Carbohydrate molecules have many internal torsional degrees of freedom in the unbound state. In particular, the glycosidic linkage can adopt different conformations around the torsional angles, Φ and Ψ (Figure 7). During binding to protein, loss of entropy by restricting the torsional angles has been estimated at 0.6 kcal/mol per torsional angle.⁵⁵ Crystallographers define these angles by the heavy atoms, whereas carbohydrate chemists who use NMR spectroscopy to determine the angles employ the definitions Φ^H and Ψ^H . In this thesis, the Φ^H and Ψ^H definitions are used, but for convenience, the superscript 'H' has been omitted (Figure 7).

Figure 7: Definition of the Φ and Ψ Torsional Angles and Their Signs



Three methods have been prominent in the field of glycobiology to determine the conformation of the oligosaccharide: X-ray analysis, NMR spectroscopy, and computer modeling.⁵⁷ As mentioned before, X-ray crystallography provides the solid state conformations of both the protein and the bound ligand. Angles and distances of the carbohydrate can be obtained directly from the crystal structure with the aid of a computer graphics program.

NMR spectroscopy can be used to measure sugar conformations of the free and bound state in solution provided certain criteria are fulfilled. Determination of nuclear Overhauser enhancements (nOe) across the glycosidic bond is the most important tool for conformational analysis of oligosaccharides.⁵⁸ The nOe enhancements from a 1D or 2D experiment can be converted to average distances for inter-residue protons across the glycosidic linkage. This method of conformational analysis is very precise if a number of distances can be measured.

Due to the availability of powerful computers, a number of theoretical calculations can be performed to compare conformations seen in crystal structures or calculated by nOe enhancements.⁵⁹ These calculations include force field programs that calculate minimum energy structures based on potential energy factors and molecular dynamics simulations that determine both the minimum energy structures and the inherent flexibility of the molecule.

E) Scope of Project

Published microcalorimetry data have identified the thermodynamic parameters associated with the binding of the 'native trisaccharide', α -L-Rhap(1 \rightarrow 3)- α -L-Rhap(1 \rightarrow 3)- β -D-GlcNAcp(1 \rightarrow OMe), **3**, with the SYA/J6 antibody, illustrated in Table 2.⁶⁰

The data suggest that the free energy is partitioned between favourable enthalpic and entropic factors for the binding of the native trisaccharide **3** to the antibody. Thus, the current project used the model binding system between the monoclonal antibody SYA/J6 and sugar antigens to improve carbohydrate-protein interactions.

Table 2: Thermodynamic Parameters for the Binding of the Native Trisaccharide (3) to SYA/J6 Antibody at 25°C

Ligand	K_A (M^{-1})	ΔG (kcal/mol)	ΔH (kcal/mol)	$-T\Delta S$ (kcal/mol)
3	9.5×10^4	-6.8	-4.3	-2.5

A two-fold design methodology was undertaken in attempts to provide tight binding ligands. Firstly, additional hydrogen bond contacts were introduced to a small ligand such as the native disaccharide to increase the enthalpy of binding to

the protein. Secondly, constraints were added to the native trisaccharide to preorganize it for binding and decrease the unfavourable loss of entropy due to flexibility in the binding event. This thesis describes the design, synthesis, and biological evaluation of new ligands to the SYA/J6 antibody.

Potentially successful ligand designs could have a great impact on the field of glycobiology because low molecular weight, tight binding ligands are rare. Possible extensions of successful ligand designs to other carbohydrate – protein systems could advance the field and result in a series of new lead pharmaceutical candidates.

Chapter 2

Synthesis of Oligosaccharides with Improved Contacts With the SYA/J6 Antibody

Experimental evidence has shown, with few exceptions, that oligosaccharide binding to protein is an enthalpically-driven process.¹⁸ One method to improve enthalpic stabilization involves the addition of new groups to the native structure. These contacts could provide stronger hydrogen bonding, stacking interactions, and van der Waals interactions.⁴⁴

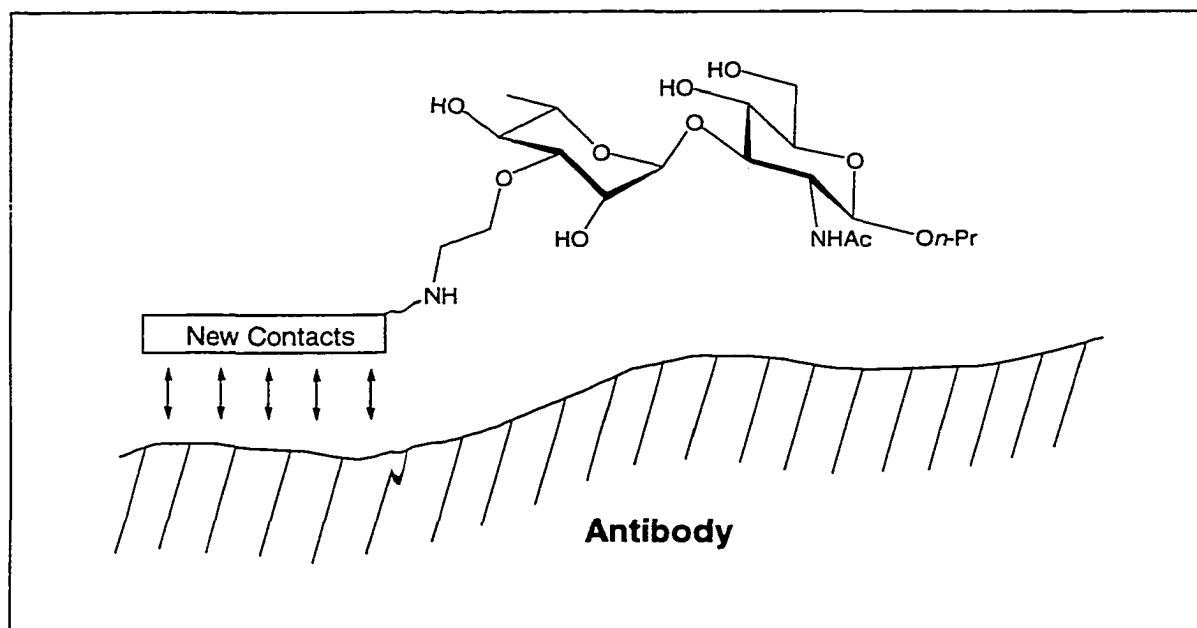
A) Ligand Design

Within the binding groove of the SYA/J6 antibody, a number of pockets of available space are present that can be filled with new hydrogen bond acceptors, donors, and hydrophobic residues that can be attached to the core α -L-Rhap(1 \rightarrow 3) β -D-GlcNAc₂ disaccharide. These new interactions could strengthen carbohydrate-protein interactions and result in tighter binding. A two-carbon linker arm was chosen to provide a source of linkage of these groups to the carbohydrate moiety at the 3 position of the rhamnose C ring (type I modification) or at the

anomeric centre of the glucosamine D ring (type II modification) (Figures 8, 9, and 10).

The linker arm was attached to the 3 position of the rhamnose C ring of the sugar for a number of reasons. Firstly, the glycosidic bond between the rhamnose B and C rings in the native antigen was simulated by the placement of the spacer arm at that position. Secondly, the other hydroxyl groups on the rhamnose C ring were involved in hydrogen bonding in the protein – carbohydrate complex.⁴⁸ Therefore, in order to retain their function in binding, these groups were not the target of modifications. Lastly, only alkylation of the 3 position would result in minimum steric clashes between the rhamnose C ring and the protein.

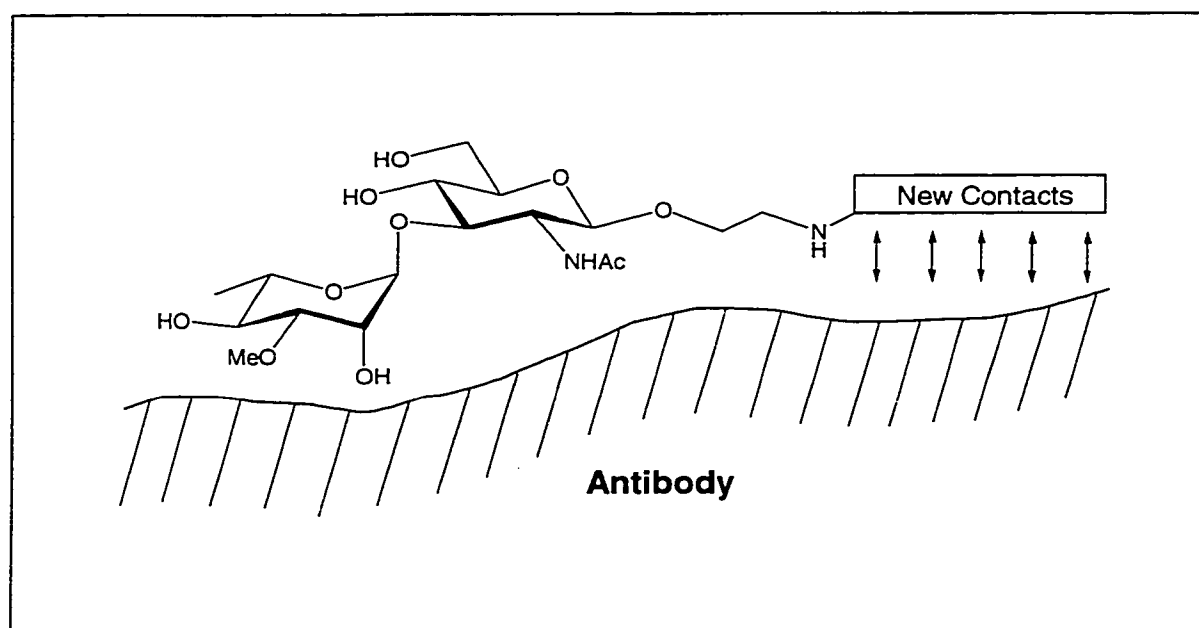
Figure 8: Introduction of New Contacts on the Rhamnose C Ring



An examination of the binding site of the antibody in the two crystal structures revealed regions of hydrophobicity. In particular, Phe 60L, Ala 103H, Val 104H, Gly 105H, and Tyr 37L were situated close to the rhamnose C ring and in the region occupied by the attached groups. Therefore, the linker on the rhamnose C ring was acylated to form ligands of type I that contained non-polar amides such as acetamide and benzamide. In addition, a non-polar amino acid, L-alanine, was linked to form a relatively hydrophobic peptide bond.

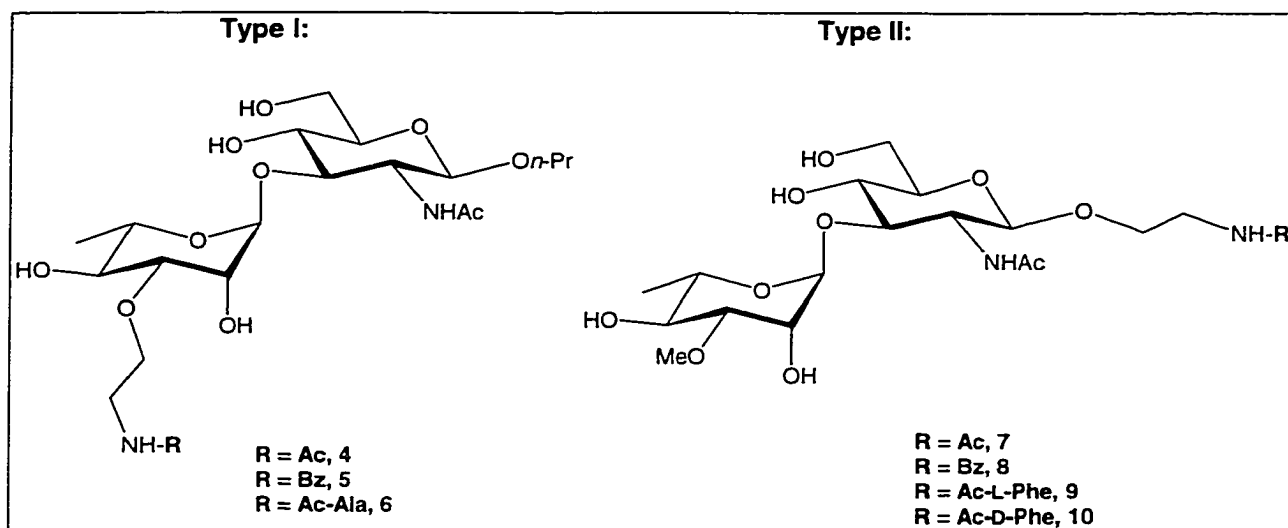
A linker arm placed at the anomeric centre of the glucosamine D ring would simulate the glycosidic bond between the glucosamine D ring and the rhamnose A' ring of the next repeating unit, keep the other positions unrestricted involvement in the hydrogen bond network, and prevent steric clash with the antibody.

Figure 9: Introduction of New Contacts on the Glucosamine D Ring



Near the anomeric centre of the glucosamine D ring, a number of aromatic residues are present, including His 98L and His 31L. Therefore, inhibitors of type II had acetyl, benzoyl, and phenylalanine residues attached to the linker at the anomeric position of the glucosamine D ring.

Figure 10: Proposed Ligands



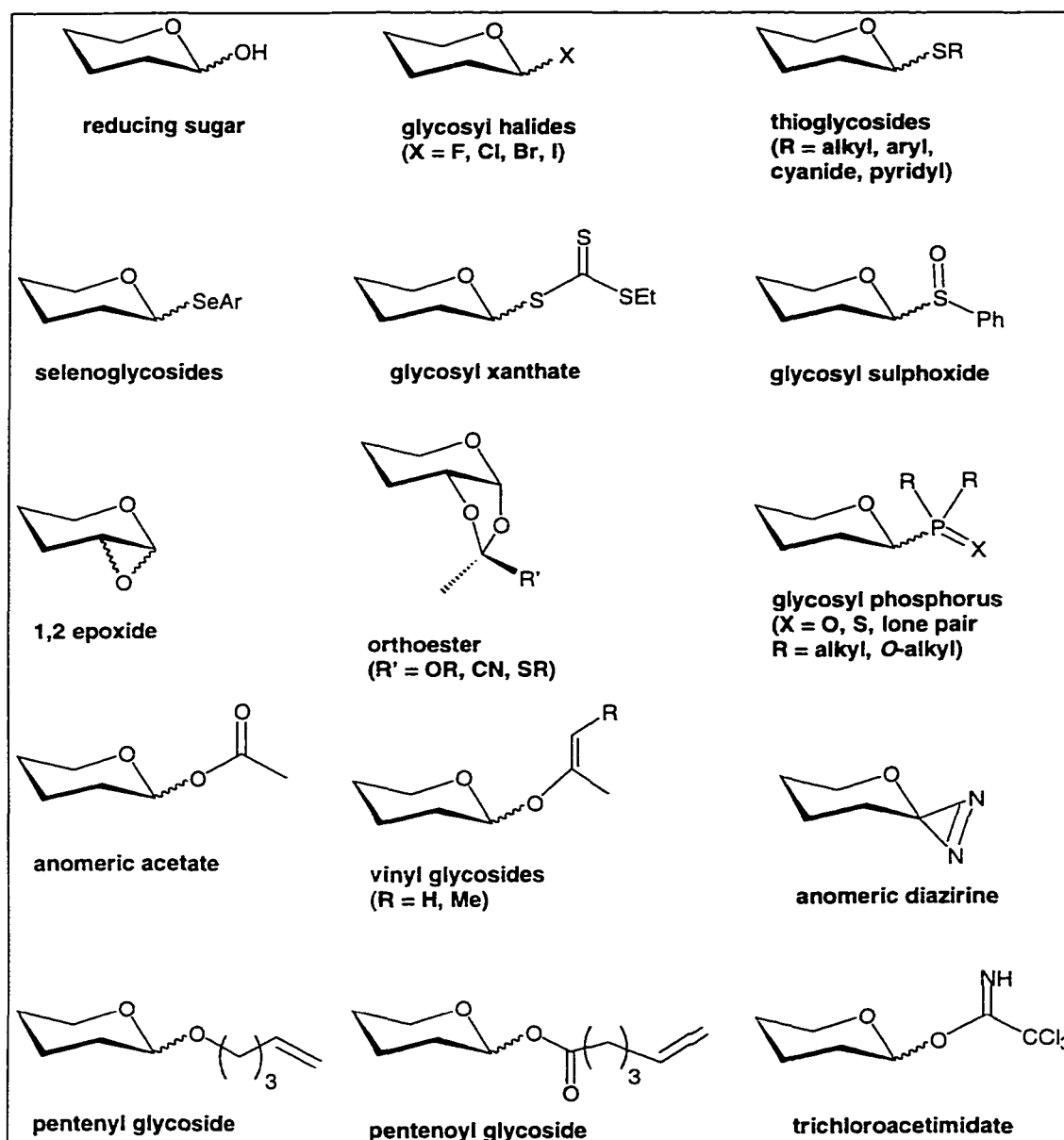
B) Synthetic Strategy

a. Choice of Anomeric Leaving Group

One of the most important reactions in the field of carbohydrate research is the glycosylation of two sugar residues to form new glycosidic linkages.⁶¹ Because of the

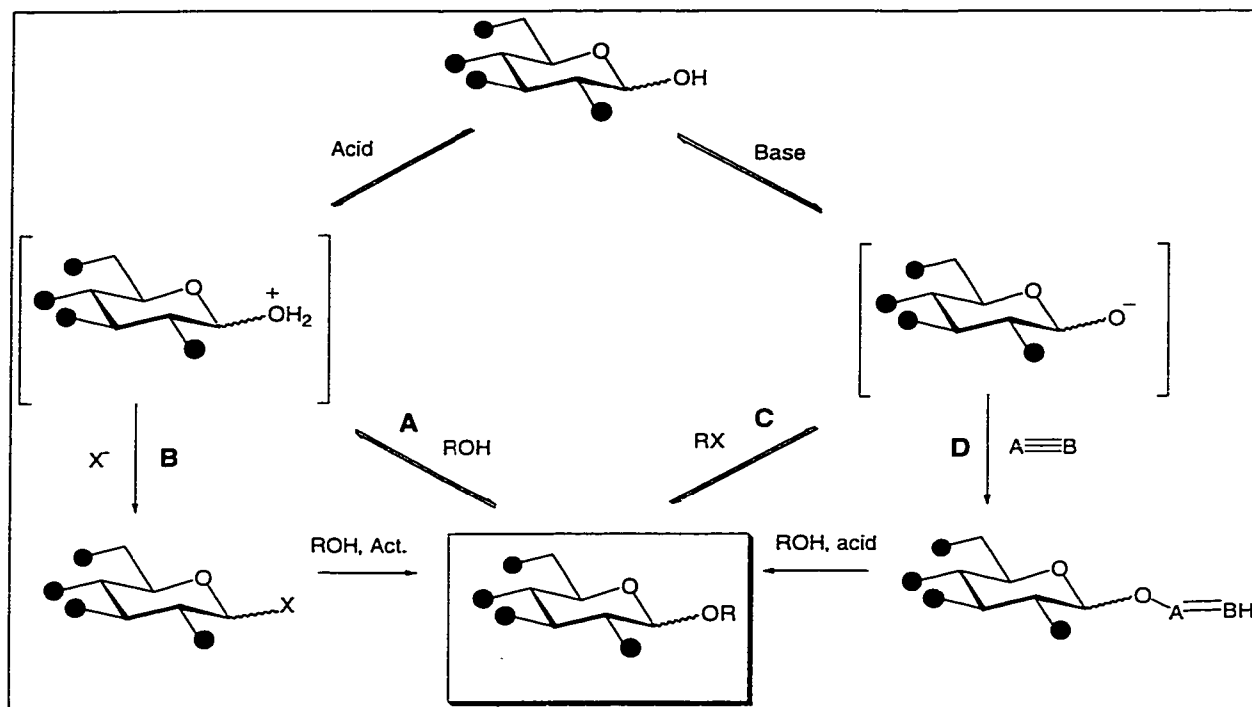
diversity of carbohydrates found in nature, chemists hoping to synthesize a wide variety of oligosaccharides have employed a number of different anomeric leaving groups to facilitate the formation of glycosidic bonds (Figure 11).^{62,63,64,65}

Figure 11: Anomeric Leaving Groups



The reactions by which the glycosyl donors listed in Figure 11 function can be promoted either by acid or base. The mechanisms are listed in Figure 12.

Figure 12: General Classes of Glycosylation Reactions



Acid facilitated glycosylations generally involve an exchange reaction between the anomeric oxygen for an oxygen from a hydroxyl group on the acceptor. These glycosylations can be divided into two classes: **A** and **B**.

Class **A** is the Fischer reaction that involves the direct conversion of the hemiacetal of a reducing sugar to an acetal with an acid catalyst. Improvements on

this theme, including orthoesters, anomeric acetates, vinyl glycosides, anomeric diaziridines and 1,2-epoxides have also been well represented in the literature.

Class **B** is the Koenigs-Knorr procedure that involves the preparation a glycosyl halide as the donor and the use of metal promoter in the glycosylation step.⁶⁶ Glycosyl fluorides, chlorides, bromides, and iodides can be prepared and purified in advance of the glycosylation.⁶⁷ Glycosyl halides can also be prepared *in situ* by the reaction of thioglycosides, selenoglycosides, glycosyl xanthates, glycosyl sulphoxides, pentenyl glycosides, pentenoyl glycosides.^{68,69,70}

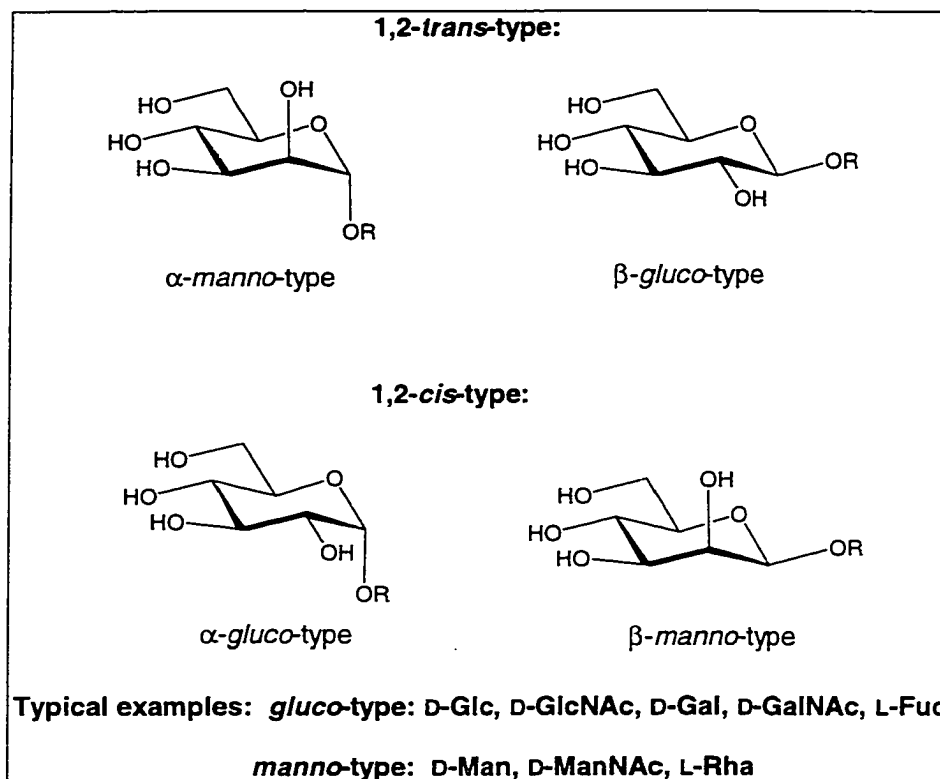
Base-promoted glycosylations can be classified into two groups: **C** and **D**. Glycosylations belonging to group **C** involve the base-promoted nucleophilic attack on an alkylating agent by the anomeric oxygen of a free sugar.

Group **D** donors-glycosyl phosphorus and trichloroacetimidates are modifications on the previous reaction that involve the activation of the anomeric oxygen with the use of base.⁷¹ Treatment of the activated donors with mild acid and acceptor affords the glycoside products.

The steric outcome of a glycosylation reaction mainly depends on the strength of the anomeric effect and on the possible neighbouring group participation of the protective groups at C-2.⁷² The anomeric effect is strongest in the formation of the α anomers of *manno*- and *gluco*-type sugars (Figure 13). Neighbouring group participation is most prevalent in 1,2-*trans*-type sugars. Hence, the formation of α -*manno*-type glycosidic linkages is relatively facile. Glycosidic linkages of α -*gluco*-type can be synthesized under thermodynamic control. Neighbouring group

participation can be used to control the formation of β -*gluco*-type linkages. The formation of β -*manno*-type linkages is quite difficult because they are not supported by the anomeric effect or by the participation of neighbouring groups.

Figure 13: Structural Types in Hexopyranosides



To prepare the synthetic disaccharide inhibitors, thioethyl anomeric groups were utilized because they can be prepared under mild conditions, are sufficiently stable for purification and may be stored for a considerable period of time, and facilitate glycosylations under mild conditions with commercially available promoter systems.⁷³

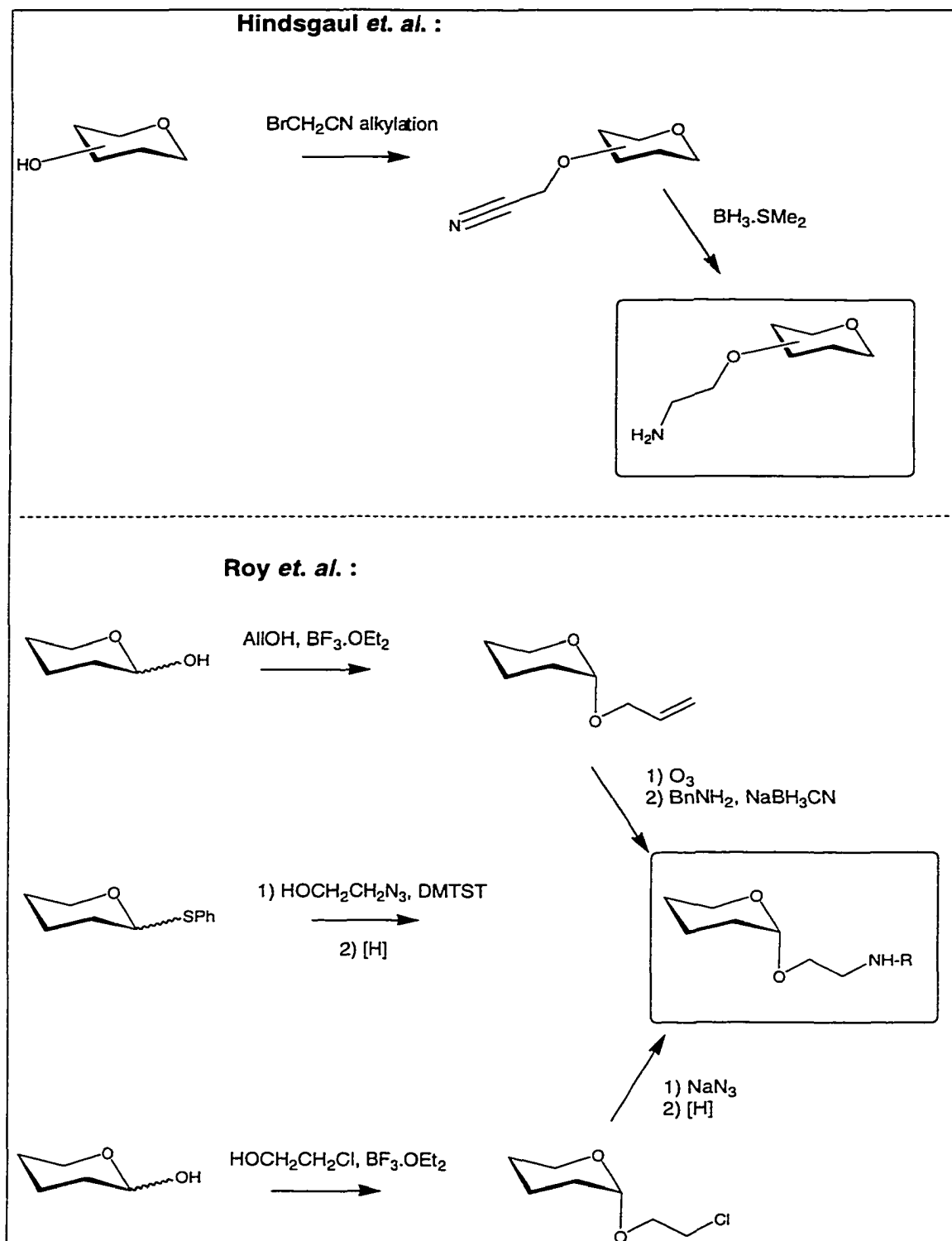
b. Method of Attachment of Linker Arm

A number of methods to introduce an ethylene-spaced amine into a molecule have been reported in the literature (Figure 14).

Hindsgaul and co-workers generated different functional groups on ligands to interact with proteins by alkylating hydroxyl groups with bromoacetonitrile followed by borane reduction to produce an amino ethylene linker arm.⁷⁴ This procedure was used to synthesize ligands of type I.

Roy and co-workers have utilized ethylene-spaced linker arms for the assembly of glycopeptoid libraries.⁷⁵ These groups were introduced in a number of ways. A reductive amination of an anomeric allyl group produced the desired amine linker arm. A glycosylation reaction with either 2-azidoethanol or 2-chloroethanol followed by displacement by azide also produced amine anchors after hydrogenation.⁷⁶ Roy's methodology was followed to make ligands of type II because the conditions necessary for reduction of the cyanomethyl group in Hindsgaul's procedure would not produce the required linker in high yield due to the presence of sensitive groups on the glucosamine D ring.

Figure 14: Introduction of an Ethylene-Spaced Amine



c. Choice of Protecting Groups

For the attachment of the linker onto the rhamnose C ring and subsequent glycosylations, benzyl ether protecting groups were used to protect the 2 and 4 positions of the rhamnose molecule because they are stable to the conditions chosen to reduce the cyanomethyl group to an alkyl amine. To reduce the number of synthetic manipulations to prepare the disaccharides with a linker arm at the anomeric centre of the glucosamine D ring, acetate groups were chosen to protect the 2 and 4 positions of the rhamnose C ring.

Because the glycosidic bond that was formed was a thermodynamically – favoured 1,2-*trans*-2-*L*-glycero linkage in all of the disaccharides, the controlling nature of the protecting groups had little effect on the steric outcome of the glycosylation reactions.

During all of the preparations of the disaccharides, a benzylidene acetal was used for the protection of the 4 and 6 positions of the glucosamine and was compatible with all of the organic transformations used in the synthetic strategy. A phthalimido group was used to protect the free amine on the glucosamine D ring.⁷⁷ This group improved solubility of the molecule in organic solvents compared with an acetamido group. The reducing end of the molecules were protected with allyl groups because of their stability and convertibility to linker arms.

d. Retrosynthetic Analyses of Ligands

After the choice of anomeric leaving groups, linking arms, and protecting groups were made, the retrosynthetic analysis of the type I ligands (Figure 15) shows the logical disconnections that would lead to the construction of the final products.

A glycosylation between ethyl 3-*O*-aminoethyl-2,4-di-*O*-benzyl-1-thio- α -L-rhamnopyranoside acylated with new contacts and allyl 4,6-*O*-benzylidene-2-deoxy-2-phthalimido- β -D-glucopyranoside **26** would furnish the proposed ligands of type I upon deprotection. An attachment of a cyanomethyl linker arm to the 3 position, reduction, and acylation with the new contacts would provide the donor.

A glycosylation between ethyl 2,4-di-*O*-acetyl-3-*O*-methyl-1-thio- α -L-rhamnopyranoside **43** and 2-azido-1-*O*-(4,6-*O*-benzylidene-2-deoxy-2-phthalimido- β -D-glucopyranosyl)-ethanol **39**, deprotection, reduction of the azido group, and acylation with new contacts would afford ligands of type II (Figure 16). The acceptor can be prepared from allyl 4,6-*O*-benzylidene-2-deoxy-2-phthalimido- β -D-glucopyranoside **26**.

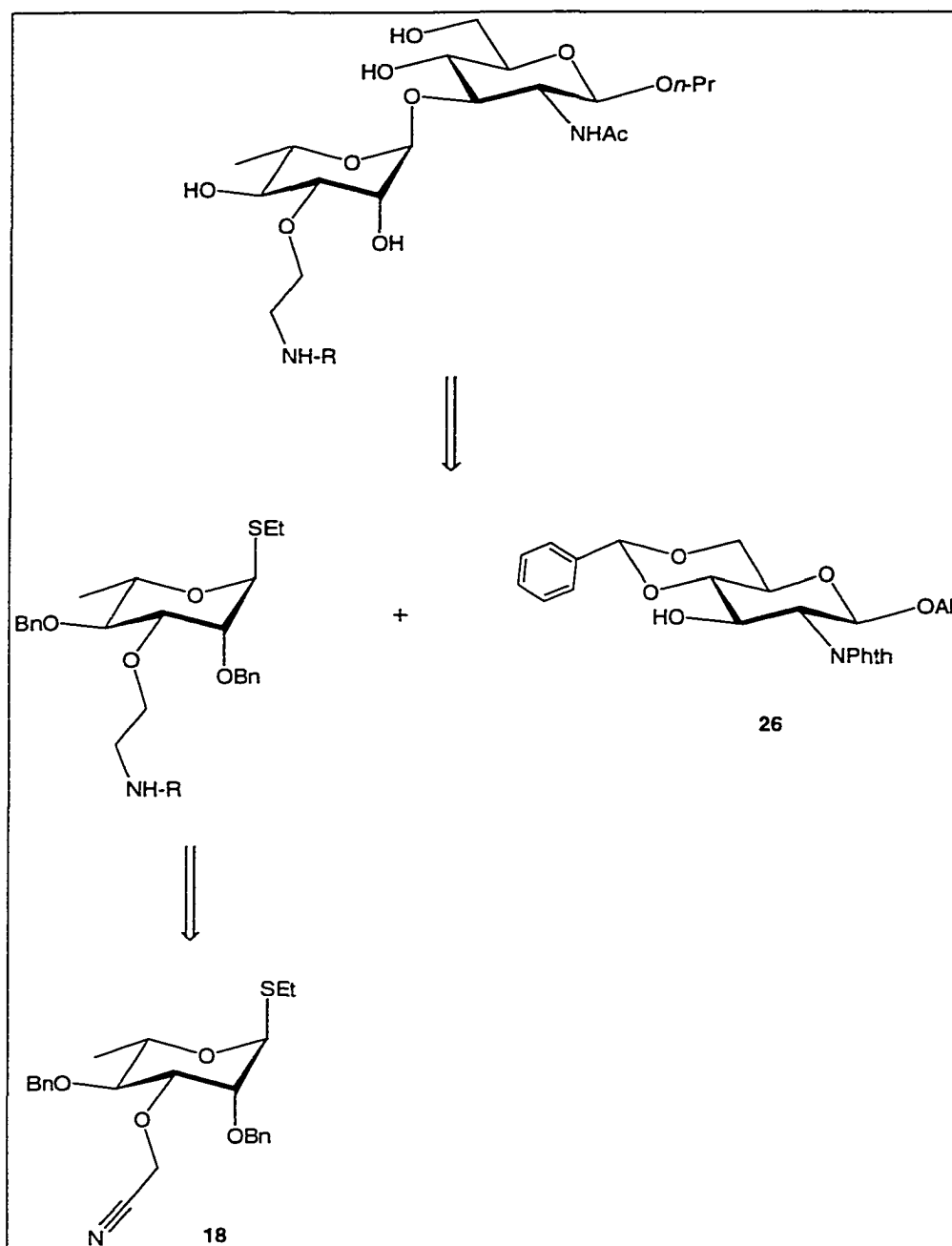
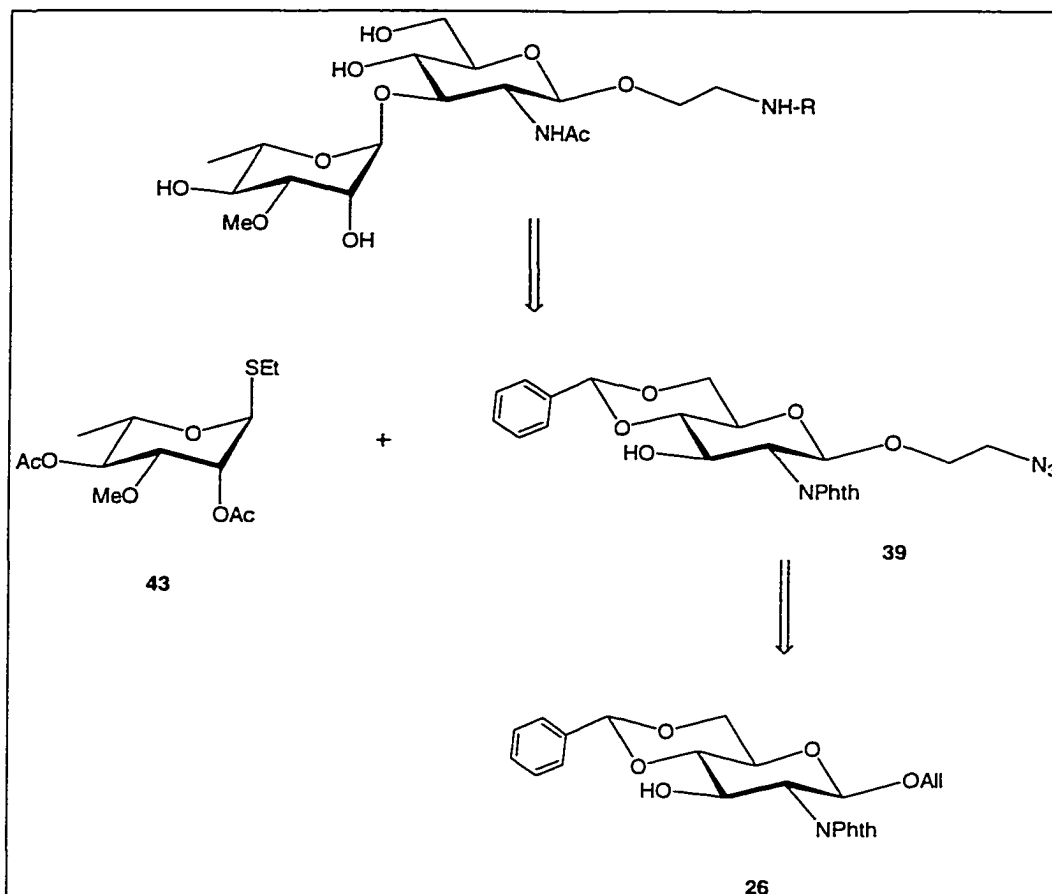
Figure 15: Retrosynthetic Analysis of Compounds of Type I

Figure 16: Retrosynthetic Analysis of Compounds of Type II



C) Syntheses of Ligands

I. Synthetic Ligands of Type I Modification

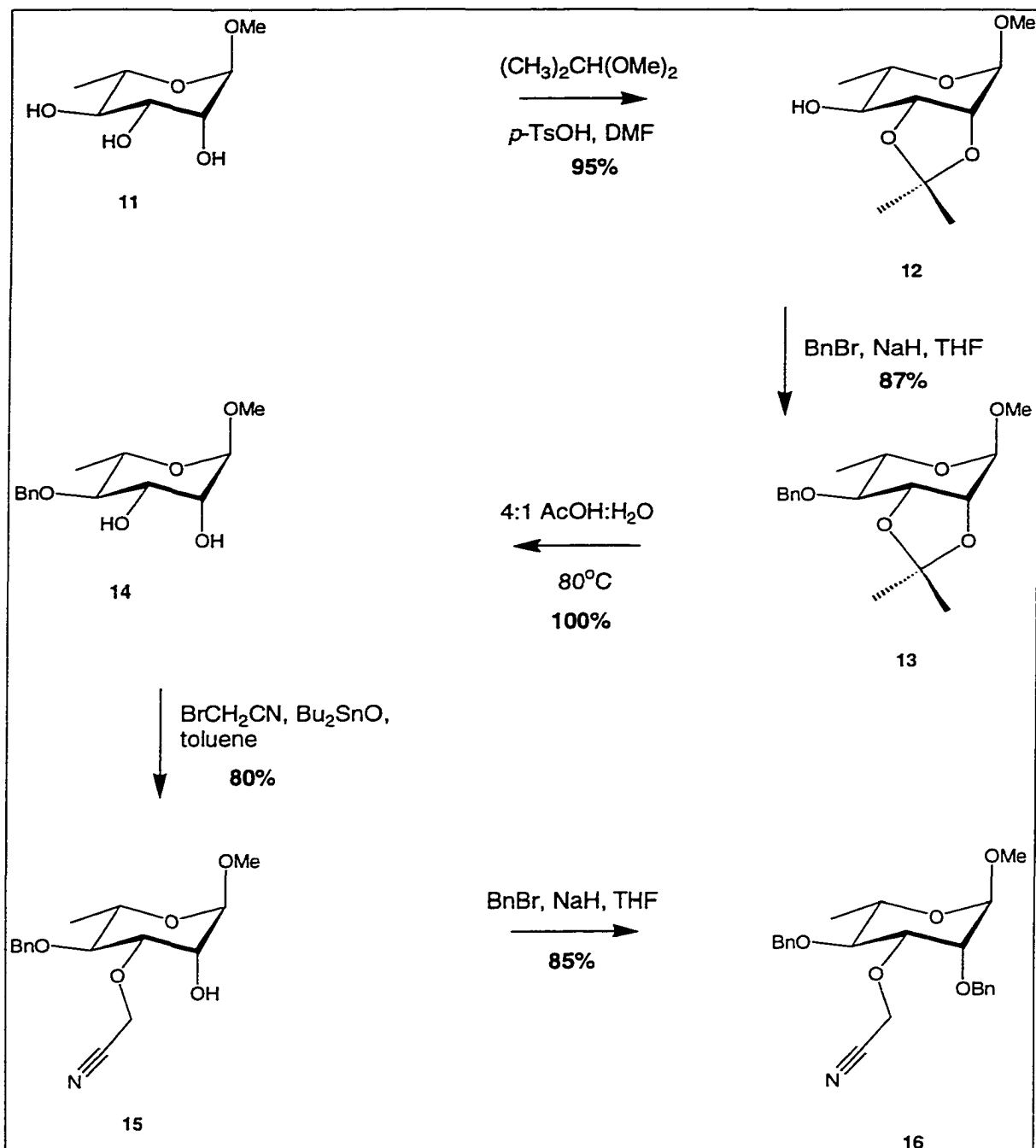
a. Introduction of the Cyanomethyl Group

The cyanomethyl group was introduced *via* an alkylation of diol **14** with dibutyltin oxide and bromoacetonitrile (Figure 17). Established procedures were

used to synthesize **14** from L-rhamnose. A Fisher glycosylation with methanol and strongly acidic cationic exchange resin yielded methyl α -L-rhamnopyranoside **11** in methanol.⁷⁸ Protection of the 2,3-*trans*-diols with 2,2-dimethoxypropane and *p*-toluenesulphonic acid in DMF furnished the acetonide **12**. Benzylation of the 4 position with benzyl bromide and sodium hydride in THF yielded the fully protected rhamnose molecule **13**.⁷⁹ The diol, **14**, was obtained by removal of the acetal protecting group by acid hydrolysis with 80% acetic acid (*aq.*) at 80 °C.

A regioselective alkylation with dibutyltin oxide and bromoacetonitrile in toluene afforded the nitrile **15**.⁸⁰ A subsequent benzylation yielded the fully-protected 3-*O*-cyanomethyl rhamnopyranoside **16**. A direct alkylation of methyl 2,4-*O*-dibenzyl- α -L-rhamnopyranoside, that was obtained by a phase-transfer benzylation of **14**, resulted in polymerization of bromoacetonitrile and did not produce the desired product **16**.⁸¹

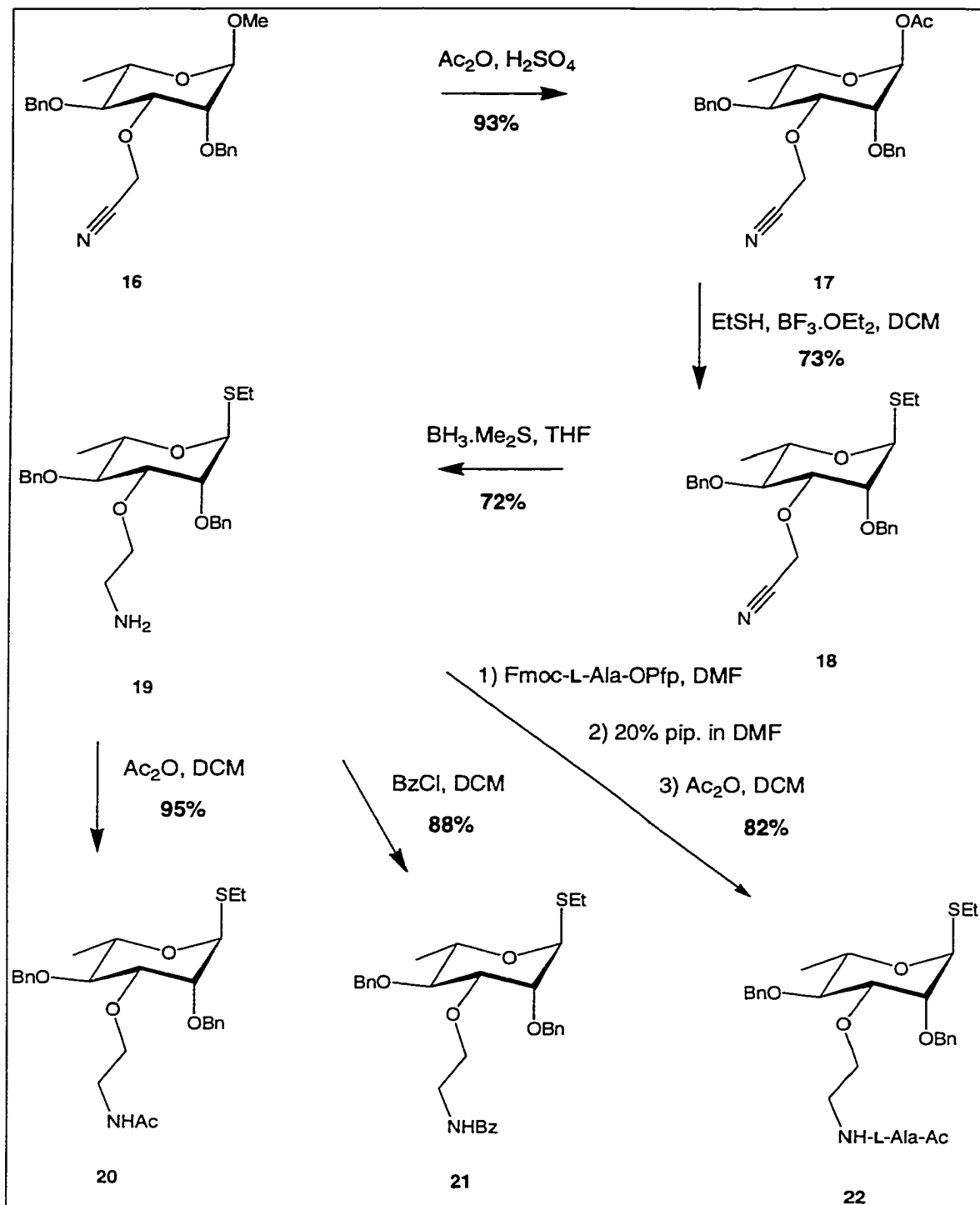
Figure 17: Synthesis of the Nitrile (16)



b. Preparation of the Glycosyl Donors (20), (21), and (22)

The methyl α -glycoside **16** was first converted to an anomeric acetate by acetolysis conditions, catalytic sulphuric acid in acetic anhydride (Figure 18). The acetate **17** was then transformed into the α -thioethyl glycoside **18** in good yield using the Lewis acid, boron trifluoride diethyl etherate, and ethanethiol in dichloromethane. Despite the possible removal of the benzyl ether protecting groups in these conditions, the yields were respectable.⁸² The nitrile group was reduced under refluxing conditions using borane-dimethyl sulphide complex in THF to produce the free amine **19**.⁸³ The desired compound was produced in the highest yield relative to other conditions such as catalytic hydrogenation and lithium aluminum hydride. The amine was acylated with either acetic anhydride or benzoyl chloride in dichloromethane to produce the glycosyl donors **20** and **21**. The third donor **22** was prepared by acylating with commercially available Fmoc-L-alanine pentafluorophenylester in DMF followed by conversion of the Fmoc group to the *N*-acetate with 20% piperidine in DMF and acetylation with acetic anhydride in dichloromethane.⁸⁴

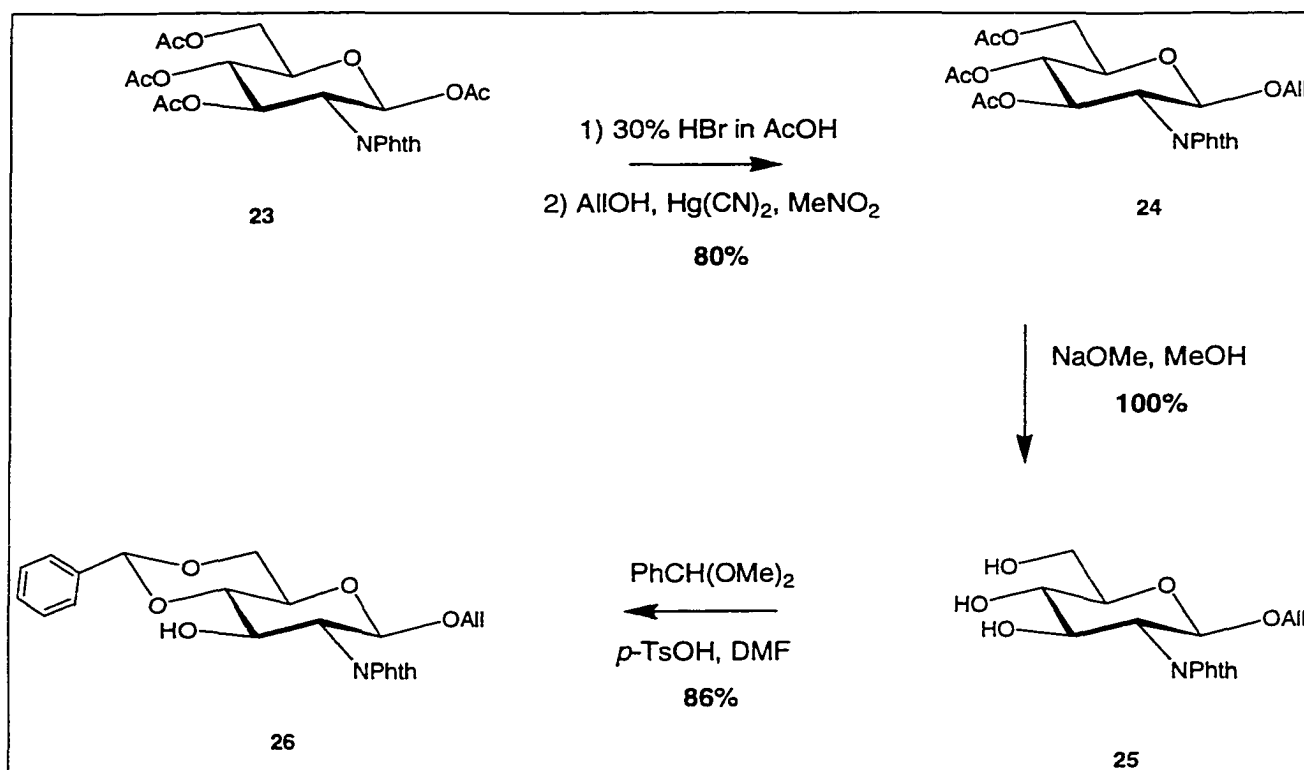
Figure 18: Syntheses of the Donors (20), (21), and (22)



c. Preparation of the Glycosyl Acceptor (26)

The glycosyl acceptor **26** was synthesized according to published methodology (Figure 19).⁸⁵

Figure 19: Preparation of the Acceptor (26)



Unprotected glucosamine was converted to the peracetylated phthalimido derivative **23** using phthalic anhydride and acetic anhydride in pyridine.⁸⁵ The anomeric acetate was converted to an allyl group by first making the glycosyl bromide using 30% HBr in AcOH, and then glycosidating with allyl alcohol and

mercury (II) cyanide in nitromethane. Transesterification of **24** with sodium methoxide in methanol yielded the partially deprotected sugar **25**. A benzylidene acetal was then installed using acid catalysis and benzaldehyde dimethyl acetal in DMF to afford the acceptor **26**.

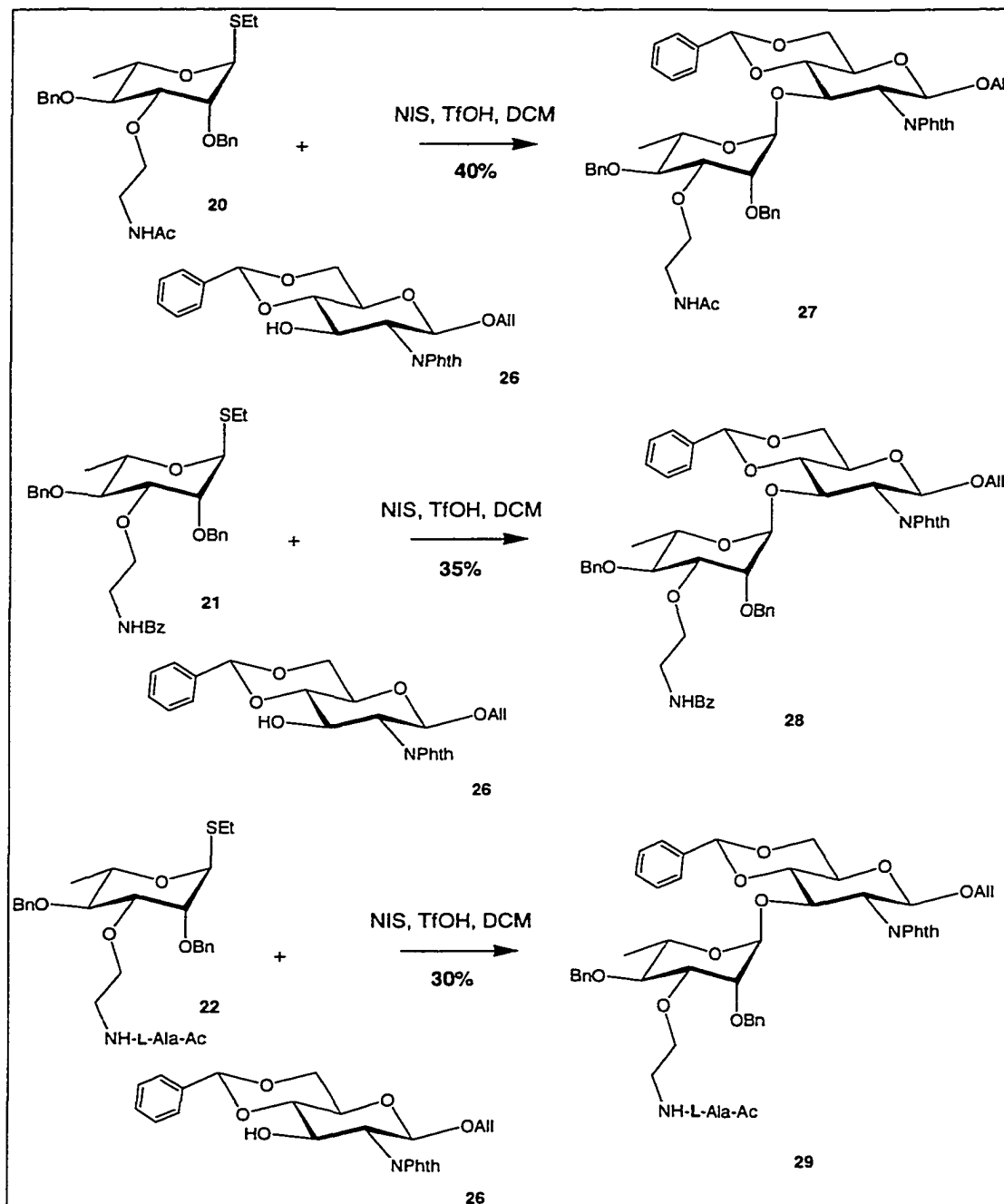
d. Preparation of the Protected Disaccharides (**27**), (**28**), and (**29**)

The glycosylation conditions to produce the disaccharides **27**, **28**, and **29** used *N*-iodosuccinimide and triflic acid promotion in dichloromethane (Figure 20). In each case, the acceptor and glycosyl donor (1.3 eq.) were allowed to stir overnight with 4 Å molecular sieves in dichloromethane. Triflic acid and *N*-iodosuccinimide were then added and the mixtures were stirred for one hour. After aqueous work up, yields of the disaccharides **27**, **28**, and **29** were somewhat disappointing (40%, 35%, and 30% respectively). The use of other promoters such as iodine, bromine, and silver triflate did not produce the desired disaccharides in higher yields.⁶¹ The large $^1J_{\text{CH}}$ coupling constants of 166.6, 167.0, and 168.5 Hz at the anomeric centres for the newly – formed glycosidic linkages in **27**, **28**, and **29**, respectively, confirmed the correct α anomeric configuration.

It is unusual that the substitution at the 3 position would have a dramatic influence on the glycosylation reaction. However, in this system, it appears that the presence of large substituents at the 3 position results in poor glycosylation yields. Further evidence of this statement is that when a Fmoc-carbamate was formed on

the free amine **19** using Fmoc succinimide in order to give the donor a combinatorial feature, the glycosylation between this donor and the acceptor **26** proceeded very poorly with a yield of less than 10%.

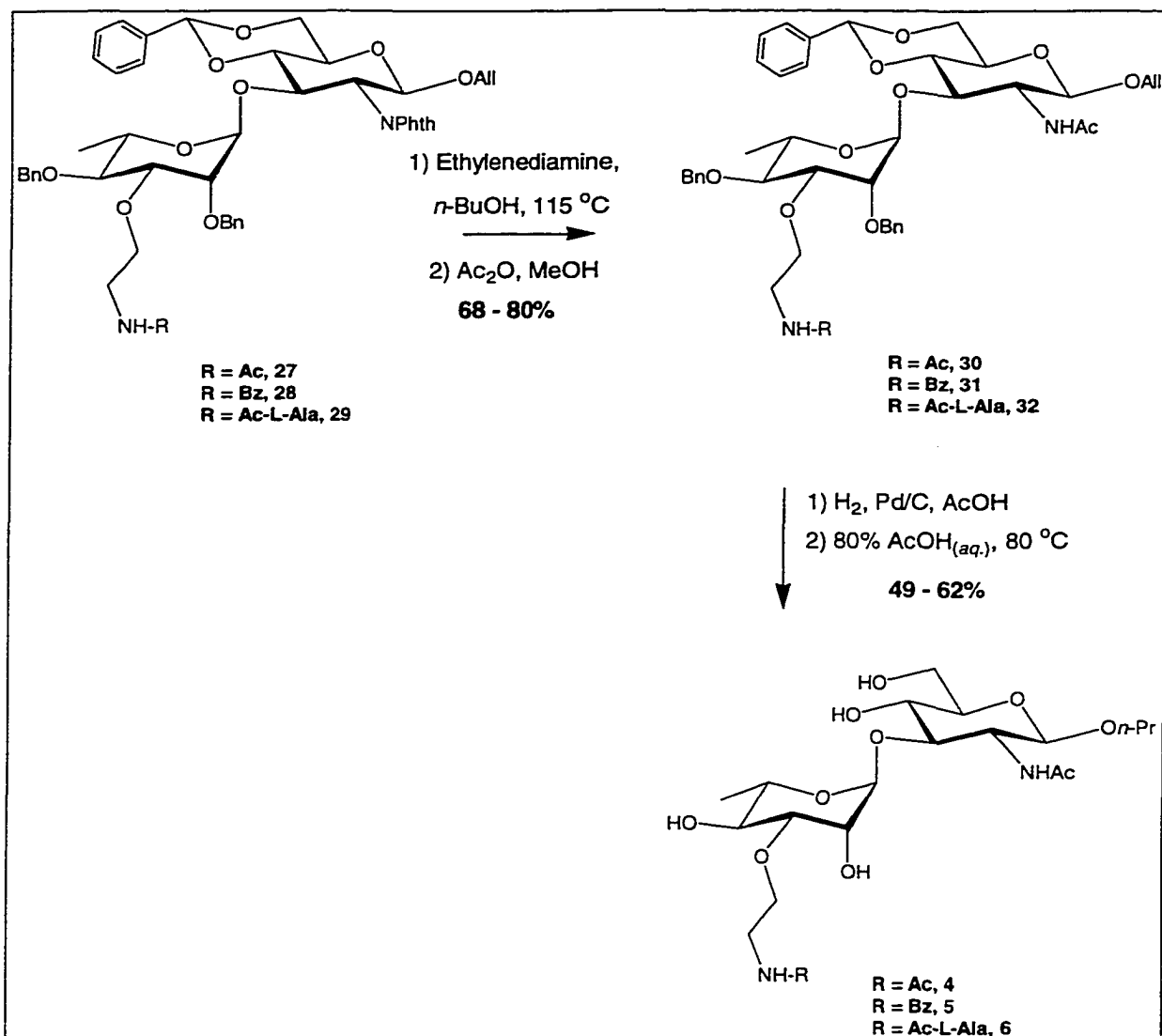
Figure 20: Syntheses of the Disaccharides (27), (28), and (29)



e. Syntheses of Test Compounds (4), (5), and (6)

To complete the syntheses of the first test compounds, the protected disaccharides **27**, **28**, and **29** were stirred in *n*-butanol and ethylenediamine at 115 °C for 18 h to remove the phthalimide group from the glucosamine residue (Figure 21).⁸⁶ Typically, hydrazine hydrate is used for this manipulation, but side reactions that may occur with the allyl protecting group would decrease yields. After the removal of solvents, methanol and acetic anhydride were added to install an acetate group on the free amine. Yields for these transformations varied from 66% for **31** to 80% for **32**. Next, the products were subjected to catalytic hydrogenation conditions using 10% palladium on carbon and a stream of hydrogen gas. Acetic acid was used as the solvent. NMR analyses of the products of the hydrogenations showed the presence of a persistent benzylidene acetal protecting group. To remove this group, the filtered solution was heated with 80% acetic acid in water at 80 °C. These procedures yielded the deprotected disaccharides **4**, **5**, and **6** in 54, 62, and 49% yields, respectively. These compounds were tested against the native trisaccharides by a solid phase binding assay. This information is provided later.

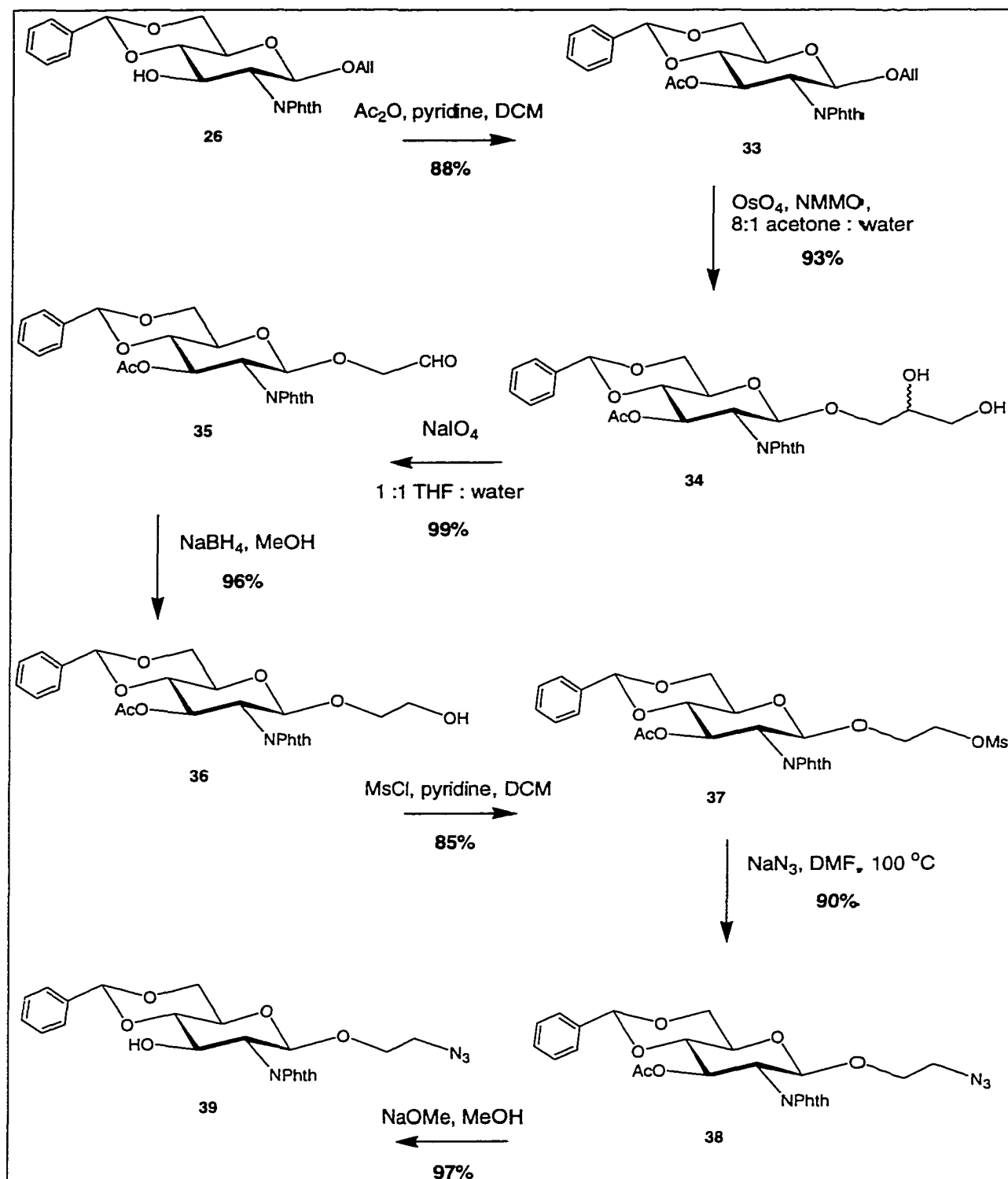
Figure 21: Syntheses of the Test Compounds (4), (5), and (6)



II. Synthetic Ligands of Type II Modification

a. Synthesis of the Glycosyl Acceptor (39) with an Ethylene-Spaced Azide

The free hydroxyl group in the partially-protected glucosamine monosaccharide **26** was acetylated to minimize side products during reactions with oxidation agents. To convert the allyl group into an ethylene – spaced azide, the olefin **33** was first oxidized with osmium tetroxide and *N*-methylmorpholine *N*-oxide in wet acetone to produce the diol **34** (Figure 22). These conditions were chosen over ozone because of the sensitivity of the benzylidene acetal towards ozone. The diol **34** was oxidatively cleaved with sodium periodate in 50% aqueous THF to yield the aldehyde **35** which was reduced to the alcohol **36** using sodium borohydride in methanol. The alcohol functional group was then transformed into a good leaving group with methanesulphonyl chloride and pyridine in dichloromethane. Displacement of the mesylate **37** with an azide group using sodium azide in DMF at high temperature resulted in the ethylene – spaced azide. A Mitsunobu reaction to replace the hydroxyl group with azide directly did not produce the azide **38** in good yield.⁸⁷ Finally, the acetate protecting group was removed with sodium methoxide in methanol to produce the glycosyl acceptor **39**.

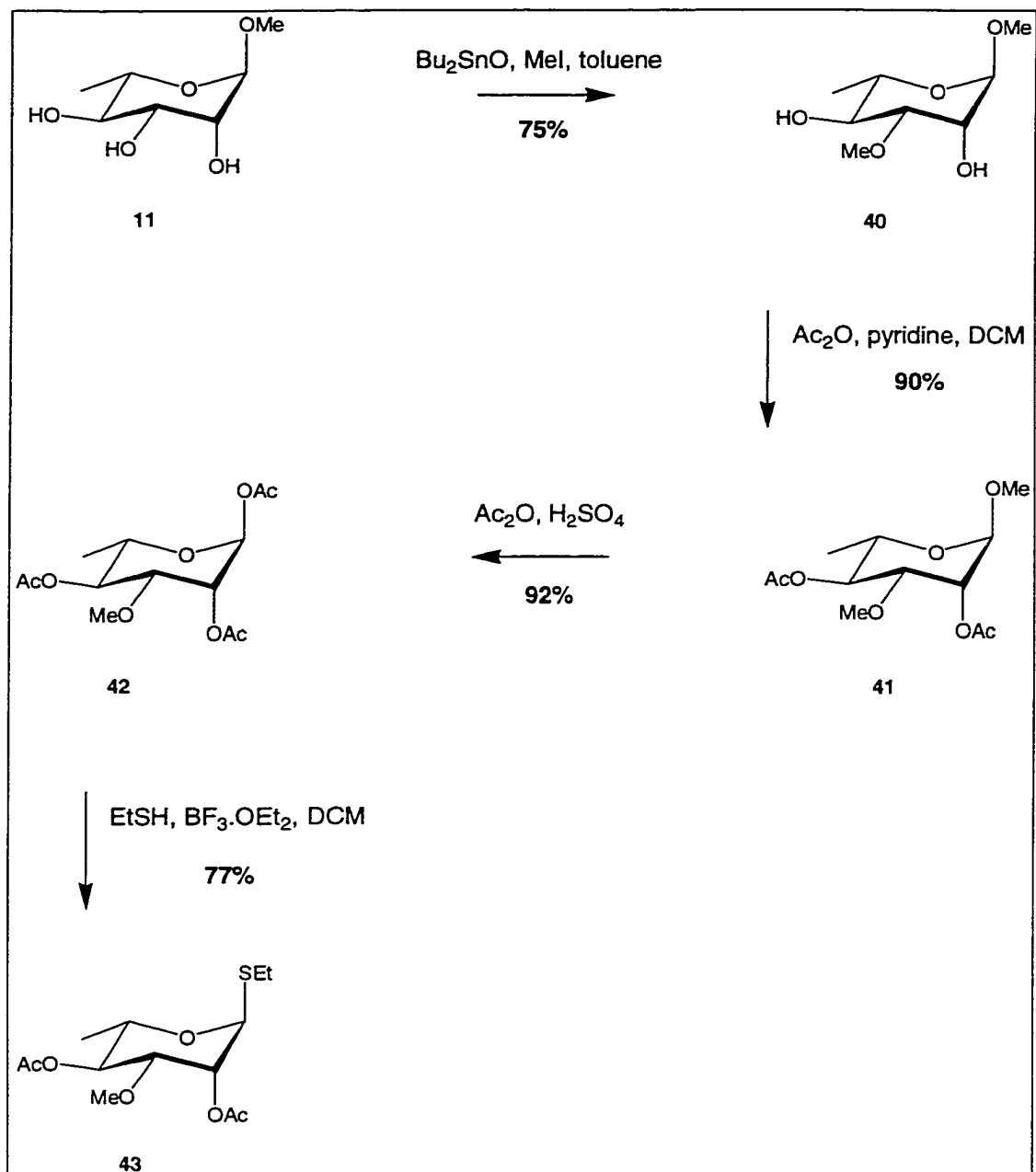
Figure 22: Synthesis of the Acceptor Molecule (39)

b. Preparation of the Rhamnose Donor (43)

To minimize differences between the synthetic analogs and the native ligand, a methyl group was installed on the O-3 atom of the rhamnose C ring. This group serves to mimic the glycosidic bond between the rhamnose B and C rings. The donor was prepared in four steps from methyl α -rhamnoside (Figure 22).

Methylation of methyl α -rhamnoside with dibutyltin oxide and methyl iodide provided **40** in good yield.⁸⁸ The free hydroxyl groups were acetylated with acetic anhydride and pyridine in dichloromethane. The methyl α -glycoside **41** was then converted by acetolysis to the anomeric acetate **42** using a drop of concentrated sulphuric acid in acetic anhydride. The glycosyl donor **43** was then obtained by stirring the acetate **42** in dichloromethane with ethanethiol and boron trifluoride diethyl etherate.

Figure 23: Preparation of the Donor (43)

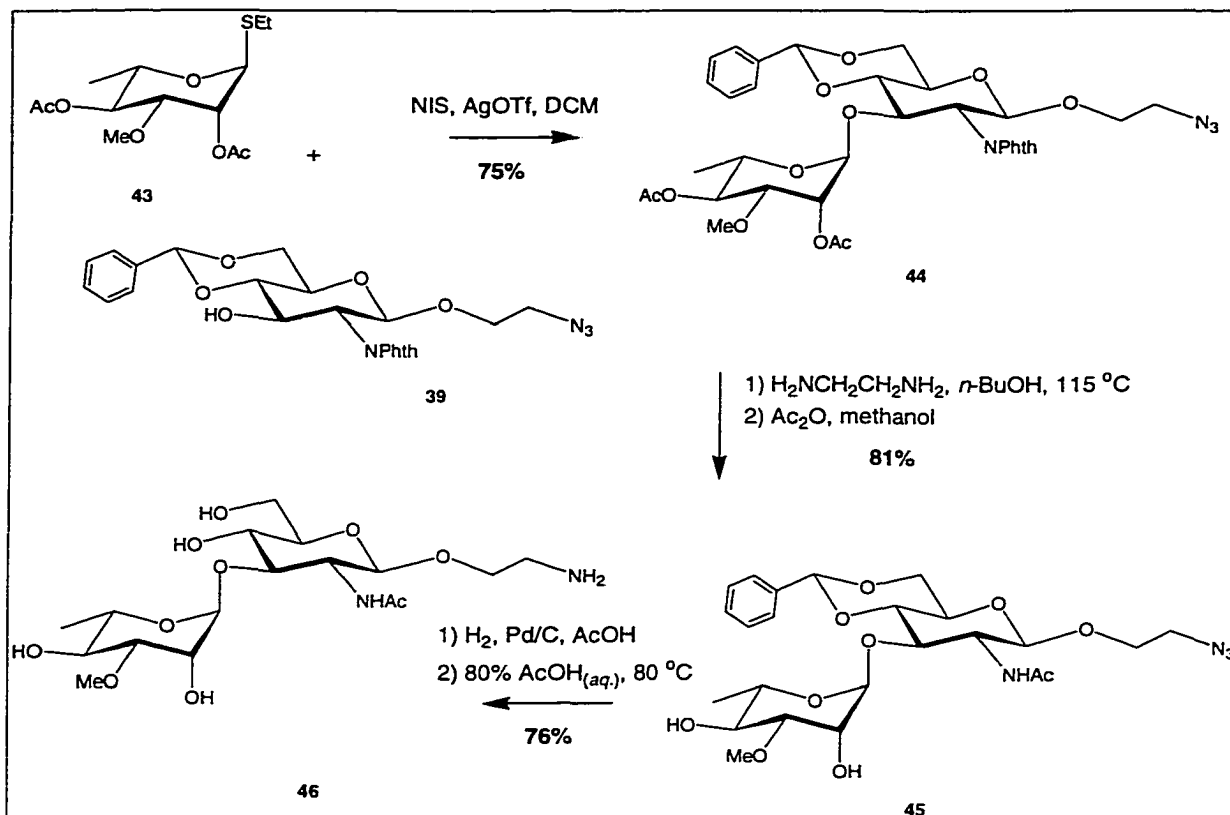


c. Synthesis of the Disaccharide (46) with an Ethylene-Spaced Amine

Glycosylation of the acceptor **39** by the donor **43** proceeded using silver triflate and *N*-iodosuccinimide as promoters in dichloromethane to produce the disaccharide **44** (Figure 24). The yield was a very respectable 75% and further validates the idea that the substituent at the 3 position influences the glycosylation reaction; because, in this glycosylation, the group at the 3 position of the donor is small and consequently, the product was formed in high yield. The large $^1J_{\text{CH}}$ coupling constant of 171.2 Hz for the newly – formed glycosidic linkage confirmed that the α configuration at the anomeric centre was achieved.

The acetate and phthalimido protecting groups were removed with ethylenediamine and an acetate was installed on the free amine of the glucosamine residue to afford the partially deprotected disaccharide **45**. The azide was reduced under hydrogenation conditions and the benzylidene acetal was removed by acid hydrolysis to produce the fully deprotected sugar **46**.

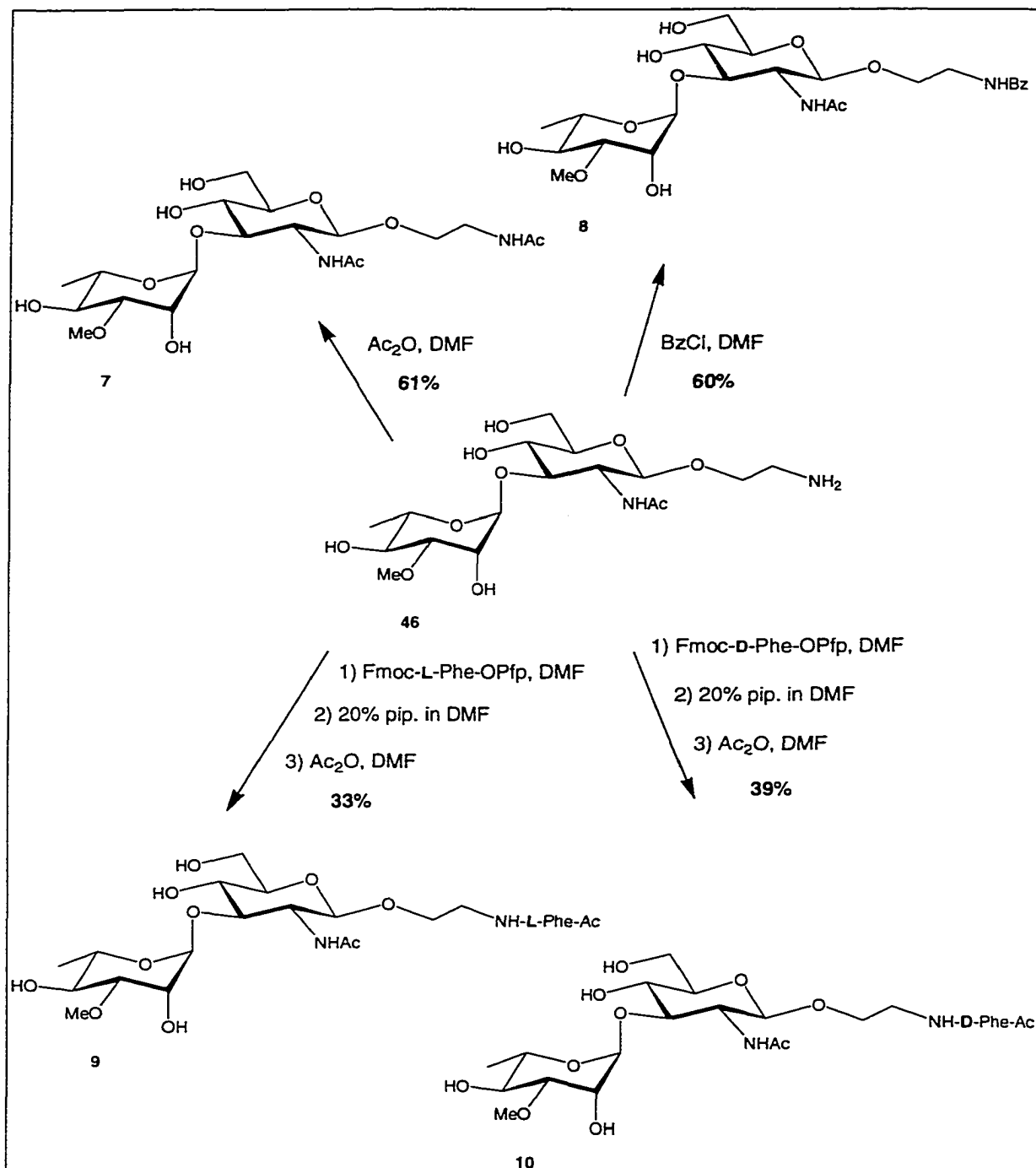
Figure 24: Synthesis of the Deprotected Disaccharide (46)



d. Syntheses of Test Compounds (7), (8), (9), and (10)

To synthesize the test compound 7 the deprotected sugar 46 was acetylated with acetic anhydride in dimethylformamide (Figure 25). Similarly 46 was benzoylated with benzoyl chloride to produce the final compound 8. To attach the amino acids, L-phenylalanine and D-phenylalanine, the pentafluorophenylesters of the Fmoc-protected amino acids were stirred with the free amine. The Fmoc groups were removed with piperidine and the resulting amines were acetylated using acetic anhydride to provide the test compounds 9 and 10.

Figure 25: Syntheses of Test Compounds (7), (8), (9) and (10)



III. Synthesis of the 3'-O-Methyl Native Disaccharide (49)

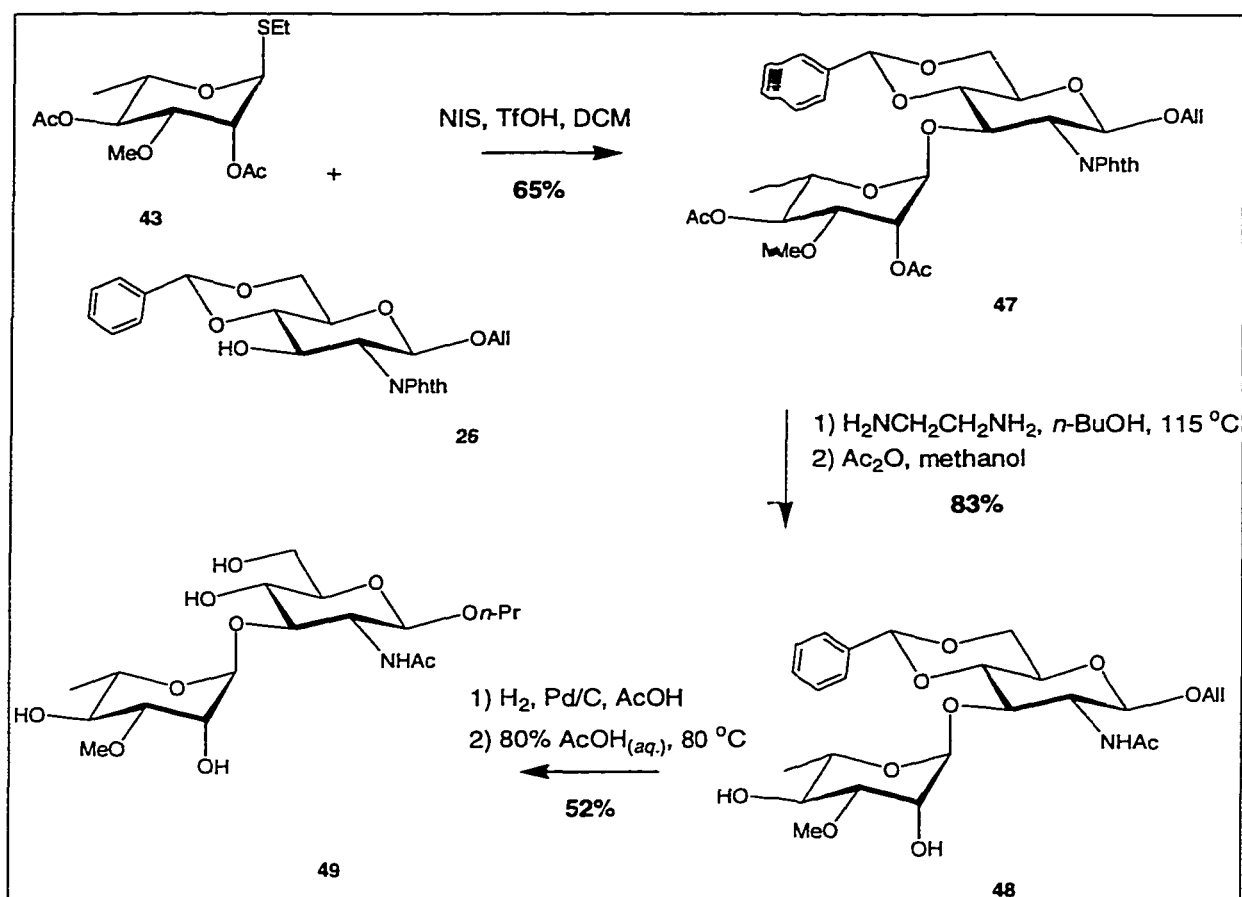
A modified 3'-O-methyl native disaccharide was synthesized as a way of showing that the modifications that were made to the Rha-GlcNAc CD disaccharide were beneficial. If the synthetic derivatives had higher association constants than this structure, the ligand design strategy can be regarded as improving the carbohydrate contacts with the protein.

a. Preparation of the Native Disaccharide Mimic

The acceptor **26** and the donor **43** were reacted in dichloromethane with triflic acid and *N*-iodosuccinimide to produce the disaccharide **47** in 65% yield (Figure 26). The large $^1J_{\text{CH}}$ coupling constant of 170.6 Hz at the anomeric centre for the newly – formed glycosidic linkage confirmed that the correct linkage was produced.

The phthalimido and acetate groups were removed from the protected disaccharide and the acetamide functionality was installed. The allyl group was reduced by hydrogenation and the benzylidene acetal was hydrolyzed to produce the native disaccharide mimic.

Figure 26: Preparation of the Disaccharide (49)



Chapter 3

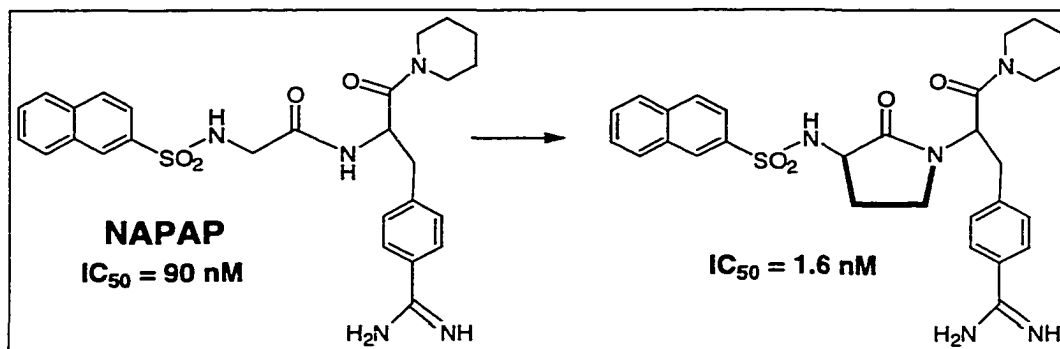
The Design and Synthesis of Constrained Trisaccharide Ligands

It has been postulated for oligosaccharides that a major contributor to the entropic barrier is the conformational loss of freedom of the ligand upon binding to protein.¹⁸ In particular, the loss of rotational freedom about the glycosidic bond has been estimated at about 0.6 kcal mol⁻¹ per torsion angle although recent work by Whitesides *et al.* suggests this number may be smaller.⁸⁹

A) Ligand Design

During the past few years, a number of research groups have designed and synthesized rigid ligands with hopes of improving binding to protein.⁴⁴ For example, Mack and co-workers have designed rigid inhibitors of thrombin.⁹⁰ Their research showed that the introduction of a lactam ring on the known inhibitor, NAPAP, improved the binding affinity by a factor of 60 (Figure 27).

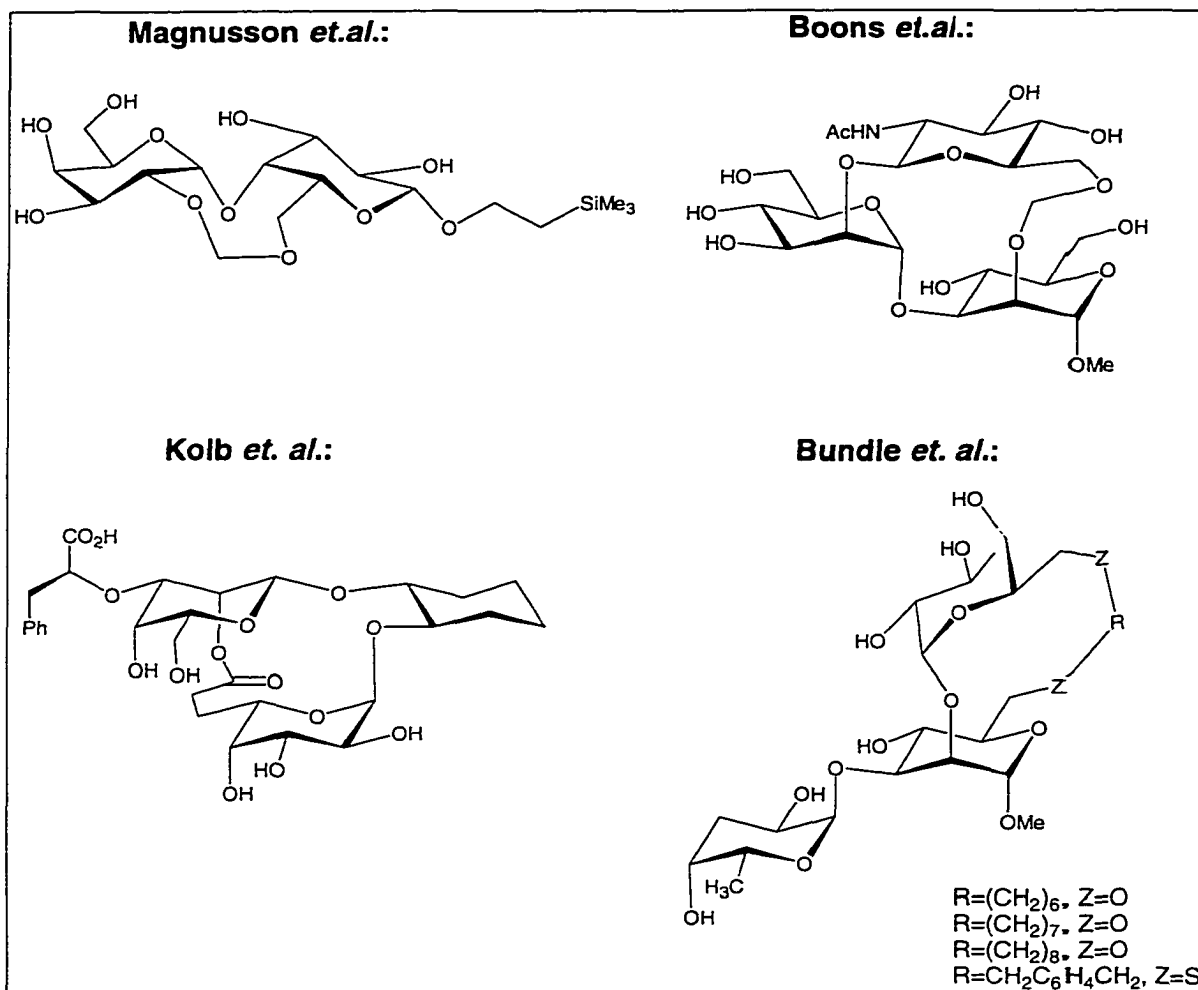
Figure 27: An Example of Improved Affinity *via* the Introduction of Constraints



In the field of glycobiology, Magnusson and co-workers have synthesized a galabioside with a methylene bridge between two key hydroxyl groups as a candidate for bacterial adhesion (Figure 28).⁹¹ Similarly, Boons and co-workers synthesized a rigid trisaccharide with a methylene acetal to mimic an intramolecular hydrogen bond to study interactions with a lectin, Concanavalin A.^{92,93} Kolb and co-workers designed and synthesized a sialyl Lewis^x mimic to probe the spatial orientation of the functional groups in the ligand bound to E-selectin.⁹⁴ All previous three ligand designs were successful in reducing the entropic barrier, but the total free energy of binding was not improved because the carbohydrates were preorganized in a conformation that was not ideal for binding. Bundle and co-workers have prepared a series of trisaccharide ligands with aryl or alkyl tethers of varying length in order to overcome the entropic barrier and produce ligands with higher affinities.⁹⁵ In this case, free energy changes no larger than 0.5 kcal/mol relative to the native trisaccharide were observed because the bound form of the

ligand placed the non-polar tethers into a solvent exposed region that resulted in hydrophobic interactions with water that produced enthalpic gains but an entropic penalty.

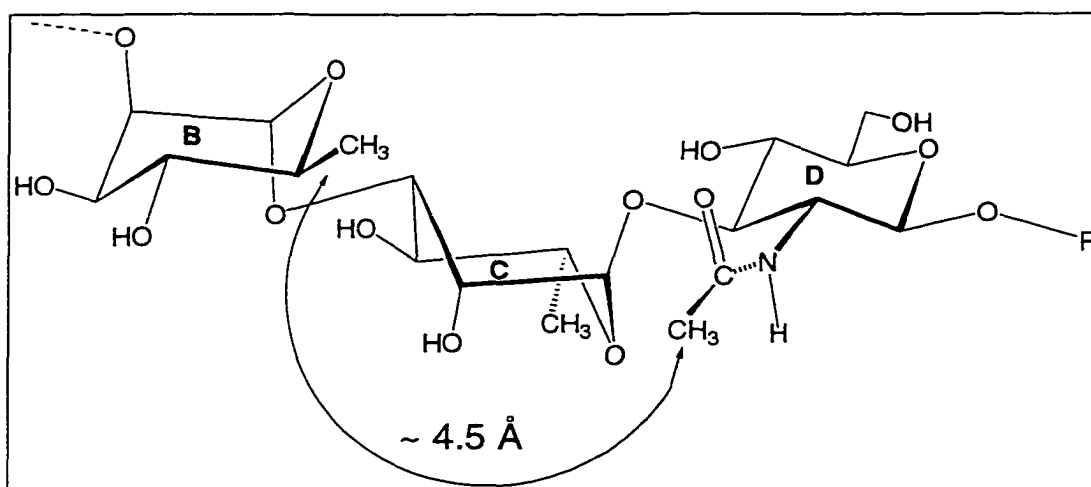
Figure 28: Examples of Constrained Ligands



In the present study, constrained ligands were designed that varied in linker size and attachment to overcome the entropic barrier involved in oligosaccharide –

protein binding.¹⁸ An examination of the crystal structures of the bound ligands in the antibody binding site revealed the proximity of the acetamido group on the 2 position of the glucosamine D ring with the 6 position of the rhamnose B ring (Figure 29). These methyl groups were approximately 4.5 Å apart and were the logical anchoring sites for the attachment of a tether that would constrain two glycosidic linkages. In addition, the linker would be in a solvent – exposed region and steric clashes between the linker and protein backbone would be avoided or minimized.

Figure 29: Proximity of Linkage Sites

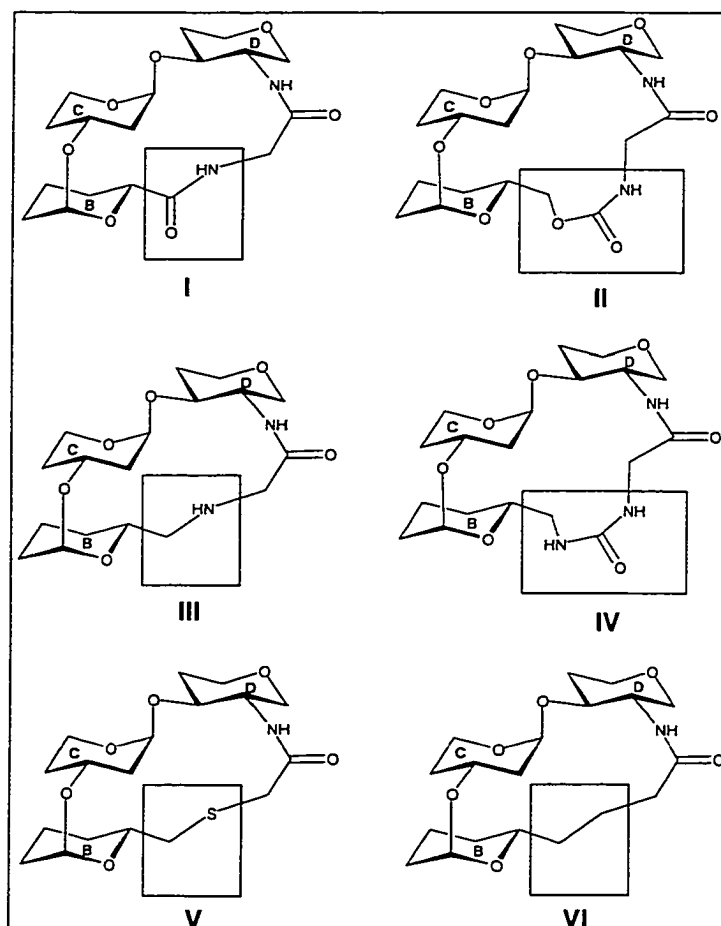


To attach the linkers, the amino group on the 2 position can be acylated with amino acids such as glycine or β -alanine instead of an acetyl group as in the native structure. This would conserve the hydrogen bonding network at the reducing end

of the molecule and provide an amine functional group that can be used in the cyclization of the molecule.

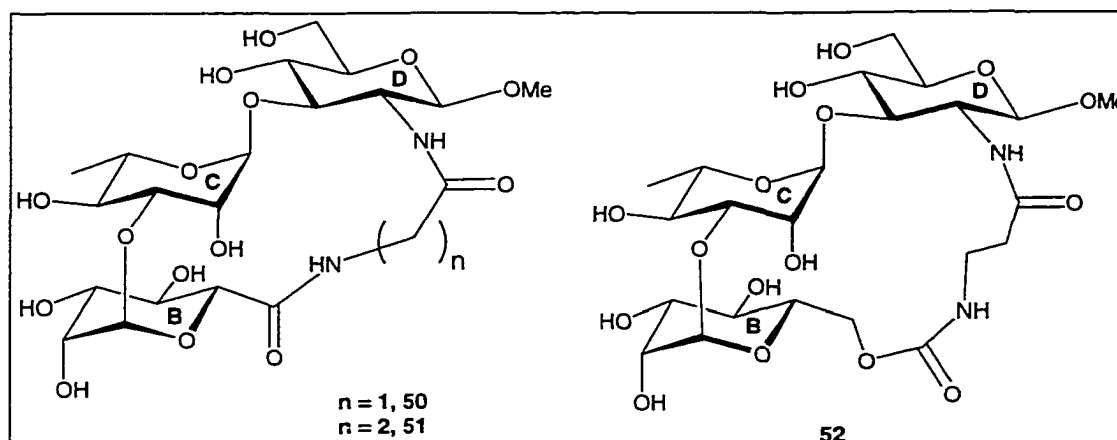
If the rhamnose B ring residue is replaced by L-mannose, the polar hydroxyl group at the 6 position can be modified to provide a variety of linkages that are shown in Figure 30 including amides (I), carbamates (II), amines (III), ureas (IV), mercaptans (V), and alkanes (VI). While the last type of linkage would require a more substantial synthetic effort, the others can be achieved through functional group manipulation of the core trisaccharide.

Figure 30: Possible Tethers



Initial efforts have focused on the syntheses of ligands of types I and II to provide constrained molecules for testing. The syntheses of these molecules would be less involved than the other types. In addition, the area that the linker would occupy is solvent – exposed and the attachment of somewhat polar linkers would minimize solvent reorganization. Hence, three ligands, lactams **50** and **51**, and cyclic carbamate **52**, have been prepared and tested by a solid phase assay for inhibitory power (Figure 31).

Figure 31: Proposed Ligands



B) Retrosynthetic Analysis of the Proposed Ligands

A retrosynthetic analysis of the lactam **75** shows the logical disconnections that would lead to the construction of the final product (Figures 32 and 33). After the glycine linker was attached to the amine at the 2 position of the glucosamine D ring

and the 6 position of the L-mannose B ring was oxidized, the cyclization would occur at the end of the synthetic scheme (Figure 32). To do this, the core trisaccharide structure would have to be constructed with temporary protecting groups at the 2 position of the glucosamine D ring and the 6 position of the L-mannose B ring. A glycosylation reaction between the disaccharide, **69** and fully protected L-mannose donor, **67**, would yield the core trisaccharide unit. The disaccharide **69** can be obtained from the glycosylation between the donor **58** and the acceptor **61** (Figure 33).

The other constrained ligands, lactam **51** and cyclic carbamate **52**, could be synthesized in the same fashion (Figure 31).

The choice of anomeric leaving groups and protecting groups were made using the criteria outlined in the previous chapter. In this strategy, benzyl ether, phthalimide, and benzylidene acetal protecting groups are stable to the conditions to be used to assemble and modify the trisaccharide ligands.

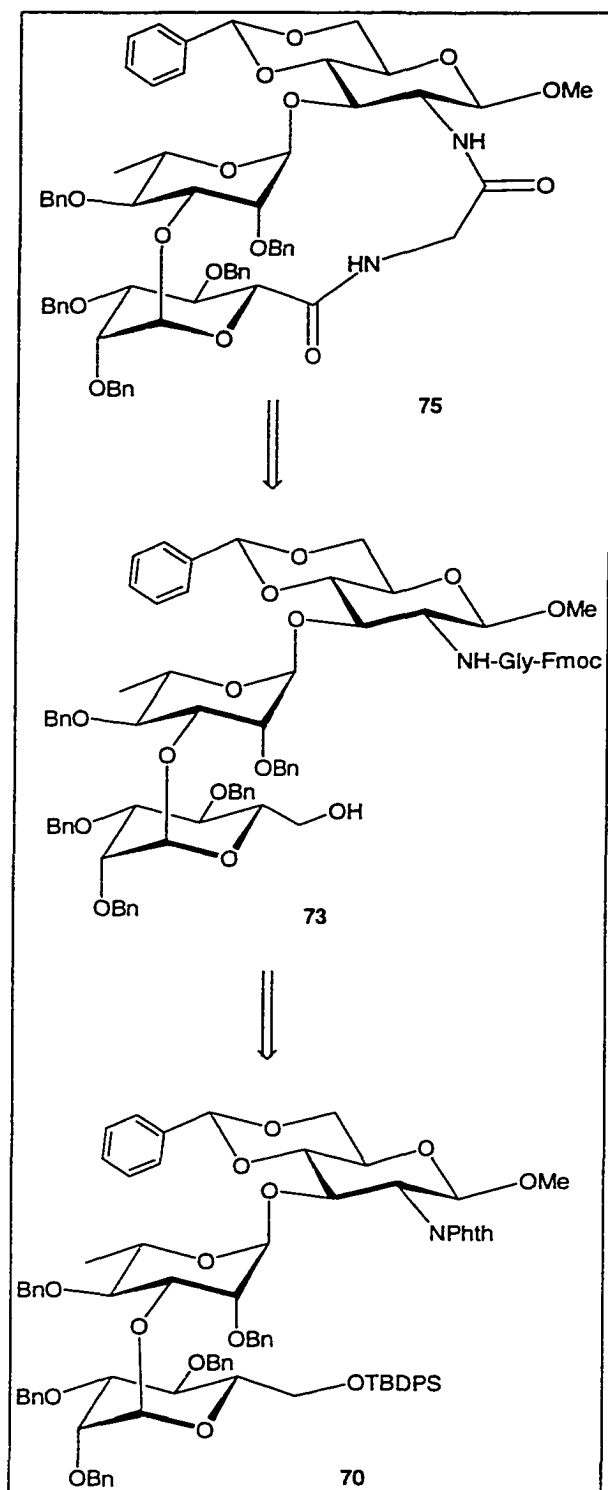
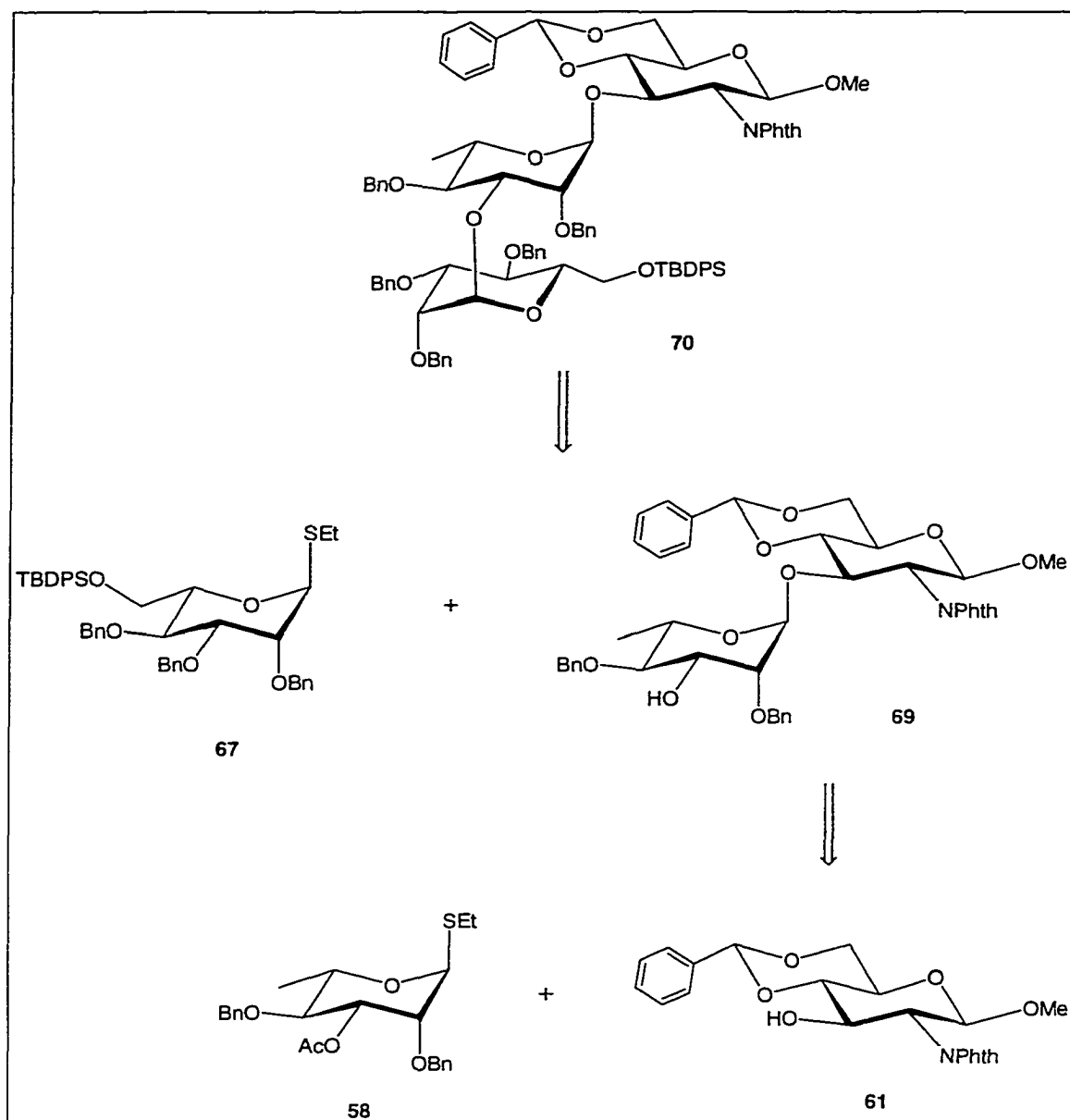
Figure 32: Retrosynthetic Analysis of the Lactam (75)

Figure 33: Retrosynthetic Analysis of the Core Trisaccharide (70)



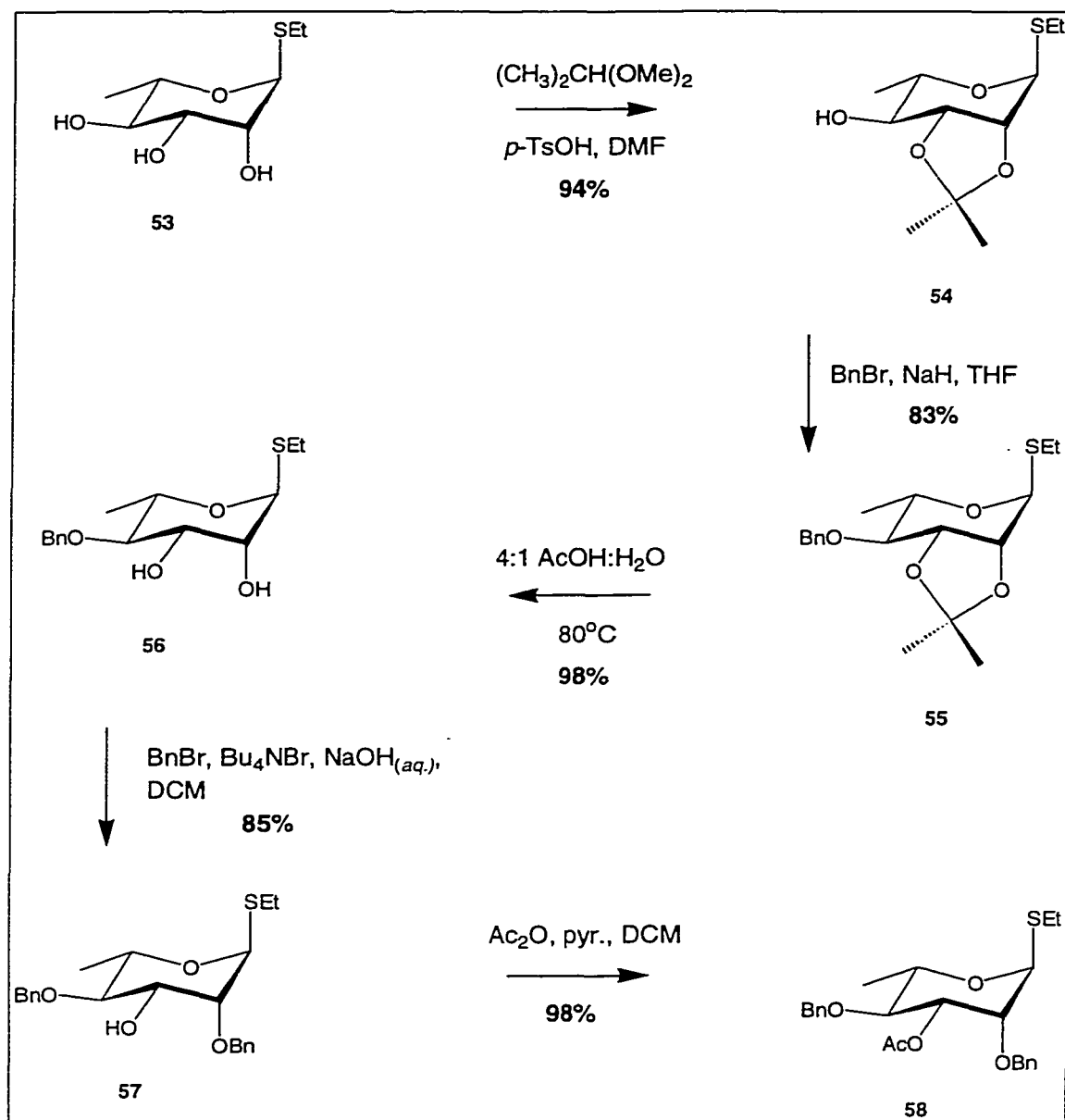
C) Synthesis of Ligands

I. Synthesis of Lactams (50) and (51)

a. Synthesis of the Rhamnose C ring of the Trisaccharide Structure

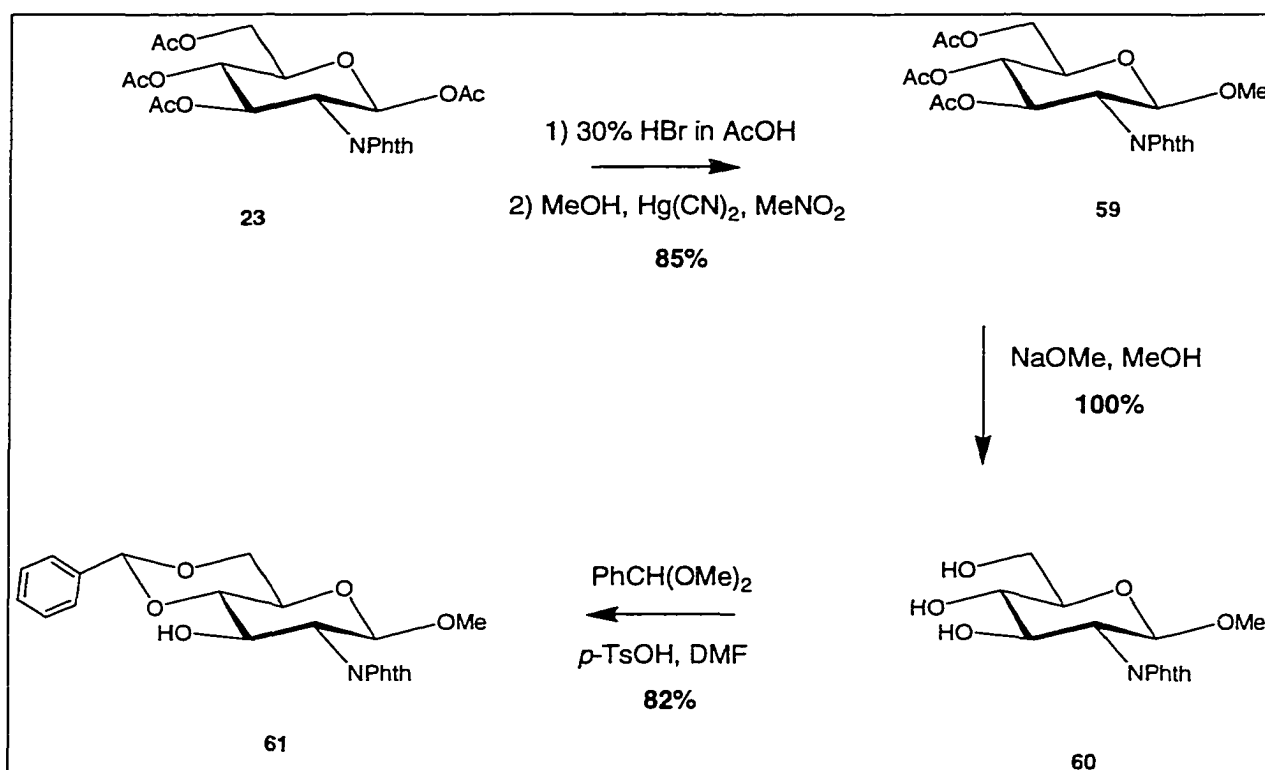
The rhamnose donor **58** has been reported in the literature and was synthesized in eight steps starting with the acetylation of L-rhamnose with acetic anhydride and pyridine in DCM (Figure 34).⁶⁶ The peracetylated compound was converted to a thioethyl glycoside through the addition of ethanethiol and boron trifluoride diethyl etherate in DCM. The remaining ester groups were removed with sodium methoxide in methanol to yield the triol **53**. The 2 and 3 positions were protected as an acetonide with 2,2-dimethoxy propane in DMF (**54**). The 4 position was protected as a benzyl ether through alkylation with benzyl bromide and sodium hydride in THF (**55**). The isopropylidene acetal was hydrolyzed with 4:1 acetic acid: water at 80 °C to obtain the partially protected sugar **56**. The dibenzyl ether-protected molecule **57** was obtained through alkylation with benzyl bromide under phase transfer conditions.⁶¹ Finally, the 3 position was temporarily protected as an acetate ester.

Figure 34: Synthesis of Rhamnose Donor (58)



b. Synthesis of the Glucosamine D ring of the Trisaccharide Structure

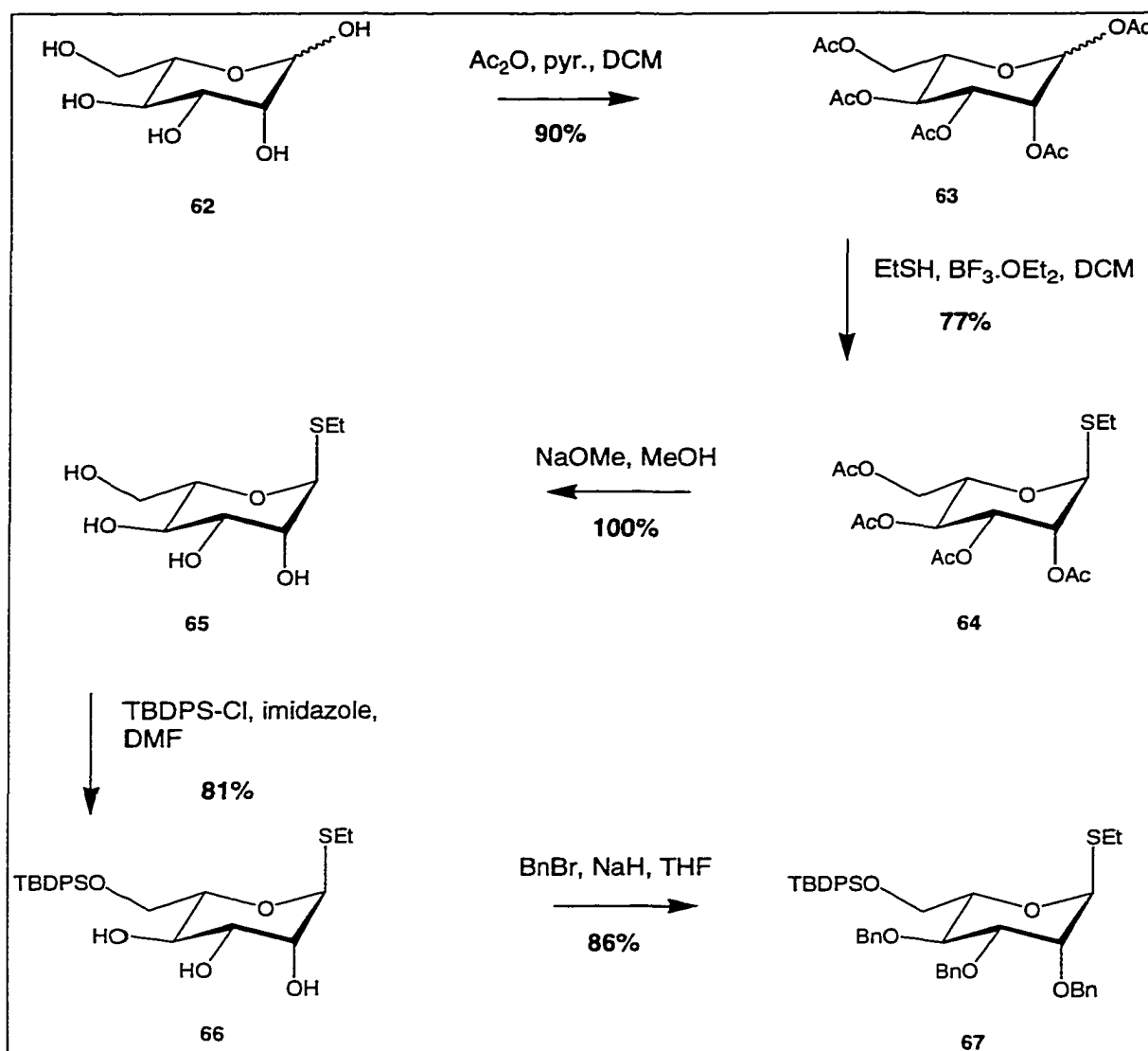
The glycosyl acceptor **61** was prepared in four steps from glucosamine by applying the same methodology that was used to make the partially-protected glucosamine residue **26** (Figure 35).⁷⁷

Figure 35: Synthesis of Glucosamine Acceptor (61)

c. Synthesis of the L-Mannose B ring of the Core Trisaccharide

The glycosyl donor **67** was prepared in five steps from L-mannose (Figure 36). A thioethyl anomeric protecting group was installed on the peracetylated L-mannose molecule **63** with ethanethiol and boron trifluoride diethyl etherate in DCM.⁹⁷ The acetate groups were removed from **64** using sodium methoxide in methanol to produce unprotected thioglycoside **65**. Attempts to selectively oxidize the 6 position of the unprotected sugar **65** were unsuccessful due to the insolubility of the sugar in the oxidation conditions.⁹⁸ Consequently, the oxidation only worked when the hydroxyl groups were protected. Therefore, the 6 position of this compound was selectively protected by a bulky silyl ether by stirring overnight with *t*-butylchlorodiphenylsilane and imidazole in DMF. The core trisaccharide was also made with a trityl group at the 6 position. It was not possible to remove the trityl group without the coincidental removal of the 4,6 benzylidene on the D ring during the assembly of the linked molecule.⁹⁹ The alcohol groups of **66** were benzylated with benzyl bromide and sodium hydride in THF to produce the fully protected L-mannose donor **67**. Benzyl ethers were chosen at this step because acyl protective groups such as benzoyl and acetyl groups could migrate during the selective removal of the silyl ether with TBAF.

Figure 36: Synthesis of L-Mannose Donor (67)



d. Assembly of the Trisaccharide Unit

The Rha-GlcNPhth glycosidic linkage was formed first in the assembly of the trisaccharide unit (Figure 37). The donor **58** and the acceptor **61** were stirred with

molecular sieves under argon overnight in DCM. Silver triflate and *N*-iodosuccinimide were then added and the disaccharide was obtained in excellent yield. The acetate on the 3 position of the rhamnose C ring was removed with sodium methoxide in methanol to yield the glycosyl acceptor **69**.

The L-Man-Rha glycosidic linkage was then installed between the donor **67** and acceptor **69** under the same conditions that were used in the penultimate step. Large quantities of the trisaccharide **70** could be synthesized because the yields of the reactions in all the synthesis schemes were very good. The large $^1J_{\text{CH}}$ coupling constants of 167.3 and 171.1 Hz at the anomeric centres for the newly – formed glycosidic linkages in **68** and **70**, respectively, confirmed the correct α anomeric configuration.

e. Partial Deprotection of the Core Trisaccharide

Ethylene diamine was stirred with the trisaccharide **70** in *n*-butanol at 115°C to produce the free amine **71** (Figure 38). After purification, tetrabutylammonium fluoride was added to the partially deprotected trisaccharide **71** in THF to remove the silyl ether protective group from the L-mannose B ring.¹⁰⁰ The product **72** was formed in good yield under these conditions. Attempts to remove the silyl ether group in the presence of the phthalimido group were unsuccessful due to the sensitivity of the amine protective group to tetrabutylammonium fluoride.

Figure 37: Assembly of the Core Trisaccharide

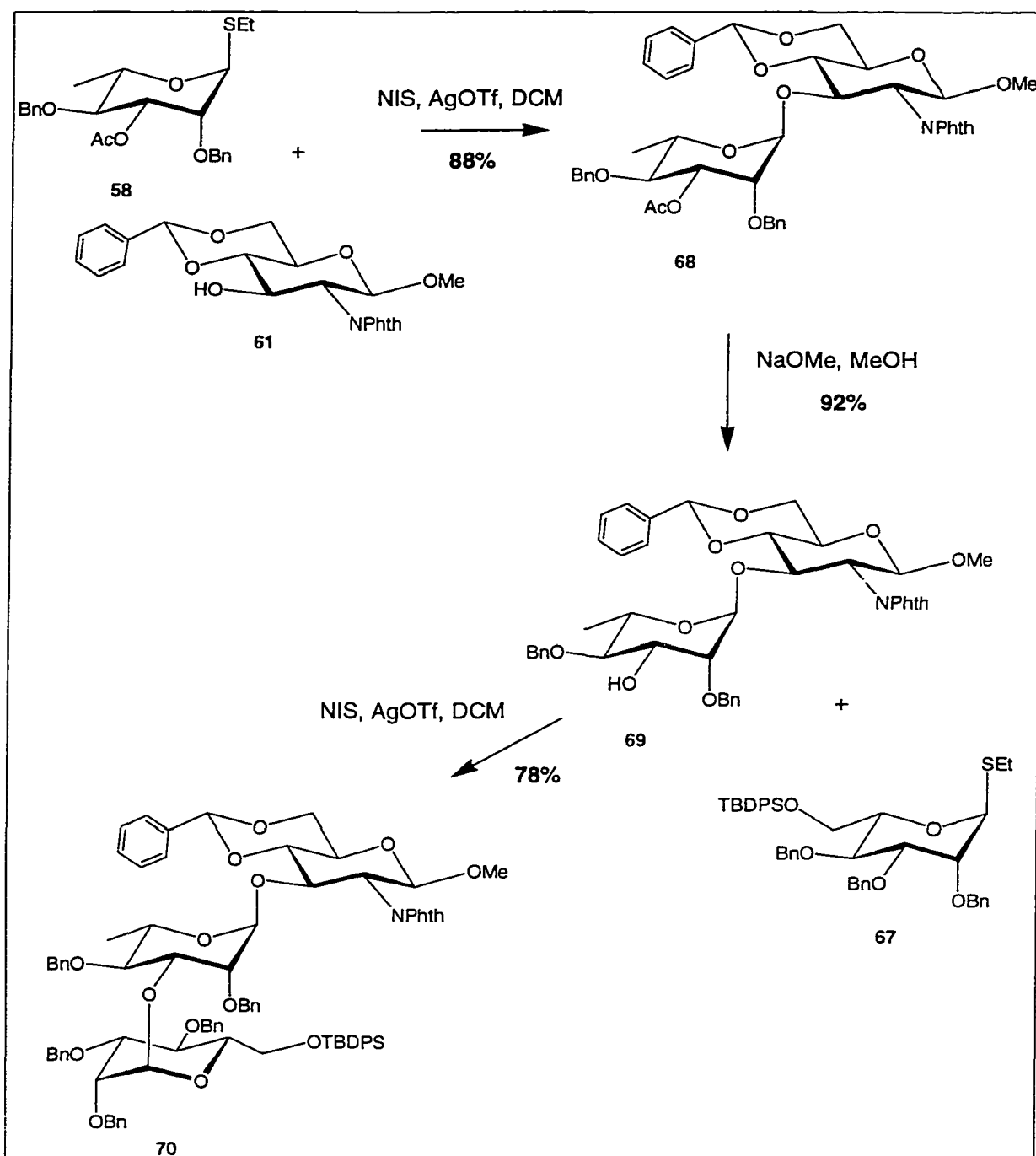
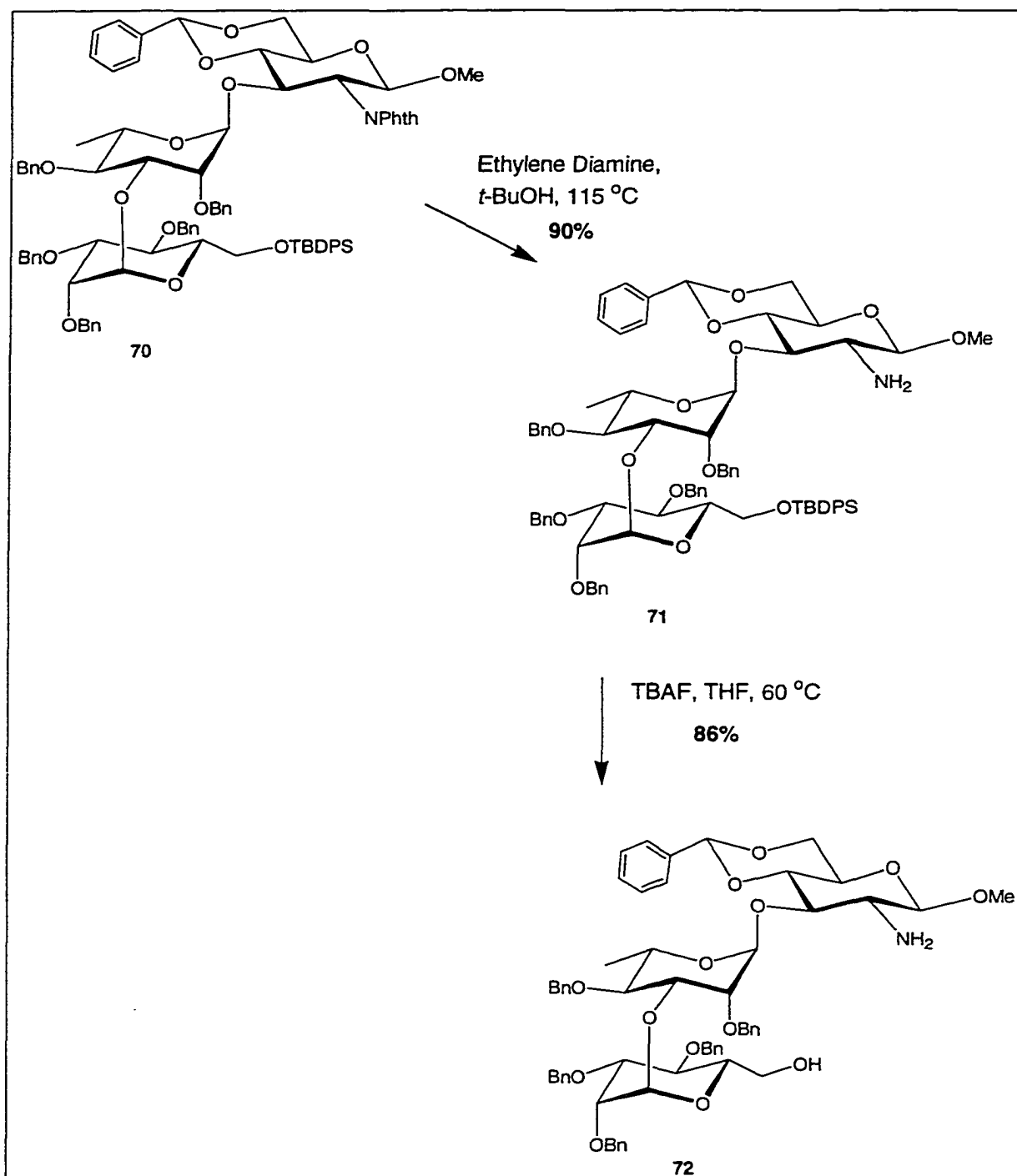


Figure 38: Partial Deprotection of the Core Trisaccharide

f. Synthesis and Deprotection of the Lactam (50)

To attach the glycine linker to the trisaccharide **72**, coupling reagents TBTU and HOBt were added to *N*- α -Fmoc-glycine and **72** along with *N*-ethylmorpholine in DMF (Figure 39).¹⁰¹ These coupling reagents were chosen because they have been shown in the literature to produce amide and peptide linkages in very high yields. In this example, the amide **73** was formed in excellent yield.

Oxidants TEMPO and sodium hypochlorite were added to the free alcohol **73** to oxidize the 6 position to a carboxylic acid under phase transfer conditions.¹⁰² The Fmoc protecting group was then removed from the linker with 20% piperidine in DMF. Coupling reagents TBTU and HOBt along with *N*-ethylmorpholine were added to this material in DMF to produce the lactam **75** in good yield (Figure 40). The lactam **75** was stirred with palladium hydroxide in wet methanol under a hydrogen atmosphere to remove all the protecting groups and yield the final compound **50**.

Figure 39: Synthesis of the Carboxylic Acid (74)

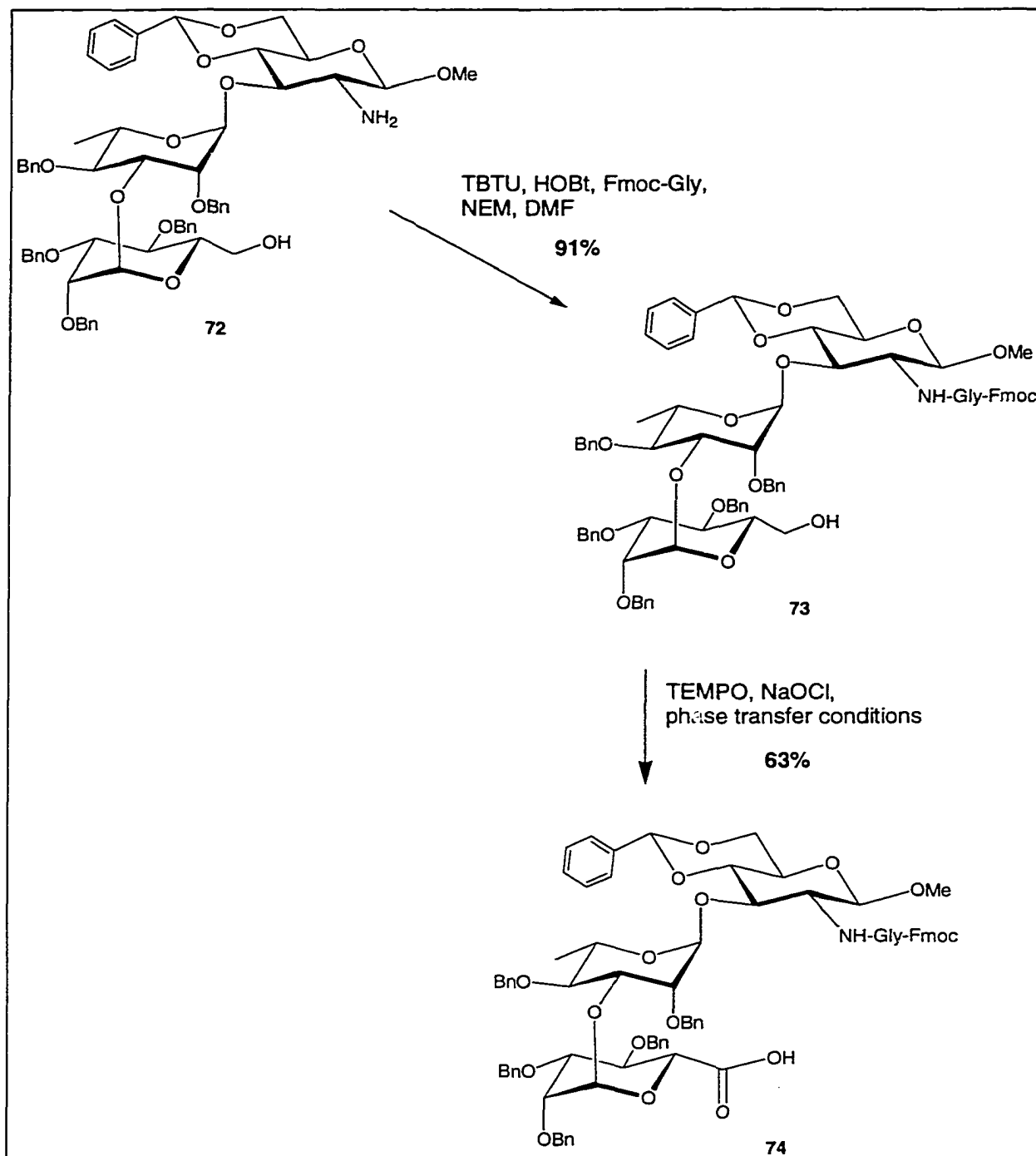
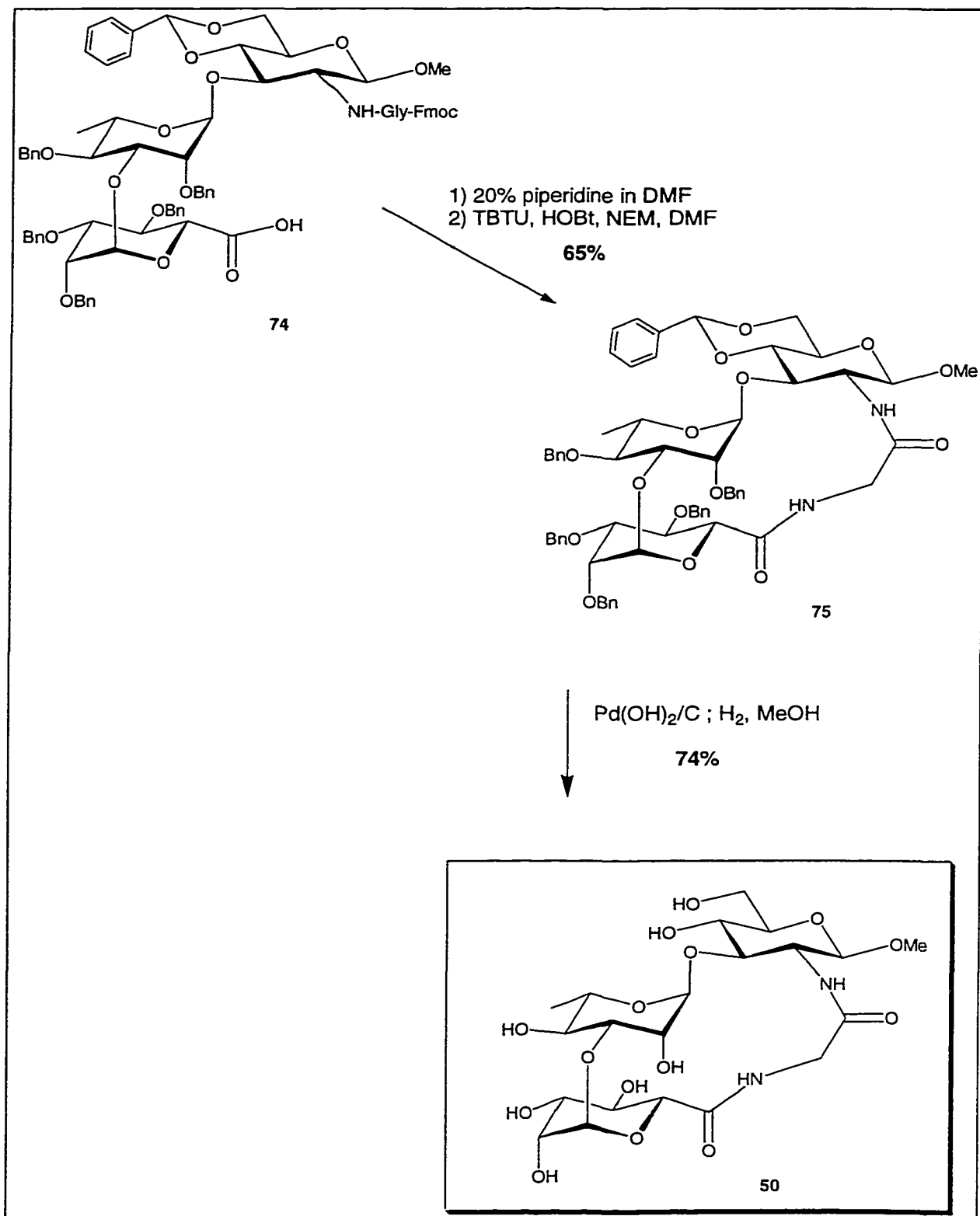


Figure 40: Synthesis and Deprotection of the Lactam (50)



g. Synthesis and Deprotection of the Lactam (51)

The methodology in the synthesis of the lactam **50** with a glycine-spaced linker was followed to synthesize the lactam **51** that possessed a β -alanine-spaced linker (Figures 41 and 42).

For this lactam, a β -alanine spacer was used to link the two anchoring positions. The same coupling reagents, TBTU and HOBt, were used to attach the linker (**76**). The 6 position of the L-mannose B ring was oxidized with TEMPO and sodium hypochlorite (**77**). The Fmoc group was removed with piperidine and TBTU and HOBt were used to form the macrocycle **78**. Removal of the protecting groups under hydrogenation conditions with palladium hydroxide produced the lactam **51**.

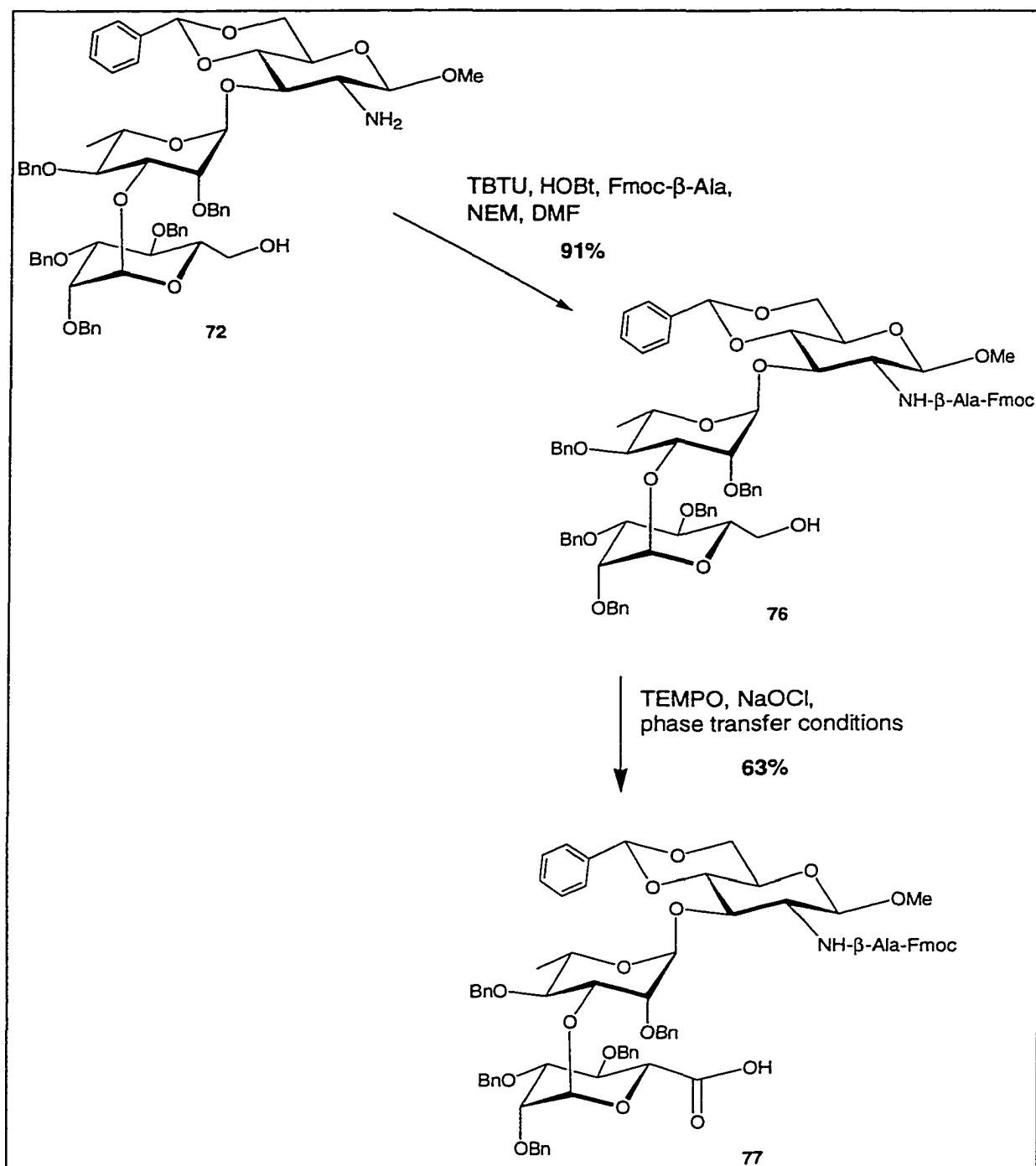
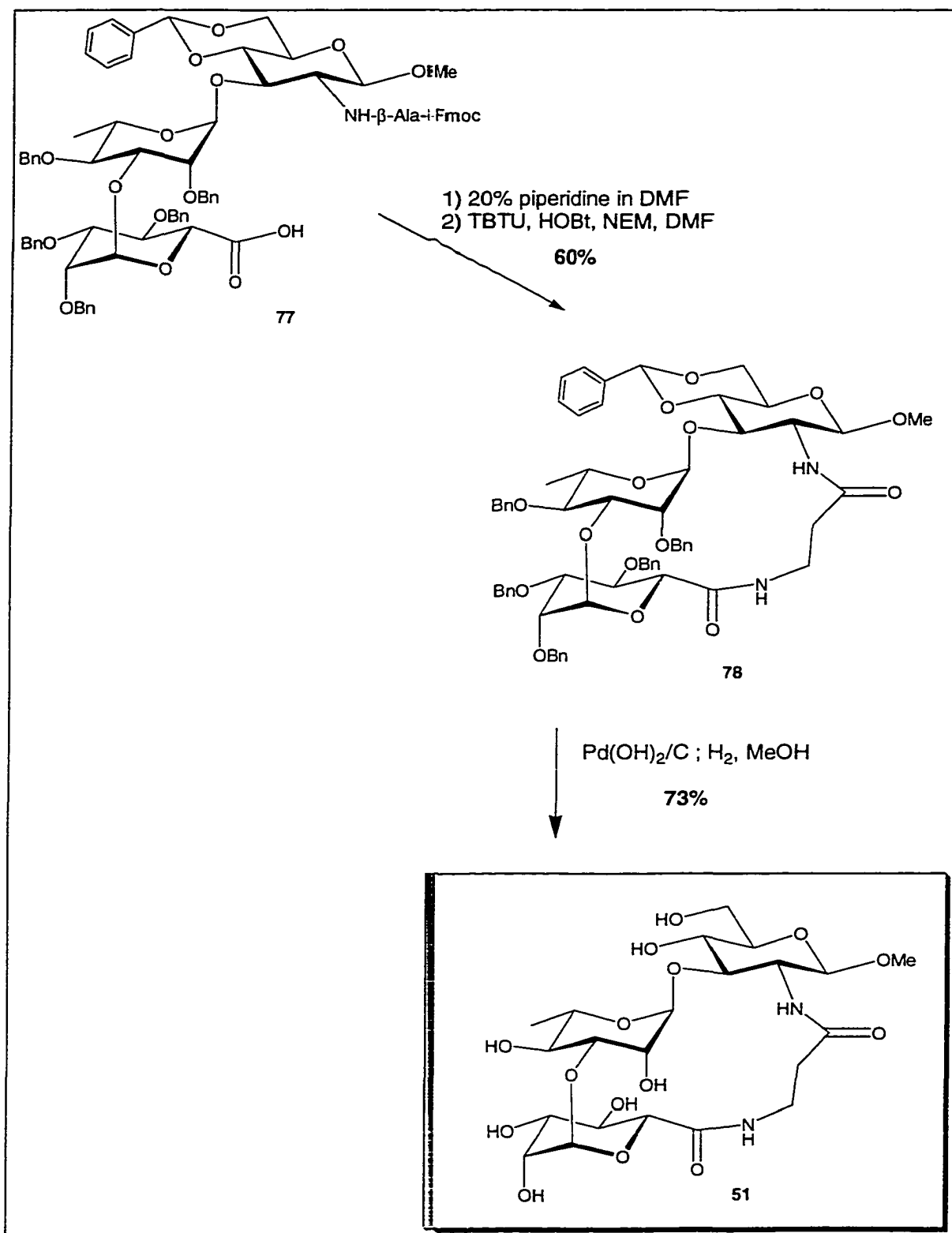
Figure 41: Synthesis of the Carboxylic Acid (77)

Figure 42: Synthesis and Deprotection of the Lactam (51)



II. Synthesis of Cyclic Carbamate (52)

To attach the β -alanine linker to the trisaccharide **72**, coupling reagents TBTU and HOBt were added to *N*- β -*t*-Boc- β -alanine and **72** along with *N*-ethylmorpholine in DMF (Figure 43). To enable the macrocyclization to occur, *p*-nitrophenyl chloroformate was added to the alcohol **79** and heated in pyridine at 100°C overnight to produce the carbonate **80**. Trifluoroacetic acid was added dropwise into a solution of the carbonate **80** in DCM to remove the benzylidene acetal and *t*-Boc protecting groups (Figure 44). When thin layer chromatography indicated that the reaction was complete, triethylamine was added to neutralize the solution. The cyclic carbamate **81** was formed after the solution was neutralized. The carbamate **81** was stirred with palladium hydroxide in wet methanol under a hydrogen atmosphere to remove all the protecting groups and yield the target compound **52**.

Figure 43: Synthesis of the Carbonate (80)

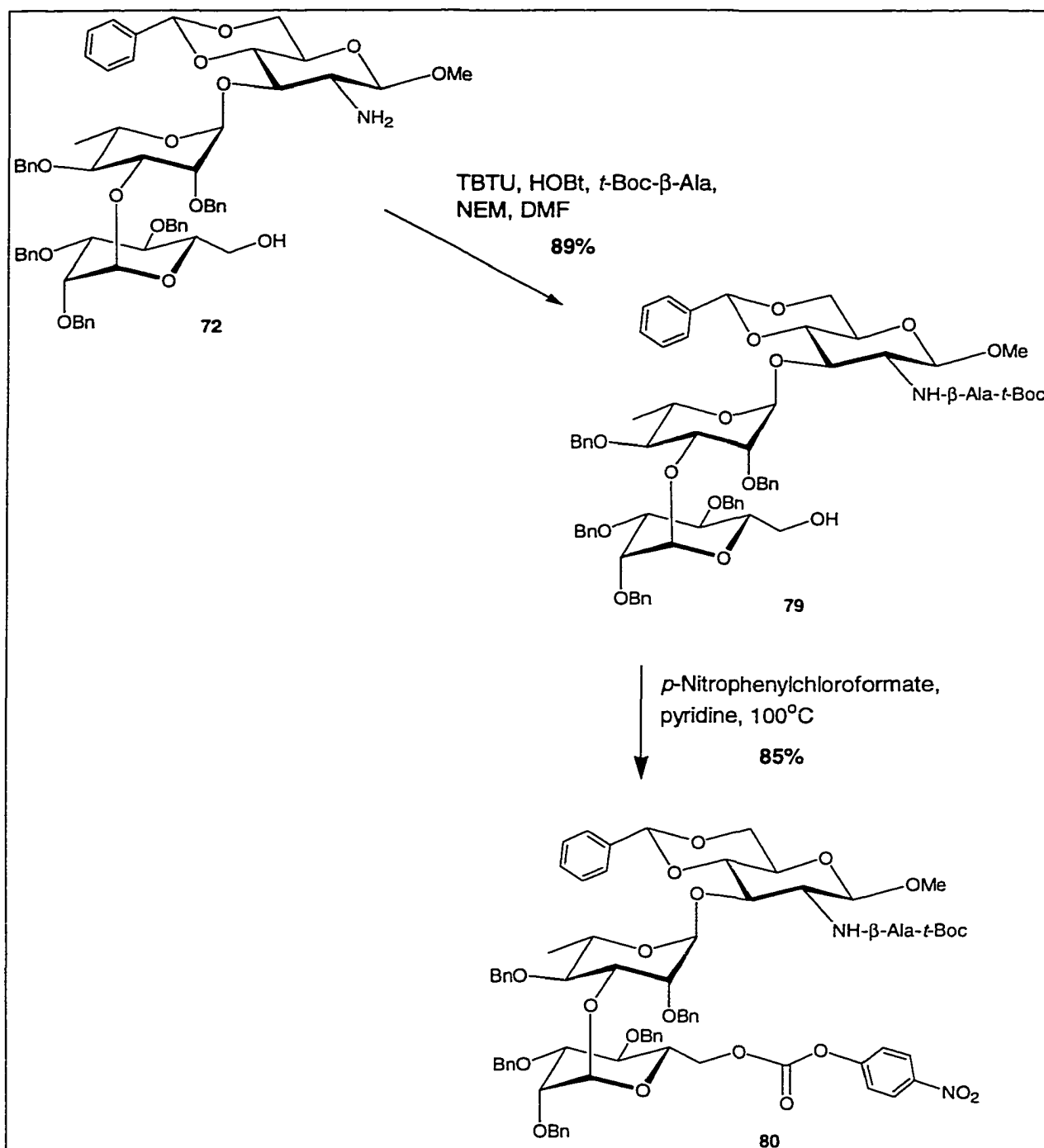
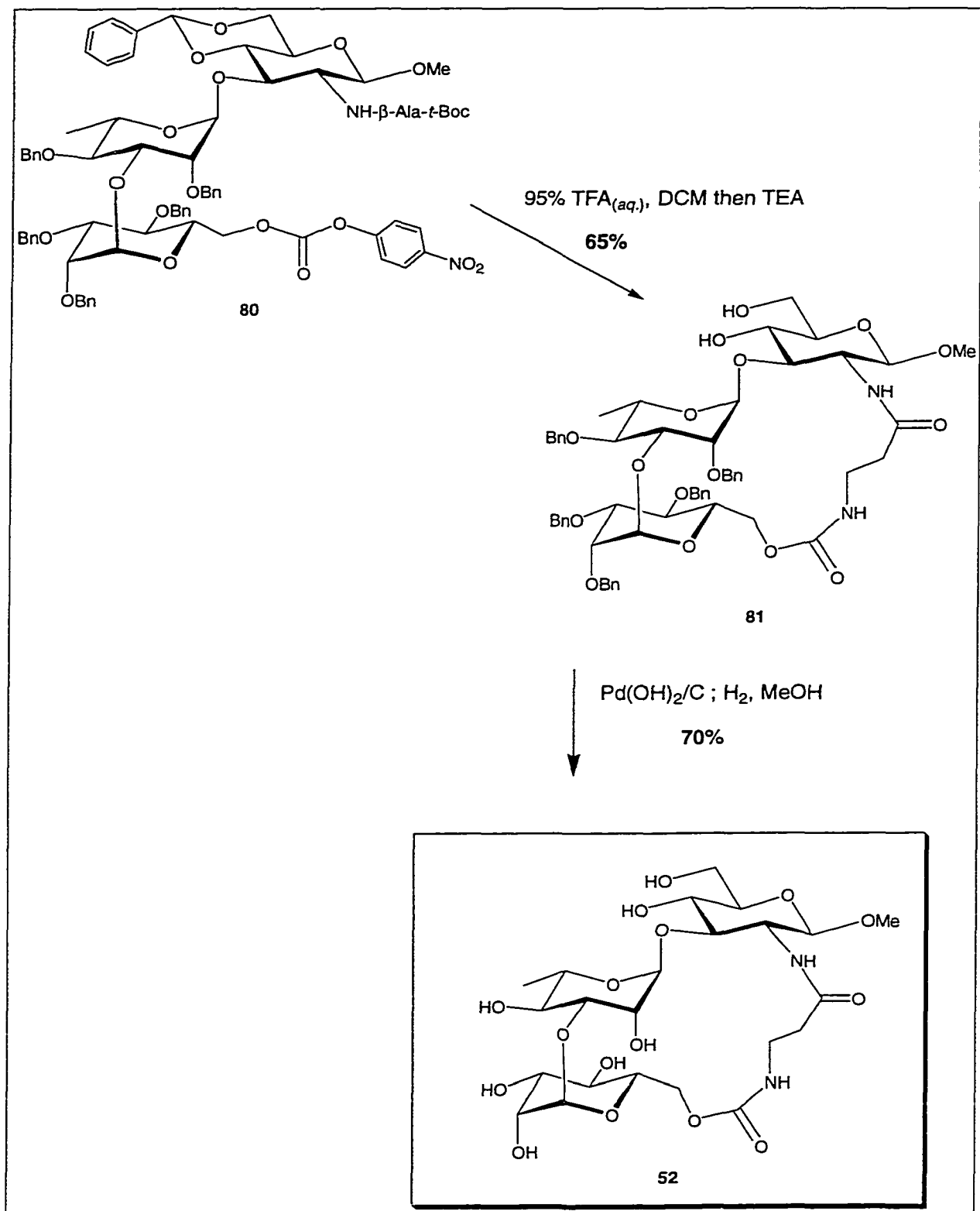


Figure 44: Synthesis and Deprotection of the Cyclic Carbamate (52)

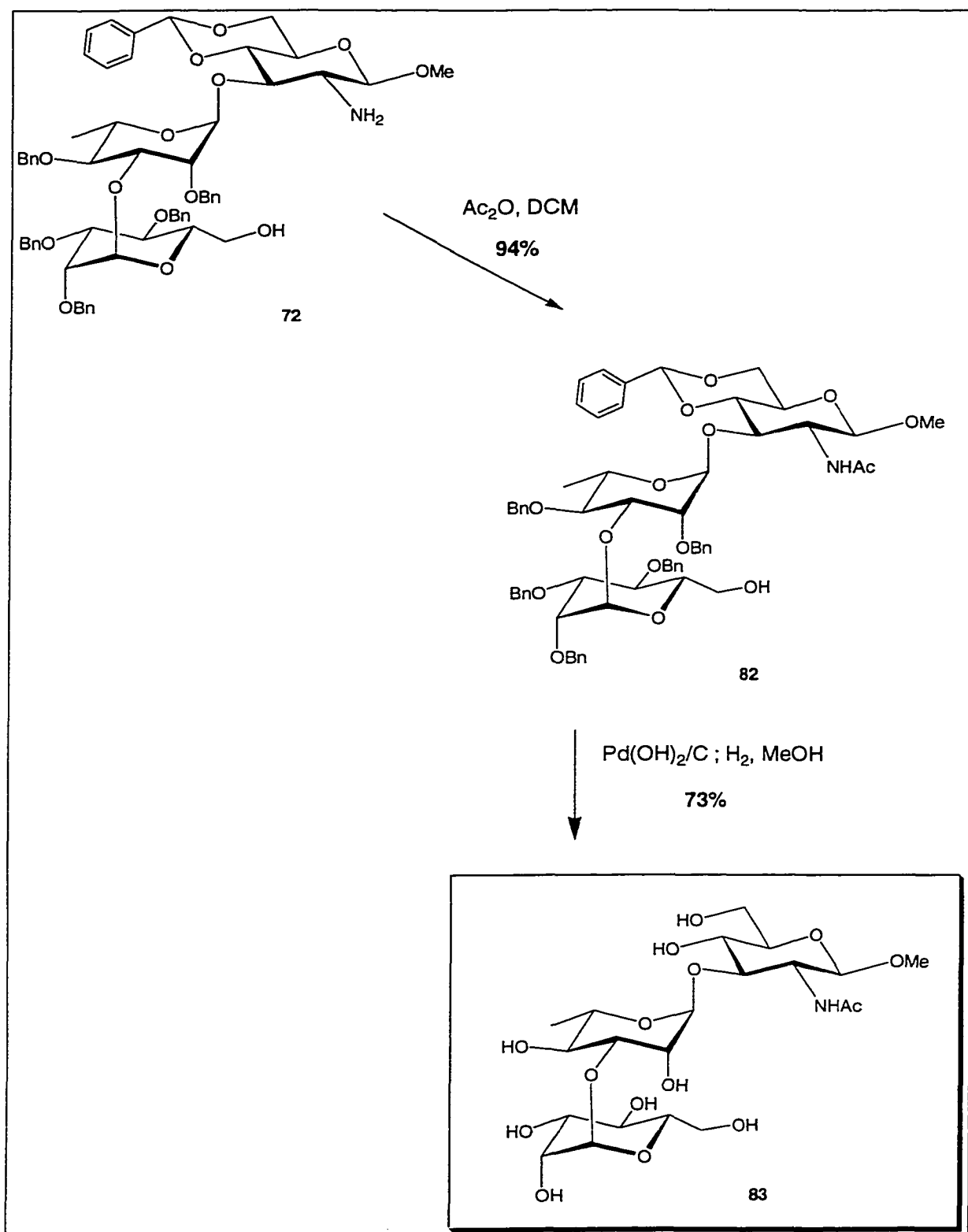
III. Synthesis of the Native Trisaccharide Comparison Ligand

(83)

A modified native trisaccharide was synthesized to compare the binding affinities determined from solid phase assays of the cyclic structures against the acyclic trisaccharide. This trisaccharide has a hydroxyl group at the 6 position of the L-mannose B ring.

a. Preparation of the Native Trisaccharide Mimic

Acetic anhydride was added to the partially protected trisaccharide **72** in DMF (Figure 45). The trisaccharide **82** was stirred with palladium hydroxide in wet methanol under a hydrogen atmosphere to remove all the protecting groups and yield the modified native trisaccharide **83**.

Fig 45: Synthesis and Deprotection of the Trisaccharide (83)

Chapter 4

Evaluation of the Biological Activities of the Synthetic Ligands

Solid phase binding assays of all the synthetic ligands were performed to establish the quantitative activity of the synthetic ligands. Solution phase titration microcalorimetry was employed to measure the thermodynamics of binding for the best ligand, 51.

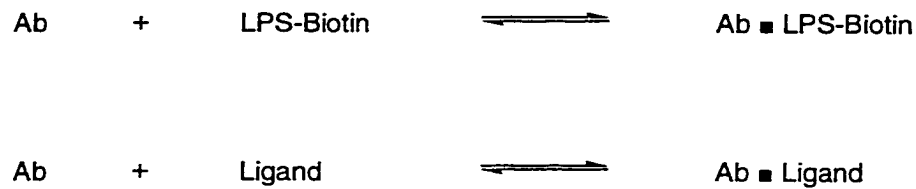
A) Solid Phase Binding Assay

A competitive enzyme linked immunosorbent assay (ELISA), developed by Bundle and co-workers, was used to evaluate the binding affinity of the synthetic ligands (Figure 46).¹⁰³ Purified SYA/J6 antibody obtained from the hybridoma technique was non-covalently adsorbed to an ELISA plate. A biotinylated lipopolysaccharide (LPS) antigen provided the signal. For this inhibition assay, variable concentrations of the synthetic ligands along with a static concentration of a biotinylated LPS solution were added to the plate and equilibrium was established over an 18 h incubation time. After removing excess reagents, a horseradish

peroxidase/streptavidin complex was added which binds strongly to the biotin moiety that is present on the bound LPS antigen. A solution of 3,3',5,5'-tetramethylbenzidine (TMB) was then added and the solution turned a blue colour due to the oxidation of TMB with horseradish peroxidase. Addition of phosphoric acid quenches the reaction and produces a stable, yellow colour.

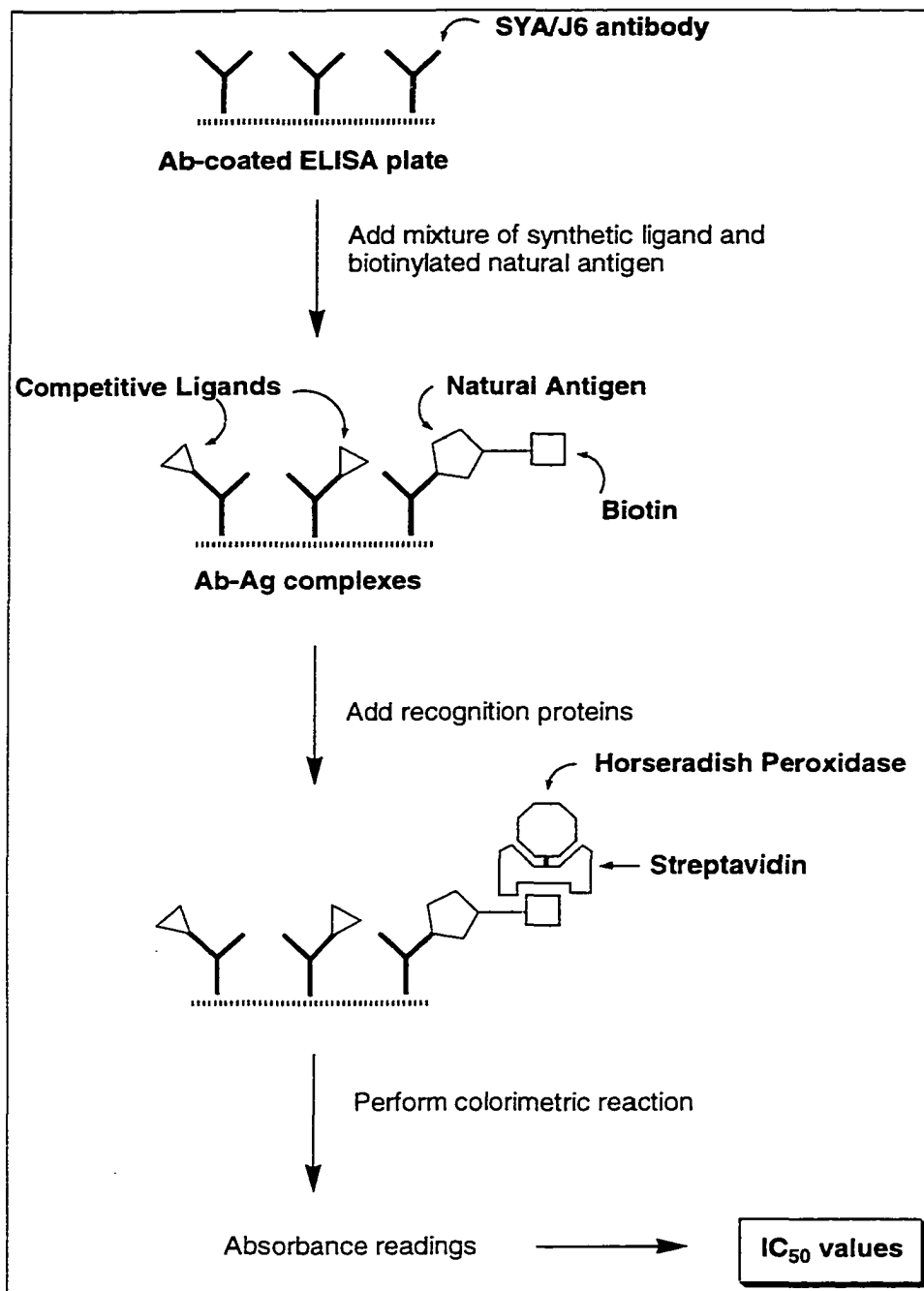
This colour is proportional to the amount of LPS-biotin complex bound to antibody on the ELISA plate. Therefore, if a synthetic ligand at a particular concentration binds strongly to the antibody, it will displace the biotinylated natural substrate and result in a low absorbance reading due to the absence of the biotin group. The plate can then be read with a spectrophotometer set at 450 nm and a plot of inhibition *versus* the \log_{10} of ligand concentration can be constructed. To determine the amount of inhibition by the ligand, the absorbance of the complex is subtracted from the absorbance of wells developed in the absence of inhibitor and converted to a percentage.

For this assay, the binding constant is represented as the concentration at 50% of the total inhibition of the LPS natural substrate by the synthetic ligand with the antibody (IC_{50} value). As a result, the smaller the IC_{50} value, the stronger the binding between the antibody and the synthetic ligand. It should be noted that the IC_{50} values that are obtained in these assays are only rough estimates of the dissociation constant.³⁹ The dissociation constants for tight binding ligands are underestimated in this assay because there are two equilibria that govern the associations – the binding of the natural substrate and the binding of the synthetic ligand to the protein.



In order to perform the assay and obtain a reasonable dynamic range in terms of the absorbance for zero inhibition, it is necessary to ensure an appropriate concentration of Ab.LPS-Biotin complex. However this removes a given concentration of antibody from the ligand-antibody equilibrium. Tight binding ligands will bind nearly the entire antibody that is present on the plate. Therefore, if the first equilibrium consumes more than 10% of the total antibody, the error between the IC_{50} and true K_D value can become large and will always underestimate the K_D of the inhibition. In the current project, the IC_{50} values were initially used to indicate the biological activities of the synthetic ligands. Because the error in the IC_{50} values is the same for all test ligands in this system, the underestimation of the K_D values is not an issue in the determination of the binding activities of the synthetic analogs.

**Figure 46: ELISA Protocol for the Evaluation
Of the Binding Affinity of the Synthetic Ligands**



a. IC_{50} Values for Synthetic Disaccharides (4), (5), and (6)

A plot of % inhibition *versus* concentration using the above ELISA protocol is shown in Figure 47 for 4, 5, and 6. The inhibition data is also shown for the native trisaccharide 3 and the native disaccharide 49.

Figure 47: Competitive Inhibition Data For (4), (5), and (6)

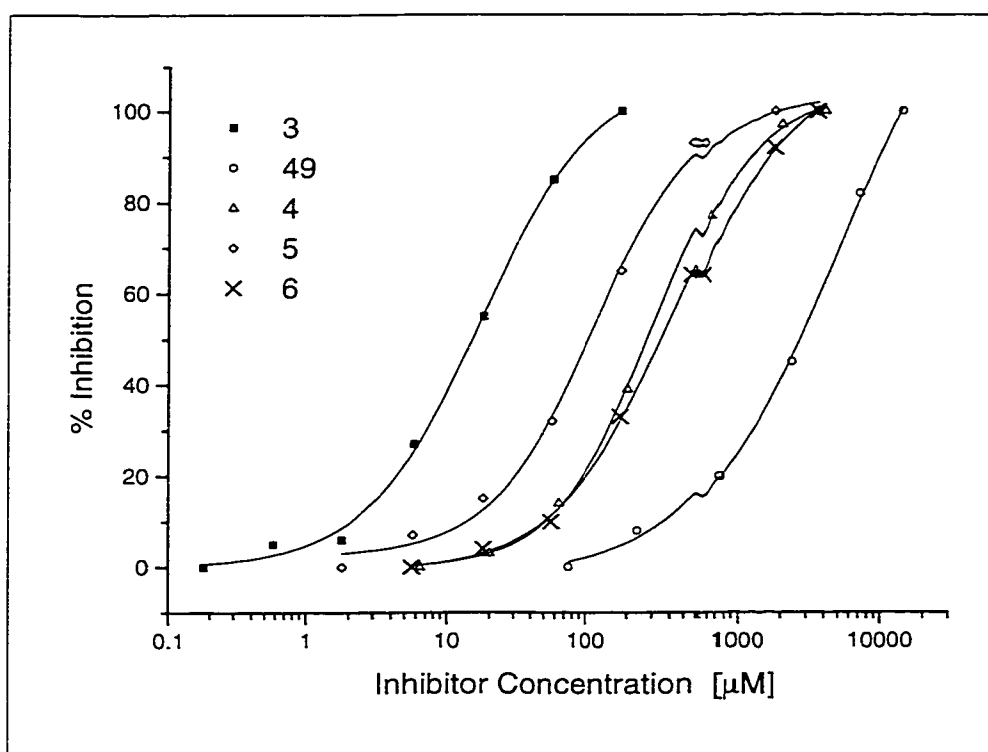
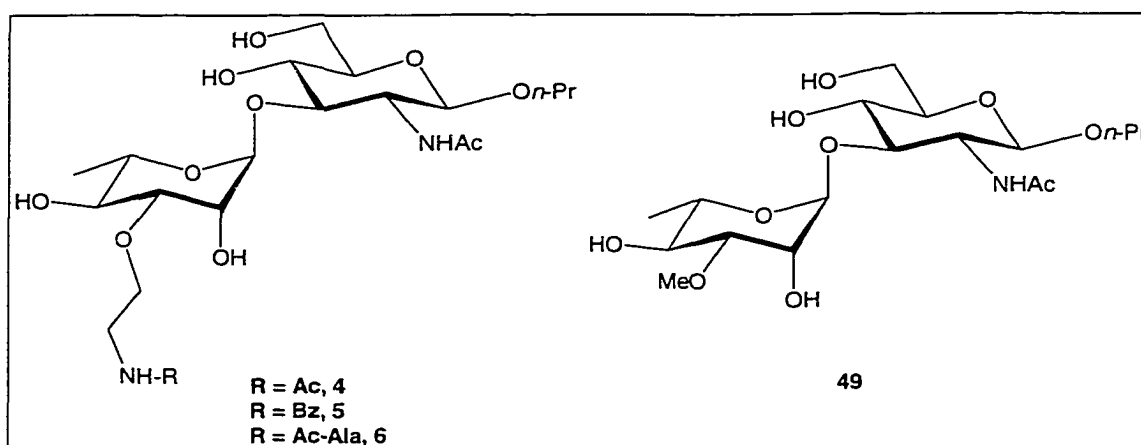


Table 3. IC₅₀ Values for (4), (5), and (6)

Ligand	IC ₅₀ (μM)
Rha-Rha-GlcNAc-OMe 3	17
49	4800
4	288
5	114
6	396

Figure 48: Test Compounds (4), (5), and (6)



All of the novel ligands had smaller IC₅₀ values than the native disaccharide inferring that they were all tighter binding ligands than the native disaccharide. However, none of the synthetic ligands were tighter binders than the native trisaccharide and only 5 was within the same order of magnitude. The data suggest

that tight-binding, low molecular weight ligands would have to be obtained from ligands at the trisaccharide level. Investigations into the source of enhancement over the native disaccharide either by crystallography or calorimetry were not undertaken because the low binding constants of the ligands would cause experimental problems and unreliable results. Computer-based predictions would also be suspect because of the inherent flexibility of the linker arm.

b. IC₅₀ Values for Synthetic Disaccharides (7), (8), (9), and (10)

A plot of % inhibition *versus* concentration using the above ELISA protocol is shown in Figure 49 for 7, 8, 9, and 10. As before, the inhibition data is shown for the native trisaccharide 3.

The estimated IC₅₀ values are given in Table 4 for 7, 8, 9, and 10. The IC₅₀ values are only estimated because none of the inhibitors were concentrated enough to quantitatively inhibit the natural substrate due to the lack of material available for testing. Because the curves did not have upper limits, accurate IC₅₀ values cannot be calculated.

Figure 49: Competitive Inhibition Data For (7), (8), (9), and (10)

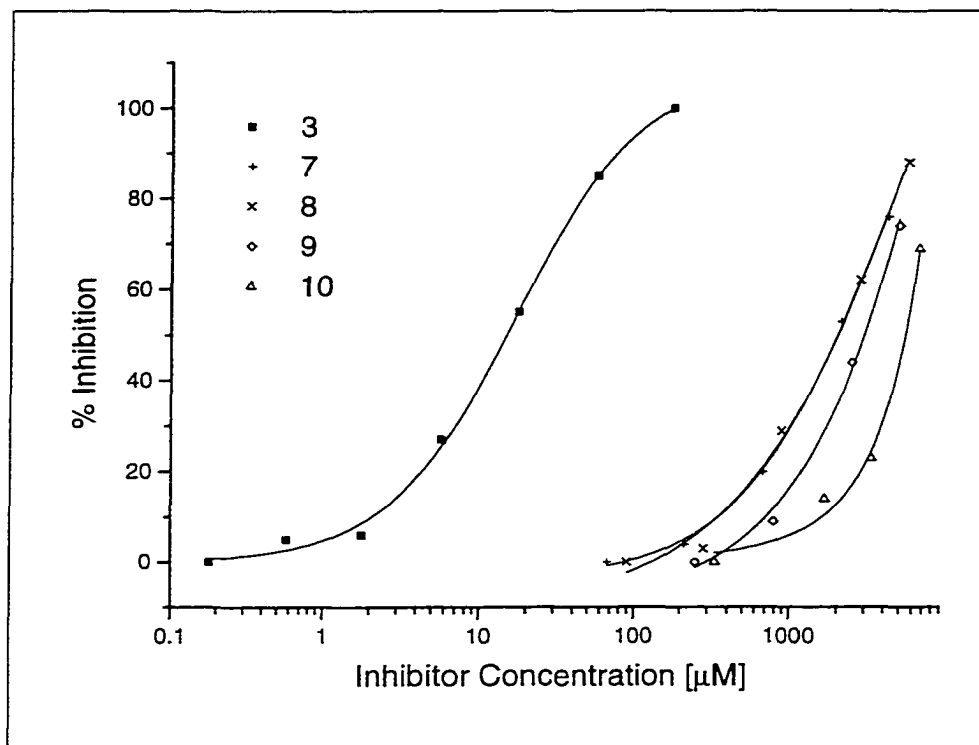
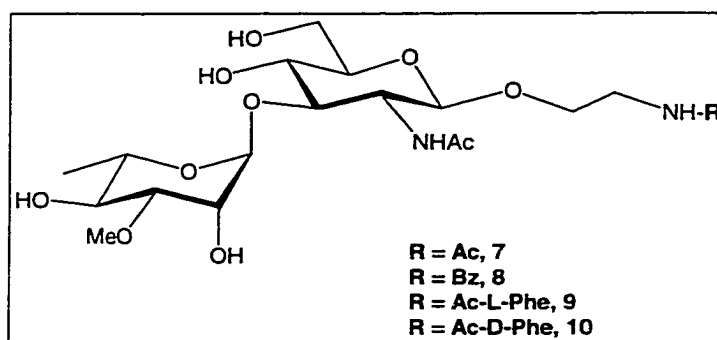


Table 4. Estimated IC_{50} Values for (7), (8), (9), and (10)

Ligand	IC_{50} (μ M)
Rha-Rha-GlcNac-OMe (3)	17
49	4800
7	2300
8	3000
9	3000
10	>5000

Figure 50: Test Compounds (7), (8), (9), and (10)

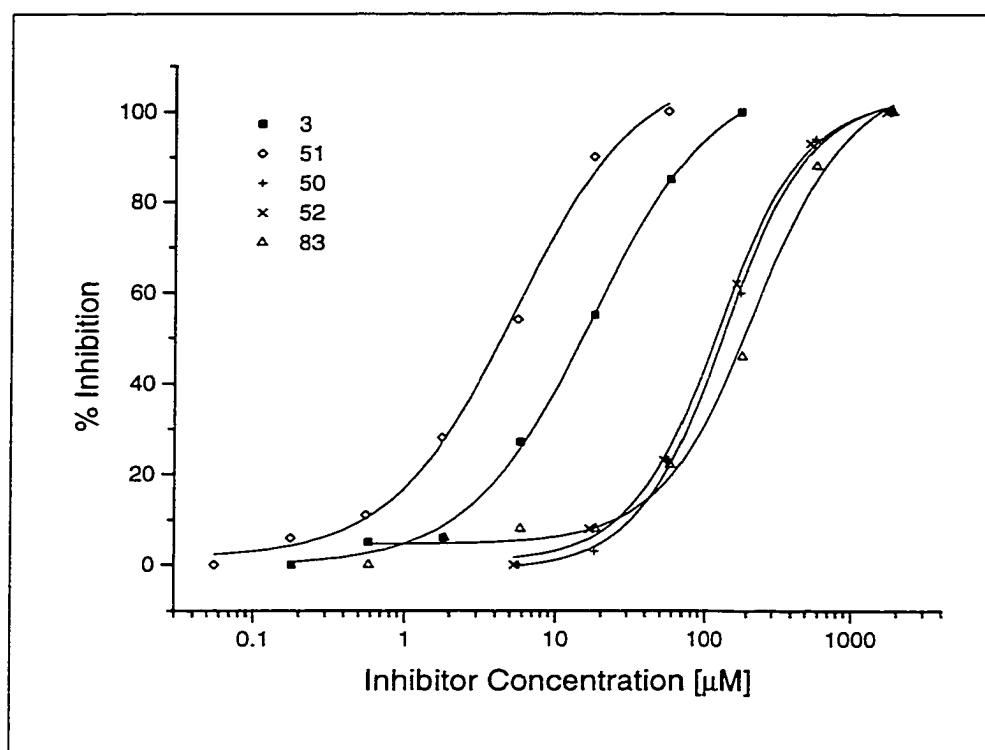


Despite the lack of accurate IC_{50} values, none of the inhibitors **7** to **10** appear to inhibit the natural substrate better than the native disaccharide **49** within experimental error. No improvement in binding affinity between the antibody and its antigen was achieved with this design strategy.

c. Inhibition Constants for Constrained Trisaccharides (50), (51), and (52)

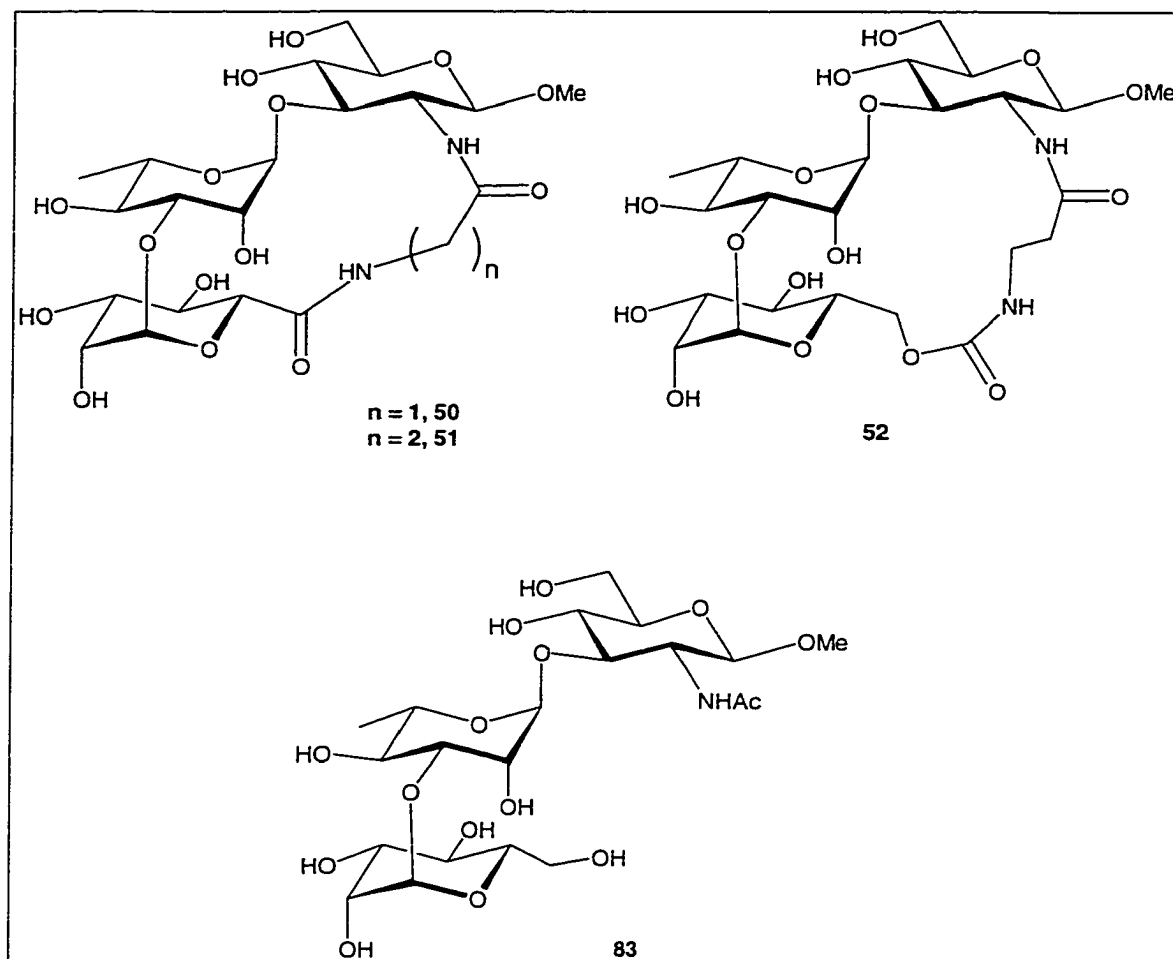
A plot of % inhibition *versus* concentration using the same ELISA protocol that was described before is shown in Figure 51 for the constrained ligands **50**, **51**, and **52**, the native trisaccharide **3**, and the modified native trisaccharide **83**.

Figure 51: Competitive Inhibition Data for (50), (51), (52) and (83)

Table 5: IC₅₀ Values for (50), (51), (52), and (83)

Ligand	IC ₅₀ (μM)
Rha-Rha-GlcNac-OMe (3)	17
51	5
50	137
52	125
83	227

Figure 52: Test Compounds (50), (51), (52), and (83)



Two of the tethered compounds, 50 and 52 had IC_{50} values that were higher than the native trisaccharide which suggest that the design strategy of these tethered compounds did not strengthen the sugar-protein binding event. The third ligand, 51, had a lower IC_{50} value than the native structure implying that this ligand design has improved the binding of the oligosaccharide to its receptor. The high IC_{50} value of the modified acyclic trisaccharide 83 verifies the previous data of Bundle that

showed the adverse effect of the $\text{CH}_3 \rightarrow \text{CH}_2\text{OH}$ substitution on the rhamnose B ring. To investigate the factors that contributed to the binding enhancement, microcalorimetry data was obtained for this compound and is presented in the next section.

B) Micro-Calorimetry Data for the Tightest-Binding Ligand, (51)

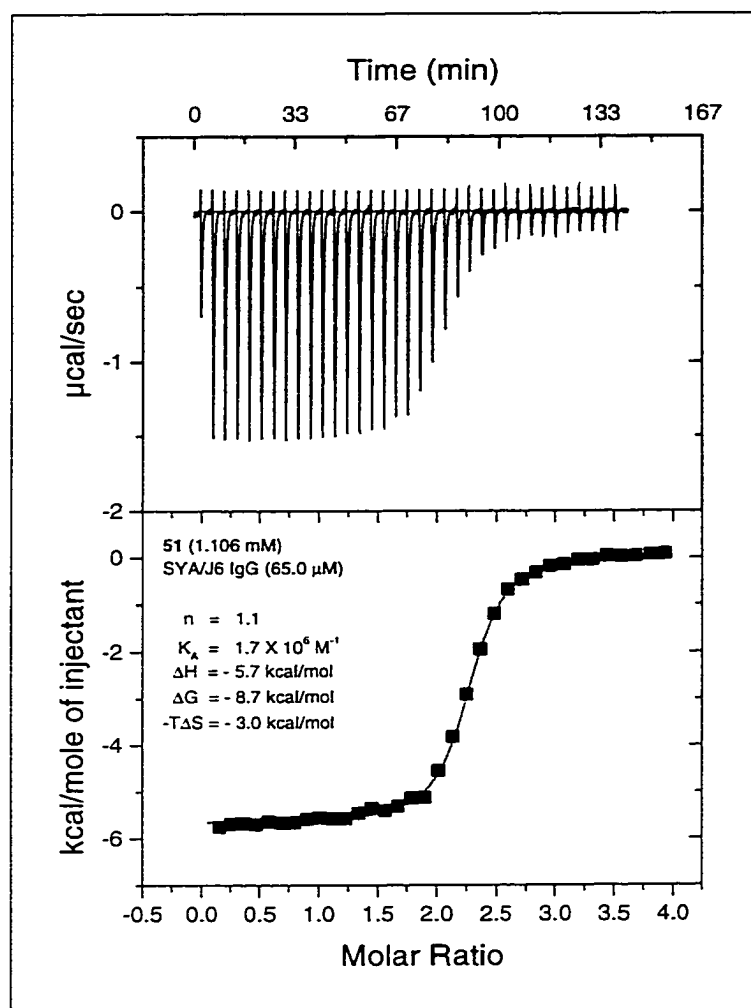
a. Microcalorimetry Data for (3) and (51)

Microcalorimetry studies were performed to determine the thermodynamic parameters associated with the binding event that took place between the SYA/J6 and the tethered trisaccharide, 51. The procedure described in the literature by Bundle and co-workers was followed.⁴⁰ A sample of the purified antibody of known concentration in buffer was placed in one of two cells of a MicroCal™ calorimeter.¹⁰⁴ The buffer present in the second reference cell is heated or cooled to maintain a constant small temperature difference between the two cells. The required electric current to do this represents the energy liberated or consumed as the ligand is titrated into the antibody solution.

Integration of the peaks that resulted from the injections gave the total enthalpy of the association whereas the saturation of the binding site furnished a binding curve. Figure 53 shows the calorimetry data for the synthetic ligand 51. The top graph is a plot of heat *versus* time that was obtained during the titration and the

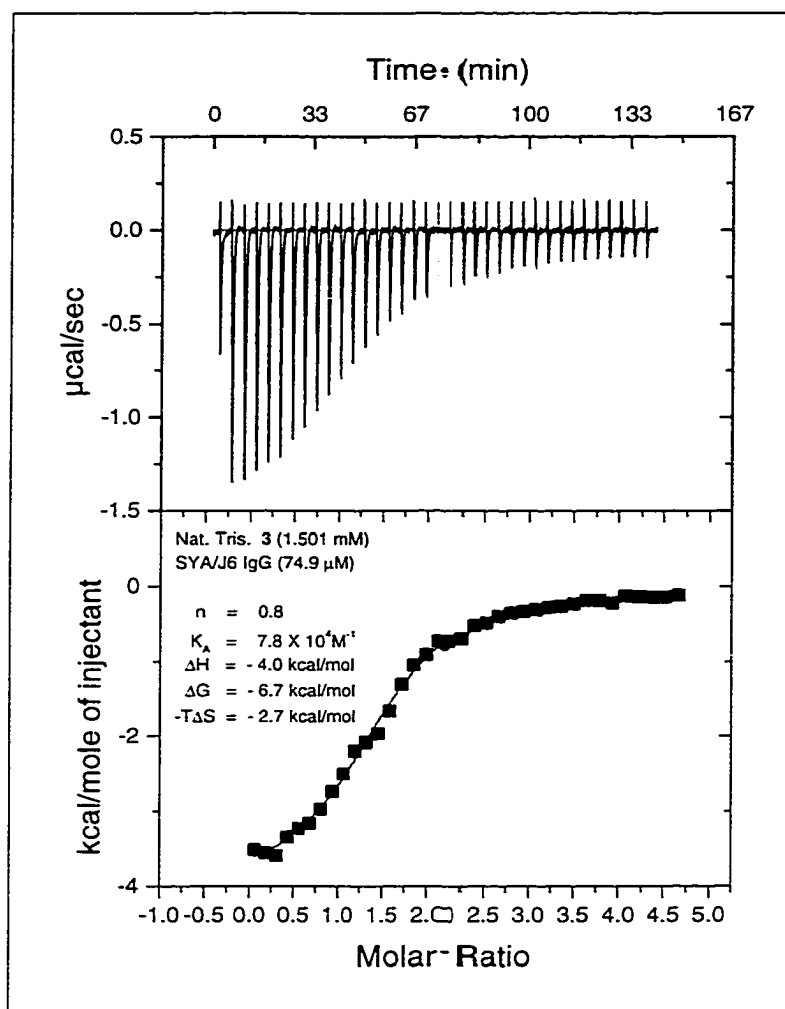
bottom graph is plot of enthalpy *versus* the ratio of sugar to protein based on the integrated raw data. This is the binding curve that was computed based on the raw heat data.

Once the binding curve was obtained for the association process, the thermodynamic parameters, K_A , ΔH , ΔG , $-T\Delta S$, and the stoichiometry of binding, n , were calculated.¹⁰⁵ The ΔH , K_A , and n values were calculated by a nonlinear least-squares fit to an equation that involved cell and concentration dimensions. The free energy of binding was calculated using the equation $\Delta G = -RT\ln K_A$ ($R = 1.98$ cal/mol•K, $T = 303$ K) and the $-T\Delta S$ term was calculated from the equation $\Delta G = \Delta H - T\Delta S$. A value of n of close to unity indicated that the concentrations of protein and ligand were optimal in the experiment.

Figure 53: Calorimetry Data for the Tethered Trisaccharide (51)

The binding curve for the native trisaccharide 3 was also obtained using the same methodology to calculate comparison numbers. Figure 54 shows the raw and integrated calorimetry data for the native trisaccharide.

Figure 54: Calorimetry Data for the Native Trisaccharide (3)



The values that were obtained with this data were slightly different from literature values (Table 6). The stoichiometry of binding, n , was less than one, which indicates less than optimal concentrations of protein and ligand were used in the experiment.

b. Interpretation and Comparison of Results

Table 6 shows the calculated thermodynamic values from the two calorimetric experiments as well as literature values for the native trisaccharide **3**.⁴⁸

Table 6: Calorimetry Results and Literature Values

Ligand	K_A (M^{-1})	ΔG (kcal/mol)	ΔH (kcal/mol)	$-T\Delta S$ (kcal/mol)
Rha-Rha-GlcNAc-OMe (3) (lit.)	9×10^4	-6.8	-4.3	-2.5
Rha-Rha-GlcNAc-OMe (3) (exp.)	8×10^4	-6.7	-4.0	-2.7
51	2×10^6	-8.7	-5.7	-3.0

The data indicate that the tethered compound **51** had a binding constant that was 20 times higher than the native trisaccharide which in turn meant the free energy of the system was increased by about 2 kcal/mol. Whereas the objective of the ligand design was partially met because the entropy term of the system was improved by about 0.5 kcal/mol, the major source of the higher binding constant was an increase of binding enthalpy of about 1.5 kcal/mol. The sources of improvements in the enthalpy and entropy terms are suggested and explained by computational and NMR studies that are presented in the next chapter.

Chapter 5

A Comparison of the Solution Conformation and Flexibility of the Native Trisaccharide (3) and (51)

The shape of a polysaccharide is very important for its biological function.^{106, 107}

An estimation of the conformation of a ligand in solution is one vital piece of information to explain binding activity in carbohydrate – protein systems. Solution conformations of oligosaccharides can in principle be determined by NMR methods.¹⁰⁸ These techniques measure distances and certain torsional angles through homo- and heteronuclear coupling constants and dipolar couplings (also referred to as nuclear Overhauser enhancements).¹⁰⁹

The difficulty in these measurements is due to the flexibility of the oligosaccharide. Sugars generally sample numerous conformations during the time interval of an NMR experiment so measured distances and torsional angles are averaged.¹¹⁰ Furthermore, it is extremely rare to be able to measure sufficient constraints to define a unique conformation. Average distances and angles determine only a ‘virtual’ conformation that may not be based in reality.

Computer modeling is often combined with physical measurements to avoid this problem.¹¹¹ Energetically favourable conformations are mapped and the

populations across the energy surfaces can be computed and the average distances or angles can be predicted for such low energy families of molecules. The results of “theoretical” predictions can be compared with the observed NMR parameters. At present, this combination of empirical observation and computer modeling is the best that can be done for carbohydrates. This treatment was applied to the ligands that had the highest affinities to the SYA/J6 antibody.

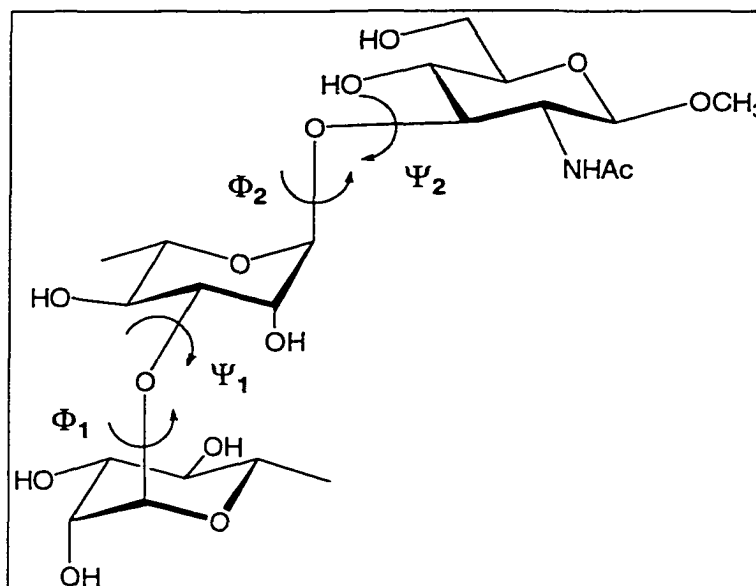
A) Introduction

It was shown that the tethered synthetic trisaccharide **51** had a higher affinity towards the SYA/J6 antibody than the native trisaccharide. The factors responsible for the increase in the association constant were investigated by computer modeling. In particular, molecular mechanics and molecular dynamics (MD) simulations of the solution conformations and flexibilities of the synthetic analog and native trisaccharide provided insights into the behaviour of the trisaccharides **3** and **51** in solution. These computations were performed with the Discover module in InsightII software[®] developed by Biosym Technologies[™]. The validity of the results was determined by crystallographic and NMR techniques.

Torsional angles across the glycosidic linkages were used to compare conformations of the trisaccharides obtained by molecular mechanics and crystallographic methods. They were also employed in molecular dynamics studies to indicate the flexibility of the molecules in solution. The diagnostic torsional angles

for the conformations are designated in Figure 55. The same designation of angles was used for the tethered ligand **51**. Hexopyranose molecules exist primarily in stable chair forms. Their conformations can be defined by the Φ and Ψ angles.

Figure 55: Definition of Torsional Angles Φ_1 , Ψ_1 , Φ_2 and Ψ_2



Interproton distances across the glycosidic linkages, which are defined later in this chapter, were used to compare the solution conformations of the native and synthetic trisaccharides predicted by theoretical methods and inferred from experimental average distances obtained from quantitative nOe values that were measured by the T-ROESY NMR technique.

B) Conformation and Flexibility of the Native Trisaccharide (3)

a. Potential Energy Minimization Studies

The key computation for any molecular simulation is the potential energy calculation for a given molecule. This energy term is calculated with the use of an empirical fit of the potential energy, called a forcefield, which employs a combination of internal coordinates, such as bond distances, bond angles, and torsions, and interatomic parameters such as electrostatic and van der Waals interactions. The calculated energies can give populations across the potential energy surface *via* a Boltzman distribution.

The AMBER_PLUS forcefield, developed by Kollman and modified for carbohydrates by Homans, was used in potential energy minimum calculations to obtain the lowest energy solution conformation of the native trisaccharide.^{112a,112b} The forcefield was derived from the combination of the monosaccharide parameters reported by Ha and the glycosidic linkage data reported by Wiberg and Murcko.^{113,114} The trisaccharide **3** was abstracted from the crystal structure of SYA/J6 **Fab** bound to the pentasaccharide ligand **1** and a potential energy minimization was run to determine the lowest energy conformation. The observed angles in the lowest energy structure were in good agreement with the angles reported for the crystal structure (Table 7).

Table 7: Computed $\Phi_1, \Psi_1, \Phi_2,$ and Ψ_2 Angles for the Native Trisaccharide (3)

	Φ_1	Ψ_1	Φ_2	Ψ_2
Crystal structure ³⁷	51.7°	-29.6°	42.2°	22.4°
Lowest energy structure	48.9°	-20.0°	44.1°	7.1°

To determine that this conformation of the trisaccharide was the global minimum, a grid search was used, whereby each Φ and Ψ angle was stepped through 360° in 18° intervals, and the energies were calculated by the forcefield. The structure determined from the original minimization studies was one of two global minima. A structure with angles of approximately 54°, 18°, 36°, and 0° for the $\Phi_1, \Psi_1, \Phi_2,$ and Ψ_2 torsional angles, respectively, also had an energy similar to the minimum structure obtained from the crystal structure. Because the first minimum energy structure was more similar to the crystallographically-determined structure, the latter structure was not used in further conformational studies.

b. Molecular Dynamics

Molecular dynamics simulations were performed on the native trisaccharide to study the movement of the molecule in water.¹¹⁵ The molecule was allowed to move as it would in solvent for one nanosecond and four thousand “snapshots” of the conformation were taken at regular intervals. Four graphs were obtained from the experiment in regards to the torsional angles across the glycosidic linkage (Figures

56 and 57). For each graph, the torsional angle that was observed in the snapshot was plotted *versus* the time of the experiment. The graphs show the extent of the fluctuations in this torsional parameter. Frequent spikes would occur in a very flexible molecule.

Figure 56: Φ_1 vs. Time (left) and Ψ_1 vs. Time (right) for the Native Trisaccharide (3)

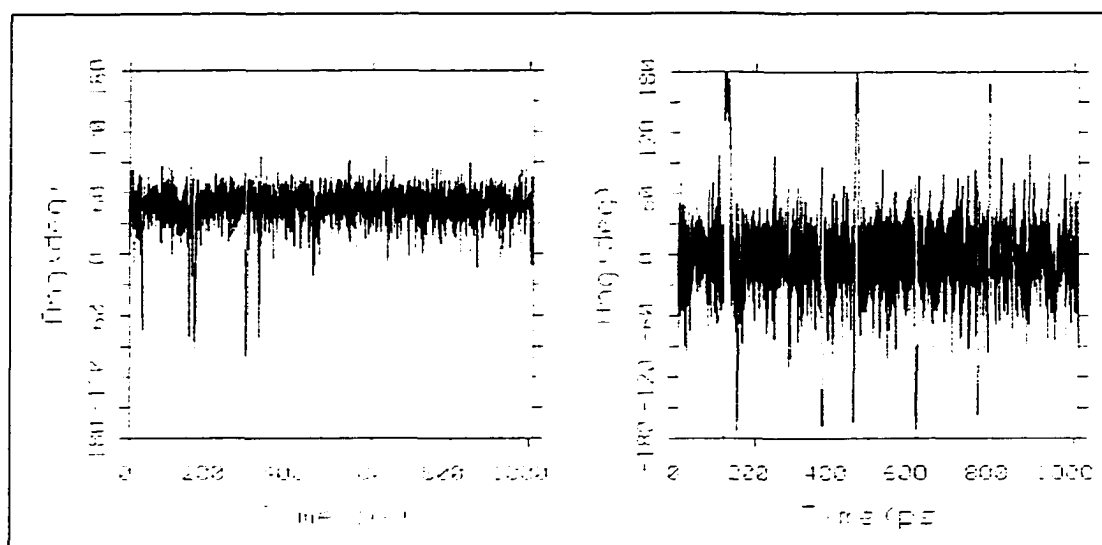
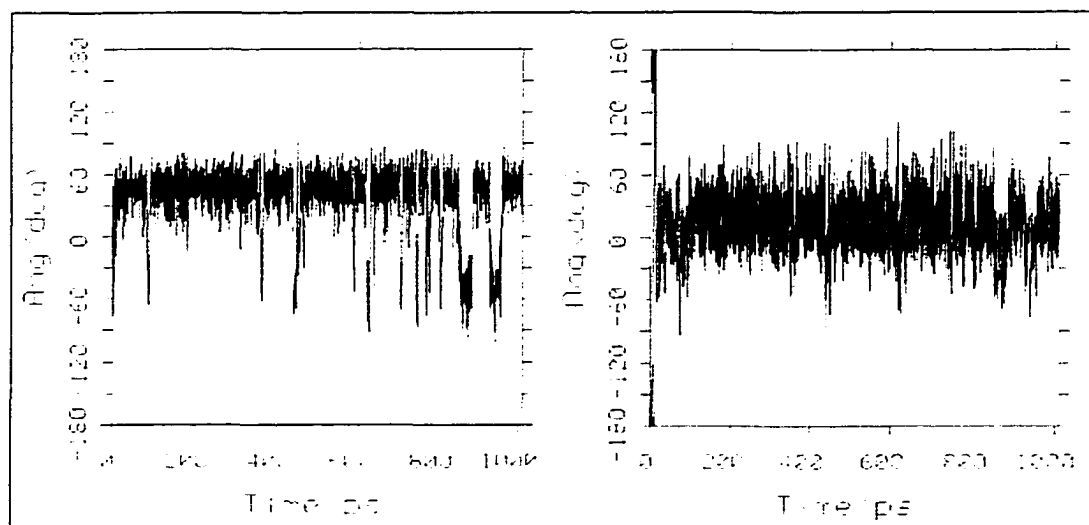
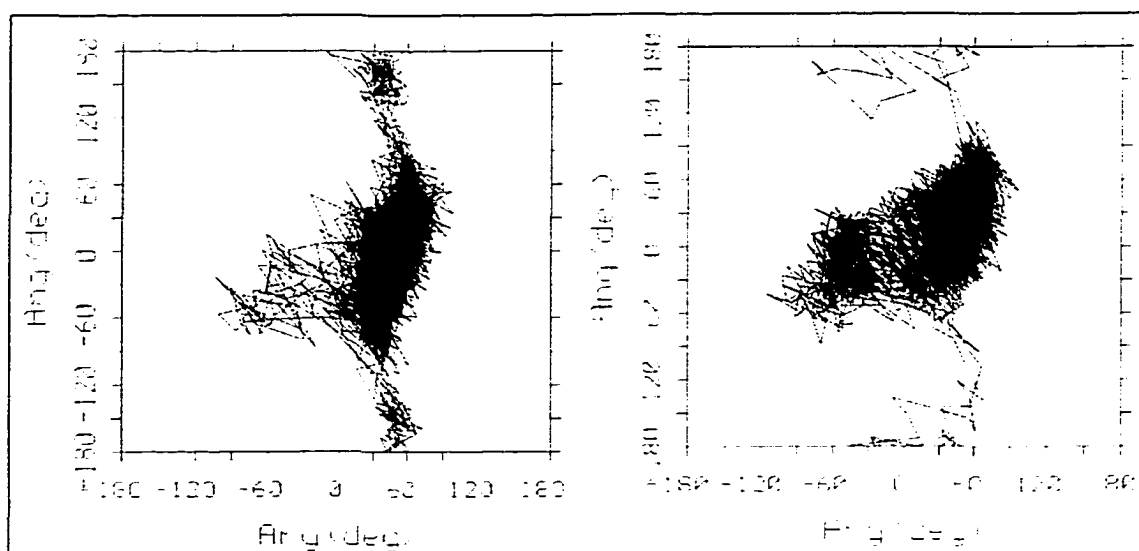


Figure 57: Φ_2 vs. Time (left) and Ψ_2 vs. Time (right) for the Native Trisaccharide (3)



The left-hand graph in Figure 56 indicates that the molecule is somewhat restricted about an angle of $+45^\circ$ for Φ_1 because the molecule made very few excursions from that angle. However, the right-hand graph in Figure 56 implies that the molecule is more flexible about the linkage defined by the Ψ_1 angle. It can be seen that the molecule adopts many more conformations about this bond. Similarly, the graphs in Figure 57 show that there are many deviations from a converged value for both Φ_2 and Ψ_2 . This implies that the molecule is flexible in this glycosidic region.

Figure 58: Ψ_1 vs. Φ_1 (left) and Ψ_2 vs. Φ_2 (right) for the Native Trisaccharide (3)



When the four previous graphs are combined to form a density map of the conformations that were adopted by the molecule during the dynamics experiment (Figure 58), the overall flexibility inherent in the trisaccharide is evident. The angles observed in the dynamics run occupy a broad region of conformational space. The

results of the potential energy minimization were verified because the torsional angles of the minimum solution structure lie well within the conformational space seen in the two plots.

C) Conformation and Flexibility of the Tethered Trisaccharide (51)

a. Potential Energy Minimization Studies

The same AMBER_PLUS forcefield was used to calculate the lowest energy conformation of the synthesized tethered trisaccharide **51** in a dipole gradient. The molecule was constructed by the addition of the linker group to the native trisaccharide. The observed angles in the lowest energy structure of the tethered compound were in excellent agreement with the angles seen in the lowest energy structure of the native trisaccharide (Table 8).

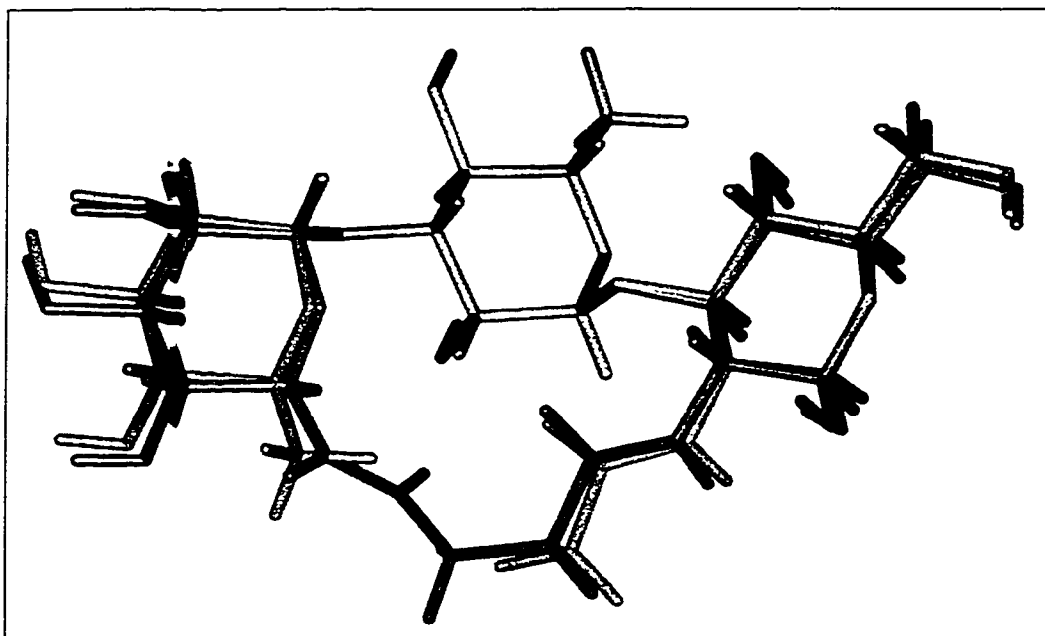
Table 8: Φ_1, Ψ_1, Φ_2 and Ψ_2 Angles of the Trisaccharides (3) and (51)

Compound	Φ_1	Ψ_1	Φ_2	Ψ_2
3	48.93°	-20.03°	44.08°	7.06°
51	53.54°	-21.35°	41.65°	1.14°

The rhamnose C ring residues of the two structures were superimposed to obtain Figure 59. The excellent overlap of these two structures would suggest that the hydrogen bond network that exists in the native trisaccharide/antibody complex

would be conserved in the binding that takes place between the modified trisaccharide and the antibody. This would account for the similarity in the thermodynamic parameters that were obtained from calorimetry in the binding of the two molecules with the protein.

Figure 59: Superimposition of the Trisaccharides (3) and (51)

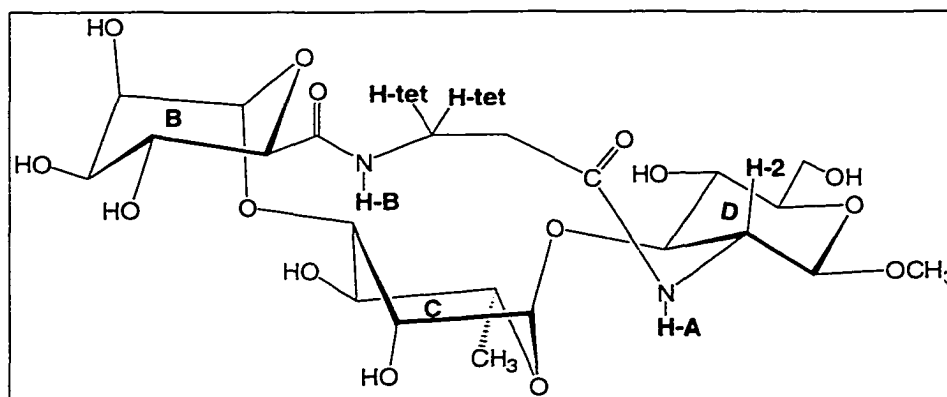


The average torsional angles could be computed by the EXSIDE NMR method.¹¹⁶ This experiment measures the $^3J_{CH}$ coupling constant across the glycosidic bond for the glycosidic carbon -proton coupling system. A Karplus relation can convert this coupling constant to a torsional angle.¹¹⁷ This type of experiment requires high sample concentrations and long acquisition times on high field NMR machines and was not recorded for practical reasons for ligands in this project.

b. Structure of the Ligand

In order to adopt a configuration that is identical to the native trisaccharide, the tethered compound is likely to be constrained to the conformation shown in Figure 60. In this conformation, both amide bonds in the structure are in the favoured *trans* orientation and the ethylene spacer is in a *cis* orientation. Experimental data confirm this postulate. The coupling constants between the amide protons, H-A and H-B, and their neighbouring coupling partners were measured by NMR spectroscopy in a 85: 15 H₂O: D₂O solvent mixture. A large $^3J_{\text{H-2,H-A}}$ coupling constant of 10 Hz signaled that the H-A and H-2 protons are $\sim 0^\circ$ apart. A $^3J_{\text{H-tet,H-B}}$ coupling constant of 6.3 Hz implied that the H-B and H-tet protons are $\sim 30^\circ$ apart.

Figure 60: Structure of (51) in Solution



c. Suggested Origins for the Improvement of the Enthalpy Term

It was shown by calorimetry that the enthalpy associated with the binding to the antibody was about 1.5 kcal/mol more favourable for the tethered trisaccharide than for the native trisaccharide. A number of hypotheses are consistent with this observation.

The increase in binding enthalpy of the tethered compound could be the consequence of the substitution of the methyl group at the 6 position of the rhamnose B ring by an amide function. New polar contacts between the synthetic ligand and the protein may have arisen in the association of this ligand compared with the native structure. This hypothesis seems unlikely because the binding constant for the acyclic trisaccharide **83** was a full order of magnitude less than the native trisaccharide **3**. In that case, the addition of a potential hydrogen bond donor and acceptor showed an adverse effect, due perhaps in part to a steric clash with the side chain of Tyr 37L which is $\sim 3.5 \text{ \AA}$ from the 6 position of the L-mannose B ring.⁴⁸

In addition to polar contacts, new van der Waals contacts between the ligand and protein may have arisen. A crystal structure of the synthetic ligand-protein complex would prove the existence of such novel contacts. This data is unavailable at the present time.

It can be seen in the lowest energy structure of the tethered ligand that the H-B amide proton is reasonably close ($\sim 2.9 \text{ \AA}$) to the hydroxyl group on the 2 position of the rhamnose C ring. A possible weak hydrogen bond may exist between these groups in the bound conformation. Previous work by Bundle and co-workers have

shown that this hydroxyl group is responsible for an unfavourable hydrophobic clash with the tryptophan H47 side chain in the bound form of the ligand.⁴⁸ The removal of this group causes a ~ 6 kcal/mol increase in enthalpy in the binding to antibody. It was postulated that this hydroxyl group points to a hydrophobic region in the binding site and is not extensively hydrogen bonded upon binding to protein.

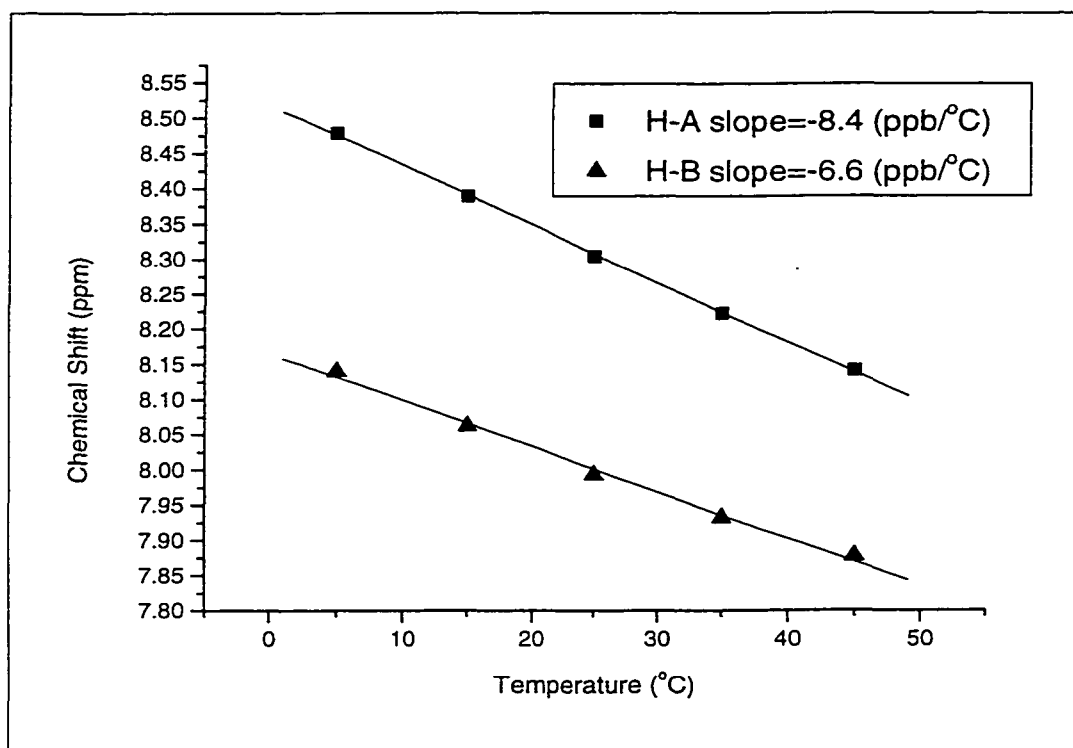
An experiment was run to check for a possible hydrogen bond between the amide proton H-B and the 2-OH of the rhamnose C ring. The NMR spectrum was obtained for the compound in a 85:15 H₂O:D₂O solvent mixture at five temperatures: 5°, 15°, 25°, 35°, and 45°. Changes in temperature of the solvent would cause smaller effects in chemical shift for hydrogen bonded protons *versus* non-hydrogen bonded protons because molecules containing intramolecular hydrogen bonds would have less interactions with the water.¹¹⁶ The chemical shifts (referenced to acetone at 2.225 ppm) of the two amides were plotted against temperature to obtain the linear dependence of chemical shift on temperature (Figure 61).

The H-B amide proton experiences a smaller downfield shift (6.6 ppb/°C) as the temperature increases compared to the H-A amide proton (8.4 ppb/°C). Although the difference in slope is small, it is significant enough to suggest a weak hydrogen bond is possible between the H-B amide and the 2-OH of the rhamnose C ring.

The presence of a weak intramolecular hydrogen bond and an extra methylene group in the tethered trisaccharide possibly adds to the overall hydrophobicity of the molecule compared to the native trisaccharide. On the other hand, **51** contains two

polar amide groups but these are bridged by two methylenes. However, the tether creates a space between itself and the trisaccharide with a separation of ~ 3.5 Å. It is likely that one or two water molecules could occupy this space but it is clear that the untethered trisaccharide would be much more solvated at this surface. In this sense, despite its polar features, we might regard the tether as possessing non-polar properties.

Figure 61: Chemical Shift vs. Temperature for the Amide Protons in (51)



If this is the case, reorganization of the high energy water molecules that surround the ligand and that are released into the bulk solvent after the binding event would contribute to the favourable enthalpy term.

In his previous work with interresidue tethering, Bundle has used this argument to provide an explanation for the increase in binding enthalpy for ligands that contained hydrophobic tethers.¹¹⁸ That conclusion, and the one presented here, is based on recent research that has been reported by Toone.⁵² With the use of calorimetric data for ligand – receptor association in heavy and light water, Toone and co-workers have proved that solvent reorganization is responsible for 25 to 100% of the binding enthalpy. One can postulate that ligands with a larger hydrophobic surface will have a greater number of unorganized water molecules on those surfaces. This will result in a larger solvent reorganization term and a higher enthalpy term associated with this process.

d. Molecular Dynamics Support Entropic Gains

In order to provide a possible explanation of the gain in entropy in the association between the tethered molecule and the antibody, compared with the native trisaccharide, molecular dynamics studies were performed on the tethered ligand. Similar to the studies with the native trisaccharide **3**, these calculations could provide information about the flexibility of the ligand in water. The following four graphs in Figures 62 and 63 show the values of the four torsional angles in the tethered ligand that were monitored during the molecular dynamics experiment.

Figure 62: Φ_1 vs. Time (left) and Ψ_1 vs. Time (right) for the Trisaccharide (51)

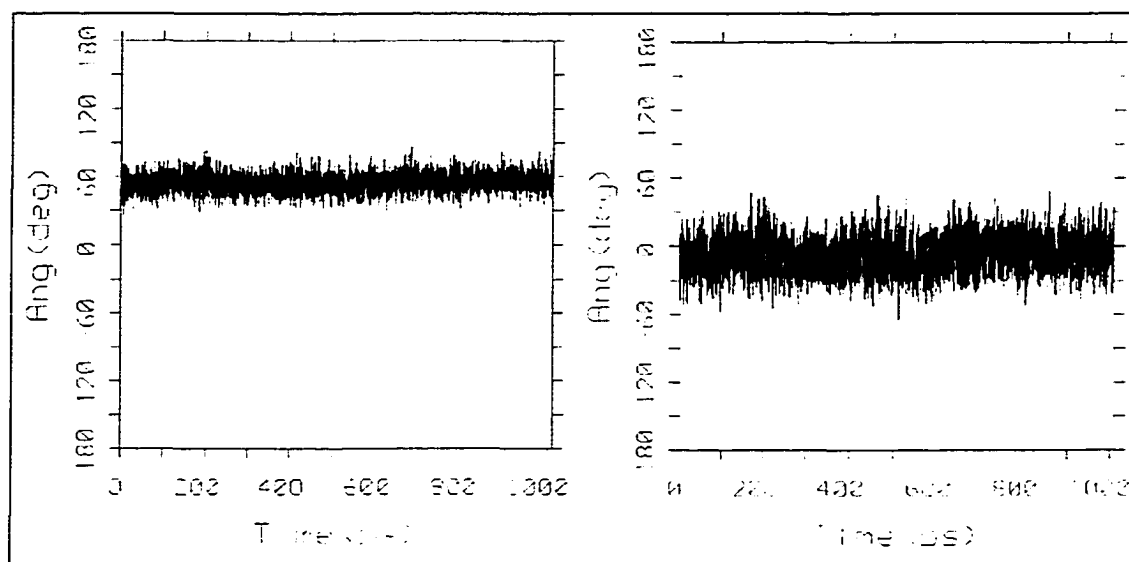
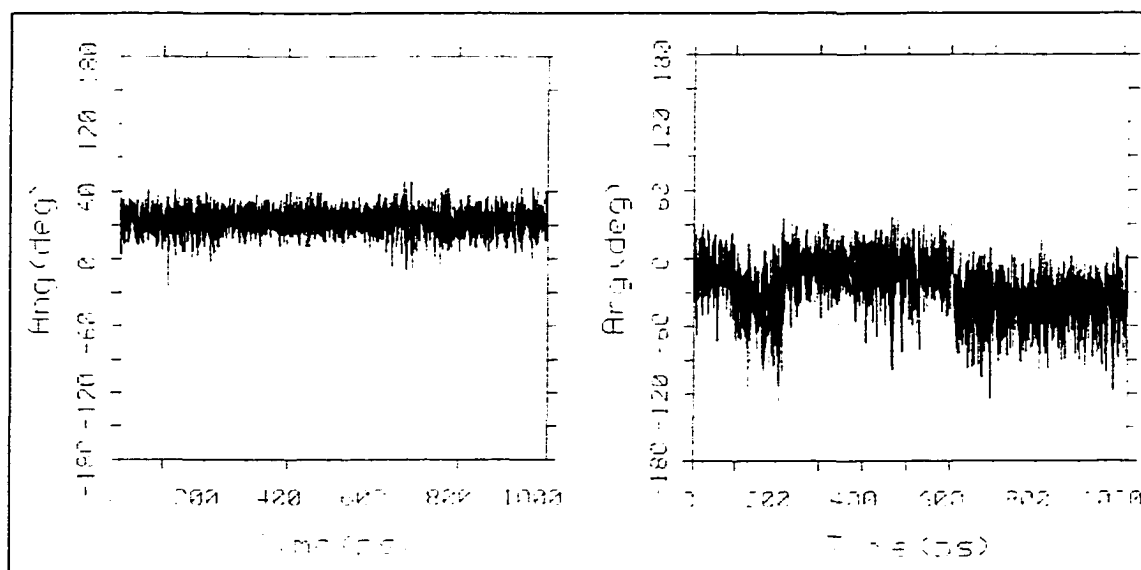


Figure 63: Φ_2 vs. Time (left) and Ψ_2 vs. Time (right) for the Trisaccharide (51)

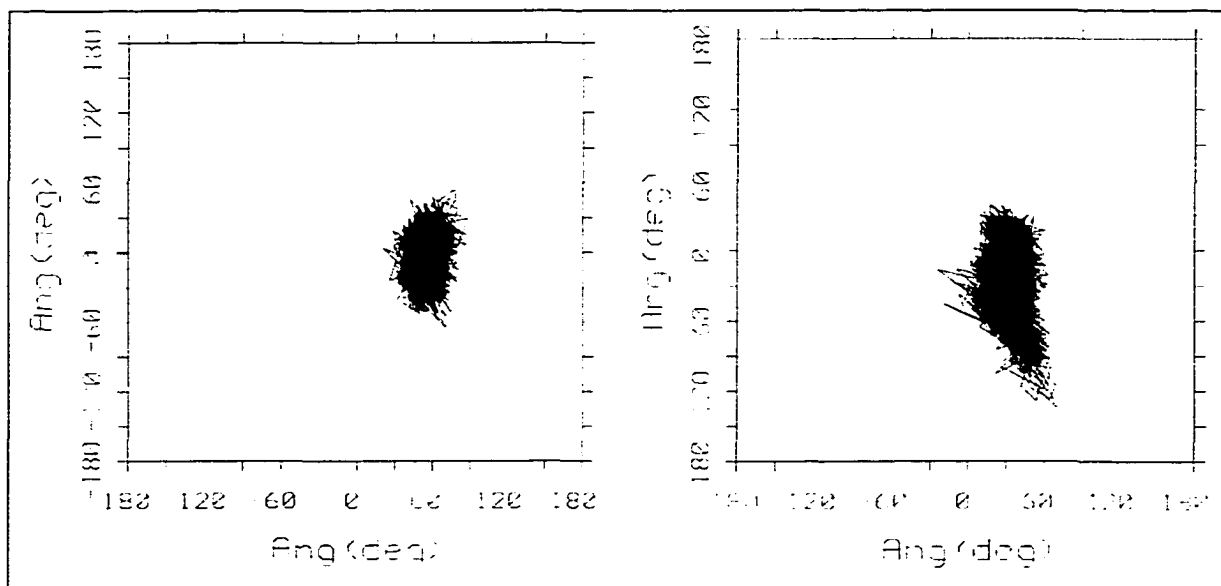


The Φ_1 versus time graph in Figure 62 indicates that the molecule is very constrained about this angle in solution because the molecule deviates by only a few degrees from $+50^\circ$ during the entire experiment. The Ψ_1 versus time graph also

shows reduced variability in this angle in comparison with the native trisaccharide. As a consequence, conformational contributions from the other global minimum that was observed during the grid search of the native trisaccharide have been reduced as seen by the near absence of conformations at about $+20^\circ$.

The lack of excursions from $+30^\circ$ in the Φ_2 *versus* time graph in Figure 63 indicates that the molecule is also very constrained about Φ_2 . In contrast, the presence of two main regions of variability in the Ψ_2 *versus* time graph about -10° and -40° suggests that the molecule is not entirely constrained about the bond defined by the Ψ_2 angle.

Figure 64: Ψ_1 vs. Φ_1 (left) and Ψ_2 vs. Φ_2 (right) for the Trisaccharide (51)



The density maps shown in Figure 64 of the four torsional angles were constructed by the combination of the previous four graphs. Both the Ψ_1 vs. Φ_1 and Ψ_2 vs. Φ_2 plots show smaller regions of allowable conformations in solution

compared with the native trisaccharide (Figure 58). Therefore, the results from the molecular dynamics show that the ligand design strategy was successful in reducing the flexibility of the sugar in aqueous medium and decreasing the unfavourable entropy term that is associated with this loss of flexibility in the ligand upon binding versus the native trisaccharide. However, the net entropy gain was limited to 0.5 kcal/mol, presumably by the persistent flexibility about the Ψ_2 angle.

To ensure that the linker did not introduce added flexibility to the molecule, two other dihedral angles across the amide linkages, φ and ω were investigated.

Figure 65: Definition of the Torsional Angles φ and ω

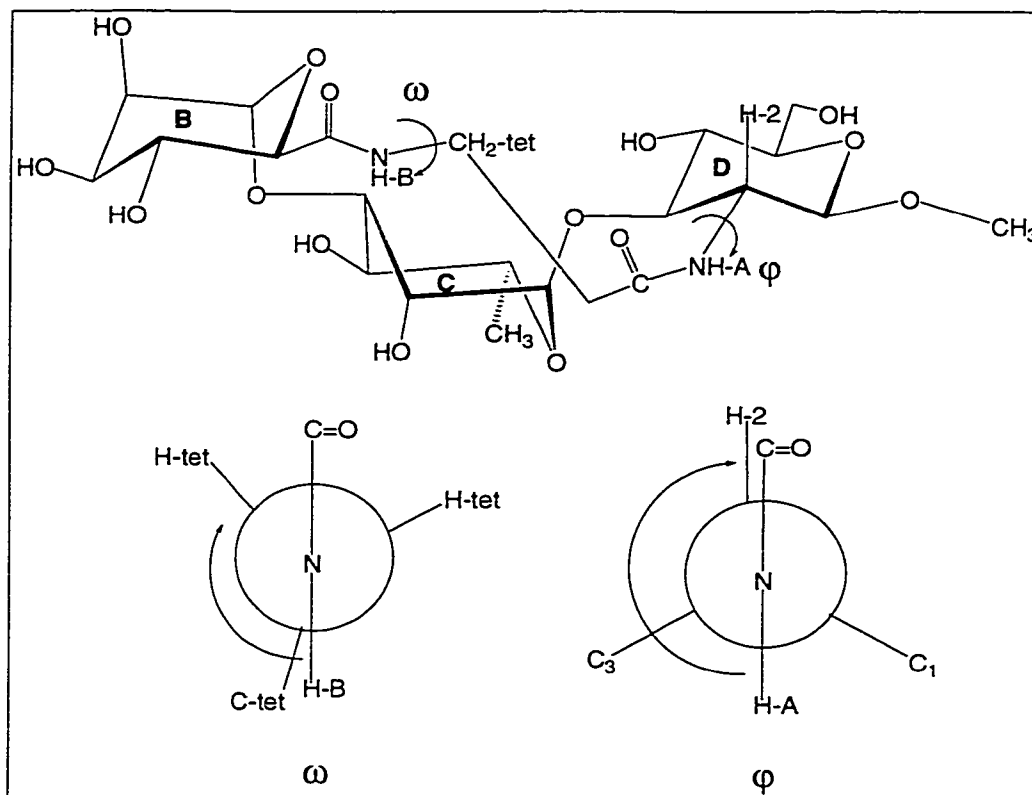
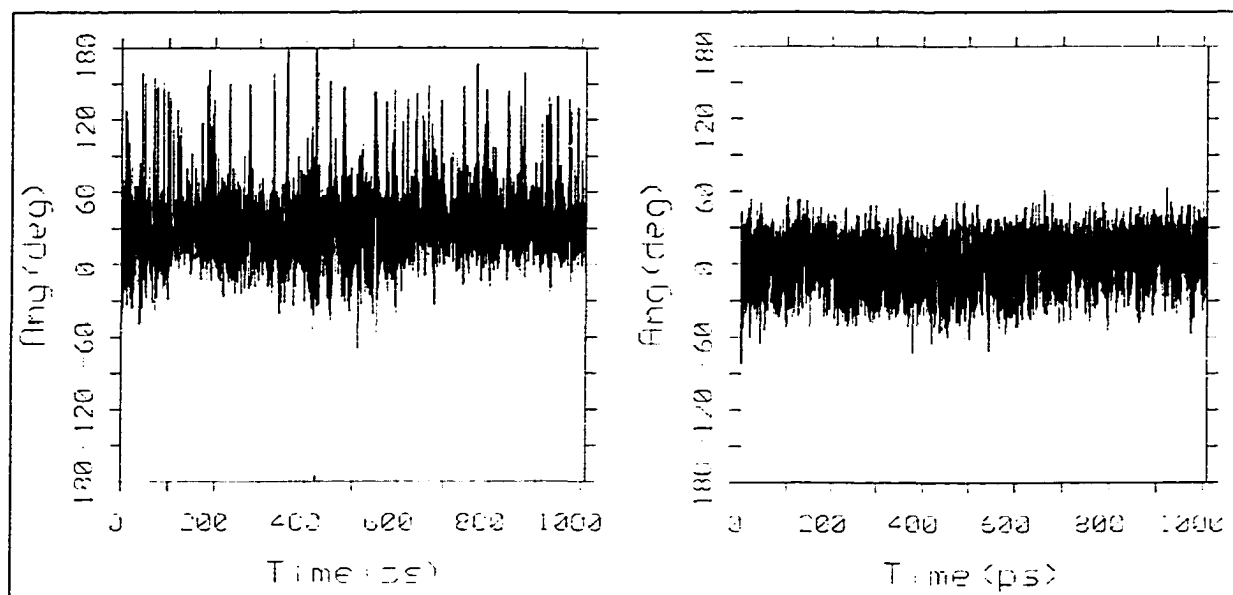


Figure 66: ω vs. Time (left) and ϕ vs. Time (right) for the Trisaccharide (51)



The ω *versus* time graph indicates that the molecule samples many conformations about this torsional angle, but the angle is generally close to $+30^\circ$. The ϕ *versus* time graph shows that this torsional angle is restricted to 0° . It can be inferred that no additional flexibility was introduced to the molecule by the choice of tether.

e. Summary of the Origin of the Favourable Thermodynamics

To summarize, the observed thermodynamics can be explained by several possibilities.

Favourable enthalpic terms can arise due to the following; the tethered trisaccharide could provide enhanced complementary and stronger hydrogen bonds

when compared to the native trisaccharide and the methylene groups of the tether come close to van der Waals contacts with His 31L and Tyr 37H. In addition, the potentially enhanced hydrophobicity of the tethered ligand could also contribute to the enthalpic gain.

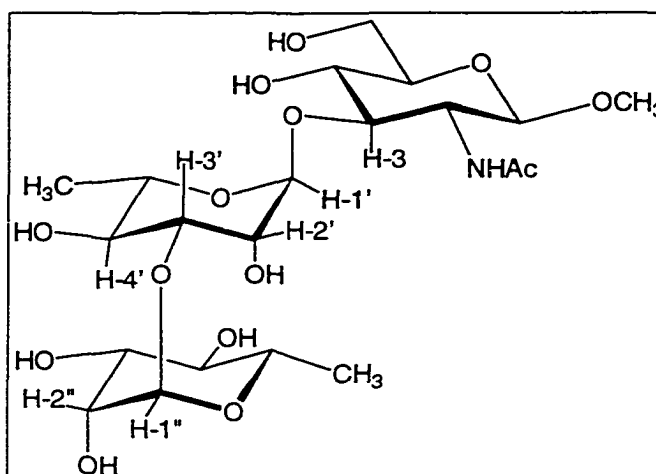
Favourable entropic contributions may arise from the preorganization of the trisaccharide.

D) NMR Studies on the Trisaccharides (3) and (51)

a. Comparison of Interproton Distances Found in Modeling with NMR-Based Experiments for the Native Trisaccharide (3)

Four interproton distances were examined to compare the conformations of the native trisaccharide in aqueous solution with those found in the molecular dynamics simulations. The proton assignments of interest are shown in Figure 67.

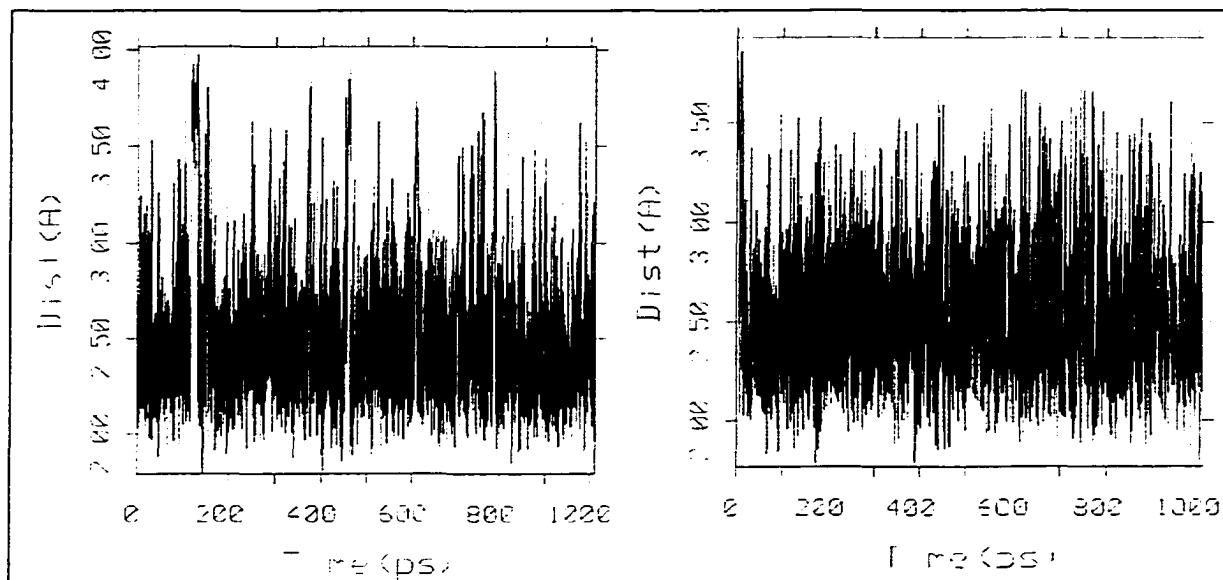
Figure 68 shows the H-1'' → H-3' distances (left graph) and the H-1' → H-3 distances (right graph) that were plotted against time from the molecular dynamics simulations that were previously described for the native trisaccharide 3. The plots show the distances measured for each particular conformation that was seen in the dynamics experiment.

Figure 67: Selected Proton Assignments for the Native Trisaccharide (3)

The distances were extracted from these plots and averaged to obtain mean distances determined from molecular dynamics. The same procedure was done for the $H-1'' \rightarrow H-2'$ and $H-1'' \rightarrow H-4'$ distances (plots not shown). These four distances serve as a comparative numbers to the distances measured by quantitative nOe's from T-ROESY experiments.

A T-ROESY experiment was performed on the native trisaccharide to determine the nOe correlations between the assigned protons. This experiment was first reported by Bothner-By and co-workers and then modified by Shaka.^{119,120}

**Figure 68: H-1'' → H-3' Distance vs. Time (left) and
H-1' → H-3 Distance vs. Time (right) for the Native Trisaccharide (3)**



In the experiment, cross peaks corresponding to the dipolar coupling of interest in the spectrum were integrated to obtain nOe volumes that were used to calculate distances with the formula¹²¹:

$$D_x = (D_{\text{std.}}) (V_{\text{std.}}/V_x)^{1/6}$$

In the formula, D_x represents the unknown distance, D_{std} is the reference distance, V_{std} is the volume of the reference correlation, and V_x is the volume of the unknown correlation. The standard correlation that was used in the calculations was the H-1'' → H-2'' correlation. The distance for this proton-pair was observed as 2.52 Å in the crystal structure as well as in the results from computer modeling. The

results of distance calculations from crystallography, dynamics and T-ROESY experiments are presented in Table 9.

Table 9: Inter-Proton Distances (Å) for Selective Correlations Calculated from Crystallography, Dynamics, and NMR for the Native Trisaccharide (3)

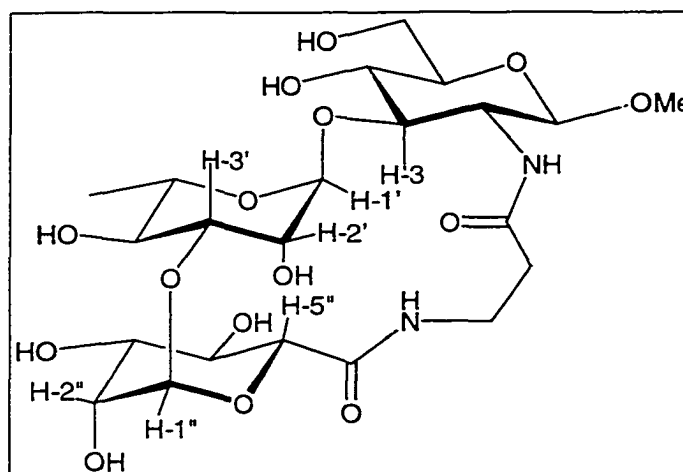
Correlation	Average Distance from Crystallography	Average Distance from Dynamics	Average Distance from NMR
H-1'' → H-3'	2.2	2.5	2.3
H-1'' → H-2'	3.3	3.8	3.4
H-1'' → H-4'	3.8	4.0	3.8
H-1' → H-3	2.4	2.6	2.3

The distances calculated from the three techniques are in good agreement and suggest that the conformations observed in the crystal structure, molecular dynamics and in aqueous solution are quite similar. In addition, the results from the minimization studies involving the torsional angles of the native trisaccharide **3** are verified by these findings.

b. A Comparison of Inter-Proton Distances Found in Modeling with NMR for the Tethered Trisaccharide (51)

As before, four distances were examined to compare the conformations of the tethered trisaccharide in aqueous solution with the conformations found in the molecular dynamics simulations. The distances that were chosen were the H-1'' \rightarrow H-3', H-1'' \rightarrow H-2', H-5'' \rightarrow H-2', and H-1' \rightarrow H-3 distances. The proton assignments of interest are shown in Figure 69.

Figure 69: Selected Proton Assignments for the Tethered Trisaccharide (51)



The average distances calculated from molecular dynamics experiment were obtained, as before, from the plots of distance against time that resulted from the dynamics experiment. A T-ROESY experiment was performed on the tethered compound and the average distances were obtained from this experiment as previously described for the native trisaccharide. The H-1'' \rightarrow H-2'' distance was

used as the reference. The results of distance calculations from the dynamics and T-ROESY experiments are presented in Table 10.

Table 10: Inter-Proton Distances for Selective Correlations Calculated from Molecular Dynamics and NMR for the Tethered Trisaccharide (51)

Correlation	Average Distance from Dynamics (Å)	Average Distance from NMR (Å)
H-1'' → H-3'	2.4	2.2
H-1'' → H-2'	3.9	3.5
H-5'' → H-2'	2.3	2.3
H-1' → H-3	2.3	2.5

Once again, the distances calculated from the two techniques were in good agreement that suggests that the conformations observed in the molecular dynamics and in aqueous solution are quite similar.

The calculated distances across the glycosidic linkages from NMR measurements were compared for the native and tethered trisaccharides to determine the conformation of the synthetic compound in solution relative to the native structure. The distances are shown in Table 11.

Table 11: Inter-Proton Distances (Å) for Correlations Across the Glycosidic Linkages for the Trisaccharides (3) and (51)

Correlation	Average Distance in (3)	Average Distance in (51)
H-1'' → H-3'	2.3	2.2
H-1'' → H-2'	3.4	3.5
H-1' → H-3	2.3	2.5

The distances across both glycosidic linkages were almost identical for the native and tethered trisaccharides and further verifies that both structures have similar conformations in solution.

Based on the torsional angles observed in the minimum structures, the distances observed in solution, and the structure observed in the crystal structure, the conclusion can be made that the tethered compound **51** is an excellent mimic of the native trisaccharide **3**.

Chapter 6

Conclusion

Two crystal structures of SYA/J6 monoclonal antibody – ligand complexes were used to design disaccharide ligands that had new hydrogen bond and hydrophobic contacts linked *via* two carbon spacer arms.

Three ligands that had either an *N*-acetate, *N*-benzoate, or an *N*-alanyl group attached to the linker arm on the 3 position of the rhamnose C ring were synthesized in good yields from simple starting materials. The new contacts were introduced through reduction and acylation of a cyanomethyl group. Four ligands that possessed an *N*-acetate, *N*-benzoate, or *N*-phenylalanyl group (D or L) on a linker arm at the anomeric centre of the glucosamine D ring *via* modification of an anomeric allyl group were produced. An analogue of the native disaccharide epitope that is recognized by the antibody was also made.

Using a solid phase binding assay, binding curves were obtained for these compounds and IC_{50} values were calculated.

The first set of ligands that had new contacts introduced to the three position of the rhamnose C ring bound more strongly to the antibody than the native disaccharide analogue. The best ligand, that had an *N*-benzoate group on the linker arm, had an IC_{50} value that was fifty times higher than the native disaccharide. This

finding suggested that the original ligand design strategy lead to small molecule, higher affinity ligands of the antibody, but did not reach the threshold activity represented by the native trisaccharide. Practical concerns prevented discovery of the source of the higher affinity of these ligands towards the protein.

The second set of test molecules that had new contacts at the reducing end had the same affinity as the native disaccharide analogue.

The 6 position of the rhamnose B ring was observed to be in close proximity to the acetamido group of the glucosamine D ring in the crystal structures. Three constrained trisaccharide ligands that connected these atoms were synthesized from a common trisaccharide intermediate and commercially available starting materials. Orthogonally protected amino acids (β -alanine and glycine) were used as spacers in these tethered trisaccharides. A condensation between a carboxylic acid group on the L-mannose B ring and an amino group on the spacer was the key step in the synthesis of two of the test molecules. A third macrocycle ligand was synthesized by forming a carbamate linkage between the hydroxyl group on the 6 position of the L-mannose and an amino group of the spacer.

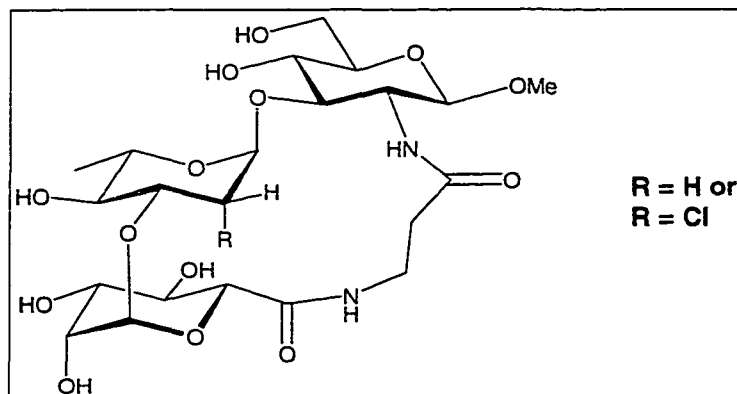
Results from the solid phase assay showed that two of the constrained ligands had lower binding affinities than the natural trisaccharide substrate of the antibody. The third analogue that had a β -alanine spacer attached by an amide group to the 6 position of the L-mannose B ring showed an increase in activity by a factor of three over that of the native structure. Microcalorimetry measurements provided a more

accurate increase in affinity of a factor of twenty for this ligand over the native trisaccharide

Microcalorimetry measurements also showed an increase in both the enthalpy and entropy terms for this ligand relative to the acyclic native trisaccharide. Investigations into the conformation in solution of this ligand by NMR experiments and theoretical calculations indicated that the constrained ligand adopted the same solution conformation as the native trisaccharide. It was suggested that the increase in enthalpy was likely due in whole or in part to one of three reasons: the creation and strengthening of contacts between the sugar and protein, the generation of polar contacts within the sugar, or solvent reorganization. Molecular dynamics simulations verified that this molecule was relatively rigid in solution thereby accounting for the decrease in the entropic barrier relative to the natural epitope.

The most successful ligand could serve as a lead compound for the spawning of other tight binding ligands, such as the 2'-deoxy or 2'-chloro-2'-deoxy analogs shown below.

Figure 70: One Possible Extension of this Project



Earlier studies with this system showed that a trisaccharide lacking a hydroxyl group at the 2 position of the rhamnose C ring had a higher affinity to the antibody than the native trisaccharide. Bundle *et al.* have shown that selective chlorodeoxygenations have led to tighter binding ligands.⁷³ If the previous and present ligand designs are complementary, a trisaccharide antigen with an exceptionally high binding affinity to an antibody (nanomolar) could be achieved.

The data presented in this thesis suggest that the ligand design approach of adding constraints to two glycosidic bonds in the ligand through a polar linker may lead to low molecular weight, tight binding ligands for this and possibly other systems. However, the total free energy gain by this approach alone produces an inhibitor of sugar-protein binding with micromolar activity.

In the search for design principles that could reliably generate nanomolar activities, the approach identified here should be successful (reach nanomolar levels) when combined with serendipitous observations, of the type suggested in Figure 70. In such circumstances, the effects of tethering should be additive to those of selective deoxygenation.

Chapter 7

Experimental

General methods

Analytical thin layer chromatography (tlc) was performed on silica gel 60-F₂₅₄ (Merck). Tlc detection was achieved by charring with 5% sulphuric acid in ethanol. All commercial reagents were used as supplied. Column chromatography used silica gel (SiliCycle) and solvents were distilled. High performance liquid chromatography (HPLC) was performed using a Waters HPLC system which consisted of a Waters 600S controller, 626 pump, and 486 tunable absorbance detector. HPLC separations were performed on a Beckmann C₁₈ semi-preparative reversed-phase column with acetonitrile and water as eluents. ¹H NMR spectra were recorded at either 300, 360, 500, or 600 MHz, and are referenced to internal standards of the residual protonated solvent peaks; δ_{H} 7.24 ppm for solutions in CDCl₃ or to 0.1% external acetone (δ_{H} 2.225 ppm) for solutions in D₂O. ¹³C NMR spectra (HMQC) were recorded at 150 MHz and are referenced to internal CDCl₃ (δ_{C} 77.0 ppm) or to external acetone (δ_{C} 31.07 ppm). Optical rotations were measured with a Perkin Elmer 241 polarimeter at 22°C. Mass spectrometric analysis was performed by positive mode electrospray

ionization on a Micromass ZabSpec Hybrid Sector-TOF. For exact measurements, the spectra were obtained by voltage scan over a narrow mass range at 10 000 resolution.

Methyl 2-acetamido-3-O-(3-O-[α -L-rhamnopyranosyl]- α -L-rhamnopyranosyl)-2-deoxy- β -D-glucopyranoside (3)

An authentic sample was available from previous work in the laboratory.

^1H NMR (600 MHz, D_2O) δ : 5.01 (d, 1H, $J_{1,2''} = 1.5$ Hz, H-1''), 4.82 (d, 1H, $J_{1,2'} = 1.4$ Hz, H-1'), 4.48 (d, 1H, $J_{1,2} = 8.8$ Hz, H-1), 4.06 (dd, 1H, $J_{1,2''} = 1.8$ Hz, $J_{2',3''} = 3.5$ Hz, H-2''), 4.04 (dq, 1H, $J_{4',5'} = 9.9$ Hz, $J_{5',6'} = 6.4$ Hz, H-5'), 3.95 (dd, 1H, $J_{5,6a} = 2.2$ Hz, $J_{6a,6b} = 12.2$ Hz, H-6a), 3.87 (dd, 1H, $J_{1,2'} = 2.0$ Hz, $J_{2',3'} = 3.1$ Hz, H-2'), 3.83 (dd, 1H, $J_{2',3''} = 3.1$ Hz, $J_{3'',4''} = 9.0$ Hz, H-3''), 3.92 (dd, 1H, $J_{1,2} = 8.8$ Hz, $J_{2,3} = 9.9$ Hz, H-2), 3.79 (dd, 1H, $J_{2',3'} = 3.1$ Hz, $J_{3',4'} = 9.9$ Hz, H-3'), 3.76 (dd, 1H, $J_{5,6b} = 6.0$ Hz, $J_{6a,6b} = 12.4$ Hz, H-6b), 3.59 (dd, 1H, $J_{2,3} = 8.6$ Hz, $J_{3,4} = 10.1$ Hz, H-3), 3.53 (t, 1H, $J_{3',4'} = J_{4',5'} = 9.9$ Hz, H-4'), 3.53 (t, 1H, $J_{3,4} = J_{4,5} = 9.9$ Hz, H-4), 3.50 (s, 3H, OMe), 3.48 (ddd, 1H, $J_{5,6a} = 2.2$ Hz, $J_{5,6b} = 5.8$ Hz, $J_{4,5} = 9.9$ Hz, H-5), 3.47 (t, 1H, $J_{3'',4''} = J_{4'',5''} = 9.7$ Hz, H-4''), 3.45 (ddd, 1H, $J_{5,6a} = 1.8$ Hz, $J_{5,6b} = 5.6$ Hz, $J_{4,5} = 9.8$ Hz, H-5''), 1.31 (d, 3H, $J_{5'',6''} = 6.2$ Hz, H-6''), 1.24 (d, 3H, $J_{5',6'} = 6.4$ Hz, H-6').

Methyl 4-O-benzyl-3-O-cyanomethyl- α -L-rhamnopyranoside (15)

Distilled methanol (90 mL) was added to a mixture of the diol **14**⁷⁹ (1.0 g, 3.73 mmol) and dibutyltin oxide (1.11 g, 4.46 mmol) in a 250 mL round-bottomed

flask. The suspension was stirred under reflux conditions for 2 h. Toluene (90 mL) was then added along with tetrabutylammonium iodide (1.65 g, 4.47 mmol) and bromoacetonitrile (1.39 mL, 20.0 mmol, 1.722 g/mL). The solution was stirred at 72 °C for 4 h. The resulting red solution was then cooled to room temperature and all of the volatiles were removed using a rotary evaporator and DCM (200 mL) was added to the residue. The solution was then equilibrated between DCM and saturated $\text{Na}_2\text{S}_2\text{O}_3$ (aq.) (50 mL) in a separatory funnel. The organic phase was drained into an Erlenmeyer flask, dried with Na_2SO_4 , and filtered through cotton. The solvent was removed using a rotary evaporator and the product was purified by silica gel chromatography using hexane-ethyl acetate, 1:1, as the eluent. The nitrile **15** was isolated as a yellow oil (0.91 g, 307.34 g/mol, 80%); R_f 0.28 in hexane-ethyl acetate, 1:1. ES HRMS: (M+Na) exact mass: 330.1317, found: 330.1320. $[\alpha]_D -34.2^\circ$ (c 0.9, CH_2Cl_2). ^1H NMR (500 MHz, CDCl_3) δ : 7.27-7.38 (m, 5H, aromatic), 4.72 (d, 1H, $J_{\text{gem}} = 11.1$ Hz, $\text{CH}_2\text{-Ph}$), 4.65 (d, 1H, $J_{1,2} = 1.8$ Hz, H-1), 4.64 (d, 1H, $J_{\text{gem}} = 11.1$ Hz, $\text{CH}_2\text{-Ph}$), 4.34 (s, 2H, $\text{CH}_2\text{-CN}$), 4.06 (dd, 1H, $J_{1,2} = 1.8$ Hz, $J_{2,3} = 3.2$ Hz, H-2), 3.76 (dd, 1H, $J_{2,3} = 3.2$ Hz, $J_{3,4} = 9.3$ Hz, H-3), 3.69 (dq, 1H, $J_{4,5} = 9.3$ Hz, $J_{5,6} = 6.3$ Hz, H-5), 3.46 (dd, 1H, $J_{3,4} = 9.3$ Hz, $J_{4,5} = 9.3$ Hz, H-4), 3.33 (s, 3H, OMe), 2.22 (bs, 1H, OH), 1.31 (d, 3H, $J_{5,6} = 6.3$ Hz, H-6).

Methyl 2,4-di-O-benzyl-3-O-cyanomethyl- α -L-rhamnopyranoside (16)

Anhydrous THF (20 mL) was added to the alcohol **15** (100 mg, 0.325 mmol) along with sodium hydride (20 mg, 0.833 mmol) in a 50 mL round-

bottomed flask and stirred under an argon atmosphere for 15 min at room temperature. Benzyl bromide (58 μ L, 0.488 mmol, 1.438 g/mL) was added and the solution was stirred at 60 $^{\circ}$ C under an argon atmosphere for 12 h. The resulting yellow, cloudy solution was then cooled and all of the volatiles were removed using a rotary evaporator and DCM (50 mL) was added to the residue. The solution was then equilibrated between DCM and water (30 mL) in a separatory funnel. The organic phase was drained into an Erlenmeyer flask, dried with Na_2SO_4 , and filtered through cotton. The solvent was removed using a rotary evaporator and the product was purified by silica gel chromatography using hexane-ethyl acetate, 5:1, as the eluent. The benzylate **16** was isolated as a pale yellow solid (110 mg, 397.46 g/mol, 85%); R_f 0.16 in hexane-ethyl acetate, 6:1. ES HRMS: (M+Na) exact mass: 420.1787, found: 420.1782. $[\alpha]_D^{25}$ -47.3° (c 0.8, CH_2Cl_2). ^1H NMR (500 MHz, CDCl_3) δ : 7.25-7.40 (m, 10H, aromatic), 4.77 (d, 1H, $J_{\text{gem}} = 11.0$ Hz, $\text{CH}_2\text{-Ph}$), 4.70 (ABX, 2H, $J_{\text{ABX}} = 12.2$ Hz, $\text{CH}_2\text{-Ph}$), 4.64 (d, 1H, $J_{1,2} = 1.7$ Hz, H-1), 4.64 (d, 1H, $J_{\text{gem}} = 11.0$ Hz, $\text{CH}_2\text{-Ph}$), 4.18 (AB, 2H, $J_{\text{AB}} = 16.0$ Hz, $\text{CH}_2\text{-CN}$), 3.80 (dd, 1H, $J_{1,2} = 1.7$ Hz, $J_{2,3} = 3.2$ Hz, H-2), 3.78 (dd, 1H, $J_{2,3} = 3.2$ Hz, $J_{3,4} = 8.9$ Hz, H-3), 3.65 (dq, 1H, $J_{4,5} = 9.0$ Hz, $J_{5,6} = 6.1$ Hz, H-5), 3.56 (dd, 1H, $J_{3,4} = 8.9$ Hz, $J_{4,5} = 9.0$ Hz, H-4), 3.30 (s, 3H, OMe), 1.31 (d, 3H, $J_{5,6} = 6.1$ Hz, H-6).

Acetyl 2,4-di-O-benzyl-3-O-cyanomethyl- α -L-rhamnopyranoside (17)

Acetic anhydride (50 mL) was added to the α -methyl glycoside **16** (1.95 g, 4.91 mmol) along with concentrated sulphuric acid (20 μ L) in a 500 mL round-

bottomed flask and stirred for 2 h at room temperature. DCM (100 mL) and saturated NaHCO_3 (aq.) (300 mL) were then added and the solution was stirred for 2 h. The resulting biphasic solution was then transferred to a separatory funnel. The organic phase was drained into an Erlenmeyer flask, dried with Na_2SO_4 , and filtered through cotton. The solvent was removed using a rotary evaporator and the product was purified by silica gel chromatography using hexane-ethyl acetate, 3:1, as the eluent. The acetate **17** was isolated as a pale yellow solid (1.96 g, 425.47 g/mol, 93%); R_f 0.35 in hexane-ethyl acetate, 2:1. ES HRMS: (M+Na) exact mass: 448.1736, found: 448.1730. $[\alpha]_D -119.4^\circ$ (c 0.9, CH_2Cl_2). $^1\text{H NMR}$ (360 MHz, CDCl_3) δ : 7.25-7.40 (m, 10H, aromatic), 6.15 (d, 1H, $J_{1,2} = 1.6$ Hz, H-1), 4.78 (d, 1H, $J_{\text{gem}} = 11.0$ Hz, CH_2 -Ph), 4.77 (d, 1H, $J_{\text{gem}} = 12.2$ Hz, CH_2 -Ph), 4.67 (d, 1H, $J_{\text{gem}} = 11.0$ Hz, CH_2 -Ph), 4.65 (d, 1H, $J_{\text{gem}} = 12.2$ Hz, CH_2 -Ph), 4.19 (AB, 2H, $J_{\text{AB}} = 16.0$ Hz, CH_2 -CN), 3.82 (dd, 1H, $J_{2,3} = 3.3$ Hz, $J_{3,4} = 9.0$ Hz, H-3), 3.79 (dd, 1H, $J_{1,2} = 1.6$ Hz, $J_{2,3} = 3.3$ Hz, H-2), 3.77 (dq, 1H, $J_{4,5} = 9.0$ Hz, $J_{5,6} = 6.1$ Hz, H-5), 3.62 (dd, 1H, $J_{3,4} = 9.0$ Hz, $J_{4,5} = 9.0$ Hz, H-4), 2.04 (s, 3H, OAc), 1.35 (d, 3H, $J_{5,6} = 6.1$ Hz, H-6).

Ethyl 2,4-di-O-benzyl-3-O-cyanomethyl-1-thio- α -L-rhamnopyranoside (18)

Anhydrous DCM (30 mL) was added to the α -acetate **17** (200 mg, 0.470 mmol) along with ethanethiol (70.0 μL , 0.945 mmol, 0.839 g/mL) and boron trifluoride diethyl etherate (238 μL , 1.88 mmol, 1.12 g/mL) in a 100 mL round-bottomed flask and stirred under an argon atmosphere for 2 h at 0 $^\circ\text{C}$ and then

stirred at room temperature for 16 h. Saturated NaHCO_3 (aq.) (50 mL) was then added and the solution was stirred for 2 h. The resulting biphasic solution was then transferred to a separatory funnel. The organic phase was drained into an Erlenmeyer flask, dried with Na_2SO_4 , and filtered through cotton. The volatile components were removed using a rotary evaporator and the product was purified by silica gel chromatography using hexane-ethyl acetate, 6:1, as the eluent. The thioglycoside **18** was isolated as a colourless oil (147 mg, 427.56 g/mol, 73%); R_f 0.23 in hexane-ethyl acetate, 6:1. ES HRMS: (M+Na) exact mass: 450.1715, found: 450.1712. $[\alpha]_D -63.0^\circ$ (c 1, CH_2Cl_2). $^1\text{H NMR}$ (360 MHz, CDCl_3) δ : 7.25-7.40 (m, 10H, aromatic), 5.26 (d, 1H, $J_{1,2} = 1.5$ Hz, H-1), 4.77 (d, 1H, $J_{\text{gem}} = 10.9$ Hz, CH_2 -Ph), 4.74 (d, 1H, $J_{\text{gem}} = 12.2$ Hz, CH_2 -Ph), 4.64 (d, 1H, $J_{\text{gem}} = 11.0$ Hz, CH_2 -Ph), 4.63 (d, 1H, $J_{\text{gem}} = 12.2$ Hz, CH_2 -Ph), 4.17 (AB, 2H, $J_{\text{AB}} = 16.1$ Hz, CH_2 -CN), 4.02 (dq, 1H, $J_{4,5} = 9.3$ Hz, $J_{5,6} = 6.2$ Hz, H-5), 3.90 (dd, 1H, $J_{1,2} = 1.5$ Hz, $J_{2,3} = 3.2$ Hz, H-2), 3.75 (dd, 1H, $J_{2,3} = 3.2$ Hz, $J_{3,4} = 9.2$ Hz, H-3), 3.59 (dd, 1H, $J_{3,4} = 9.2$ Hz, $J_{4,5} = 9.3$ Hz, H-4), 2.55-2.60 (m, 2H, SCH_2CH_3), 1.35 (d, 3H, $J_{5,6} = 6.2$ Hz, H-6), 1.11 (t, 3H, $J = 7.3$ Hz, SCH_2CH_3).

Ethyl 3-O-(2-aminoethyl)-2,4-di-O-benzyl-1-thio- α -L-rhamnopyranoside (19)

Anhydrous THF (20 mL) was added to the nitrile **18** (180 mg, 0.421 mmol) along with borane-methyl sulphide complex (630 μL , 1.26 mmol, 2.0 M in THF) in a 100 mL round-bottomed flask and stirred under an argon atmosphere for 15 h under reflux. The resulting clear solution was then cooled to room

temperature and methanol was added (5 mL) and the solution was left to stir for 2 h. The volatiles were then removed using a rotary evaporator and DCM (50 mL) was added to the residue. The solution was then equilibrated between DCM and water (30 mL) in a separatory funnel. The organic phase was drained into an Erlenmeyer flask, dried with Na_2SO_4 , and filtered through cotton. The solvent was removed using a rotary evaporator and the product was purified by silica gel chromatography using DCM – methanol, 10:1, as the eluent. The amine **19** was isolated as a colourless oil (131 mg, 431.59 g/mol, 72%); R_f 0.39 in toluene-ethyl acetate – methanol, 7.5:2:0.5. ES HRMS: (M+H) exact mass: 432.2209, found: 432.2201. $[\alpha]_D^{25}$ -67.7° (c 0.9, CH_2Cl_2). ^1H NMR (300 MHz, CDCl_3) δ : 7.24-7.41 (m, 10H, aromatic), 5.29 (bs, 1H, H-1), 4.83 (d, 1H, $J_{\text{gem}} = 11.1$ Hz, CH_2 -Ph), 4.74 (d, 1H, $J_{\text{gem}} = 12.2$ Hz, CH_2 -Ph), 4.64 (d, 2H, $J_{\text{gem}} = 11.0$ Hz, CH_2 -Ph), 4.01 (dq, 1H, $J_{4,5} = 9.1$ Hz, $J_{5,6} = 6.2$ Hz, H-5), 3.87 (bt, 1H, $J_{2,3} = 2.3$ Hz, H-2), 3.63 (dd, 1H, $J_{2,3} = 2.3$ Hz, $J_{3,4} = 9.3$ Hz, H-3), 3.55 (dd, 1H, $J_{3,4} = 9.3$ Hz, $J_{4,5} = 9.1$ Hz, H-4), 3.45-3.55 (m, 2H, $\text{CH}_2\text{CH}_2\text{NH}_2$), 2.83 (bt, 2H, $\text{CH}_2\text{CH}_2\text{NH}_2$), 2.55-2.60 (m, 4H, SCH_2CH_3 , NH_2), 1.31 (d, 3H, $J_{5,6} = 6.2$ Hz, H-6), 1.23 (t, 3H, $J = 7.3$ Hz, SCH_2CH_3).

Ethyl 3-O-(2-N-acetyl-amidoethyl)-2,4-di-O-benzyl-1-thio- α -L-rhamnopyranoside (20)

Distilled DCM (20 mL) was added to the amine **19** (40 mg, 0.0927 mmol) along with acetic anhydride (50 μL , 0.530 mmol, 1.082 g/mL) in a 50 mL round-bottomed flask and stirred for 15 h at room temperature. The volatiles were then removed using a rotary evaporator and the product was purified by silica gel

chromatography using toluene-ethyl acetate, 2:1, as the eluent. The acetamide **20** was isolated as a colourless oil (42 mg, 473.63 g/mol, 95%); R_f 0.14 in toluene-ethyl acetate, 2:1. ES HRMS: (M+Na) exact mass: 496.2134, found: 496.2138. $[\alpha]_D$ -57.8° (c 0.9, CH_2Cl_2). ^1H NMR (360 MHz, CDCl_3) δ : 7.24-7.39 (m, 10H, aromatic), 5.84 (bs, 1H, NHAc), 5.29 (d, 1H, $J_{1,2} = 1.7$ Hz, H-1), 4.82 (d, 1H, $J_{\text{gem}} = 11.2$ Hz, $\text{CH}_2\text{-Ph}$), 4.75 (d, 1H, $J_{\text{gem}} = 12.4$ Hz, $\text{CH}_2\text{-Ph}$), 4.68 (d, 1H, $J_{\text{gem}} = 11.2$ Hz, $\text{CH}_2\text{-Ph}$), 4.60 (d, 1H, $J_{\text{gem}} = 12.4$ Hz, $\text{CH}_2\text{-Ph}$), 4.03 (dq, 1H, $J_{4,5} = 8.7$ Hz, $J_{5,6} = 6.2$ Hz, H-5), 3.82 (dd, 1H, $J_{1,2} = 1.7$ Hz, $J_{2,3} = 2.7$ Hz, H-2), 3.61 (dd, 1H, $J_{2,3} = 2.7$ Hz, $J_{3,4} = 9.4$ Hz, H-3), 3.56 (dd, 1H, $J_{3,4} = 9.4$ Hz, $J_{4,5} = 8.7$ Hz, H-4), 3.53-3.31 (m, 4H, $\text{CH}_2\text{CH}_2\text{NHAc}$), 2.56-2.61 (m, 2H, SCH_2CH_3), 1.36 (d, 3H, $J_{5,6} = 6.2$ Hz, H-6), 1.23 (t, 3H, $J = 7.3$ Hz, SCH_2CH_3).

Ethyl 3-O-(2-N-benzoyl-aminoethyl)-2,4-di-O-benzyl-1-thio- α -L-rhamnopyranoside

(**21**)

Distilled DCM (20 mL) was added to the amine **19** (80 mg, 0.185 mmol) along with benzoyl chloride (100 μL , 0.862 mmol, 1.211 g/mL) in a 50 mL round-bottomed flask and stirred for 15 h at room temperature. The volatiles were then removed using a rotary evaporator and the product was purified by silica gel chromatography using toluene-ethyl acetate, 4:1, as the eluent. The benzamide **21** was isolated as a colourless oil (87 mg, 535.70 g/mol, 88%); R_f 0.44 in toluene-ethyl acetate, 3:1. ES HRMS: (M+Na) exact mass: 558.2290, found: 558.2300. $[\alpha]_D$ -21.0° (c 1, CH_2Cl_2). ^1H NMR (360 MHz, CDCl_3) δ : 7.20-7.61 (m, 15H, aromatic),

6.60 (bs, 1H, NHBz), 5.30 (d, 1H, $J_{1,2} = 1.4$ Hz, H-1), 4.86 (d, 1H, $J_{\text{gem}} = 11.2$ Hz, $\text{CH}_2\text{-Ph}$), 4.73 (d, 1H, $J_{\text{gem}} = 12.3$ Hz, $\text{CH}_2\text{-Ph}$), 4.67 (d, 1H, $J_{\text{gem}} = 11.2$ Hz, $\text{CH}_2\text{-Ph}$), 4.62 (d, 1H, $J_{\text{gem}} = 12.3$ Hz, $\text{CH}_2\text{-Ph}$), 4.03 (dq, 1H, $J_{4,5} = 8.9$ Hz, $J_{5,6} = 6.2$ Hz, H-5), 3.87 (dd, 1H, $J_{1,2} = 1.4$ Hz, $J_{2,3} = 3.1$ Hz, H-2), 3.68 (dd, 1H, $J_{2,3} = 3.1$ Hz, $J_{3,4} = 9.3$ Hz, H-3), 3.67 (dd, 1H, $J_{3,4} = 9.3$ Hz, $J_{4,5} = 8.9$ Hz, H-4), 3.65-3.50 (m, 4H, $\text{CH}_2\text{CH}_2\text{NHBz}$), 2.56-2.61 (m, 2H, SCH_2CH_3), 1.37 (d, 3H, $J_{5,6} = 6.2$ Hz, H-6), 1.23 (t, 3H, $J = 7.3$ Hz, SCH_2CH_3).

Ethyl 3-O-(2-N-[N- α -acetamido-L-alanyl-]-aminoethyl)-2,4-di-O-benzyl-1-thio- α -L-rhamnopyranoside (22)

Dry DMF (10 mL) was added to the amine **19** (40 mg, 0.0927 mmol) along with *N- α -Fmoc-L-alanine* pentafluorophenyl ester (66 mg, 0.138 mmol) in a 50 mL round-bottomed flask and stirred for 15 h at room temperature. The volatiles were then removed using a rotary evaporator and the intermediate was purified by silica gel chromatography using toluene-ethyl acetate, 3:1, as the eluent. The Fmoc-protected intermediate was isolated as a colourless oil (64 mg, 95%). Dry DMF (10 mL) was added to this material along with piperidine (2 mL) and the solution was stirred for 1 h at room temperature. The volatiles were removed using a rotary evaporator and DCM (10 mL) and acetic anhydride (50 μL , 0.530 mmol, 1.082 g/mL) were added to the solution and the solution was stirred for 3 h at room temperature. The volatiles were then removed using a rotary evaporator and the product was purified by silica gel chromatography

using toluene-ethyl acetate – methanol, 7.5:2:0.5, as the eluent. The amide **22** was isolated as a colourless oil (41 mg, 544.70 g/mol, 82%); R_f 0.23 in hexane-ethyl acetate, 7.5:2:0.5. ES HRMS: (M+Na) exact mass: 567.2505, found: 567.2498. $[\alpha]_D^{+5.0}$ (c 0.8, CH_2Cl_2). ^1H NMR (300 MHz, CDCl_3) δ : 7.24-7.40 (m, 10H, aromatic), 6.28 (bt, 1H, $\text{CH}_2\text{CH}_2\text{NHCO}$), 5.97 (bd, 1H, NHAc), 5.27 (d, 1H, $J_{1,2} = 0.8$ Hz, H-1), 4.81 (d, 1H, $J_{\text{gem}} = 11.1$ Hz, $\text{CH}_2\text{-Ph}$), 4.73 (d, 1H, $J_{\text{gem}} = 12.3$ Hz, $\text{CH}_2\text{-Ph}$), 4.68 (d, 1H, $J_{\text{gem}} = 11.1$ Hz, $\text{CH}_2\text{-Ph}$), 4.62 (d, 1H, $J_{\text{gem}} = 12.3$ Hz, $\text{CH}_2\text{-Ph}$), 4.09 (p, 1H, $J = 7.0$ Hz, NHCHCH_3), 4.00 (dq, 1H, $J_{4,5} = 8.1$ Hz, $J_{5,6} = 6.2$ Hz, H-5), 3.81 (dd, 1H, $J_{1,2} = 0.8$ Hz, $J_{2,3} = 3.5$ Hz, H-2), 3.57 (dd, 1H, $J_{2,3} = 3.5$ Hz, $J_{3,4} = 10.4$ Hz, H-3), 3.55 (dd, 1H, $J_{3,4} = 10.4$ Hz, $J_{4,5} = 8.1$ Hz, H-4), 3.52-3.21 (m, 4H, $\text{CH}_2\text{CH}_2\text{NHCO}$), 2.55-2.60 (m, 2H, SCH_2CH_3), 1.89 (s, 3H, NHAc), 1.32 (d, 3H, $J_{5,6} = 6.2$ Hz, H-6), 1.23 (t, 3H, $J = 7.3$ Hz, SCH_2CH_3), 1.15 (d, 3H, $J = 7.0$ Hz, NHCHCH_3).

Allyl 3-O-(3-O-[2-N-acetyl-aminoethyl]-2,4-di-O-benzyl- α -L-rhamnopyranosyl)-4,6-O-benzylidene-2-deoxy-2-phthalimido- β -D-glucoopyranoside (27)

Anhydrous DCM (20 mL) was added to the glycosyl donor **20** (35 mg, 0.0739 mmol) along with the acceptor **26**⁸⁵ (25 mg, 0.0572 mmol) and 4 Å molecular sieves (500 mg) in a 50 mL round-bottomed flask and stirred under an argon atmosphere for 12 h at room temperature. Trifluoromethanesulphonic acid (2 μL , 0.00203 mmol, 1.696 g/mL) and *N*-iodosuccinimide (33 mg, 0.147 mmol) were then added and the solution was stirred for 1 h. The resulting dark purple solution was then filtered through celite in a sintered glass funnel and the

supernatant solution was equilibrated between DCM and saturated $\text{Na}_2\text{S}_2\text{O}_3$ (aq.) (30 mL) in a separatory funnel. The organic phase was drained into an Erlenmeyer flask, dried with Na_2SO_4 , and filtered through cotton. The volatile components were removed using a rotary evaporator and the product was purified by silica gel chromatography using toluene-ethyl acetate, 1:1, as the eluent. The disaccharide **27** was isolated as a colourless oil (19 mg, 848.93 g/mol, 40%); R_f 0.26 in toluene-ethyl acetate, 1:1. ES HRMS: (M+Na) exact mass: 871.3418, found: 871.3417. $[\alpha]_D -20.2^\circ$ (c 0.5, CH_2Cl_2). ^1H NMR (500 MHz, CDCl_3) δ : 7.87-7.72 (m, 4H, Phth), 7.48-7.42 (m, 14H, aromatic), 6.92-6.95 (m, 2H, aromatic), 5.77 (bs, 1H, NHAc), 5.64-5.69 (m, 1H, $\text{O-CH}_2\text{-CH=CH}_2$), 5.53 (s, 1H, CH-Ph), 5.31 (d, 1H, $J_{1,2} = 8.6$ Hz, H-1), 5.03-5.10 (m, 2H, $\text{O-CH}_2\text{-CH=CH}_2$), 4.66 (d, 1H, $J_{\text{gem}} = 11.3$ Hz, $\text{CH}_2\text{-Ph}$), 4.64 (d, 1H, $J_{1,2} = 1.7$ Hz, H-1'), 4.60 (dd, 1H, $J_{2,3} = 10.2$ Hz, $J_{3,4} = 8.9$ Hz, H-3), 4.51 (d, 1H, $J_{\text{gem}} = 11.3$ Hz, $\text{CH}_2\text{-Ph}$), 4.39 (dd, 1H, $J_{5,6a} = 4.2$ Hz, $J_{6a,6b} = 10.3$ Hz, H-6a), 4.28 (dd, 1H, $J_{1,2} = 8.6$ Hz, $J_{2,3} = 10.2$ Hz, H-2), 4.22-4.30 (m, 1H, $\text{O-CH}_2\text{-CH=CH}_2$), 4.02-4.06 (m, 1H, $\text{O-CH}_2\text{-CH=CH}_2$), 4.01 (d, 1H, $J_{\text{gem}} = 12.0$ Hz, $\text{CH}_2\text{-Ph}$), 3.86 (d, 1H, $J_{\text{gem}} = 12.0$ Hz, $\text{CH}_2\text{-Ph}$), 3.84 (ddd, 1H, $J_{4,5} = 10.1$ Hz, $J_{5,6a} = 4.2$ Hz, $J_{5,6b} = 2.2$ Hz, H-5), 3.84 (dq, 1H, $J_{4,5'} = 9.6$ Hz, $J_{5,6'} = 6.1$ Hz, H-5'), 3.65 (dd, 1H, $J_{3,4} = 8.9$ Hz, $J_{4,5} = 10.1$ Hz, H-4), 3.65 (dd, 1H, $J_{5,6b} = 2.2$ Hz, $J_{6a,6b} = 10.3$ Hz, H-6b), 3.53-3.31 (m, 4H, $\text{CH}_2\text{CH}_2\text{NHAc}$), 3.52 (dd, 1H, $J_{2,3} = 3.2$ Hz, $J_{3,4'} = 9.5$ Hz, H-3'), 3.35 (dd, 1H, $J_{1,2} = 1.7$ Hz, $J_{2,3} = 3.2$ Hz, H-2'), 3.29 (dd, 1H, $J_{3,4'} = 9.5$ Hz, $J_{4,5'} = 9.6$ Hz, H-4'), 1.52 (s, 3H, NHAc), 0.83 (d, 3H, $J_{5,6'} = 6.1$ Hz, H-6'). ^{13}C NMR (125 MHz, CDCl_3)

δ : 97.7 ($J_{C-1,H-1} = 165.2$ Hz, C-1), 97.6 ($J_{C-1',H-1'} = 166.6$ Hz, C-1').

Allyl 3-O-(3-O-[2-N-benzoyl-aminoethyl]-2,4-di-O-benzyl- α -L-rhamnopyranosyl)-4,6-O-benzylidene-2-deoxy-2-phthalimido- β -D-glucopyranoside (28)

Anhydrous DCM (20 mL) was added to the glycosyl donor **21** (80 mg, 0.149 mmol) along with the acceptor **26** (50 mg, 0.114 mmol) and 4 Å molecular sieves (500 mg) in a 50 mL round-bottomed flask and stirred under an argon atmosphere for 16 h at room temperature. Trifluoromethanesulphonic acid (3 μ L, 0.00310 mmol, 1.696 g/mL) and *N*-iodosuccinimide (67 mg, 0.298 mmol) were then added and the solution was stirred for 1 h. The resulting dark purple suspension was then filtered through celite in a sintered glass funnel and the supernatant solution was equilibrated between DCM and saturated Na₂S₂O₃ (aq.) (30 mL) in a separatory funnel. The organic phase was drained into an Erlenmeyer flask, dried with Na₂SO₄, and filtered through cotton. The volatile components were removed using a rotary evaporator and the product was purified by silica gel chromatography using toluene-ethyl acetate, 3:1, as the eluent. The disaccharide **28** was isolated as a colourless oil (36 mg, 911.00 g/mol, 35%); *R*_f 0.45 in toluene-ethyl acetate, 2:1. ES HRMS: (M+Na) exact mass: 933.3574, found: 933.3575. $[\alpha]_D^{25} -32.9^\circ$ (*c* 1.0, CH₂Cl₂). ¹H NMR (300 MHz, CDCl₃) δ : 7.83-7.68 (m, 4H, Phth), 7.54-7.10 (m, 19H, aromatic), 6.84-6.90 (m, 2H, aromatic), 6.45 (bt, 1H, NHBz), 5.64-5.71 (m, 1H, O-CH₂-CH=CH₂), 5.49 (s, 1H, CH-Ph), 5.30 (d, 1H, $J_{1,2} = 8.5$ Hz, H-1), 5.04-5.07 (m, 2H, O-CH₂-CH=CH₂), 4.68

(d, 1H, $J_{\text{gem}} = 11.3$ Hz, $\text{CH}_2\text{-Ph}$), 4.64 (d, 1H, $J_{1,2'} = 1.7$ Hz, H-1'), 4.58 (dd, 1H, $J_{2,3} = 10.3$ Hz, $J_{3,4} = 8.9$ Hz, H-3), 4.49 (d, 1H, $J_{\text{gem}} = 11.3$ Hz, $\text{CH}_2\text{-Ph}$), 4.38 (dd, 1H, $J_{5,6a} = 4.3$ Hz, $J_{6a,6b} = 10.3$ Hz, H-6a), 4.28 (dd, 1H, $J_{1,2} = 8.5$ Hz, $J_{2,3} = 10.3$ Hz, H-2), 4.25-4.29 (m, 1H, $\text{O-CH}_2\text{-CH=CH}_2$), 4.00-4.04 (m, 1H, $\text{O-CH}_2\text{-CH=CH}_2$), 3.96 (d, 1H, $J_{\text{gem}} = 12.1$ Hz, $\text{CH}_2\text{-Ph}$), 3.87 (d, 1H, $J_{\text{gem}} = 12.1$ Hz, $\text{CH}_2\text{-Ph}$), 3.85 (dq, 1H, $J_{4',5'} = 9.5$ Hz, $J_{5',6'} = 6.2$ Hz, H-5'), 3.81 (ddd, 1H, $J_{4,5} = 10.1$ Hz, $J_{5,6a} = 4.3$ Hz, $J_{5,6b} = 2.1$ Hz, H-5), 3.63 (dd, 1H, $J_{5,6b} = 2.1$ Hz, $J_{6a,6b} = 10.3$ Hz, H-6b), 3.61-3.45 (m, 4H, $\text{CH}_2\text{CH}_2\text{NHIBz}$), 3.59 (dd, 1H, $J_{3,4} = 8.9$ Hz, $J_{4,5} = 10.1$ Hz, H-4), 3.57 (dd, 1H, $J_{2,3'} = 3.0$ Hz, $J_{3',4'} = 9.5$ Hz, H-3'), 3.37 (dd, 1H, $J_{1,2'} = 1.7$ Hz, $J_{2,3'} = 3.0$ Hz, H-2'), 3.31 (dd, 1H, $J_{3',4'} = 9.5$ Hz, $J_{4',5'} = 9.5$ Hz, H-4'), 0.81 (d, 3H, $J_{5',6'} = 6.2$ Hz, H-6'). ^{13}C NMR (125 MHz, CDCl_3) δ : 97.8 ($J_{\text{C-1',H-1'}} = 167.0$ Hz, C-1'), 97.6 ($J_{\text{C-1,H-1}} = 165.2$ Hz, C-1).

Allyl 3-O-(3-O-[2-N-{N- α -acetamido-L-alanyl-}-aminoethyl]-2,4-di-O-benzyl- α -L-rhamnopyranosyl)-4,6-O-benzylidene-2-deoxy-2-phthalimido- β -D-glucopyranoside (29)

Anhydrous DCM (20 mL) was added to the glycosyl donor **22** (50 mg, 0.0916 mmol) along with the acceptor **26** (31 mg, 0.0709 mmol) and 4 Å molecular sieves (500 mg) in a 50 mL round-bottomed flask and stirred under an argon atmosphere for 12 h at room temperature. The suspension was then cooled to -78 °C and trifluoromethanesulfonic acid (2 μL , 0.002 mmol, 1.696 g/mL) and *N*-iodosuccinimide (41 mg, 0.182 mmol) were then added and the solution was stirred for 1 h. The resulting dark purple solution was then filtered through celite in a sintered glass funnel and the supernatant solution was

equilibrated between DCM and saturated $\text{Na}_2\text{S}_2\text{O}_3$ (aq.) (30 mL) in a separatory funnel. The organic phase was drained into an Erlenmeyer flask, dried with Na_2SO_4 , and filtered through cotton. The volatile components were removed using a rotary evaporator and the product was purified by silica gel chromatography using toluene-ethyl acetate-methanol, 7.5:2:0.5, as the eluent. The disaccharide **29** was isolated as a colourless oil (23 mg, 1100.21 g/mol, 30%); R_f 0.18 in toluene-ethyl acetate-methanol, 7.5:2:0.5. ES HRMS: (M+Na) exact mass: 942.3789, found: 942.3796. $[\alpha]_D -10.5^\circ$ (c 1.0, CH_2Cl_2). ^1H NMR (500 MHz, CDCl_3) δ : 7.86-7.71 (m, 4H, Phth), 7.45-7.18 (m, 14H, aromatic), 6.90-6.96 (m, 2H, aromatic), 6.06 (bt, 1H, $\text{CH}_2\text{-CH}_2\text{-NH-CO}$), 5.94 (bd, 1H, $J = 7.1$ Hz, NHAc), 5.64-6.67 (m, 1H, $\text{O-CH}_2\text{-CH=CH}_2$), 5.51 (s, 1H, CH-Ph), 5.31 (d, 1H, $J_{1,2} = 8.6$ Hz, H-1), 5.04-5.09 (m, 2H, $\text{O-CH}_2\text{-CH=CH}_2$), 4.65 (d, 1H, $J_{\text{gem}} = 11.3$ Hz, $\text{CH}_2\text{-Ph}$), 4.61 (d, 1H, $J_{1,2'} = 1.8$ Hz, H-1'), 4.59 (dd, 1H, $J_{2,3} = 10.4$ Hz, $J_{3,4} = 8.5$ Hz, H-3), 4.51 (d, 1H, $J_{\text{gem}} = 11.3$ Hz, $\text{CH}_2\text{-Ph}$), 4.38 (dd, 1H, $J_{5,6a} = 4.7$ Hz, $J_{6a,6b} = 10.8$ Hz, H-6a), 4.27 (dd, 1H, $J_{1,2} = 8.6$ Hz, $J_{2,3} = 10.4$ Hz, H-2), 4.23-4.27 (m, 1H, $\text{O-CH}_2\text{-CH=CH}_2$), 4.03 (p, 1H, $J = 7.1$ Hz, $\text{CO-CH}(\text{CH}_3)\text{-NH}$), 4.00-4.05 (m, 1H, $\text{O-CH}_2\text{-CH=CH}_2$), 3.97 (d, 1H, $J_{\text{gem}} = 12.1$ Hz, $\text{CH}_2\text{-Ph}$), 3.86 (d, 1H, $J_{\text{gem}} = 12.0$ Hz, $\text{CH}_2\text{-Ph}$), 3.83 (dq, 1H, $J_{4,5'} = 9.6$ Hz, $J_{5,6'} = 6.1$ Hz, H-5'), 3.82 (ddd, 1H, $J_{4,5} = 9.3$ Hz, $J_{5,6a} = 4.7$ Hz, $J_{5,6b} = 3.4$ Hz, H-5), 3.66 (dd, 1H, $J_{5,6b} = 3.4$ Hz, $J_{6a,6b} = 10.8$ Hz, H-6b), 3.63 (dd, 1H, $J_{3,4} = 8.5$ Hz, $J_{4,5} = 9.3$ Hz, H-4), 3.49 (dd, 1H, $J_{2,3'} = 3.2$ Hz, $J_{3',4'} = 9.5$ Hz, H-3'), 3.34-3.17 (m, 4H, $\text{CH}_2\text{-CH}_2\text{-NH-CO}$), 3.33 (dd, 1H, $J_{1,2'} = 1.8$ Hz, $J_{2,3'} = 3.2$ Hz, H-2'), 3.27 (dd, 1H, $J_{3',4'} = 9.5$ Hz, $J_{4',5'} = 9.6$ Hz, H-4'), 1.88 (s, 3H, NHAc), 1.13 (d, 3H, $\text{CO-CH}(\text{CH}_3)\text{-NH}$),

0.81 (d, 3H, $J_{5,6} = 6.1$ Hz, H-6'). ^{13}C NMR (125 MHz, CDCl_3) δ : 97.8 ($J_{\text{C-1}',\text{H-1}'} = 168.5$ Hz, C-1'),
97.7 ($J_{\text{C-1},\text{H-1}} = 166.3$ Hz, C-1).

Allyl 2-acetamido-3-O-(3-O-[2-N-acetyl-aminoethyl]-2,4-di-O-benzyl- α -L-rhamnopyranosyl)-4,6-O-benzylidene-2-deoxy- β -D-glucofuranoside (30)

Ethylenediamine (3 mL) and *t*-butyl alcohol (10 mL) were added to the phthalimide **27** (40 mg, 0.0471 mmol) in a 50 mL round-bottomed flask and stirred under an argon atmosphere for 15 h at 115°C. The resulting pale yellow solution was then cooled to room temperature. The volatiles were then removed using a rotary evaporator and methanol (10 mL) was added to the residue along with acetic anhydride (50 μL , 0.530 mmol, 1.082 g/mL) and the solution was stirred for 2 h at room temperature. The volatiles were removed using a rotary evaporator and the product was purified by silica gel chromatography using toluene-ethyl acetate-methanol, 7.5:2:0.5, as the eluent. The acetamide **30** was isolated as a white solid (28 mg, 760.87 g/mol, 78%); R_f 0.09 in toluene-ethyl acetate-methanol, 7.5:2:0.5. ES HRMS: (M+Na) exact mass: 783.3469, found: 783.3476. $[\alpha]_D^{25} +12.6^\circ$ (*c* 0.8, MeOH). ^1H NMR (300 MHz, CDCl_3) δ : 7.46-7.22 (m, 15H, aromatic), 5.80-5.87 (m, 2H, O-CH₂-CH=CH₂, NHAc), 5.58 (bd, 1H, NHAc, $J_{\text{NH}_2} = 8.3$ Hz), 5.48 (s, 1H, CH-Ph), 5.22-5.26 (m, 2H, O-CH₂-CH=CH₂), 4.98 (bs, 1H, H-1'), 4.79 (d, 1H, $J_{1,2} = 8.2$ Hz, H-1), 4.76 (d, 1H, $J_{\text{gem}} = 11.2$ Hz, CH₂-Ph), 4.66 (d, 1H, $J_{\text{gem}} = 12.5$ Hz, CH₂-Ph), 4.56 (d, 2H, $J_{\text{gem}} = 12.0$ Hz, 2 X CH₂-Ph), 4.30-4.36

(m, 2H, O-CH₂-CH=CH₂, H-6a), 4.24 (dd, 1H, J_{2,3} = 10.2 Hz, J_{3,4} = 8.9 Hz, H-3), 4.02-4.07 (m, 1H, O-CH₂-CH=CH₂), 3.93 (dq, 1H, J_{4,5'} = 9.6 Hz, J_{5,6'} = 6.1 Hz, H-5'), 3.34-3.37 (m, 2H, CH₂CH₂NHAc, H-2'), 3.52 (dd, 1H, J_{2,3'} = 3.1 Hz, J_{3,4'} = 9.3 Hz, H-3'), 3.59-3.26 (m, 7H, CH₂CH₂NHAc, H-2, H-4, H-5, H-6b), 3.42 (dd, 1H, J_{3,4'} = 9.5 Hz, J_{4,5'} = 9.6 Hz, H-4'), 1.88 (s, 3H, NHAc), 1.56 (s, 3H, NHAc), 0.91 (d, 3H, J_{5,6'} = 6.2 Hz, H-6').

n-Propyl 2-deoxy-2-acetamido-3-O-(3-O-[2-N-acetyl-aminoethyl- α -L-rhamnopyranosyl)- β -D-glucopyranoside (4)

Acetic acid (10 mL) was added to the protected disaccharide **30** (20 mg, 0.0263 mmol) in a 25 mL round-bottomed flask along with palladium (10 mg, 10% on carbon) and the suspension was stirred under a hydrogen atmosphere for 24 h at room temperature. The resulting solution was then filtered through celite using a sintered glass funnel. The volatiles were then removed using a rotary evaporator. Acetic acid (8 mL) and water (2 mL) were added and the solution was stirred for 2 h at 80°C. The volatiles were removed using a rotary evaporator. Distilled water (5 mL) was added to the residue and the solution was passed through a Sep-Pak cartridge. The product was purified by reversed-phase high performance liquid chromatography using water – acetonitrile, 20:1, as the eluent. The deprotected disaccharide **4** was isolated as a colourless oil (7 mg, 494.53 g/mol, 54%); R_f 0.39 in ethyl acetate – methanol – water, 7:2:1. ES HRMS: (M+H) exact mass: 495.2554, found: 495.2563.

$[\alpha]_D -37.2^\circ$ (c 0.5, CH_2Cl_2). $^1\text{H NMR}$ (500 MHz, D_2O) δ : 4.88 (d, 1H, $J_{1,2} = 1.7\text{ Hz}$, H-1'), 4.56 (d, 1H, $J_{1,2} = 8.6\text{ Hz}$, H-1), 4.01 (dq, 1H, $J_{4,5'} = 9.3\text{ Hz}$, $J_{5',6} = 6.3\text{ Hz}$, H-5'), 3.95 (dd, 1H, $J_{1,2} = 1.7\text{ Hz}$, $J_{2,3'} = 2.6\text{ Hz}$, H-2'), 3.90 (dd, 1H, $J_{5,6a} = 1.9\text{ Hz}$, $J_{6a,6b} = 12.2\text{ Hz}$, H-6a), 3.80-3.85 (m, 2H, $-\text{O}-\text{CH}_2\text{CH}_2\text{CH}_3$), 3.78 (dd, 1H, $J_{1,2} = 8.5\text{ Hz}$, $J_{2,3} = 10.2\text{ Hz}$, H-2), 3.72 (dd, 1H, $J_{5,6b} = 5.5\text{ Hz}$, $J_{6a,6b} = 11.7\text{ Hz}$, H-6b), 3.65-3.38 (m, 4H, $\text{CH}_2\text{CH}_2\text{NHAc}$), 3.59 (dd, 1H, $J_{2,3} = 10.2\text{ Hz}$, $J_{3,4} = 8.9\text{ Hz}$, H-3), 3.52 (dd, 1H, $J_{2,3'} = 2.2\text{ Hz}$, $J_{3,4'} = 9.1\text{ Hz}$, H-3'), 3.48 (dd, 1H, $J_{3,4'} = J_{4',5} = 9.1\text{ Hz}$, H-4'), 3.45 (dd, 1H, $J_{3,4} = 8.9\text{ Hz}$, $J_{4,5} = 10.1\text{ Hz}$, H-4), 3.42 (ddd, 1H, $J_{4,5} = 10.1\text{ Hz}$, $J_{5,6a} = 1.7\text{ Hz}$, $J_{5,6b} = 5.5\text{ Hz}$, H-5), 2.06 (s, 3H, NHAc), 2.01 (s, 3H, NHAc), 1.59 (sextuplet, 2H, $J = 7.3\text{ Hz}$, $\text{OCH}_2\text{CH}_2\text{CH}_3$), 1.24 (d, 3H, $J_{5',6} = 6.2\text{ Hz}$, H-6'), 0.88 (t, 3H, $-\text{OCH}_2\text{CH}_2\text{CH}_3$).

Allyl 2-acetamido-3-O-(3-O-[2-N-benzoyl-aminoethyl]-2,4-di-O-benzyl- α -L-rhamnopyranosyl)-4,6-O-benzylidene-2-deoxy- β -D-glucopyranoside (31)

Ethylenediamine (3 mL) and *t*-butyl alcohol (10 mL) were added to the phthalimide **28** (45 mg, 0.494 mmol) in a 50 mL round-bottomed flask and stirred under an argon atmosphere for 16 h at 115°C . The resulting pale yellow solution was then cooled to room temperature. The volatiles were then removed using a rotary evaporator and methanol (10 mL) was added to the residue along with acetic anhydride (50 μL , 0.530 mmol, 1.082 g/mL) and the solution was stirred for 2 h at room temperature. The volatiles were removed using a rotary evaporator and the product was purified by silica gel chromatography using

toluene-ethyl acetate-methanol, 7.5:2:0.5, as the eluent. The acetamide **31** was isolated as a white solid (27 mg, 822.94 g/mol, 66%); R_f 0.18 in toluene-ethyl acetate-methanol, 7.5:2:0.5. ES HRMS: (M+Na) exact mass: 845.3625, found: 845.3629. $[\alpha]_D^{25} +15.3^\circ$ (c 0.7, CH_2Cl_2). $^1\text{H NMR}$ (300 MHz, CDCl_3) δ : 7.58-7.17 (m, 20H, aromatic), 6.56 (bt, 1H, NHBz), 5.66-5.70 (m, 1H, $\text{O-CH}_2\text{-CH=CH}_2$), 5.70 (d, 1H, $J_{2,\text{NH}} = 8.1$ Hz, NHAc), 5.41 (s, 1H, CH-Ph), 5.18-5.22 (m, 2H, $\text{O-CH}_2\text{-CH=CH}_2$), 4.96 (d, 1H, $J_{1',2'} = 1.0$ Hz, H-1'), 4.79 (d, 1H, $J_{1,2} = 8.3$ Hz, H-1), 4.75 (d, 1H, $J_{\text{gem}} = 11.1$ Hz, $\text{CH}_2\text{-Ph}$), 4.56-4.60 (m, 3H, $\text{CH}_2\text{-Ph}$), 4.26-4.30 (m, 2H, $\text{O-CH}_2\text{-CH=CH}_2$, H-6a), 4.23 (t, 1H, $J_{2,3} = J_{3,4} = 9.1$ Hz, H-3), 4.01-4.04 (m, 1H, $\text{O-CH}_2\text{-CH=CH}_2$), 3.85 (dq, 1H, $J_{4',5'} = 9.5$ Hz, $J_{5',6'} = 6.2$ Hz, H-5'), 3.75 (dd, 1H, $J_{1',2'} = 1.7$ Hz, $J_{2,3'} = 2.2$ Hz, H-2'), 3.70 (ddd, 1H, $J_{4,5} = 9.2$ Hz, $J_{5,6a} = 3.6$ Hz, $J_{5,6b} = 2.1$ Hz, H-5), 3.61-3.50 (m, 4H, $\text{CH}_2\text{CH}_2\text{NHBz}$), 3.49-3.40 (m, 5H, H-2, H-4, H-6b, H-3', H-4'), 1.85 (s, 3H, NHAc), 0.88 (d, 3H, $J_{5',6'} = 6.2$ Hz, H-6').

n-Propyl 2-acetamido-3-O-(3-O-[2-N-benzoyl-aminoethyl]- α -L-rhamnopyranosyl)-2-deoxy- β -D-glucopyranoside (**5**)

Acetic acid (10 mL) was added to the protected disaccharide **31** (19 mg, 0.0231 mmol) in a 25 mL round-bottomed flask along with palladium (12 mg, 10% on carbon) and the suspension was stirred under a hydrogen atmosphere for 36 h at room temperature. The resulting solution was then filtered through celite using a sintered glass funnel. The volatiles were then removed using a rotary evaporator. Acetic acid (8 mL) and water (2 mL) were added and the

solution was stirred for 2 h at 80°C. The volatiles were removed using a rotary evaporator. Distilled water (5 mL) was added to the residue and the solution was passed through a C₁₈ Sep-Pak cartridge. The product was purified by reversed-phase high performance liquid chromatography using water – acetonitrile, 20:1, as the eluent. The deprotected disaccharide **5** was isolated as a colourless oil (8 mg, 556.60 g/mol, 62%); R_f 0.64 in ethyl acetate – methanol – water, 7:2:1. ES HRMS: (M+H) exact mass: 557.2710, found: 557.2710. [α]_D -22.7° (c 0.3, H₂O). ¹H NMR (300 MHz, D₂O) δ: 7.42-7.20 (m, 5H, aromatic), 4.89 (bs, 1H, H-1'), 4.56 (d, 1H, J_{1,2} = 8.5 Hz, H-1), 4.03 (dq, 1H, J_{4',5'} = 9.2 Hz, J_{5',6'} = 6.3 Hz, H-5'), 3.98 (dd, 1H, J_{1',2'} = 1.6 Hz, J_{2',3'} = 2.6 Hz, H-2'), 3.90 (dd, 1H, J_{5,6a} = 1.7 Hz, J_{6a,6b} = 12.2 Hz, H-6a), 3.84-3.87 (m, 2H, -OCH₂CH₂CH₃), 3.78 (dd, 1H, J_{1,2} = 8.5 Hz, J_{2,3} = 10.2 Hz, H-2), 3.72 (dd, 1H, J_{5,6b} = 5.3 Hz, J_{6a,6b} = 11.9 Hz, H-6b), 3.65-3.38 (m, 4H, CH₂CH₂NHAc), 3.59 (dd, 1H, J_{2,3} = 10.2 Hz, J_{3,4} = 8.9 Hz, H-3), 3.52 (dd, 1H, J_{2,3'} = 2.2 Hz, J_{3',4'} = 9.1 Hz, H-3'), 3.48 (dd, 1H, J_{3',4'} = J_{4',5'} = 9.1 Hz, H-4'), 3.45 (dd, 1H, J_{3,4} = 8.9 Hz, J_{4,5} = 10.1 Hz, H-4), 3.42 (ddd, 1H, J_{4,5} = 10.1 Hz, J_{5,6a} = 1.7 Hz, J_{5,6b} = 5.5 Hz, H-5), 2.06 (s, 3H, NHAc), 2.01 (s, 3H, NHAc), 1.59 (sextuplet, 2H, J = 7.3 Hz, -OCH₂CH₂CH₃), 1.24 (d, 3H, J_{5',6'} = 6.2 Hz, H-6'), 0.89 (t, 3H, -OCH₂CH₂CH₃).

Allyl 2-acetamido-3-O-(3-O-[2-N-{N-α-acetamido-L-alanyl-}aminoethyl]-2,4-di-O-benzyl-α-L-rhamnopyranosyl)-4,6-O-benzylidene-2-deoxy-β-D-glucopyranoside (32)

Ethylenediamine (3 mL) and *t*-butyl alcohol (10 mL) were added to the phthalimide **29** (38 mg, 0.0345 mmol) in a 50 mL round-bottomed flask and

stirred under an argon atmosphere for 20 h at 115°C. The resulting pale yellow solution was then cooled to room temperature. The volatiles were then removed using a rotary evaporator and methanol (10 mL) was added to the residue along with acetic anhydride (50 μ L, 0.530 mmol, 1.082 g/mL) and the solution was stirred for 2 h at room temperature. The volatiles were removed using a rotary evaporator and the product was purified by silica gel chromatography using toluene-acetone-methanol, 7.5:2:0.5, as the eluent. The acetamide **32** was isolated as a white solid (23 mg, 831.95 g/mol, 80%); R_f 0.31 in toluene-acetone-methanol, 7.5:2:0.5. ES HRMS: (M+Na) exact mass: 854.3840, found: 854.3840. $[\alpha]_D -23.4^\circ$ (c 0.5, MeOH). ^1H NMR (360 MHz, CDCl_3) δ : 7.36-7.12 (m, 15H, aromatic), 5.73-5.76 (m, 1H, $\text{OCH}_2\text{-CH}=\text{CH}_2$), 5.38 (s, 1H, CH-Ph), 5.12-5.16 (m, 2H, $\text{OCH}_2\text{CH}=\text{CH}_2$), 4.88 (d, 1H, $J_{1,2} = 1.5$ Hz, H-1'), 4.61 (d, 1H, $J_{1,2} = 8.2$ Hz, H-1), 4.60 (d, 1H, $J_{\text{gem}} = 11.2$ Hz, $\text{CH}_2\text{-Ph}$), 4.56 (d, 1H, $J_{\text{gem}} = 12.5$ Hz, $\text{CH}_2\text{-Ph}$), 4.54 (d, 2H, $J_{\text{gem}} = 12.0$ Hz, 2 X $\text{CH}_2\text{-Ph}$), 4.16-4.20 (m, 3H, $\text{OCH}_2\text{CH}=\text{CH}_2$, H-3, H-6a), 4.02 (q, 1H, $J = 7.1$ Hz, $\text{CO-CH}(\text{CH}_3)\text{-NH}$), 3.94-3.96 (m, 1H, $\text{OCH}_2\text{CH}=\text{CH}_2$), 3.83 (dq, 1H, $J_{4,5} = 9.6$ Hz, $J_{5,6'} = 6.1$ Hz, H-5'), 3.63-3.67 (m, 2H, $\text{CH}_2\text{CH}_2\text{NHAc}$, H-2'), 3.52 (dd, 1H, $J_{2,3'} = 3.1$ Hz, $J_{3,4'} = 9.2$ Hz, H-3'), 3.59-3.26 (m, 7H, $\text{CH}_2\text{CH}_2\text{NHAc}$, H-2, H-4, H-5, H-6b), 3.32 (dd, 1H, $J_{3,4'} = 9.5$ Hz, $J_{4,5'} = 9.6$ Hz, H-4'), 1.88 (s, 3H, NHAc), 1.86 (s, 3H, NHAc), 1.01 (d, 3H, $J_{5,6'} = 7.1$ Hz, CH-CH_3), 0.81 (d, 3H, $J_{5,6'} = 6.2$ Hz, H-6').

n-Propyl 2-acetamido-3-O-(3-O-[2-N-{N- α -acetamido-L-alanyl-}-aminoethyl]- α -L-rhamnopyranosyl)-2-deoxy- β -D-glucopyranoside (6)

Acetic acid (10 mL) was added to the protected disaccharide **32** (18 mg, 0.0216 mmol) in a 25 mL round-bottomed flask along with palladium (15 mg, 10% on carbon) and the suspension was stirred under a hydrogen atmosphere for 24 h. The resulting solution was then filtered through celite using a sintered glass funnel. The volatiles were then removed using a rotary evaporator. Acetic acid (8 mL) and water (2 mL) were added and the solution was stirred for 2 h at 80°C. The volatiles were removed using a rotary evaporator. Distilled water (5 mL) was added to the residue and the solution was passed through a Sep-Pak cartridge. The product was purified by reversed-phase high performance liquid chromatography using water – acetonitrile, 20:1, as the eluent. The deprotected disaccharide **6** was isolated as a clear oil (6 mg, 565.61 g/mol, 49%); R_f 0.33 in ethyl acetate – methanol – water, 7:2:1. ES HRMS: (M+H) exact mass: 566.2925, found: 566.2927. ^1H NMR (500 MHz, D_2O) δ : 4.88 (bs, 1H, H-1'), 4.56 (d, 1H, $J_{1,2} = 8.5$ Hz, H-1), 4.24 (q, 1H, $J = 7.0$ Hz, $\text{CH}_2\text{-CH}_3$), 4.01 (dq, 1H, $J_{4',5'} = 9.2$ Hz, $J_{5',6'} = 6.3$ Hz, H-5'), 3.96 (dd, 1H, $J_{1',2'} = 1.9$ Hz, $J_{2',3'} = 2.6$ Hz, H-2'), 3.90 (dd, 1H, $J_{5,6a} = 1.6$ Hz, $J_{6a,6b} = 12.2$ Hz, H-6a), 3.84-3.87 (m, 2H, $-\text{O-CH}_2\text{CH}_2\text{CH}_3$), 3.78 (dd, 1H, $J_{1,2} = 8.5$ Hz, $J_{2,3} = 10.2$ Hz, H-2), 3.72 (dd, 1H, $J_{5,6b} = 5.5$ Hz, $J_{6a,6b} = 11.7$ Hz, H-6b), 3.65-3.38 (m, 4H, $\text{CH}_2\text{CH}_2\text{NHAc}$), 3.59 (dd, 1H, $J_{2,3} = 10.2$ Hz, $J_{3,4} = 8.9$ Hz, H-3), 3.52 (dd, 1H, $J_{2',3'} = 2.2$ Hz, $J_{3',4'} = 9.1$ Hz, H-3'), 3.48 (dd, 1H, $J_{3',4'} = J_{4',5'} = 9.1$ Hz, H-4'), 3.45 (dd, 1H, $J_{3,4} = 8.9$ Hz, $J_{4,5} = 10.1$ Hz, H-4), 3.42 (ddd, 1H, $J_{4,5} = 10.1$ Hz, $J_{5,6a} = 1.7$ Hz,

$J_{5,6b} = 5.5$ Hz, H-5), 2.06 (s, 3H, NHAc), 2.01 (s, 3H, NHAc), 1.59 (sextuplet, 2H, $J = 7.3$ Hz, $-\text{OCH}_2\text{CH}_2\text{CH}_3$), 1.38 (d, 3H, $J_{5,6'} = 7.1$ Hz, $\text{CH}-\text{CH}_3$), 1.25 (d, 3H, $J_{5,6'} = 6.3$ Hz, H-6'), 0.89 (t, 3H, $-\text{OCH}_2\text{CH}_2\text{CH}_3$).

1-O-(3-O-acetyl-4,6-O-benzylidene-2-deoxy-2-phthalimido- β -D-glucopyranosyl)-(2R/2S)-glycerol (34)

Distilled acetone (16 mL) and water (2 mL) were added to the olefin **33**⁸⁵ (333 mg, 0.695 mmol) along with *N*-methyilmorpholine *N*-oxide (163 mg, 1.39 mmol) and osmium tetroxide (50 μL , 10% solution in *t*-butanol) in a 100 mL round-bottomed flask and stirred for 16 h at 50°C. Ethyl acetate (50 mL) and saturated NaHSO_3 (aq.) (50 mL) were then added and the solution was stirred for 2 h. The resulting biphasic solution was then transferred to a separatory funnel. The organic phase was drained into an Erlenmeyer flask, dried with Na_2SO_4 , and filtered through cotton. The solvent was removed using a rotary evaporator and the product was purified by silica gel chromatography using toluene-ethyl acetate, 1:1, as the eluent. The racemic diol **34** was isolated as a white morpous solid (332 mg, 513.49 g/mol, 93%); R_f 0.15 in toluene-ethyl acetate, 1:1. ES HRMS: (M+Na) exact mass: 536.1533, found: 536.1531. ^1H NMR (300 MHz, CDCl_3) δ : 7.87-7.72 (m, 4H, Phth), 7.48-7.32 (m, 5H, aromatic), 5.83-5.87 (m, 1H, H-3), 5.53 (s, 1H, $\text{CH}-\text{Ph}$), 5.46 (2 X d, 1H, $J_{1,2} = 8.5$ Hz, H-1), 4.40 (dd, 1H, $J_{5,6a} = 5.5$ Hz, $J_{6a,6b} = 9.8$ Hz, H-6a), 4.29 (dd, 1H, $J_{1,2} = 8.5$ Hz, $J_{3,4} = 10.2$ Hz, H-2), 3.86-3.44 (m, 7H, H-4, H-5, $\text{O}-\text{CH}_2-\text{CH}(\text{OH})-\text{CH}_2\text{OH}$), 1.80 (s, 3H, OAc).

2-O-(3-O-Acetyl-4,6-O-benzylidene-2-deoxy-2-phthalimido-β-D-glucopyranosyl)-2-hydroxy-ethan-1-al (35)

Distilled THF (10 mL) and water (10 mL) were added to the diol **34** (275 mg, 0.536 mmol) along with sodium periodate (172 mg, 0.804 mmol) in a 100 mL round-bottomed flask and stirred for 1 h at room temperature. Diethyl ether (75 mL) and water (50 mL) were then added and the resulting biphasic solution was then transferred to a separatory funnel. The organic phase was drained into an Erlenmeyer flask, dried with Na₂SO₄, and filtered through cotton. The solvent was removed using a rotary evaporator and the product was purified by silica gel chromatography using toluene-ethyl acetate, 2:1, as the eluent. The aldehyde **35** was isolated as a colourless oil (255 mg, 481.45 g/mol, 99%); R_f 0.29 in toluene – ethyl acetate, 2:1. ES HRMS: (M+Na) exact mass: 504.1270, found: 504.1275. [α]_D +54.0° (c 0.9, CH₂Cl₂). ¹H NMR (300 MHz, CDCl₃) δ: 9.56 (s, 1H, CHO), 7.87-7.72 (m, 4H, Phth), 7.48-7.32 (m, 5H, aromatic), 5.90 (dd, 1H, J_{2,3} = 8.9 Hz, J_{3,4} = 10.2 Hz, H-3), 5.53 (s, 1H, CH-Ph), 5.47 (d, 1H, J_{1,2} = 8.5 Hz, H-1), 4.40 (dd, 1H, J_{5,6a} = 5.5 Hz, J_{6a,6b} = 9.8 Hz, H-6a), 4.40 (dd, 1H, J_{1,2} = 8.5 Hz, J_{3,4} = 10.2 Hz, H-2), 4.19 (s, 2H, CH₂CHO), 3.75-3.80 (m, 3H, H-4, H-5, H-6b) 1.90 (s, 3H, OAc).

2-O-(3-O-Acetyl-4,6-O-benzylidene-2-deoxy-2-phthalimido-β-D-glucopyranosyl)-ethanediol (36)

Distilled methanol (40 mL) was added to the aldehyde **35** (210 mg, 0.436 mmol) along with sodium borohydride (33 mg, 0.872 mmol) in a 100 mL round-

bottomed flask and stirred for 1 h at room temperature. The volatiles were removed using a rotary evaporator and DCM (100 mL) was added to the residue. The solution was then equilibrated between DCM and water (50 mL) in a separatory funnel. The organic phase was drained into an Erlenmeyer flask, dried with Na_2SO_4 , and filtered through cotton. The solvent was removed using a rotary evaporator and the product was purified by silica gel chromatography using toluene-ethyl acetate, 1:1, as the eluent. The alcohol **36** was isolated as a white solid (202 mg, 483.47 g/mol, 96%); R_f 0.30 in toluene – ethyl acetate, 1:1. ES HRMS: (M+Na) exact mass: 506.1427, found: 506.1436. $[\alpha]_D^{25} +67.1^\circ$ (c 1, CH_2Cl_2). $^1\text{H NMR}$ (300 MHz, CDCl_3) δ : 7.87-7.72 (m, 4H, Phth), 7.48-7.36 (m, 5H, aromatic), 5.86 (dd, 1H, $J_{2,3} = 8.9$ Hz, $J_{3,4} = 10.3$ Hz, H-3), 5.53 (s, 1H, CH-Ph), 5.49 (d, 1H, $J_{1,2} = 8.5$ Hz, H-1), 4.40 (dd, 1H, $J_{5,6a} = 3.3$ Hz, $J_{6a,6b} = 9.5$ Hz, H-6a), 4.30 (dd, 1H, $J_{1,2} = 8.5$ Hz, $J_{3,4} = 10.2$ Hz, H-2), 3.75-3.81 (m, 5H, H-4, H-5, H-6b, $\text{O-CH}_2\text{-CH}_2\text{-OH}$), 3.60 (t, 2H, $\text{O-CH}_2\text{-CH}_2\text{-OH}$) 1.90 (s, 3H, OAc).

2-O-(3-O-Acetyl-4,6-O-benzylidene-2-deoxy-2-phthalimido- β -D-glucopyranosyl)-1-O-methanesulphonyl ethanediol (37)

Distilled DCM (40 mL) was added to the alcohol **36** (170 mg, 0.352 mmol) along with methanesulphonyl chloride (100 μL , 1.29 mmol, 1.480 g/mL) and pyridine (100 μL , 1.24 mmol, 0.978 g/mL) in a 50 mL round-bottomed flask and stirred for 10 h at room temperature. The solution was then equilibrated between DCM and 5% HCl (aq.) (20 mL) in a separatory funnel. The organic

phase was drained into an Erlenmeyer flask, dried with Na_2SO_4 , and filtered through cotton. The volatiles were then removed using a rotary evaporator and the product was purified by silica gel chromatography toluene-ethyl acetate, 3:1 as the eluent. The methane sulphonate **37** was isolated as a colourless oil (168 mg, 561.56 g/mol, 85%); R_f 0.24 in toluene-ethyl acetate, 3:1. ES HRMS: (M+Na) exact mass: 584.1202, found: 584.1198. $[\alpha]_D^{25} +37.3^\circ$ (c 0.8, CH_2Cl_2). ^1H NMR (300 MHz, CDCl_3) δ : 7.87-7.72 (m, 4H, Phth), 7.48-7.36 (m, 5H, aromatic), 5.86 (dd, 1H, $J_{2,3} = 8.9$ Hz, $J_{3,4} = 10.4$ Hz, H-3), 5.53 (s, 1H, CH-Ph), 5.49 (d, 1H, $J_{1,2} = 8.4$ Hz, H-1), 4.40 (dd, 1H, $J_{5,6a} = 4.1$ Hz, $J_{6a,6b} = 10.0$ Hz, H-6a), 4.28 (dd, 1H, $J_{1,2} = 8.4$ Hz, $J_{3,4} = 10.4$ Hz, H-2), 4.21 (t, 2H, $\text{O-CH}_2\text{-CH}_2\text{-OMs}$) 4.00-4.05 (m, 1H, $\text{O-CH}_2\text{-CH}_2\text{-OMs}$), 3.75-3.80 (m, 4H, H-4, H-5, H-6b, $\text{O-CH}_2\text{-CH}_2\text{-OMs}$), 2.80 (s, 3H, OMs), 1.90 (s, 3H, OAc).

1-O-(3-O-Acetyl-4,6-O-benzylidene-2-deoxy-2-phthalimido- β -D-glucopyranosyl)-2-azidoethanol (38)

Dry DMF (20 mL) was added to the methane sulphonate **37** (150 mg, 0.267 mmol) along with sodium azide (52 mg, 0.800 mmol) in a 50 mL round-bottomed flask and stirred for 16 h at 100°C. The volatiles were removed using a rotary evaporator and DCM (50 mL) was added to the residue. The solution was then equilibrated between DCM and water (50 mL) in a separatory funnel. The organic phase was drained into an Erlenmeyer flask, dried with Na_2SO_4 , and

filtered through cotton. The solvent was removed using a rotary evaporator and the product was purified by silica gel chromatography using toluene-ethyl acetate, 4:1, as the eluent. The azide **38** was isolated as a white solid (122 mg, 508.48 g/mol, 90%); R_f 0.51 in toluene – ethyl acetate, 3:1. ES HRMS: (M+Na) exact mass: 531.1492, found: 531.1505. $[\alpha]_D^{25} +23.0^\circ$ (c 0.7, CH_2Cl_2). ^1H NMR (300 MHz, CDCl_3) δ : 7.87-7.68 (m, 4H, Phth), 7.48-7.32 (m, 5H, aromatic), 5.86 (dd, 1H, $J_{2,3} = 8.9$ Hz, $J_{3,4} = 10.3$ Hz, H-3), 5.53 (s, 1H, CH-Ph), 5.52 (d, 1H, $J_{1,2} = 8.6$ Hz, H-1), 4.40 (dd, 1H, $J_{5,6a} = 4.2$ Hz, $J_{6a,6b} = 10.1$ Hz, H-6a), 4.30 (dd, 1H, $J_{1,2} = 8.4$ Hz, $J_{3,4} = 10.4$ Hz, H-2), 3.94-3.97 (m, 1H, $\text{O-CH}_2\text{-CH}_2\text{-N}_3$), 3.76-3.79 (m, 3H, H-4, H-5, H-6b), 3.63-3.65 (m, 1H, $\text{O-CH}_2\text{-CH}_2\text{-N}_3$), 3.32-3.34 (m, 1H, $\text{O-CH}_2\text{-CH}_2\text{-N}_3$), 3.15-3.18 (m, 1H, $\text{O-CH}_2\text{-CH}_2\text{-N}_3$), 1.90 (s, 3H, OAc).

1-O-(4,6-O-Benzylidene-2-deoxy-2-phthalimido- β -D-glucopyranosyl)-2-azido-ethanol

(39)

Distilled methanol (50 mL) was added to the acetate **38** (110 mg, 0.216 mmol) along with sodium (10 mg, 0.435 mmol) in a 100 mL round-bottomed flask and stirred for 12 h at room temperature. Strongly-acidic cationic exchange resin was then added until the solution became neutral. The solution was filtered through celite and the filtrate was concentrated using a rotary evaporator. The product was purified by silica gel chromatography toluene-ethyl acetate, 3:1, as the eluent. The alcohol **39** was isolated as a white solid (98 mg, 466.44 g/mol, 97%); R_f 0.40 in toluene-ethyl acetate, 3:1. ES HRMS: (M+Na)

exact mass: 489.1386, found: 489.1391. $[\alpha]_D +4.7^\circ$ (*c* 0.9, CH₂Cl₂). ¹H NMR (300 MHz, CDCl₃) δ : 7.87-7.70 (m, 4H, Phth), 7.48-7.36 (m, 5H, aromatic), 5.56 (s, 1H, CH-Ph), 5.34 (d, 1H, $J_{1,2} = 8.4$ Hz, H-1), 4.62 (ddd, 1H, $J_{2,3} = 8.9$ Hz, $J_{3,4} = 10.3$ Hz, $J_{3,\text{OH}} = 3.5$ Hz, H-3), 4.38 (dd, 1H, $J_{5,6a} = 4.2$ Hz, $J_{6a,6b} = 10.1$ Hz, H-6a), 4.27 (dd, 1H, $J_{1,2} = 8.4$ Hz, $J_{3,4} = 10.4$ Hz, H-2), 3.96-3.99 (m, 1H, O-CH₂-CH₂-N₃), 3.83 (dd, 1H, $J_{5,6b} = 0.9$ Hz, $J_{6a,6b} = 10.1$ Hz, H-6b), 3.66-3.68 (m, 1H, O-CH₂-CH₂-N₃), 3.63-3.65 (m, 2H, H-4, H-5), 3.34-3.37 (m, 1H, O-CH₂-CH₂-N₃), 3.19-3.21 (m, 1H, O-CH₂-CH₂-N₃), 2.32 (d, 1H, $J = 3.5$ Hz, OH).

1,2,4-Tri-O-acetyl-3-O-methyl- α -L-rhamnopyranose (42)

Acetic anhydride (50 mL) was added to the methyl α -glycoside **41**⁸⁸ (2.12 g, 7.67 mmol) along with concentrated sulphuric acid (20 μ L) in a 500 mL round-bottomed flask and stirred for 2 h. DCM (100 mL) and saturated NaHCO₃ (aq.) (300 mL) were then added and the solution was stirred for 2 h at room temperature. The resulting biphasic solution was then transferred to a separatory funnel. The organic phase was drained into an Erlenmeyer flask, dried with Na₂SO₄, and filtered through cotton. The solvent was removed using a rotary evaporator and the product was purified by silica gel chromatography using hexane-ethyl acetate, 2:1, as the eluent. The α -acetate **42** was isolated as a white solid (2.15 g, 304.29 g/mol, 92%); R_f 0.23 in hexane – ethyl acetate, 2:1. ES HRMS: (M+Na) exact mass: 327.1056, found: 327.1052. $[\alpha]_D -66.7^\circ$ (*c* 1.0, CH₂Cl₂). ¹H NMR (360 MHz, CDCl₃) δ : 6.02 (d, 1H, $J_{1,2} = 1.9$ Hz, H-1), 5.29 (dd, 1H, $J_{1,2} = 1.9$

Hz, $J_{2,3} = 3.3$ Hz, H-2), 5.00 (t, 1H, $J_{3,4} = J_{4,5} = 9.9$ Hz, H-4), 3.86 (dq, 1H, $J_{4,5} = 9.9$ Hz, $J_{5,6} = 6.3$ Hz, H-5), 3.58 (dd, 1H, $J_{2,3} = 3.3$ Hz, $J_{3,4} = 9.8$ Hz, H-3), 3.32 (s, 3H, OCH₃), 2.03 (s, 3H, OAc), 2.02 (s, 3H, OAc), 1.98 (s, 3H, OAc), 1.20 (d, 3H, $J_{5,6} = 6.3$ Hz, H-6).

Ethyl 2,4-di-O-acetyl-3-O-methyl-1-thio- α -L-rhamnopyranoside (43)

Anhydrous DCM (100 mL) was added to the α -acetate **42** (1.53 g, 5.03 mmol) along with ethanethiol (1.12 mL, 15.1 mmol, 0.839 g/mL) and boron trifluoride diethyletherate (1.91 mL, 15.1 mmol, 1.12 g/mL) in a 250 mL round-bottomed flask and stirred under an argon atmosphere for 2 h at 0 °C and then stirred at room temperature for 16 h. Saturated NaHCO₃ (aq.) (100 mL) was then added and the solution was stirred for 2 h. The resulting biphasic solution was then transferred to a separatory funnel. The organic phase was drained into an Erlenmeyer flask, dried with Na₂SO₄, and filtered through cotton. The volatile components were removed using a rotary evaporator and the product was purified by silica gel chromatography using hexane-ethyl acetate, 6:1, as the eluent. The thioglycoside **43** was isolated as a colourless oil (1.19 g, 306.38 g/mol, 77%); R_f 0.21 in hexane – ethyl acetate, 6:1. ES HRMS: (M+Na) exact mass: 329.1035, found: 329.1039. $[\alpha]_D -47.8^\circ$ (c 0.9, CH₂Cl₂). ¹H NMR (300 MHz, CDCl₃) δ : 5.38 (dd, 1H, $J_{1,2} = 1.7$ Hz, $J_{2,3} = 3.6$ Hz, H-2), 5.19 (d, 1H, $J_{1,2} = 1.7$ Hz, H-1), 4.97 (t, 1H, $J_{3,4} = J_{4,5} = 9.8$ Hz, H-4), 4.10 (dq, 1H, $J_{4,5} = 9.8$ Hz, $J_{5,6} = 6.2$ Hz, H-5), 3.51 (dd, 1H, $J_{2,3} = 3.3$ Hz, $J_{3,4} = 9.7$ Hz, H-3), 3.31 (s, 3H, OCH₃), 2.61-2.64 (m, 2H,

SCH₂CH₃), 2.12 (s, 3H, OAc), 2.07 (s, 3H, OAc), 1.28 (t, 3H, SCH₂CH₃), 1.18 (d, 3H, J_{5,6} = 6.3 Hz, H-6).

1-O-(3-O-[2,4-Di-O-acetyl-3-O-methyl- α -L-rhamnopyranosyl]-4,6-O-benzylidene-2-deoxy-2-phthalimido- β -D-glucopyranosyl)-2-azidoethanol (44)

Anhydrous DCM (50 mL) was added to the glycosyl donor **43** (77 mg, 0.251 mmol) along with the acceptor **39** (90 mg, 0.193 mmol) and 4 Å molecular sieves (500 mg) in a 100 mL round-bottomed flask and stirred under an argon atmosphere for 4 h at room temperature. Silver trifluoromethanesulphonate (13 mg, 0.051 mmol) and *N*-iodosuccinimide (113 mg, 0.502 mmol) were added and the solution was stirred for 1 h. The resulting dark purple solution was then filtered through celite in a sintered glass funnel and the supernatant was equilibrated between DCM and saturated Na₂S₂O₃ (aq.) (50 mL) in a separatory funnel. The organic phase was drained into an Erlenmeyer flask, dried with Na₂SO₄, and filtered through cotton. The volatile components were removed using a rotary evaporator and the product was purified by silica gel chromatography using toluene-ethyl acetate, 3:1, as the eluent. The disaccharide **44** was isolated as a colourless oil (103 mg, 710.68 g/mol, 75%); R_f 0.31 in toluene-ethyl acetate, 4:1. ES HRMS: (M+Na) exact mass: 733.2333, found: 733.2335. [α]_D +13.6° (c 0.9, CH₂Cl₂). ¹H NMR (600 MHz, CDCl₃) δ : 7.87-7.69 (m, 4H, Phth), 7.48-7.32 (m, 5H, aromatic), 5.57 (s, 1H, CH-Ph), 5.33 (d, 1H, J_{1,2} = 8.6 Hz, H-1), 5.38 (dd, 1H, J_{1',2'}} = 1.8 Hz, J_{2',3'}} = 3.3 Hz, H-2'), 4.97 (t, 1H, J_{3',4'}} = J_{4',5'}} = 9.9

Hz, H-4'), 4.58 (dd, 1H, $J_{2,3} = 9.0$ Hz, $J_{3,4} = 10.5$ Hz, H-3), 5.19 (d, 1H, $J_{1,2} = 1.8$ Hz, H-1'), 4.38 (dd, 1H, $J_{5,6a} = 4.4$ Hz, $J_{6a,6b} = 10.6$ Hz, H-6a), 4.27 (dd, 1H, $J_{1,2} = 8.4$ Hz, $J_{3,4} = 10.3$ Hz, H-2), 3.96-3.98 (m, 1H, O-CH₂-CH₂-N₃), 3.87 (dq, 1H, $J_{4,5'} = 9.8$ Hz, $J_{5,6'} = 6.3$ Hz, H-5'), 3.81-3.84 (m, 1H, $J_{5,6b} = 1.1$ Hz, $J_{6a,6b} = 10.6$ Hz, H-6b), 3.67-3.69 (m, 2H, H-4, H-5), 3.61-3.64 (m, 1H, O-CH₂-CH₂-N₃), 3.51 (dd, 1H, $J_{2,3'} = 3.3$ Hz, $J_{3,4'} = 9.8$ Hz, H-3'), 3.32-3.34 (m, 1H, O-CH₂-CH₂-N₃), 3.18-3.20 (m, 1H, O-CH₂-CH₂-N₃), 3.18 (s, 3H, OCH₃), 1.98 (s, 3H, OAc), 1.76 (s, 3H, OAc), 0.6 (d, 3H, $J_{5,6'} = 6.3$ Hz, H-6').

1-O-(2-Acetamido-4,6-O-benzylidene-3-O-[3-O-methyl- α -L-rhamnopyranosyl]-2-deoxy- β -D-glucopyranosyl)-2-azidoethanol (45)

Ethylenediamine (5 mL) and *t*-butyl alcohol (20 mL) were added to the phthalimide **44** (90 mg, 0.127 mmol) in a 50 mL round-bottomed flask and stirred under an argon atmosphere for 28 h at 115°C. The resulting pale yellow solution was then cooled to room temperature. The volatiles were then removed using a rotary evaporator and methanol (30 mL) was added to the residue along with acetic anhydride (100 μ L, 1.60 mmol, 1.082 g/mL) and the solution was stirred for 10 h at room temperature. The volatiles were removed using a rotary evaporator and the product was purified by silica gel chromatography using toluene-acetone-methanol, 7.5:2:0.5, as the eluent. The acetamide **45** was isolated as a white solid (55 mg, 538.55 g/mol, 81%); R_f 0.14 in toluene-acetone-methanol, 7.5:2:0.5. ES HRMS: (M+Na) exact mass: 561.2173, found: 561.2169. $[\alpha]_D -9.9^\circ$ (c

0.5, MeOH). ^1H NMR (300 MHz, CDCl_3) δ : 7.48-7.32 (m, 5H, aromatic), 5.90 (d, 1H, $J = 8.7$ Hz, NHAc), 5.49 (s, 1H, CH-Ph), 5.19 (d, 1H, $J_{1,2'} = 1.5$ Hz, H-1'), 4.76 (d, 1H, $J_{1,2} = 8.4$ Hz, H-1), 4.32 (dd, 1H, $J_{5,6a} = 4.4$ Hz, $J_{6a,6b} = 10.5$ Hz, H-6a), 4.58 (t, 1H, $J_{2,3} = J_{3,4} = 10.5$ Hz, H-3), 4.10 (dd, 1H, $J_{1,2'} = 1.7$ Hz, $J_{2,3'} = 2.6$ Hz, H-2'), 3.95-3.98 (m, 1H, $\text{O-CH}_2\text{-CH}_2\text{-N}_3$), 3.87 (dq, 1H, $J_{4,5'} = 9.8$ Hz, $J_{5,6'} = 6.2$ Hz, H-5'), 3.74-3.77 (m, 2H, H-2, H-6b), 3.61-3.64 (m, 1H, $\text{O-CH}_2\text{-CH}_2\text{-N}_3$), 3.52-3.54 (m, 2H, H-4, H-5), 3.42-3.45 (m, 1H, $\text{O-CH}_2\text{-CH}_2\text{-N}_3$), 3.43 (s, 3H, OCH_3), 3.36-3.38 (m, 1H, H-3', H-4'), 3.24-3.27 (m, 1H, $\text{O-CH}_2\text{-CH}_2\text{-N}_3$), 1.99 (s, 3H, NHAc), 0.8 (d, 3H, $J_{5,6'} = 6.3$ Hz, H-6').

1-O-(2-Acetamido-3-O-[3-O-methyl- α -L-rhamnopyranosyl]-2-deoxy- β -D-glucopyranosyl)-2-aminoethanol (46)

Acetic acid (20 mL) was added to the partially-protected disaccharide **45** (90 mg, 0.167 mmol) in a 50 mL round-bottomed flask along with palladium (30 mg, 10% on carbon) and the suspension was stirred under a hydrogen atmosphere for 24 h at room temperature. The resulting solution was then filtered through celite using a sintered glass funnel. The volatiles were then removed using a rotary evaporator. Acetic acid (16 mL) and water (4 mL) were added and the solution was stirred for 2 h at 80°C. The volatiles were removed using a rotary evaporator. Distilled water (10 mL) was added to the residue and the solution was passed through two Sep-Pak cartridges. The deprotected disaccharide **46** was isolated as a clear oil (54 mg, 424.44 g/mol, 76%); R_f 0.25 in

ethyl acetate – methanol – water, 7:2:1. ES HRMS: (M+Na) exact mass: 447.1955, found: 447.1954. $[\alpha]_D -24.8^\circ$ (c 0.5, H₂O). ¹H NMR (600 MHz, D₂O) δ : 4.90 (d, 1H, $J_{1,2} = 2.0$ Hz, H-1'), 4.62 (d, 1H, $J_{1,2} = 8.6$ Hz, H-1), 4.06-4.09 (m, 1H, O-CH₂-CH₂-NH₂), 4.02 (dd, 1H, $J_{1,2} = 2.1$ Hz, $J_{2,3} = 2.9$ Hz, H-2'), 3.99 (dq, 1H, $J_{4,5} = 9.8$ Hz, $J_{5,6} = 6.2$ Hz, H-5'), 3.95 (dd, 1H, $J_{5,6a} = 2.2$ Hz, $J_{6a,6b} = 12.4$ Hz, H-6a), 3.92-3.95 (m, 1H, O-CH₂-CH₂-NH₂), 3.87 (dd, 1H, $J_{1,2} = 8.8$ Hz, $J_{2,3} = 10.0$ Hz, H-2), 3.75-3.77 (m, 1H, H-6b), 3.63 (dd, 1H, $J_{2,3} = 10.1$, $J_{3,4} = 8.9$ Hz, H-3), 3.53 (t, 1H, $J_{3,4} = J_{4,5} = 8.9$ Hz, H-4), 3.50-3.52 (m, 1H, H-5), 3.46 (t, 1H, $J_{3,4} = J_{4,5} = 9.5$, H-4'), 3.46 (dd, 1H, $J_{2,3} = J_{3,4} = 9.5$, H-3'), 3.46 (s, 3H, OCH₃), 3.20-3.22 (m, 2H, O-CH₂-CH₂-NH₂), 2.08 (s, 3H, NHAc), 1.33 (d, 3H, $J_{5,6} = 6.2$ Hz, H-6').

2-N-Acetyl-1-O-(2-acetamido-3-O-[3-O-methyl- α -L-rhamnopyranosyl]-2-deoxy- β -D-glucopyranosyl)-2-aminoethanol (7)

Dry DMF (10 mL) was added to the amine **46** (12 mg, 0.028 mmol) along with acetic anhydride (50 μ L, 0.530 mmol, 1.082 g/mL) in a 50 mL round-bottomed flask and stirred for 15 h at room temperature. The volatiles were then removed using a rotary evaporator and the product was purified by reversed-phase high performance liquid chromatography using water-acetonitrile, 20:1, as the eluent. The acetamide **7** was isolated as a clear oil (8 mg, 466.48 g/mol, 61%); R_f 0.22 in ethyl acetate – methanol – water, 7:2:1. ES HRMS: (M+Na) exact mass: 489.2060, found: 489.2060. $[\alpha]_D -42.7^\circ$ (c 0.4, H₂O). ¹H NMR (600 MHz, D₂O) δ : 4.89 (d, 1H, $J_{1,2} = 1.5$ Hz, H-1'), 4.57 (d, 1H, $J_{1,2} = 8.4$ Hz, H-1), 4.02 (dd, 1H, $J_{1,2} =$

1.7 Hz, $J_{2,3'} = 2.9$ Hz, H-2'), 3.99 (dq, 1H, $J_{4,5'} = 9.8$ Hz, $J_{5,6'} = 6.2$ Hz, H-5'), 3.94 (dd, 1H, $J_{5,6a} = 1.5$ Hz, $J_{6a,6b} = 12.8$ Hz, H-6a), 3.92-3.94 (m, 1H, O-CH₂-CH₂-NHAc), 3.82 (t, 1H, $J_{1,2} = J_{2,3} = 9.7$ Hz, H-2), 3.75 (dd, 1H, $J_{5,6b} = 5.7$ Hz, $J_{6a,6b} = 12.4$ Hz, H-6b), 3.72-3.74 (m, 1H, O-CH₂-CH₂-NHAc), 3.60 (t, 1H, $J_{2,3} = J_{3,4} = 9.1$ Hz, H-3), 3.51-3.53 (m, 2H, H-4, H-5), 3.45-3.48 (m, 3H, H-3', H-4', O-CH₂-CH₂-NHAc), 3.41 (s, 3H, OCH₃), 3.36-3.39 (m, 1H, O-CH₂-CH₂-NHAc), 2.06 (s, 3H, NHAc), 1.99 (s, 3H, NHAc), 1.24 (d, 3H, $J_{5,6'} = 6.3$ Hz, H-6').

1-O-(2-Acetamido-3-O-[3-O-methyl- α -L-rhamnopyranosyl]-2-deoxy- β -D-glucopyranosyl)-2-N-benzamido-2-aminoethanol (8)

Dry DMF (10 mL) was added to the amine **46** (12 mg, 0.028 mmol) along with benzoyl chloride (100 μ L, 0.861 mmol, 1.211 g/mL) in a 50 mL round-bottomed flask and stirred for 15 h at room temperature. The volatiles were then removed using a rotary evaporator and the product was purified by reversed-phase high performance liquid chromatography using water – acetonitrile, 20:1, as the eluent. The benzamide **8** was isolated as a clear oil (9 mg, 528.55 g/mol, 60%); R_f 0.49 in ethyl acetate – methanol – water, 7:2:1. ES HRMS: (M+Na) exact mass: 551.2217, found: 551.2219. $[\alpha]_D -10.7^\circ$ (c 0.4, H₂O). ¹H NMR (600 MHz, D₂O) δ : 7.79-7.53 (m, 5H, aromatic), 4.85 (d, 1H, $J_{1,2'} = 1.5$ Hz, H-1'), 4.59 (d, 1H, $J_{1,2} = 8.6$ Hz, H-1), 4.05-4.08 (m, 1H, O-CH₂-CH₂-NH₂), 3.99 (dq, 1H, $J_{4,5'} = 9.8$ Hz, $J_{5,6'} = 6.2$ Hz, H-5'), 3.98 (dd, 1H, $J_{1,2'} = 1.7$ Hz, $J_{2,3'} = 2.9$ Hz, H-2'), 3.91 (dd, 1H, $J_{5,6a} = 2.1$ Hz, $J_{6a,6b} = 12.3$ Hz, H-6a), 3.84-3.87 (m, 1H, O-CH₂-CH₂-NHBz), 3.81 (t, 1H, $J_{1,2}$

= $J_{2,3} = 9.9$ Hz, H-2), 3.73 (dd, 1H, $J_{5,6b} = 5.5$ Hz, $J_{6a,6b} = 12.4$ Hz, H-6b), 3.64-3.67 (m, 2H, O-CH₂-CH₂-NHBz), 3.59 (t, 1H, $J_{2,3} = J_{3,4} = 9.1$ Hz, H-3), 3.47-3.49 (m, 2H, H-4, H-5), 3.45 (t, 1H, $J_{3',4'} = J_{4',5'} = 9.7$ Hz, H-4'), 3.42-3.44 (m, 1H, O-CH₂-CH₂-NHBz), 3.41 (dd, 1H, $J_{2,3'} = 2.9$ Hz, $J_{3',4'} = 9.7$ Hz, H-3'), 3.39 (s, 3H, OCH₃), 1.75 (s, 3H, NHAc), 1.23 (d, 3H, $J_{5',6'} = 6.2$ Hz, H-6').

1-O-(2-Acetamido-3-O-[3-O-methyl- α -L-rhamnopyranosyl]-2-deoxy- β -D-glucopyranosyl)-2-N-(N- α -acetamido-L-phenylalanyl)-2-aminoethanol (9)

Dry DMF (10 mL) was added to the amine **46** (12 mg, 0.028 mmol) along with *N*- α -Fmoc-L-phenylalanine pentafluorophenyl ester (23 mg, 0.042 mmol) in a 50 mL round-bottomed flask and stirred for 15 h at room temperature. Piperidine (2 mL) was then added and the solution was stirred for 1 h at room temperature. The volatiles were removed using a rotary evaporator and dry DMF (10 mL) and acetic anhydride (150 μ L, 1.59 mmol, 1.082 g/mL) were added and the solution was stirred for 10 h at room temperature. The volatiles were then removed using a rotary evaporator. Water (10 mL) was added to the residue and the solution was passed through a Sep-Pak cartridge. The product was purified by reversed-phase high performance liquid chromatography using water – acetonitrile, 20:1, as the eluent. The amide **9** was isolated as a clear oil (5 mg, 613.48 g/mol, 33%); R_f 0.40 in ethyl acetate – methanol – water, 7:2:1. ES HRMS: (M+Na) exact mass: 636.2744, found: 636.2746. ¹H NMR (600 MHz, D₂O) δ : 7.42-7.27 (m, 5H, aromatic), 4.89 (s, 1H, H-1'), 4.53 (d, 1H, $J_{1,2} = 8.6$ Hz, H-1),

4.53 (t, 1H, $J = 3.3$ Hz, $\underline{\text{CH}}\text{-CH}_2\text{-Ph}$), 4.03 (bs, 1H, H-2'), 4.00 (dq, 1H, $J_{4,5'} = 9.7$ Hz, $J_{5',6'} = 6.6$ Hz, H-5'), 3.94 (dd, 1H, $J_{5,6a} = 2.1$ Hz, $J_{6a,6b} = 12.3$ Hz, H-6a), 3.81 (t, 1H, $J_{1,2} = J_{2,3} = 9.3$ Hz, H-2), 3.76-3.78 (m, 2H, H-6b, $\text{O-CH}_2\text{-CH}_2\text{-NH-R}$), 3.64-3.66 (m, 1H, $\text{O-CH}_2\text{-CH}_2\text{-NH-R}$), 3.59 (t, 1H, $J_{2,3} = J_{3,4} = 9.3$ Hz, H-3), 3.50 (t, 1H, $J_{3,4} = J_{4,5} = 9.2$ Hz, H-4), 3.46-3.48 (m, 3H, H-5, H-3', H-4'), 3.41 (s, 3H, OCH_3), 3.33-3.35 (m, 2H, $\text{O-CH}_2\text{-CH}_2\text{-NH-R}$), 3.12-2.98 (m, 2H, $\text{CH-CH}_2\text{-Ph}$), 2.06 (s, 3H, NHAc), 1.98 (s, 3H, NHAc), 1.24 (d, 3H, $J_{5,6'} = 6.4$ Hz, H-6').

1-O-(2-Acetamido-3-O-[3-O-methyl- α -L-rhamnopyranosyl]-2-deoxy- β -D-glucopyranosyl)-2-N-(N- α -acetamido-D-phenylalanyl)-2-aminoethanol (10)

Dry DMF (10 mL) was added to the amine **46** (12 mg, 0.028 mmol) along with *N- α -Fmoc-D-phenylalanine* pentafluorophenyl ester (23 mg, 0.041 mmol) in a 50 mL round-bottomed flask and stirred for 17 h at room temperature. Piperidine (2 mL) was then added and the solution was stirred for 1 h at room temperature. The volatiles were removed using a rotary evaporator and dry DMF (10 mL) and acetic anhydride (150 μL , 1.59 mmol, 1.082 g/mL) were added and the solution was stirred for 10 h at room temperature. The volatiles were then removed using a rotary evaporator. Distilled water (10 mL) was added to the residue and the solution was passed through two Sep-Pak cartridges. The product was purified by reversed-phase high performance liquid chromatography using water – acetonitrile, 20:1, as the eluent. The amide **10** was isolated as a clear oil (6 mg, 613.48 g/mol, 39%); R_f 0.40 in ethyl acetate –

methanol – water, 7:2:1. ES HRMS: (M+Na) exact mass: 636.2744, found: 636.2748. ¹H NMR (600 MHz, D₂O) δ: 7.42-7.27 (m, 5H, aromatic), 4.88 (s, 1H, H-1'), 4.54 (d, 1H, J_{1,2} = 8.4 Hz, H-1), 4.52 (t, 1H, J = 7.9 Hz, CH-CH₂-Ph), 4.03 (bt, 1H, H-2'), 4.00 (dq, 1H, J_{4',5'} = 9.7 Hz, J_{5',6'} = 6.4 Hz, H-5'), 3.94 (dd, 1H, J_{5,6a} = 1.8 Hz, J_{6a,6b} = 12.6 Hz, H-6a), 3.80-3.84 (m, 2H, H-2, O-CH₂-CH₂-NH-R), 3.74 (dd, 1H, J_{5,6b} = 5.5 Hz, J_{6a,6b} = 12.3 Hz, H-6b), 3.64-3.68 (m, 1H, O-CH₂-CH₂-NH-R), 3.59 (t, 1H, J_{2,3} = J_{3,4} = 9.3 Hz, H-3), 3.50 (t, 1H, J_{3',4'} = J_{4',5'} = 10.1 Hz, H-4'), 3.43-3.47 (m, 3H, H-4, H-5, H-3'), 3.41 (s, 3H, OCH₃), 3.33-3.36 (m, 2H, O-CH₂-CH₂-NH-R), 3.12-2.98 (m, 2H, CH-CH₂-Ph), 2.04 (s, 3H, NHAc), 1.97 (s, 3H, NHAc), 1.24 (d, 3H, J_{5',6'} = 6.2 Hz, H-6').

Allyl 3-O-(2,4-di-O-acetyl-3-O-methyl- α -L-rhamnopyranosyl)-4,6-O-benzylidene-2-deoxy-2-phthalimido- β -D-glucopyranoside (47)

Anhydrous DCM (100 mL) was added to the glycosyl donor **43** (1.0 g, 3.26 mmol) along with the acceptor **26** (1.1 g, 2.51 mmol) and 4 Å molecular sieves (1.0 g) in a 250 mL round-bottomed flask and stirred under an argon atmosphere for 14 h at room temperature. The suspension was then cooled to 0 °C and trifluoromethanesulphonic acid (58 μ L, 0.39 mmol, 1.696 g/mL) and *N*-iodosuccinimide (1.5 g, 6.67 mmol) were added. The solution was then allowed to reach room temperature and stirred for 1 h. The resulting dark purple solution was then filtered through celite in a sintered glass funnel and the supernatant solution was equilibrated between DCM and saturated Na₂S₂O₃,

(aq.) (100 mL) in a separatory funnel. The organic phase was drained into an Erlenmeyer flask, dried with Na_2SO_4 , and filtered through cotton. The volatile components were removed using a rotary evaporator and the product was purified by silica gel chromatography using toluene-ethyl acetate, 3:1, as the eluent. The disaccharide **47** was isolated as a white solid (1.1 g, 681.68 g/mol, 65%); R_f 0.29 in toluene – ethyl acetate, 3:1. ES HRMS: (M+Na) exact mass: 704.231911, found: 704.231608. $[\alpha]_D^{25} +14.7^\circ$ (c 0.7, CH_2Cl_2). ^1H NMR (600 MHz, CDCl_3) δ : 7.87-7.72 (m, 4H, Phth), 7.48-7.42 (m, 5H, aromatic), 5.66-5.69 (m, 1H, O- CH_2 - $\text{CH}=\text{CH}_2$), 5.55 (s, 1H, CH -Ph), 5.28 (d, 1H, $J_{1,2} = 8.5$ Hz, H-1), 5.05-5.10 (m, 2H, O- CH_2 - $\text{CH}=\text{CH}_2$), 4.79 (dd, 1H, $J_{1,2'} = 1.8$ Hz, $J_{2,3'} = 3.5$ Hz, H-2'), 4.73 (dd, 1H, $J_{3,4'} = J_{4,5'} = 9.6$ Hz, H-4'), 4.60 (dd, 1H, $J_{2,3} = 10.4$ Hz, $J_{3,4} = 8.8$ Hz, H-3), 4.53 (d, 1H, $J_{1,2'} = 1.8$ Hz, H-1'), 4.39 (dd, 1H, $J_{5,6a} = 4.4$ Hz, $J_{6a,6b} = 10.6$ Hz, H-6a), 4.31 (dd, 1H, $J_{1,2} = 8.6$ Hz, $J_{2,3} = 10.2$ Hz, H-2), 4.23-4.27 (m, 1H, O- CH_2 - $\text{CH}=\text{CH}_2$), 4.02-4.06 (m, 1H, O- CH_2 - $\text{CH}=\text{CH}_2$), 3.84 (dq, 1H, $J_{4,5'} = 9.6$ Hz, $J_{5,6'} = 6.3$ Hz, H-5'), 3.82 (dd, 1H, $J_{5,6b} = 2.2$ Hz, $J_{6a,6b} = 10.3$ Hz, H-6b), 3.66 (ddd, 1H, $J_{4,5} = 10.1$ Hz, $J_{5,6a} = 4.2$ Hz, $J_{5,6b} = 2.2$ Hz, H-5), 3.66 (dd, 1H, $J_{3,4} = 8.9$ Hz, $J_{4,5} = 10.1$ Hz, H-4), 3.46 (dd, 1H, $J_{2,3'} = 3.4$ Hz, $J_{3,4'} = 9.8$ Hz, H-3'), 1.99 (s, 3H, OAc), 1.76 (s, 3H, OAc), 0.83 (d, 3H, $J_{5,6'} = 6.1$ Hz, H-6'). ^{13}C NMR (125 MHz, CDCl_3) δ : 97.7 ($J_{\text{C-1,H-1}} = 165.8$ Hz, C-1), 97.6 ($J_{\text{C-1',H-1'}} = 170.6$ Hz, C-1').

Allyl 2-acetamido-4,6-O-benzylidene-3-O-(3-O-methyl- α -L-rhamnopyranosyl)-2-deoxy- β -D-glucopyranoside (48)

Ethylenediamine (5 mL) and *t*-butyl alcohol (20 mL) were added to the phthalimide **47** (215 mg, 0.315 mmol) in a 50 mL round-bottomed flask and stirred under an argon atmosphere for 24 h at 115°C. The resulting pale yellow solution was then cooled to room temperature. The volatiles were then removed using a rotary evaporator and methanol (20 mL) was added to the residue along with acetic anhydride (100 μ L, 1.06 mmol, 1.082 g/mL) and the solution was stirred for 12 h at room temperature. The volatiles were removed using a rotary evaporator and the product was purified by silica gel chromatography using toluene-acetone-methanol, 7.5:2:0.5, as the eluent. The acetamide **48** was isolated as a white solid (133 mg, 509.55 g/mol, 83%); R_f 0.16 in toluene-acetone-methanol, 7.5:2:0.5. ES HRMS: (M+Na) exact mass: 532.2159, found: 532.2150. $[\alpha]_D^{25}$ -12.6° (c 1.0, MeOH). ^1H NMR (300 MHz, CDCl_3) δ : 7.48-7.32 (m, 5H, aromatic), 5.79-5.84 (m, 2H, O-CH₂-CH=CH₂, NHAc), 5.50 (s, 1H, CH-Ph), 5.16-5.20 (m, 2H, O-CH₂-CH=CH₂), 4.93 (bs, 1H, H-1'), 4.66 (d, 1H, $J_{1,2} = 8.3$ Hz, H-1), 4.36 (dd, 1H, $J_{5,6a} = 4.9$ Hz, $J_{6a,6b} = 10.6$ Hz, H-6a), 4.25-4.30 (m, 1H, O-CH₂-CH=CH₂), 4.10 (dd, 1H, $J_{2,3} = 10.4$ Hz, $J_{3,4} = 9.3$ Hz, H-3), 4.02-4.07 (m, 1H, O-CH₂-CH=CH₂), 4.02 (bs, 1H, H-2'), 3.84 (dq, 1H, $J_{4,5'} = 9.6$ Hz, $J_{5',6'} = 6.3$ Hz, H-5'), 3.80 (dd, 1H, $J_{1,2} = 8.6$ Hz, $J_{2,3} = 10.2$ Hz, H-2), 3.76 (dd, 1H, $J_{5,6b} = 2.2$ Hz, $J_{6a,6b} = 10.1$ Hz, H-6b), 3.56 (t, 1H, $J_{3,4} = J_{4,5} = 9.3$ Hz, H-4), 3.50 (ddd, 1H, $J_{4,5} = 10.1$ Hz, $J_{5,6a} = 4.2$

Hz, $J_{5,6b} = 2.2$ Hz, H-5), 3.43 (s, 3H, OMe), 3.33-3.36 (m, 2H, H-3', H-4'), 1.99 (s, 3H, NHAc), 0.81 (d, 3H, $J_{5,6'} = 6.1$ Hz, H-6').

n-Propyl 2-acetamido-3-O-(3-O-methyl- α -L-rhamnopyranosyl)-2-deoxy- β -D-glucopyranoside (**49**)

Acetic acid (20 mL) was added to the partially-protected disaccharide **48** (51 mg, 0.100 mmol) in a 50 mL round-bottomed flask along with palladium (30 mg, 10% on carbon) and the suspension was stirred under a hydrogen atmosphere for 36 h at room temperature. The resulting solution was then filtered through celite using a sintered glass funnel. The volatiles were then removed using a rotary evaporator. Acetic acid (8 mL) and water (2 mL) were added and the solution was stirred for 2 h at 80°C. The volatiles were removed using a rotary evaporator. Distilled water (10 mL) was added to the residue and the solution was passed through two Sep-Pak cartridges. The product was purified by reversed-phase high performance liquid chromatography using water – acetonitrile, 20:1, as the eluent. The deprotected disaccharide **49** was isolated as a clear oil (22 mg, 565.61 g/mol, 52%); R_f 0.51 in ethyl acetate – methanol – water, 7:2:1. ES HRMS: (M+H) exact mass: 424.2183, found: 424.2184. $[\alpha]_D -17.2^\circ$ (c 0.3, H₂O). ¹H NMR (360 MHz, D₂O) δ : 4.98 (d, 1H, $J_{1,2'} = 1.9$ Hz, H-1'), 4.58 (d, 1H, $J_{1,2} = 8.5$ Hz, H-1), 4.11 (dq, 1H, $J_{4,5'} = 9.2$ Hz, $J_{5,6'} = 6.2$ Hz, H-5'), 3.96 (dd, 1H, $J_{1,2'} = 1.9$ Hz, $J_{2,3'} = 2.6$ Hz, H-2'), 3.93-3.99 (m, 2H, -O-CH₂CH₂CH₃), 3.90 (dd, 1H, $J_{5,6a} = 1.9$ Hz, $J_{6a,6b} = 11.8$ Hz, H-6a), 3.78 (dd, 1H, $J_{1,2} = 8.5$ Hz, $J_{2,3} =$

10.2 Hz, H-2), 3.72 (dd, 1H, $J_{5,6b} = 5.5$ Hz, $J_{6a,6b} = 11.9$ Hz, H-6b), 3.59 (dd, 1H, $J_{2,3} = 10.2$ Hz, $J_{3,4} = 9.0$ Hz, H-3), 3.52 (dd, 1H, $J_{2,3'} = 2.6$ Hz, $J_{3',4'} = 9.1$ Hz, H-3'), 3.47 (dd, 1H, $J_{3',4'} = J_{4',5'} = 9.0$ Hz, H-4'), 3.45 (dd, 1H, $J_{3,4} = 8.9$ Hz, $J_{4,5} = 10.1$ Hz, H-4), 3.41 (s, 3H, OMe), 3.40 (ddd, 1H, $J_{4,5} = 10.1$ Hz, $J_{5,6a} = 1.9$ Hz, $J_{5,6b} = 5.5$ Hz, H-5), 1.95 (s, 3H, NHAc), 1.65 (sextuplet, 2H, $J = 7.1$ Hz, $-\text{OCH}_2\text{CH}_2\text{CH}_3$), 1.29 (d, 3H, $J_{5',6'} = 6.2$ Hz, H-6'), 0.89 (t, 3H, $-\text{O}-\text{CH}_2\text{CH}_2\text{CH}_3$).

Ethyl 2,3,4,6-tetra-O-acetyl-1-thio- α -L-mannopyranoside (64)

Anhydrous DCM (100 mL) was added to the pentaacetate **63**⁹⁷ (2.1 g, 5.38 mmol) along with ethanethiol (1.20 mL, 16.2 mmol, 0.839 g/mL) and boron trifluoride diethyl etherate (2.00 mL, 15.8 mmol, 1.12 g/mL) in a 500 mL round-bottomed flask and stirred under an argon atmosphere for 2 h at 0 °C and then stirred at room temperature for 16 h. Saturated NaHCO₃ (aq.) (250 mL) was then added and the solution was stirred for 2 h. The resulting biphasic solution was then transferred to a separatory funnel. The organic phase was drained into an Erlenmeyer flask, dried with Na₂SO₄, and filtered through cotton. The volatile components were removed using a rotary evaporator and the product was purified by silica gel chromatography using toluene-ethyl acetate, 3:1, as the eluent. The thioglycoside **64** was isolated as a white solid (1.6 g, 392.42 g/mol, 77%); R_f 0.33 in toluene-ethyl acetate, 3:1. ES HRMS: (M+Na) exact mass: 415.1039, found: 415.1033. $[\alpha]_D^{25} -110.6^\circ$ (c 0.9, CH₂Cl₂). ¹H NMR (300 MHz, CDCl₃) δ : 5.34-5.25 (m, 4H, H-1, H-2, H-3, H-4), 4.38 (ddd, 1H, $J_{4,5} = 9.9$ Hz, $J_{5,6a} =$

5.3 Hz, $J_{5,6b} = 2.3$ Hz, H-5), 4.29 (dd, 1H, $J_{5,6a} = 5.3$ Hz, $J_{6a,6b} = 12.1$ Hz, H-6a), 4.08 (dd, 1H, $J_{5,6b} = 2.3$ Hz, $J_{6a,6b} = 12.1$ Hz, H-6b), 2.60-2.66 (m, 2H, SCH_2CH_3), 2.16 (s, 3H, OAc), 2.08 (s, 3H, OAc), 2.03 (s, 3H, OAc), 2.02 (s, 3H, OAc), 1.97 (s, 3H, OAc), 1.28 (t, 3H, SCH_2CH_3). Anal. Calcd for $\text{C}_{16}\text{H}_{24}\text{O}_9\text{S}$ (392.4): C, 48.97; H, 6.16; S, 8.17. Found: C, 48.86; H, 6.17; S, 8.24.

Ethyl 1-thio- α -L-mannopyranoside (65)

Distilled methanol (100 mL) was added to the tetraacetate **64** (1.5 g, 3.82 mmol) along with sodium (105 mg, 4.56 mmol) in a 250 mL round-bottomed flask and stirred for 18 h at room temperature. Strongly-acidic cationic exchange resin was then added until the solution became neutral. The solution was filtered through celite and the filtrate was concentrated using a rotary evaporator. The alcohol **65** was obtained without purification as a white solid (0.86 g, 224.28 g/mol, 100%); R_f 0.54 in ethyl acetate – methanol – water, 7:2:1. ES HRMS: (M+Na) exact mass: 247.0616, found: 247.0619. ^1H NMR (600 MHz, D_2O) δ : 5.33 (d, 1H, $J_{1,2} = 1.6$ Hz, H-1), 4.05 (dd, 1H, $J_{1,2} = 1.6$ Hz, $J_{2,3} = 3.3$ Hz, H-2), 4.00 (ddd, 1H, $J_{4,5} = 9.7$ Hz, $J_{5,6a} = 2.3$ Hz, $J_{5,6b} = 6.2$ Hz, H-5), 3.89 (dd, 1H, $J_{5,6a} = 2.3$ Hz, $J_{6a,6b} = 12.4$ Hz, H-6a), 3.79 (dd, 1H, $J_{5,6b} = 6.1$ Hz, $J_{6a,6b} = 12.4$ Hz, H-6b), 3.78 (dd, 1H, $J_{2,3} = 3.3$ Hz, $J_{3,4} = 9.7$ Hz, H-3), 3.68 (dd, 1H, $J_{3,4} = J_{4,5} = 9.7$ Hz, H-4), 2.66-2.71 (m, 2H, SCH_2CH_3), 1.28 (t, 3H, SCH_2CH_3).

Ethyl 6-O-t-butyl-diphenylsilyl-1-thio- α -L-mannopyranoside (66)

Dry DMF (30 mL) was added to the alcohol **65** (700 mg, 3.12 mmol) along with *t*-butylchlorodiphenylsilane (1.60 mL, 6.15 mmol, 1.057 g/mL) and imidazole (425 mg, 6.24 mmol) in a 100 mL round-bottomed flask and stirred for 20 h at room temperature. The volatiles were then removed using a rotary evaporator and DCM (100 mL) was added to the residue. The solution was then equilibrated between DCM and 5% HCl(aq.) (50 mL) in a separatory funnel. The organic phase was drained into an Erlenmeyer flask, dried with Na₂SO₄, and filtered through cotton. The volatiles were then removed using a rotary evaporator and the product was purified by silica gel chromatography using toluene-acetone-methanol, 7.5:1:0.5, as the eluent. The silyl ether **66** was isolated as a colourless oil (1.2 g, 462.68 g/mol, 81%); R_f 0.41 in toluene-acetone-methanol, 7.5:2:0.5. ES HRMS: (M+Na) exact mass: 485.1794, found: 485.1790. $[\alpha]_D^{20}$ -81.7° (c 1.0, MeOH). ¹H NMR (300 MHz, CDCl₃) δ : 7.69-7.34 (m, 10H, aromatic), 5.28 (d, 1H, J_{1,2} = 2.8 Hz, H-1), 4.00-4.06 (m, 2H, H-2, H-5), 3.94-3.78 (m, 4H, H-3, H-4, H-6a, H-6b), 2.50-2.58 (m, 2H, SCH₂CH₃), 1.21 (t, 3H, SCH₂CH₃), 1.04 (s, 9H, *t*-Bu). Anal. Calcd for C₂₄H₃₄O₅SSi (462.68): C, 62.30; H, 7.41. Found: C, 61.83; H, 7.49.

Ethyl 2,3,4-tri-O-benzyl-6-O-t-butyl-diphenylsilyl-1-thio- α -L-mannopyranoside (67)

Anhydrous THF (100 mL) was added to the alcohol **66** (950 mg, 2.05 mmol) along with sodium hydride (250 mg, 10.4 mmol) in a 500 mL round-

bottomed flask and stirred under an argon atmosphere for 15 min. Benzyl bromide (1.20 mL, 10.1 mmol, 1.438 g/mL) was added and the solution was stirred at 60 °C under an argon atmosphere for 24 h. The resulting yellow, cloudy solution was then cooled then methanol (6 mL) was carefully added and the solution was stirred for 15 min. All of the volatiles were removed using a rotary evaporator and DCM (150 mL) was added to the residue. The solution was then equilibrated between DCM and water (100 mL) in a separatory funnel. The organic phase was drained into an Erlenmeyer flask, dried with Na₂SO₄, and filtered through cotton. The solvent was removed using a rotary evaporator and the product was purified by silica gel chromatography using hexane-ethyl acetate, 15:1, as the eluent. The benzylate **67** was isolated as a yellow oil (1.3 g, 717.04 g/mol, 86%); R_f 0.46 in hexane-ethyl acetate, 6:1. ES HRMS: (M+Na) exact mass: 755.3202, found: 755.3202. [α]_D -52.6° (c 1.2, CH₂Cl₂). ¹H NMR (300 MHz, CDCl₃) δ: 7.75-7.15 (m, 25H, aromatic), 5.37 (d, 1H, J_{1,2} = 1.3 Hz, H-1), 4.92-4.56 (m, 6H, CH₂-Ph), 4.00-4.07 (m, 3H, H-4, H-5, H-6a), 3.89 (dd, 1H, J_{5,6b} = 1.2 Hz, J_{6a,6b} = 10.4 Hz, H-6b), 3.88 (dd, 1H, J_{2,3} = 3.2 Hz, J_{3,4} = 9.7 Hz, H-3), 3.68 (dd, 1H, J_{1,2} = 1.6 Hz, J_{2,3} = 3.1 Hz, H-2), 2.56-2.60 (m, 2H, SCH₂CH₃), 1.20 (t, 3H, SCH₂CH₃), 1.04 (s, 9H, *t*-Bu). Anal. Calcd for C₄₅H₅₂O₄SSi (733.0): C, 73.73; H, 7.15. Found: C, 73.85; H, 7.20.

Methyl 3-O-(3-O-acetyl-2,4-di-O-benzyl- α -L-rhamnopyranosyl)-4,6-O-benzylidene-2-deoxy-2-phthalimido- β -D-glucopyranoside (68)

Anhydrous DCM (125 mL) was added to the glycosyl donor **58**⁸¹ (710 mg, 1.65 mmol) along with the acceptor **61**⁷⁷ (523 mg, 1.27 mmol) and 4 Å molecular sieves (1.5 g) in a 250 mL round-bottomed flask and stirred under an argon atmosphere for 14 h at room temperature. The solution was cooled to -78°C and silver trifluoromethanesulphonate (85 mg, 0.33 mmol) and *N*-iodosuccinimide (742 mg, 3.30 mmol) were added and the solution was allowed to reach room temperature. The resulting dark purple solution was then filtered through celite in a sintered glass funnel and the supernatant was equilibrated between DCM and saturated Na₂S₂O₃ (aq.) (100 mL) in a separatory funnel. The organic phase was drained into an Erlenmeyer flask, dried with Na₂SO₄, and filtered through cotton. The volatile components were removed using a rotary evaporator and the product was purified by silica gel chromatography using hexane-ethyl acetate, 2:1, as the eluent. The disaccharide **68** was isolated as a white morphous solid (872 mg, 779.83 g/mol, 88%); *R*_f 0.20 in hexane-ethyl acetate, 2:1. ES HRMS: (M+Na) exact mass: 802.2839, found: 802.2832. [α]_D -24.0° (*c* 0.9, CH₂Cl₂). ¹H NMR (300 MHz, CDCl₃) δ : 7.85-7.68 (m, 4H, Phth), 7.32-7.14 (m, 13H, aromatic), 6.90-6.95 (m, 2H, aromatic), 5.55 (s, 1H, CH-Ph), 5.19 (d, 1H, *J*_{1,2} = 8.6 Hz, H-1), 5.08 (dd, 1H, *J*_{2,3'} = 3.5 Hz, *J*_{3',4'} = 9.5 Hz, H-3'), 4.66 (dd, 1H, *J*_{2,3} = 9.7 Hz, *J*_{3,4} = 10.3 Hz, H-3), 4.59 (d, 1H, *J*_{1,2'} = 1.8 Hz, H-1'), 4.46-4.50 (m, 2H, CH₂-Ph), 4.41 (dd, 1H, *J*_{5,6a} = 4.0 Hz, *J*_{6a,6b} = 12.5 Hz, H-6a), 4.30 (dd, 1H, *J*_{1,2} = 8.5 Hz, *J*_{2,3} = 10.2 Hz, H-2),

3.96 (dq, 1H, $J_{4,5'} = 9.7$ Hz, $J_{5',6'} = 6.2$ Hz, H-5'), 3.94 (d, 1H, $\text{CH}_2\text{-Ph}$), 3.83-3.86 (m, 1H, H-6b), 3.76 (d, 1H, $\text{CH}_2\text{-Ph}$), 3.68-3.73 (m, 2H, H-4, H-5), 3.51 (dd, 1H, $J_{1,2} = 2.0$ Hz, $J_{2,3'} = 3.5$ Hz, H-2'), 3.42 (s, 3H, OMe), 3.35 (t, 1H, $J_{3',4'} = J_{4',5'} = 9.5$ Hz, H-4'), 1.90 (s, 3H, OAc), 0.79 (d, 3H, $J_{5',6'} = 6.2$ Hz, H-6'). ^{13}C NMR (125 MHz, CDCl_3) δ : 99.5 ($J_{\text{C-1,H-1}} = 164.6$ Hz, C-1), 97.7 ($J_{\text{C-1',H-1'}} = 167.3$ Hz, C-1'). Anal. Calcd for $\text{C}_{44}\text{H}_{45}\text{NO}_{12}$ (779.8): C, 67.77; H, 5.82; N, 1.80. Found: C, 67.40; H, 5.83; N, 1.74.

Methyl 3-O-(2,4-di-O-benzyl- α -L-rhamnopyranosyl)-4,6-O-benzylidene-2-deoxy-2-phthalimido- β -D-glucopyranoside (69)

Distilled methanol (100 mL) was added to the acetate **68** (535 mg, 0.686 mmol) along with sodium (50 mg, 2.17 mmol) in a 250 mL round-bottomed flask and stirred for 18 h at room temperature. Strongly-acidic cationic exchange resin was then added until the solution became neutral. The solution was filtered through celite and the filtrate was concentrated using a rotary evaporator. The product was purified by silica gel chromatography using toluene-ethyl acetate, 5:1, as the eluent. The alcohol **69** was isolated as a white morphous solid (466 mg, 737.79 g/mol, 92%); R_f 0.49 in toluene-ethyl acetate, 3:1. ES HRMS: (M+Na) exact mass: 760.2734, found: 760.2748. $[\alpha]_D^{25} -37.2^\circ$ (c 1.0, CH_2Cl_2). ^1H NMR (600 MHz, CDCl_3) δ : 7.88-7.68 (m, 4H, Phth), 7.32-7.14 (m, 13H, aromatic), 6.86-6.91 (m, 2H, aromatic), 5.56 (s, 1H, $\text{CH}_2\text{-Ph}$), 5.19 (d, 1H, $J_{1,2} = 8.5$ Hz, H-1), 4.70 (d, 1H, $\text{CH}_2\text{-Ph}$), 4.64 (d, 1H, $J_{1,2} = 1.3$ Hz, H-1'), 4.60 (dd, 1H, $J_{2,3} = 9.6$ Hz, $J_{3,4} = 10.4$ Hz, H-3), 4.46 (d, 1H, $\text{CH}_2\text{-Ph}$), 4.41 (dd, 1H, $J_{5,6a} = 4.3$ Hz, $J_{6a,6b} = 10.3$ Hz, H-6a), 4.26

(dd, 1H, $J_{1,2} = 8.5$ Hz, $J_{2,3} = 10.2$ Hz, H-2), 3.78-3.82 (m, 4H, H-6b, H-3', H-5', CH_2 -Ph), 3.63-3.67 (m, 3H, H-4, H-5, CH_2 -Ph), 3.42 (s, 3H, OMe), 3.35 (dd, 1H, $J_{1,2} = 1.6$ Hz, $J_{2,3} = 3.8$ Hz, H-2'), 3.05 (t, 1H, $J_{3,4} = J_{4,5} = 9.5$ Hz, H-4'), 2.01 (d, 1H, OH), 0.72 (d, 3H, $J_{5,6} = 6.2$ Hz, H-6'). Anal. Calcd for $\text{C}_{42}\text{H}_{43}\text{NO}_{11}$ (737.8): C, 68.37; H, 5.87; N, 1.90. Found: C, 68.14; H, 6.02; N, 1.88.

Methyl 3-O-(2,4-di-O-benzyl-3-O-[2,3,4-tri-O-benzyl-6-O-t-butyl-diphenylsilyl- α -L-mannopyranosyl]- α -L-rhamnopyranosyl)-4,6-O-benzylidene-2-deoxy-2-phthalimido- β -D-glucopyranoside (70)

Anhydrous DCM (70 mL) was added to the glycosyl donor **67** (425 mg, 0.593 mmol) along with the acceptor **69** (336 mg, 0.455 mmol) and 4 Å molecular sieves (1 g) in a 250 mL round-bottomed flask and stirred under an argon atmosphere for 10 h at room temperature. The solution was cooled to -78°C and silver trifluoromethanesulphonate (30 mg, 0.12 mmol) and *N*-iodosuccinimide (267 mg, 1.19 mmol) were added and the solution was allowed to reach room temperature. The resulting dark purple solution was then filtered through celite in a sintered glass funnel and the supernatant was equilibrated between DCM and saturated $\text{Na}_2\text{S}_2\text{O}_3$ (aq.) (100 mL) in a separatory funnel. The organic phase was drained into an Erlenmeyer flask, dried with Na_2SO_4 , and filtered through cotton. The volatile components were removed using a rotary evaporator and the product was purified by silica gel chromatography using hexane-ethyl acetate, 2:1, as the eluent. The trisaccharide **70** was isolated as a white morpous

solid (500 mg, 1408.70 g/mol, 78%); R_f 0.33 in hexane-ethyl acetate, 2:1. ES HRMS: (M+Na) exact mass: 1430.5838, found: 1430.5848. $[\alpha]_D^{25}$ -112.3° (c 1.1, CH_2Cl_2). ^1H NMR (600 MHz, CDCl_3) δ : 7.82-6.78 (m, 44H, aromatic), 5.54 (s, 1H, CH -Ph), 5.19 (d, 1H, $J_{1,2} = 8.5$ Hz, H-1), 5.12 (bs, 1H, H-1''), 4.92 (d, 1H, CH_2 -Ph), 4.65 (d, 1H, CH_2 -Ph), 4.56 (dd, 1H, $J_{2,3} = 9.6$ Hz, $J_{3,4} = 10.4$ Hz, H-3), 4.53 (d, 1H, $J_{1,2} = 1.3$ Hz, H-1'), 4.51 (dd, 1H, $J_{5,6a} = 4.3$ Hz, $J_{6a,6b} = 10.3$ Hz, H-6a), 4.36-4.44 (m, 6H, CH_2 -Ph), 4.36 (t, 1H, $J_{3',4'} = J_{4',5'} = 9.6$ Hz, H-4''), 4.18 (dd, 1H, $J_{1,2} = 8.5$ Hz, $J_{2,3} = 10.1$ Hz, H-2), 3.97 (dd, 1H, $J_{5',6a'} = 2.5$ Hz, $J_{6a',6b'} = 11.5$ Hz, H-6a''), 3.76-3.86 (m, 7H, H-6b, H-3', H-5', H-3'', H-5'', H-6b'', CH_2 -Ph), 3.60-3.70 (m, 4H, H-4, H-5, H-2'', CH_2 -Ph), 3.42 (s, 3H, OMe), 3.26 (m, 2H, H-2', H-4'), 1.04 (s, 9H, *t*-Bu), 0.74 (d, 3H, $J_{5',6'} = 6.2$ Hz, H-6'). ^{13}C NMR (125 MHz, CDCl_3) δ : 99.5 ($J_{\text{C-1},\text{H-1}} = 165.0$ Hz, C-1), 99.5 ($J_{\text{C-1}'',\text{H-1}''} = 171.1$ Hz, C-1''), 97.6 ($J_{\text{C-1}',\text{H-1}'} = 168.0$ Hz, C-1'). Anal. Calcd for $\text{C}_{85}\text{H}_{89}\text{NO}_{16}$ (1408.7): C, 72.47; H, 6.37; N, 0.99. Found: C, 72.24; H, 6.24; N, 1.01.

*Methyl 2-amino-3-O-(2,4-di-O-benzyl-3-O-[2,3,4-tri-O-benzyl-6-O-*t*-butyldiphenylsilyl- α -L-mannopyranosyl]- α -L-rhamnopyranosyl)-4,6-O-benzylidene-2-deoxy- β -D-glucopyranoside (71)*

Ethylenediamine (3 mL) and *t*-butyl alcohol (30 mL) were added to the phthalimide **70** (450 mg, 0.319 mmol) in a 100 mL round-bottomed flask and stirred under an argon atmosphere for 20 h at 115°C. The resulting pale yellow solution was then cooled to room temperature. The volatiles were removed using a rotary evaporator and the product was purified by silica gel

chromatography using toluene-ethyl acetate, 5:1, as the eluent. The amine **71** was isolated as a white morphous solid (368 mg, 1278.60 g/mol, 90%); R_f 0.63 in toluene-ethyl acetate, 2:1. ES HRMS: (M+Na) exact mass: 1278.5974, found: 1278.5968. $[\alpha]_D -75.2^\circ$ (c 0.9, CH_2Cl_2). $^1\text{H NMR}$ (600 MHz, CDCl_3) δ : 7.82-7.14 (m, 40H, aromatic), 5.50 (s, 1H, $\text{CH}_2\text{-Ph}$), 5.22 (bs, 1H, H-1''), 5.08 (d, 1H, $J_{1,2'} = 1.7$ Hz, H-1'), 4.97 (d, 1H, $\text{CH}_2\text{-Ph}$), 4.40-4.71 (m, 9H, $\text{CH}_2\text{-Ph}$), 4.34 (dd, 1H, $J_{5,6a} = 4.5$ Hz, $J_{6a,6b} = 10.6$ Hz, H-6a), 4.20 (t, 1H, $J_{3',4'} = J_{4',5'} = 9.4$ Hz, H-4''), 4.08 (d, 1H, $J_{1,2} = 8.0$ Hz, H-1), 3.95-4.07 (m, 3H, H-3', H-5', H-3''), 3.90 (dd, 1H, $J_{5',6a'} = 4.2$ Hz, $J_{6a',6b'} = 11.4$ Hz, H-6a''), 3.73-3.77 (m, 3H, H-6b, H-2'', H-5''), 3.61-3.69 (m, 2H, H-2', H-6b''), 3.56 (t, 1H, $J_{2,3} = J_{3,4} = 9.0$ Hz, H-3), 3.50 (s, 3H, OMe), 3.45-3.51 (m, 3H, H-4, H-5, H-4'), 2.62 (t, 1H, $J_{1,2} = J_{2,3} = 8.4$ Hz, H-2), 1.02 (s, 9H, *t*-Bu), 0.82 (d, 3H, $J_{5',6'} = 6.1$ Hz, H-6'). Anal. Calcd for $\text{C}_{77}\text{H}_{87}\text{NO}_{14}\text{Si}$ (1278.60): C, 72.33; H, 6.86; N, 1.10. Found: C, 71.80; H, 6.77; N, 1.09.

Methyl 2-amino-3-O-(2,4-di-O-benzyl-3-O-[2,3,4-tri-O-benzyl- α -L-mannopyranosyl]- α -L-rhamnopyranosyl)-4,6-O-benzylidene-2-deoxy- β -D-glucopyranoside (72)

Anhydrous THF (50 mL) was added to the silyl ether **71** (310 mg, 0.242 mmol) along with tetrabutylammonium fluoride (480 μL , 0.480 mmol, 1.0 mol/L in THF) in a 100 mL round-bottomed flask and stirred under an argon atmosphere for 15 h at 60°C. The resulting pale yellow solution was then cooled to room temperature. The volatiles were removed using a rotary evaporator and DCM (100 mL) was added to the residue. The solution was then equilibrated

between DCM and water (50 mL) in a separatory funnel. The organic phase was drained into an Erlenmeyer flask, dried with Na_2SO_4 , and filtered through cotton. The solvent was removed using a rotary evaporator and the product was purified by silica gel chromatography using toluene-ethyl acetate-methanol, 7.5:2:0.5, as the eluent. The alcohol **72** was isolated as a white solid (217 mg, 1040.20 g/mol, 86%); R_f 0.32 in toluene-ethyl acetate-methanol, 7.5:2:0.5. ES HRMS: (M+Na) exact mass: 1062.4616, found: 1062.4628. $[\alpha]_D -59.5^\circ$ (c 0.8, CH_2Cl_2). ^1H NMR (300 MHz, CDCl_3) δ : 7.45-7.16 (m, 30H, aromatic), 5.52 (s, 1H, CH-Ph), 5.30 (d, 1H, $J_{1,2''} = 1.6$ Hz, H-1''), 5.14 (d, 1H, $J_{1,2'} = 1.6$ Hz, H-1'), 4.88 (d, 1H, $\text{CH}_2\text{-Ph}$), 4.60 (m, 9H, $\text{CH}_2\text{-Ph}$), 4.31 (dd, 1H, $J_{5,6a} = 4.9$ Hz, $J_{6a,6b} = 10.5$ Hz, H-6a), 4.19 (d, 1H, $J_{1,2} = 7.8$ Hz, H-1), 3.96-4.02 (m, 2H, H-2'', H-3''), 3.85-3.89 (m, 2H, H-5', H-6a''), 3.61-3.69 (m, 5H, H-4, H-6b, H-2', H-5'', H-6b''), 3.53-3.58 (m, 3H, H-3, H-4', H-4''), 3.51 (s, 3H, OMe), 3.40 (ddd, 1H, $J_{4,5} = 9.7$ Hz, $J_{5,6a} = 4.9$ Hz, $J_{5,6b} = 1.2$ Hz, H-5), 2.79 (t, 1H, $J_{1,2} = J_{2,3} = 8.7$ Hz, H-2), 1.10 (d, 3H, $J_{5,6'} = 6.1$ Hz, H-6'). Anal. Calcd for $\text{C}_{61}\text{H}_{69}\text{NO}_{14}$ (1040.2): C, 70.43; H, 6.69; N, 1.35. Found: C, 70.06; H, 6.68; N, 1.31.

Methyl 3-O-(2,4-di-O-benzyl-3-O-[2,3,4-tri-O-benzyl- α -L-mannopyranosyl]- α -L-rhamnopyranosyl)-4,6-O-benzylidene-2-deoxy-2-(N- α -fluorenylmethoxycarbonyl-glyciny!)-amido- β -D-glucopyranoside (73)

Dry DMF (20 mL) was added to the amine **72** (70 mg, 0.067 mmol) along with N- α -Fmoc-L-glycine (40 mg, 0.14 mmol), TBTU (43 mg, 0.134 mmol), HOBt

(18 mg, 0.13 mmol), and *N*-ethylmorpholine (34 μ L, 0.26 mmol, 0.905 g/mL) in a 25 mL round-bottomed flask and stirred for 18 h at room temperature. The volatiles were removed using a rotary evaporator. The product was purified by silica gel chromatography using toluene-ethyl acetate-methanol, 7.5:2:0.5, as the eluent. The amide **73** was isolated as a white morpous solid (76 mg, 1319.49 g/mol, 86%); R_f 0.36 in toluene-ethyl acetate-methanol, 7.5:2:0.5. ES HRMS: (M+Na) exact mass: 1341.5511, found: 1341.5512. $[\alpha]_D -13.2^\circ$ (c 0.7, CH_2Cl_2). ^1H NMR (300 MHz, CDCl_3) δ : 7.69-7.08 (m, 38H, aromatic), 6.43-6.45 (m, 1H, NH-Glc-NH_2), 5.68 (bt, 1H, NH-Fmoc), 5.48 (s, 1H, CH-Ph), 5.18 (bs, 1H, H-1''), 4.96 (bs, 1H, H-1'), 4.80 (d, 1H, $\text{CH}_2\text{-Ph}$), 4.60-4.24 (m, 10H, H-1, $\text{CH}_2\text{-Ph}$), 4.28 (dd, 1H, $J_{5,6a} = 5.7$ Hz, $J_{6a,6b} = 10.5$ Hz, H-6a), 4.12 (bt, $\text{O-CH}_2\text{-CH[Fmoc]}$), 4.01 (dd, 1H, $J_{2,3'} = 2.8$ Hz, $J_{3',4'} = 9.7$ Hz, H-3'), 4.00 (t, 1H, $J_{3',4'} = J_{4',5'} = 9.3$ Hz, H-4''), 3.92 (dd, 1H, $J_{2,3'} = 2.9$ Hz, $J_{3',4'} = 9.0$ Hz, H-3''), 3.80-3.88 (m, 5H, H-2', H-5', H-6a'', linker), 3.70 (t, 1H, $J_{1',2'} = J_{2,3'} = 1.9$ Hz, H-2''), 3.61-3.69 (m, 4H, H-3, H-4, H-6b, H-6b''), 3.52 (t, 1H, $J_{3,4'} = J_{4',5'} = 9.3$ Hz, H-4'), 3.40-3.45 (m, 6H, H-2, H-5, $\text{O-CH}_2\text{-CH[Fmoc]}$, H-5'', H-6b''), 3.38 (s, 3H, OMe), 0.73 (d, 3H, $J_{5,6'} = 6.0$ Hz, H-6').

*Methyl 3-O-(2,4-di-O-benzyl-3-O-[2,3,4-tri-O-benzyl- α -L-mannopyranosyluronic acid]- α -L-rhamnopyranosyl)-4,6-O-benzylidene-2-deoxy-2-(*N*- α -fluorenyl-methoxycarbonyl-glyciny)-amido- β -D-glucopyranoside (**74**)*

Distilled DCM (4 mL) was added to alcohol **73** (60 mg, 0.045 mmol) along with TEMPO (4 mg, 0.02 mmol) in a 25 mL round-bottomed flask. A solution of

potassium bromide (8 mg, 0.07 mmol) and tetrabutylammonium chloride (10 mg, 0.036 mmol) in saturated NaHCO_3 (aq.) (1.5 mL) was added and the biphasic solution was cooled to 0°C . A solution of sodium hypochlorite (1.5 mL, 5% solution in water), saturated NaHCO_3 (aq.) (0.6 mL), and saturated NaCl (aq.) (1.3 mL) was added dropwise over 45 min. The solution was acidified with 5% HCl (aq.) (5 mL) and transferred to a separatory funnel. The organic phase was drained into an Erlenmeyer flask, dried with Na_2SO_4 , and filtered through cotton. The volatiles were removed using a rotary evaporator and the product was purified by silica gel chromatography using toluene-ethyl acetate-methanol, 4:4:1, as the eluent. The carboxylic acid **74** was isolated as a white morphous solid (26 mg, 1333.47 g/mol, 43%); R_f 0.39 in toluene-acetone-methanol, 7.5:2:0.5. ES HRMS: (M+Na) exact mass: 1355.5304, found: 1355.5314. $[\alpha]_D^{25} +0.4^\circ$ (c 0.6, MeOH). ^1H NMR (300 MHz, CDCl_3) δ : 7.75-7.00 (m, 38H, aromatic), 5.42 (bs, 1H, CH -Ph), 5.18 (bs, 1H, H-1''), 5.04 (bs, 1H, H-1'), 4.83 (bd, 1H, CH_2 -Ph), 4.63-4.34 (m, 10H, H-1, CH_2 -Ph), 4.30-3.20 (m, 19H, H-2, H-3, H-4, H-5, H-6a, H-6b, H-2', H-3', H-4', H-5', H-2'', H-3'', H-4'', H-5'', linker, O- CH_2 - CH [Fmoc], O- CH_2 - CH [Fmoc]), 3.32 (s, 3H, OMe), 0.73 (d, 3H, $J_{5,6} = 5.7$ Hz, H-6'). Anal. Calcd for $\text{C}_{78}\text{H}_{80}\text{N}_2\text{O}_{18}$ (1333.5): C, 70.26; H, 6.05; N, 2.10. Found: C, 69.90; H, 6.44; N, 2.01.

Methyl 2-(2-aminoacetamido)-3-O-(2,4-di-O-benzyl-3-O-[2,3,4-tri-O-benzyl- α -L-mannopyranosyluronic acid]- α -L-rhamnopyranosyl)-4,6-O-benzylidene-2-deoxy- β -D-glucopyranoside lactam (75)

Dry DMF (12 mL) was added to the carboxylic acid **74** (36 mg, 0.027 mmol) along with piperidine (2 mL) in a 25 mL round-bottomed flask and stirred for 1 h at room temperature. The volatiles were removed using a rotary evaporator. Dry DMF (10 mL) was added to the residue along with TBTU (17 mg, 0.054 mmol), HOBT (7 mg, 0.054 mmol), and *N*-ethylmorpholine (14 μ L, 0.11 mmol, 0.905 g/mL) and stirred for 24 h at room temperature. The volatiles were removed using a rotary evaporator. The product was purified by silica gel chromatography using toluene-ethyl acetate-methanol, 7.5:2:0.5, as the eluent. The lactam **75** was isolated as a white morphous solid (19 mg, 1093.22 g/mol, 65%); R_f 0.24 in toluene-ethyl acetate-methanol, 7.5:2:0.5. ES HRMS: (M+Na) exact mass: 1115.4517, found: 1115.4527. $[\alpha]_D^{25}$ -27.1° (*c* 0.4, CH₂Cl₂). ¹H NMR (300 MHz, CDCl₃) δ : 7.50-7.13 (m, 30H, aromatic), 7.00 (bt, 1H, NH-Fmoc), 6.20 (d, 1H, NH-Glc-NH₂), 5.51 (s, 1H, CH-Ph), 5.24 (d, 1H, $J_{1,2'} = 2.7$ Hz, H-1''), 5.03 (d, 1H, $J_{1,2'} = 1.6$ Hz, H-1'), 4.98 (d, 1H, $J_{1,2} = 8.3$ Hz, H-1), 4.71-4.38 (m, 10H, CH₂Ph), 4.30 (dd, 1H, $J_{5,6a} = 5.0$ Hz, $J_{6a,6b} = 10.7$ Hz, H-6a), 4.23-4.26 (m, 1H, linker), 4.14 (d, 1H, $J_{4,5''} = 9.3$ Hz, H-5''), 4.08 (dd, 1H, $J_{2,3'} = 3.0$ Hz, $J_{3',4'} = 9.7$ Hz, H-3'), 3.90-4.00 (m, 4H, H-6b, H-5', H-3'', H-4''), 3.59 (m, 2H, H-3, H-2''), 3.86 (t, 1H, $J_{3,4} = J_{4,5} = 9.1$ Hz, H-4), 3.79 (bt, 1H, $J_{1,2'} = J_{2,3'} = 2.3$ Hz, H-2'), 3.54-3.57 (m, 2H, H-5, H-4'), 3.45 (s, 3H, OMe), 3.02-3.07 (m, 1H, linker), 2.92 (bq, 1H, $J_{1,2} = J_{2,3} = J_{2,NH} = 8.6$ Hz, H-2), 0.83

(d, 3H, $J_{5,6'} = 6.2$ Hz, H-6'). Anal. Calcd for $C_{63}H_{68}N_2O_{15}$ (1093.2): C, 69.22; H, 6.27; N, 2.56. Found: C, 69.35; H, 6.02; N, 2.64.

Methyl 2-(2-aminoacetamido)-3-O-(3-O-[α -L-mannopyranosyluronic acid]- α -L-rhamnopyranosyl)-2-deoxy- β -D-glucopyranoside lactam (50)

Distilled methanol (15 mL) and distilled water (1 mL) were added to the protected cyclic trisaccharide **75** (16 mg, 0.014 mmol) along with palladium (II) hydroxide (23 mg, 20% on carbon) and the suspension was stirred under a hydrogen atmosphere for 24 h at room temperature. The resulting solution was then filtered through celite using a sintered glass funnel. The volatiles were then removed using a rotary evaporator. Distilled water (5 mL) was added to the residue and the solution was passed through a Sep-Pak cartridge. The product was purified by reversed-phase high performance liquid chromatography using water – acetonitrile, 10:1, as the eluent. The deprotected cyclic trisaccharide **50** was isolated as a white solid (6 mg, 554.50 g/mol, 74%); R_f 0.12 in ethyl acetate – methanol – water, 7:2:1. ES HRMS: (M+Na) exact mass: 577.1857, found: 577.1863. ^1H NMR (600 MHz, D_2O) δ : 5.22 (d, 1H, $J_{1,2''} = 1.9$ Hz, H-1''), 4.99 (d, 1H, $J_{1,2} = 1.5$ Hz, H-1'), 4.76 (d, 1H, $J_{1,2} = 8.4$ Hz, H-1), 4.14 (d, 1H, $J_{4,5''} = 9.5$ Hz, H-5''), 3.95-4.00 (m, 2H, H-5', H-6a), 3.92-3.94 (m, 3H, H-2', H-3'', H-4''), 3.84 (bt, 1H, $J_{1,2''} = J_{2,3''} = 3.2$ Hz, H-2''), 3.83 (dd, 1H, $J_{2,3''} = 3.3$ Hz, $J_{3,4''} = 9.9$ Hz, H-3'), 3.79 (dd, 1H, $J_{1,2'} = 2.0$ Hz, $J_{2,3'} = 3.2$ Hz, H-2'), 3.76 (dd, 1H, $J_{5,6b} = 5.8$ Hz, $J_{6a,6b} = 12.2$ Hz, H-6b), 3.63-3.67 (m, 1H, linker), 3.50-3.58 (m, 4H, H-4', H-3, H-4, linker), 3.50 (s, 3H,

OMe), 3.46 (ddd, 1H, $J_{5,6a} = 2.3$ Hz, $J_{5,6b} = 5.2$ Hz, $J_{4,5} = 10.1$ Hz, H-5), 1.29 (d, 3H, $J_{5',6'} = 6.4$ Hz, H-6').

Methyl 3-O-(2,4-di-O-benzyl-3-O-[2,3,4-tri-O-benzyl- α -L-mannopyranosyl]- α -L-rhamnopyranosyl)-4,6-O-benzylidene-2-deoxy-2-(N- β -fluorenylmethoxycarbonyl- β -alanyl)-amido- β -D-glucopyranoside (76)

Dry DMF (20 mL) was added to the amine 72 (90 mg, 0.087 mmol) along with N- β -Fmoc- β -alanine (54 mg, 0.174 mmol), TBTU (56 mg, 0.174 mmol), HOBT (23 mg, 0.17 mmol), and N-ethylmorpholine (44 μ L, 0.34 mmol, 0.905 g/mL) in a 50 mL round-bottomed flask and stirred for 15 h at room temperature. The volatiles were removed using a rotary evaporator. The product was purified by silica gel chromatography using toluene-ethyl acetate-methanol, 7.5:2:0.5, as the eluent. The amide 76 was isolated as a white morphous solid (105 mg, 1333.52 g/mol, 91%); R_f 0.32 in toluene-ethyl acetate-methanol, 7.5:2:0.5. ES HRMS: (M+Na) exact mass: 1355.366770, found: 1355.567507. $[\alpha]_D -21.0^\circ$ (c 0.7, CH_2Cl_2). ^1H NMR (300 MHz, CDCl_3) δ : 7.69-7.08 (m, 38H, aromatic), 6.00 (bt, 1H, NH -Fmoc), 5.52 (s, 1H, CH -Ph), 5.11 (d, 1H, $J_{1',2''} = 2.2$ Hz, H-1''), 4.86 (bs, 1H, H-1'), 4.80 (d, 1H, CH_2 -Ph), 4.60-4.24 (m, 10H, H-1, CH_2 -Ph), 4.27 (dd, 1H, $J_{5,6a} = 5.5$ Hz, $J_{6a,6b} = 10.5$ Hz, H-6a), 4.08 (bt, O- CH_2 - CH [Fmoc]), 4.01 (dd, 1H, $J_{2',3'} = 2.8$ Hz, $J_{3',4'} = 9.7$ Hz, H-3'), 4.01 (t, 1H, $J_{3',4'} = J_{4',5'} = 9.3$ Hz, H-4''), 3.80-3.90 (m, 6H, H-2', H-5', H-3'', H-6a'', linker), 3.73-3.77 (m, 3H, H-3, H-6b, H-6b''), 3.66-3.69 (m, 2H, H-4, linker), 3.67 (t, 1H, $J_{1',2''} = J_{2',3'} = 2.6$ Hz, H-2''), 3.56-3.58 (m, 1H, linker), 3.52 (t, 1H,

$J_{3,4'} = J_{4,5'} = 9.3$ Hz, H-4'), 3.37-3.42 (m, 5H, H-5, O-CH₂-CH[Fmoc], H-5'', H-6b''), 3.30 (s, 3H, OMe), 3.24-3.27 (m, 1H, H-2), 2.16-2.19 (m, 2H, linker), 0.73 (d, 3H, $J_{5,6'}$ = 6.0 Hz, H-6'). Anal. Calcd for C₇₉H₈₄N₂O₁₇ (1333.5): H, 6.35; N, 2.10. Found: H, 6.24; N, 2.20.

Methyl 3-O-(2,4-di-O-benzyl-3-O-[2,3,4-tri-O-benzyl- α -L-mannurono]- α -L-rhamnopyranosyl)-4,6-O-benzylidene-2-deoxy-2-(2-N-Fluorenylmethoxycarbonyl- β -alanyl)-amido- β -D-glucopyranoside (77)

Distilled DCM (4 mL) was added to the alcohol **76** (85 mg, 0.064 mmol) along with TEMPO (3 mg, 0.02 mmol) in a 25 mL round-bottomed flask. A solution of potassium bromide (7 mg, 0.06 mmol) and tetrabutylammonium chloride (10 mg, 0.036 mmol) in saturated NaHCO₃ (aq.) (1.5 mL) was added and the biphasic solution was cooled to 0°C. A solution of sodium hypochlorite (1.5 mL, 5% solution in water), saturated NaHCO₃ (aq.) (0.6 mL), and saturated NaCl (aq.) (1.3 mL) was added dropwise over 45 min. The solution was acidified with 5% HCl (aq.) (5mL) and transferred to a separatory funnel. The organic phase was drained into an Erlenmeyer flask, dried with Na₂SO₄, and filtered through cotton. The volatiles were removed using a rotary evaporator and the product was purified by silica gel chromatography using toluene-ethyl acetate-methanol, 4:4:1, as the eluent. The carboxylic acid **77** was isolated as a white solid (54 mg, 1347.50 g/mol, 63%); R_f 0.39 in toluene-acetone-methanol, 7.5:2:0.5. ES HRMS: (M+Na) exact mass: 1369.5460, found: 1369.5464. $[\alpha]_D^{25} +13.6^\circ$ (c 1.0, MeOH). ¹H

NMR (300 MHz, CDCl₃) δ : 7.69-7.06 (m, 38H, aromatic), 5.42 (bs, 1H, CH-Ph), 5.18 (bs, 1H, H-1''), 4.85 (bs, 1H, H-1'), 4.80 (d, 1H, CH₂-Ph), 4.60-4.24 (m, 10H, H-1, CH₂-Ph), 4.30-3.20 (m, 19H, H-2, H-3, H-4, H-5, H-6a, H-6b, H-2', H-3', H-4', H-5', H-2'', H-3'', H-4'', H-5'', linker, O-CH₂-CH[Fmoc], O-CH₂-CH[Fmoc]), 3.20 (s, 3H, OMe), 2.16-2.21 (m, 2H, linker), 0.73 (d, 3H, $J_{5,6} = 5.7$ Hz, H-6'). Anal. Calcd for C₇₉H₈₂N₂O₁₈ (1347.5): H, 6.13; N, 2.08. Found: H, 5.59; N, 2.11.

Methyl 2-(3-aminopropionamido)-3-O-(2,4-di-O-benzyl-3-O-[2,3,4-tri-O-benzyl- α -L-mannopyranosyluronic acid]- α -L-rhamnopyranosyl)-4,6-O-benzylidene-2-deoxy- β -D-glucopyranoside lactam (78)

Dry DMF (10 mL) was added to the carboxylic acid 77 (40 mg, 0.030 mmol) along with piperidine (2 mL) in a 25 mL round-bottomed flask and stirred for 1 h at room temperature. The volatiles were removed using a rotary evaporator. Dry DMF (10 mL) was added to the residue along with TBTU (19 mg, 0.060 mmol), HOBt (8 mg, 0.06 mmol), and *N*-ethylmorpholine (15 μ L, 0.12 mmol, 0.905 g/mL) and stirred for 15 h at room temperature. The volatiles were removed using a rotary evaporator. The product was purified by silica gel chromatography using toluene-ethyl acetate-methanol, 7.5:2:0.5, as the eluent. The lactam 78 was isolated as a white morphous solid (20 mg, 1107.25 g/mol, 60%); R_f 0.25 in toluene-ethyl acetate-methanol, 7.5:2:0.5. ES HRMS: (M+Na) exact mass: 1129.4674, found: 1129.4684. $[\alpha]_D^{25} +12.1^\circ$ (*c* 0.5, CH₂Cl₂). ¹H NMR (600 MHz, CDCl₃) δ : 7.50-7.13 (m, 30H, aromatic), 6.89 (bs, 1H, NH-Fmoc), 5.48 (s, 1H,

CH-Ph), 5.42 (d, 1H, NH-Glc-NH₂), 5.14 (d, 1H, $J_{1,2''} = 2.3$ Hz, H-1''), 4.91 (d, 1H, $J_{1,2'} = 1.3$ Hz, H-1'), 4.71-4.38 (m, 10H, CH₂Ph), 4.30 (dd, 1H, $J_{5,6a} = 5.0$ Hz, $J_{6a,6b} = 10.7$ Hz, H-6a), 4.22 (d, 1H, $J_{1,2} = 8.6$ Hz, H-1), 4.04 (d, 1H, $J_{4',5''} = 9.3$ Hz, H-5''), 3.92 (bt, 1H, $J_{1,2} = J_{2,3} = 8.6$ Hz, H-2), 3.96 (dd, 1H, $J_{2,3'} = 3.0$ Hz, $J_{3',4'} = 9.7$ Hz, H-3'), 3.89 (t, 1H, $J_{3',4'} = J_{4',5''} = 9.3$ Hz, H-4''), 3.70-3.80 (m, 4H, H-6b, H-5', H-3'', NH-CH₂-CH₂-NH), 3.59-3.69 (m, 2H, H-3, H-2''), 3.76 (t, 1H, $J_{3,4} = J_{4,5} = 9.1$ Hz, H-4), 3.79 (bt, 1H, $J_{1,2'} = J_{2,3'} = 2.3$ Hz, H-2'), 3.52-3.58 (m, 4H, H-4', H-5, NH-CH₂-CH₂-NH), 3.45 (s, 3H, OMe), 2.37-2.39 (m, 2H, NH-CH₂-CH₂-NH), 0.81 (d, 3H, $J_{5,6'} = 6.2$ Hz, H-6'). Anal. Calcd for C₆₄H₇₀N₂O₁₅ (1107.3): H, 6.37; N, 2.53. Found: H, 6.48; N, 2.62.

Methyl 2-(2-aminopropionamido)-3-O-(3-O-[α-L-mannopyranosyluronic acid]-α-L-rhamnopyranosyl)-2-deoxy-β-D-glucopyranoside lactam (51)

Distilled methanol (15 mL) and distilled water (1 mL) were added to the protected cyclic trisaccharide **78** (32 mg, 0.029 mmol) along with palladium (II) hydroxide (25 mg, 20% on carbon) and the suspension was stirred under a hydrogen atmosphere for 24 h at room temperature. The resulting solution was then filtered through celite using a sintered glass funnel. The volatiles were then removed using a rotary evaporator. Distilled water (5 mL) was added to the residue and the solution was passed through a Sep-Pak cartridge. The product was purified by reversed-phase high performance liquid chromatography using water – acetonitrile, 10:1, as the eluent. The deprotected cyclic trisaccharide **51**

was isolated as a white solid (12 mg, 568.53 g/mol, 73%); R_f 0.21 in ethyl acetate – methanol – water, 7:2:1. ES HRMS: (M+Na) exact mass: 591.2013, found: 591.2006. $[\alpha]_D -36.3^\circ$ (c 0.5, H_2O). 1H NMR (600 MHz, D_2O) δ : 5.11 (d, 1H, $J_{1,2''} = 1.5$ Hz, H-1''), 4.77 (d, 1H, $J_{1,2} = 2.2$ Hz, H-1'), 4.41 (d, 1H, $J_{1,2} = 8.6$ Hz, H-1), 4.09 (dd, 1H, $J_{1,2''} = 1.5$ Hz, $J_{2,3''} = 3.2$ Hz, H-2''), 4.04 (d, 1H, $J_{4,5''} = 9.5$ Hz, H-5''), 3.95-3.99 (m, 2H, H-5', H-6a), 3.92 (dd, 1H, $J_{1,2} = 8.5$ Hz, $J_{2,3} = 10.3$ Hz, H-2), 3.89 (t, 1H, $J_{3,4''} = J_{4,5''} = 9.5$ Hz, H-4''), 3.85 (dd, 1H, $J_{3,4''} = 9.3$ Hz, $J_{2,3''} = 3.3$ Hz, H-3''), 3.83 (dd, 1H, $J_{2,3''} = 3.3$ Hz, $J_{3,4''} = 9.9$ Hz, H-3'), 3.79 (dd, 1H, $J_{1,2} = 2.2$ Hz, $J_{2,3''} = 3.2$ Hz, H-2'), 3.76 (dd, 1H, $J_{5,6a} = 5.8$ Hz, $J_{6a,6b} = 12.2$ Hz, H-6b), 3.65-3.70 (m, 1H, NH-CH₂-CH₂-NH), 3.52-3.57 (m, 4H, H-4', H-3, H-4, NH-CH₂-CH₂-NH), 3.50 (s, 3H, OMe), 3.46 (ddd, 1H, $J_{5,6a} = 2.2$ Hz, $J_{5,6b} = 6.1$ Hz, $J_{4,5} = 8.1$ Hz, H-5), 2.58-2.61 (m, 2H, NH-CH₂-CH₂-NH), 1.27 (d, 3H, $J_{5,6'} = 6.4$ Hz, H-6').

Methyl 3-O-(2,4-di-O-benzyl-3-O-[2,3,4-tri-O-benzyl- α -L-mannopyranosyl]- α -L-rhamnopyranosyl)-4,6-O-benzylidene-2-deoxy-2-(N- β -t-butoxycarbonyl- β -alanyl)-amido- β -D-glucopyranoside (79)

Dry DMF (20 mL) was added to the amine **72** (88 mg, 0.085 mmol) along with *N*- β -t-Boc- β -alanine (48 mg, 0.17 mmol), TBTU (54 mg, 0.17 mmol), HOBT (23 mg, 0.17 mmol), and *N*-ethylmorpholine (43 μ L, 0.34 mmol, 0.905 g/mL) in a 25 mL round-bottomed flask and stirred for 24 h at room temperature. The volatiles were removed using a rotary evaporator. The product was purified by silica gel chromatography using toluene-ethyl acetate-methanol, 7.5:2:0.5, as the

eluent. The amide **79** was isolated as a white morphous solid (91 mg, 1211.39 g/mol, 89%); R_f 0.20 in toluene-ethyl acetate-methanol, 7.5:2:0.5. ES HRMS: (M+Na) exact mass: 1233.5511, found: 1233.5520. $[\alpha]_D -33.3^\circ$ (c 0.7, CH₂Cl₂). ¹H NMR (300 MHz, CDCl₃) δ : 7.69-7.08 (m, 30H, aromatic), 6.40 (bt, 1H, NH-Boc), 5.52 (s, 1H, CH-Ph), 5.19 (d, 1H, $J_{1,2'} = 1.0$ Hz, H-1''), 5.00 (bd, 1H, NH-Glc-NH₂), 4.91 (bs, 1H, H-1'), 4.90 (d, 1H, CH₂-Ph), 4.74 (d, 1H, $J_{1,2} = 8.3$ Hz, H-1), 4.60-4.24 (m, 9H, CH₂-Ph), 4.27 (dd, 1H, $J_{5,6a} = 4.2$ Hz, $J_{6a,6b} = 10.2$ Hz, H-6a), 4.10 (dd, 1H, $J_{2,3} = 2.6$ Hz, $J_{3,4'} = 9.4$ Hz, H-3'), 3.83-3.88 (m, 5H, H-5', H-3'', H-6a'', linker), 3.83 (t, 1H, $J_{3',4'} = J_{4',5'} = 9.3$ Hz, H-4''), 3.78 (t, 1H, $J_{1,2'} = J_{2,3'} = 2.7$ Hz, H-2''), 3.73-3.79 (m, 3H, H-3, H-6b, H-6b''), 3.68-3.70 (m, 1H, linker), 3.65 (t, 1H, $J_{1,2'} = J_{2,3'} = 2.6$ Hz, H-2''), 3.62-3.65 (m, 1H, H-5''), 3.56-3.58 (m, 1H, linker), 3.48-3.55 (m, 3H, H-4, H-5, H-4'), 3.42 (s, 3H, OMe), 3.35-3.37 (m, 1H, H-2), 2.14-2.17 (m, 2H, linker), 1.40 (s, 9H, *t*-Bu), 0.73 (d, 3H, $J_{5',6'} = 6.0$ Hz, H-6'). Anal. Calcd for C₆₉H₈₂N₂O₁₇ (1211.4): H, 6.82; N, 2.31. Found: H, 6.92; N, 2.30.

*Methyl 3-O-(2,4-di-O-benzyl-3-O-[2,3,4-tri-O-benzyl-6-O-p-nitrophenylformate- α -L-mannopyranosyl]- α -L-rhamnopyranosyl)-4,6-O-benzylidene-2-deoxy-2-(N- β -t-butoxycarbonyl- β -alanyl)-amido- β -D-glucopyranoside (**80**)*

Dry pyridine (3 mL) was added to the alcohol **79** (77 mg, 0.064 mmol) along with *p*-nitrophenyl chloroformate (51 mg, 0.25 mmol) in a 50 mL round-bottomed flask and stirred for 20 h at 100°C. The solution was cooled to room temperature and DCM (30 mL) was added. The solution was equilibrated

between DCM and 5% HCl (aq.) (20 mL) in a separatory funnel. The organic phase was drained into an Erlenmeyer flask, dried with Na_2SO_4 , and filtered through cotton. The volatiles were then removed using a rotary evaporator and the product was purified by silica gel chromatography using toluene-ethyl acetate, 3:1, as the eluent. The *p*-nitrophenyl carbonate **80** was isolated as a white morphous solid (74 mg, 1376.50 g/mol, 85%); R_f 0.50 in toluene-ethyl acetate, 2:1. ES HRMS: (M+Na) exact mass: 1397.5733, found: 1397.5727. $[\alpha]_D -64.7^\circ$ (*c* 0.8, CH_2Cl_2). ^1H NMR (300 MHz, CDCl_3) δ : 8.18-8.20 (m, 2H, aromatic), 7.49-7.15 (m, 32H, aromatic), 6.00 (bs, 1H, NH-Boc), 5.48 (s, 1H, CH-Ph), 5.19 (bs, 1H, H-1''), 5.00 (bs, 1H, NH-Glc-NH_2), 4.94 (d, 1H, $\text{CH}_2\text{-Ph}$), 4.91 (d, 1H, $J_{1,2'} = 1.9$ Hz, H-1'), 4.69 (d, 1H, $J_{1,2} = 8.3$ Hz, H-1), 4.60-4.54 (m, 8H, $\text{CH}_2\text{-Ph}$), 4.47 (dd, 1H, $J_{5',6a'} = 2.0$ Hz, $J_{6a',6b'} = 11.3$ Hz, H-6a''), 4.37 (dd, 1H, $J_{5,6a} = 3.2$ Hz, $J_{6a,6b} = 10.2$ Hz, H-6a), 4.37 (dd, 1H, $J_{5',6b'} = 4.5$ Hz, $J_{6a',6b'} = 11.3$ Hz, H-6b''), 4.34 (d, 1H, $\text{CH}_2\text{-Ph}$), 4.25 (t, 1H, $J_{2,3} = J_{3,4} = 9.5$ Hz, H-3), 4.09 (dd, 1H, $J_{2,3'} = 2.9$ Hz, $J_{3',4'} = 9.5$ Hz, H-3'), 3.92 (dd, 1H, $J_{2',3'} = 1.9$ Hz, $J_{3',4'} = 9.5$ Hz, H-3''), 3.82-3.88 (m, 3H, H-5', H-4'', H-5''), 3.73 (t, 1H, $J_{1,2'} = J_{2,3'} = 2.2$ Hz, H-2'), 3.70 (t, 1H, $J_{1,2'} = J_{2',3'} = 2.2$ Hz, H-2''), 3.66 (t, 1H, $J_{3,4} = J_{4,5} = 10.1$ Hz, H-4), 3.45-3.50 (m, 3H, H-5, H-6b, H-4'), 3.38 (s, 3H, OMe), 3.36-3.39 (m, 1H, H-2), 3.24-3.27 (m, 2H, linker), 2.15-2.18 (m, 2H, linker), 1.40 (s, 9H, *t*-Bu), 0.83 (d, 3H, $J_{5',6'} = 6.3$ Hz, H-6'). Anal. Calcd for $\text{C}_{76}\text{H}_{85}\text{N}_3\text{O}_{21}$ (1376.5): C, 66.31; H, 6.22; N, 3.05. Found: C, 66.40; H, 6.49; N, 3.82.

Methyl 2-amino-3-O-(2,4-di-O-benzyl-3-O-[2,3,4-tri-O-benzyl-6-O-(2-carboxyethyl carbamoyl)- α -L-mannopyranosyl]- α -L-rhamnopyranosyl)-2-deoxy- β -D-glucopyranoside lactam (81)

Distilled DCM (10 mL) was added to the *p*-nitrophenyl carbonate **80** (50 mg, 0.036 mmol) in a 25 mL round-bottomed flask and trifluoroacetic acid was added dropwise until the reaction was complete by thin layer chromatography. The solution was then neutralized by adding triethylamine. The solution was equilibrated between DCM and 5% HCl(aq.) (10 mL) in a separatory funnel. The organic phase was drained into an Erlenmeyer flask, dried with Na₂SO₄, and filtered through cotton. The volatiles were then removed using a rotary evaporator and the product was purified by silica gel chromatography using toluene-ethyl acetate-methanol, 4:4:1, as the eluent. The cyclic carbamate **81** was isolated as a white solid (25 mg, 1049.16 g/mol, 65%); R_f 0.30 in toluene-ethyl acetate-methanol, 4:4:1. ES HRMS: (M+Na) exact mass: 1071.4466, found: 1071.4453. ¹H NMR (300 MHz, CDCl₃) δ : 7.30-7.10 (m, 25H, aromatic), 5.19 (bs, 1H, H-1''), 5.00 (bs, 1H, NH-Glc-NH₂), 4.94 (d, 1H, CH₂-Ph), 4.91 (d, 1H, J_{1',2'} = 1.9 Hz, H-1'), 4.60-4.54 (m, 9H, H-1, CH₂-Ph), 4.37 (dd, 1H, J_{5,6a} = 3.2 Hz, J_{6a,6b} = 10.2 Hz, H-6a), 4.34 (d, 1H, CH₂-Ph), 4.20 (bt, 1H, J_{2,3} = J_{3,4} = 9.5 Hz, H-3), 4.00-4.04 (m, 2H, H-3', H-3''), 3.80-3.90 (m, 4H, H-5', H-4'', H-5'', H-6a''), 3.73 (t, 1H, J_{1',2'} = J_{2',3'} = 2.2 Hz, H-2'), 3.70 (dd, 1H, J_{5',6b'} = 4.3 Hz, J_{6a',6b'} = 11.8 Hz, H-6b''), 3.68-3.73 (m, 1H, H-2''), 3.66 (t, 1H, J_{3',4'} = J_{4',5'} = 9.4 Hz, H-4'), 3.45-3.49 (m, 3H, H-5, H-6b, H-4), 3.38 (s, 3H, OMe), 3.32-3.34 (m, 1H, H-2), 3.25-3.29 (m, 1H, linker), 2.80-2.83 (m,

1H, linker), 2.50-2.53 (m, 1H, linker), 2.16-2.19 (m, 1H, linker), 1.40 (d, 3H, $J_{5',6'} = 6.3$ Hz, H-6').

Methyl 2-amino-3-O-(3-O-[6-O-(2-carboxyethylcarbamoyl)- α -L-mannopyranosyl]- α -L-rhamnopyranosyl-2-deoxy- β -D-glucopyranoside lactam (52)

Distilled methanol (10 mL) and distilled water (1 mL) were added to the protected cyclic trisaccharide **81** (20 mg, 0.019 mmol) along with palladium (II) hydroxide (26 mg, 20% on carbon) and the suspension was stirred under a hydrogen atmosphere for 20 h at room temperature. The resulting solution was then filtered through celite using a sintered glass funnel. The volatiles were then removed using a rotary evaporator. Distilled water (5 mL) was added to the residue and the solution was passed through a Sep-Pak cartridge. The product was purified by reversed-phase high performance liquid chromatography using water – acetonitrile, 10:1, as the eluent. The deprotected cyclic trisaccharide **52** was isolated as a white solid (8 mg, 598.55 g/mol, 70%); R_f 0.23 in ethyl acetate – methanol – water, 7:2:1. ES HRMS: (M+Na) exact mass: 621.211903, found: 621.212945. $[\alpha]_D -13.5^\circ$ (c 0.4, H₂O). ¹H NMR (300 MHz, CDCl₃) δ : 5.10 (d, 1H, $J_{1',2'} = 1.7$ Hz, H-1''), 4.88 (d, 1H, $J_{1',2'} = 1.5$ Hz, H-1'), 4.57 (d, 1H, $J_{1,2} = 8.3$ Hz, H-1), 4.21 (dd, 1H, $J_{5,6a} = 3.2$ Hz, $J_{6a,6b} = 10.2$ Hz, H-6a), 3.90-3.95 (m, 2H, H-3', H-3''), 3.82-3.87 (m, 4H, H-5', H-4'', H-5'', H-6a''), 3.73-3.76 (m, 3H, H-2', H-2'', H-6b''), 3.66 (t, 1H, $J_{3',4'} = J_{4',5'} = 9.4$ Hz, H-4'), 3.61 (bt, 1H, $J_{2,3} = J_{3,4} = 9.6$ Hz, H-3), 3.42-3.47 (m, 3H, H-5, H-6b, H-4), 3.38 (s, 3H, OMe), 3.35-3.37 (m, 1H, H-2), 2.90-2.93 (m,

1H, linker), 2.81-2.83 (m, 1H, linker), 2.47-2.49 (m, 1H, linker), 2.16-2.18 (m, 1H, linker), 1.40 (d, 3H, $J_{5,6} = 6.3$ Hz, H-6').

Methyl 2-deoxy-2-acetamido-3-O-(2,4-di-O-benzyl-3-O-[2,3,4-tri-O-benzyl- α -L-mannopyranosyl]- α -L-rhamnopyranosyl)-4,6-O-benzylidene- β -D-glucopyranoside (82)

Distilled DCM (20 mL) was added to the amine **72** (45 mg, 0.043 mmol) along with acetic anhydride (50 μ L, 0.53 mmol, 1.082 g/mL) in a 50 mL round-bottomed flask and stirred for 15 h at room temperature. The volatiles were then removed using a rotary evaporator and the product was purified by silica gel chromatography using toluene-ethyl acetate-methanol, 7.5:2:0.5, as the eluent. The acetamide **82** was isolated as a white morphous solid (44 mg, 1082.24 g/mol, 94%); R_f 0.15 in toluene-ethyl acetate-methanol, 7.5:2:0.5. ES HRMS: (M+Na) exact mass: 1104.4721, found: 1104.4719.

$[\alpha]_D -65.8^\circ$ (c 0.8, CH_2Cl_2). ^1H NMR (300 MHz, CDCl_3) δ : 7.45-7.16 (m, 30H, aromatic), 6.21 (d, 1H, $J = 7.8$, NHAc), 5.49 (s, 1H, CH-Ph), 5.20 (bs, 1H, H-1''), 4.98 (d, 1H, $\text{CH}_2\text{-Ph}$), 4.98 (d, 1H, $J_{1,2} = 1.1$ Hz, H-1'), 4.82 (d, 1H, $J_{1,2} = 8.3$ Hz, H-1), 4.40-4.70 (m, 9H, $\text{CH}_2\text{-Ph}$), 4.32 (dd, 1H, $J_{5,6a} = 4.9$ Hz, $J_{6a,6b} = 10.5$ Hz, H-6a), 4.25 (dd, 1H, $J_{2,3} = J_{3,4} = 9.1$ Hz, H-3), 4.13 (dd, 1H, $J_{2,3} = 2.7$ Hz, $J_{3,4} = 9.7$ Hz, H-3'), 3.90 (dd, 1H, $J_{2,3} = 3.1$ Hz, $J_{3,4} = 8.4$ Hz, H-3''), 3.85-3.87 (m, 2H, H-5', H-6a''), 3.76 (bt, 1H, $J_{1,2} = J_{2,3} = 2.4$, H-2''), 3.69-3.76 (m, 4H, H-6b, H-2', H-5'', H-6b''), 3.62-3.65 (m, 1H, H-4), 3.54-3.58 (m, 2H, H-4', H-4''), 3.51 (s, 3H, OMe), 3.40 (ddd, 1H, $J_{4,5} =$

9.7 Hz, $J_{5,6a} = 4.9$ Hz, $J_{5,6b} = 1.2$ Hz, H-5), 3.16-3.19 (m, 1H, H-2), 1.77 (s, 3H, NHAc), 0.92 (d, 3H, $J_{5,6'} = 6.2$ Hz, H-6').

Methyl 2-deoxy-2-acetamido-3-O-(3-O-[α -L-mannopyranosyl]- α -L-rhamnopyranosyl)- β -D-glucopyranoside (83)

Distilled methanol (15 mL) and distilled water (1 mL) were added to the protected trisaccharide **82** (30 mg, 0.028 mmol) along with palladium (II) hydroxide (32 mg, 20% on carbon) and the suspension was stirred under a hydrogen atmosphere for 24 h at room temperature. The resulting solution was then filtered through celite using a sintered glass funnel. The volatiles were then removed using a rotary evaporator. Distilled water (5 mL) was added to the residue and the solution was passed through a Sep-Pak cartridge. The product was purified by reversed-phase high performance liquid chromatography using water – acetonitrile, 10:1, as the eluent. The deprotected trisaccharide **83** was isolated as a white solid (11 mg, 543.52 g/mol, 73%); R_f 0.23 in ethyl acetate – methanol – water, 7:2:1. ES HRMS: (M+Na) exact mass: 566.2061, found: 566.2066. $[\alpha]_D -71.8^\circ$ (c 0.5, H₂O). ¹H NMR (600 MHz, D₂O) δ : 5.10 (d, 1H, $J_{1,2''} = 1.6$ Hz, H-1''), 4.82 (d, 1H, $J_{1,2'} = 1.9$ Hz, H-1'), 4.48 (d, 1H, $J_{1,2} = 8.6$ Hz, H-1), 4.04 (dd, 1H, $J_{1,2''} = 1.8$ Hz, $J_{2,3''} = 3.5$ Hz, H-2''), 4.02 (dq, 1H, $J_{4,5'} = 9.9$ Hz, $J_{5,6'} = 6.4$ Hz, H-5'), 3.95 (dd, 1H, $J_{5,6a} = 2.2$ Hz, $J_{6a,6b} = 12.2$ Hz, H-6a), 3.88 (dd, 1H, $J_{5',6a''} = 1.8$ Hz, $J_{6a'',6b''} = 12.5$ Hz, H-6a''), 3.87 (dd, 1H, $J_{1,2'} = 2.0$ Hz, $J_{2,3'} = 3.1$ Hz, H-2'), 3.83 (dd, 1H, $J_{2',3''} = 3.1$ Hz, $J_{3'',4''} = 9.0$ Hz, H-3''), 3.92 (dd, 1H, $J_{1,2} = 8.8$ Hz, $J_{2,3} = 9.9$ Hz, H-2),

3.79 (dd, 1H, $J_{2',3'} = 3.1$ Hz, $J_{3',4'} = 9.9$ Hz, H-3'), 3.77 (dq, 1H, $J_{4',5'} = 9.7$ Hz, $J_{5',6'} = 6.2$ Hz, H-5''), 3.76 (dd, 1H, $J_{5,6b} = 6.0$ Hz, $J_{6a,6b} = 12.4$ Hz, H-6b), 3.70 (dd, 1H, $J_{5',6b'} = 5.8$ Hz, $J_{6a',6b'} = 12.5$ Hz, H-6b''), 3.59 (dd, 1H, $J_{2,3} = 8.4$ Hz, $J_{3,4} = 10.1$ Hz, H-3), 3.53 (t, 1H, $J_{3',4'} = J_{4',5'} = 9.9$ Hz, H-4'), 3.53 (t, 1H, $J_{3,4} = J_{4,5} = 9.9$ Hz, H-4), 3.50 (s, 3H, OMe), 3.48 (ddd, 1H, $J_{5,6a} = 2.2$ Hz, $J_{5,6b} = 5.8$ Hz, $J_{4,5} = 9.9$ Hz, H-5), 3.47 (t, 1H, $J_{3',4'} = J_{4',5'} = 9.7$ Hz, H-4''), 3.45 (ddd, 1H, $J_{5,6a} = 1.8$ Hz, $J_{5,6b} = 5.6$ Hz, $J_{4,5} = 9.8$ Hz, H-5''), 1.31 (d, 3H, $J_{5',6'} = 6.2$ Hz, H-6''), 1.24 (d, 3H, $J_{5',6'} = 6.4$ Hz, H-6').

Purification of SYA/J6 IgG Antibody from Ascites Solution

A saturated ammonium sulphate solution (20 mL) was added to a 20 mL solution of ascites and stirred at 4 °C for 2 h. The solution was centrifuged for 10 min at 10 000 r.p.m. The precipitate was dissolved in 40 mL of 1 M tris[hydroxymethyl]aminomethane (Tris) buffer, pH 8, and added to 40 mL of a saturated ammonium sulphate solution, and left to stir at 4 °C for 1 h. The solution was centrifuged at 10 000 r.p.m. for 10 min. The precipitate was dissolved in 15 mL of a 0.05 M Tris buffer solution containing 0.15 M sodium chloride and dialyzed against the same buffer solution (2 L) for 24 h. A protein A/agarose affinity column was used to purify the dialyzed antibody. The sample was loaded onto the column and washed with 0.05 M Tris, 0.15 M NaCl, pH 8 buffer to remove unbound protein. The antibody was eluted with a 0.1 M citric acid/sodium citrate buffer solution, 0.15 M NaCl, pH 3 until all bound protein was released. The protein solution was dialyzed against 0.05 M Tris, 0.15

M NaCl, pH 8 buffer overnight. The protein concentration (m.w. 145 380.67 g/mol) was determined with a Beckmann DU 7400 spectrophotometer set at 280 nm. Absorbance readings were divided by the $E_{280}^{1\%}$ value of 1.53 to calculate the concentration in mg/mL.

Typical Competitive ELISA Testing Procedure

A stock solution of SYA/J6 antibody (~ 6 mg/mL) was diluted with 0.01 M sodium phosphate, 0.15 M NaCl (PBS) buffer solution to obtain a 0.005 mg/mL solution. A 96-well Nunc-Immuno ELISA plate (MaxiSorp F96) was coated with 100 μ L of the antibody solution and allowed to sit at 4 °C overnight. Excess solution was discarded, and the plate was washed 4 times with PBS buffer that also contained 0.1 % polyoxyethylene-sorbitan monolaurate detergent (PBST). A 2.5 % milk solution in PBS buffer (100 μ L) was added and the plate was left to stand at room temperature for 1 h to block empty hydrophobic sites. The milk solution was discarded from the plate and serially-diluted solutions of synthetic ligand (50 μ L) containing 0.04 μ g/mL solution of the biotinylated lipopolysaccharide antigen (50 μ L) in PBST were added in triplicate to the wells. The plate was allowed to stand at room temperature overnight. The plate was washed 4 times with PBST. A solution of streptavidin/horseradish peroxidase complex in PBST (100 μ L, 25 ng/mL) was added to each well and allowed to equilibrate for 1 h. The plate was washed 4 times with PBST and a 3, 3', 5, 5' tetramethylbenzidine (TMB) solution (100 μ L) was added to each well and the

colorimetric reaction was allowed to proceed for 1 min. A 1 M phosphoric acid solution (100 μ L) was added to each to quench the reaction and the plate was placed into a Dynatech MR5000 ELISA plate reader and read at 450 nm. Inhibition data were calculated from the absorbance readings.

Typical Micro-Calorimetry Experiment

Optimal calorimetry conditions occur when the product of the protein concentration multiplied by the dissociation constant is between 10 and 100. To obtain the optimum protein concentration of about 50 μ M, the purified antibody solution was concentrated using an Amicon protein concentrator. Nitrogen gas was used to push the solution through a 10 000 cut off membrane until the desired concentration of antibody solution was obtained. The protein solution (approximately 2 mL) was then degassed under vacuum for 5 min to remove air bubbles and injected into the MicroCal MCS ITC Unit micro-calorimeter cell and allowed to equilibrate for 15 min. A 17-fold excess test ligand solution in Tris buffer was drawn into the calorimetry stirrer/syringe and inserted into the cell. When a stable baseline reading was attained, 35 injections of 8 μ L were then made into the cell. The heat data that were measured during the calorimetry run were converted to thermodynamic values according to the published procedure of Bundle *et al.*¹⁰⁵

Chapter 8

Bibliography

1. A.Varki, *Glycobiology*, **3**, (1993) 97-130.
2. F.A. Quijcho, *Ann. Rev. Biochem.*, **55**, (1986) 287-315.
3. F.A. Quijcho and N.K. Nyas, *Nature*, **310**, (1984) 381-386.
4. R.U. Lemieux, *Chem. Soc. Rev.*, **18**, (1989) 347-374.
5. I. Brockhausen and H. Schacter, in *Glycosciences*, Chapman and Hall, (1997) 79-113.
6. Y. Ichikawa, G.C. Look, and C-H. Wong, *Anal. Biochem.*, **202**, (1992) 215-238.
7. R.D. Cummings, in *Glycosciences*, Chapman and Hall, (1997) 191-199.
8. Y. Bourne, H. van Tilbeurgh, and C. Cambillau, *Current Opinion in Structural Biology*, **3**, (1993) 681-686.
9. D.R. Bundle, in *Carbohydrates*, Oxford Press, (1998) 370-440.
10. C.J. Honsik, R.A. Reisfeld, and G. Jung, *Proc. Natl. Acad. Sci. USA*, **83**, (1986) 7893-7897.
11. D.B. Weiner and R.C. Kennedy, *Sci. Am.*, (1999) 799-808.
12. H.J. Jennings, *Adv. Carbohydr. Chem. Biochem.*, **41**, (1983) 155-208.
13. K-A. Karlsson, *Trends Pharmacol. Sci.*, **12**, (1991) 1-56.

14. M.S. Mulligan, J.C. Paulsen, S. De Frees, Z-L. Zheng, J.B. Lowe, and P.A. Ward, *Nature*, **364**, (1993) 149-151.
15. C.A.A. van Boeckel and M. Petitou, *Angew. Chem. Int. Ed.*, **32**, (1993) 1671-1690.
16. J. C. McAuliffe and O. Hindsgaul, *Chem. and Ind.*, (1997) 170-174.
17. R.B. Raffa and F. Porreca, *Life Sciences*, **44**, (1989) 245-258.
18. J.P. Carver, *Pure and Appl. Chem.*, **65**, (1993) 763-770.
19. M.Mammen, S-K. Choi, and G. Whitesides, *Angew. Chem. Int. Ed.*, **37**, (1998) 2754-2794.
20. Z.J. Witczak, *Curr. Med. Chem.*, **1**, (1995) 392-405.
21. O. Hindsgaul, *Current Topics in Cell Biology*, **2**, (1991) 319-326.
22. R.A. Laine, *Glycobiology*, **4**, (1994) 1-9.
23. E.A. Kabat, *Structural Concepts in Immunology and Immunochemistry*, Holt, Rinehart, and Winston, (1976).
24. F.A. Quijcho, *Biochemical Society Trans.*, **21**, (1993) 442-448.
25. E.A. Kabat and M.M. Mayer, *Experimental Immunochemistry*, C.C. Thomas, (1961).
26. G. Kohler and C. Milstein, *Nature*, **256**, (1975) 495-497.
27. N.I.A. Carlin, M.A. J. Gidney, A.A. Lindberg, and D.R. Bundle, *J. Immunol.*, **137**, (1986) 2361-2366.
28. N.I.A. Carlin, A.A. Lindberg, and D.R. Bundle, *J. Immunol.*, **138**, (1987) 4419-4427.
29. B.M. Pinto and D.R. Bundle, *Carbohydr. Res.*, **124**, (1983) 313-318.
30. N.I.A. Carlin, A.A. Lindberg, K. Bock, and D.R. Bundle, *Eur. J. Biochem.*, **139**, (1984) 189-194.

31. A. Nishinoff, *Introduction to Molecular Immunology*, Sunderland, (1982).
32. M.N. Vyas, N.K. Vyas, P.J. Meikle, B. Sinnott, B.M. Pinto, D.R. Bundle, and F.A. Quioco, *J. Mol. Biol.*, **231**, (1993) 133-136.
33. F. Berstein, *J. Mol. Biol.*, **112**, (1977) 535-542.
34. B.M. Pinto, K.B. Reimer, D.G. Morissette, and D.R. Bundle, *J. Chem. Soc., Perkin Trans. I*, (1990) 293-299.
35. H.R. Hanna and D.R. Bundle, *Can. J. Chem.*, **71**, (1993) 125-134.
36. D.R. Bundle, E. Altman, F-I. Auzanneau, H. Bauman, E. Eichler, and B. W. Sigurskjold, *The Alfred Benzon Symposium No. 36, Complex Carbohydrates in Drug Research*, (1994) 168-181.
37. D.R. Bundle and N.M. Young, *Current Opinion in Structural Biology*, **2**, (1992) 666-673.
38. D.R. Bundle, J.W. Cherwonogrodzky, M.A.J. Gidney, P.J. Meikle, M.B. Perry, and T. Peters, *Infect. Immun.*, **57**, (1989) 2829-2836.
39. E. Vorberg and D.R. Bundle, *J. Immunol. Methods*, **132**, (1990) 81-89.
40. D.R. Bundle and B.W. Sigurskjold, *Methods in Enzymology*, **247**, (1994) 288-305.
41. J.F. Brandts, *Am. Lab (Shelton Conn.)* **30**, (1990) 30-41.
42. D. Williams, *J. Am. Chem. Soc.*, **113**, (1991) 7020-7030.
43. G.A. Jeffrey and W. Saenger, *Hydrogen Bonding in Biological Systems*, Springer, (1991) 95-112.
44. H-J. Bohm and G. Klebe, *Angew. Chem. Int. Ed.*, **35**, (1996) 2588-2614.
45. J.H. Arevalo, *J. Mol. Biol.*, **231**, (1993) 103-118.

46. C.P.J. Glaudemons, *Chem. Rev.*, **91**, (1991) 25-33.
47. B.L. Jacobsen, *J. Biol. Chem.*, **266**, (1991) 5220-5225.
48. D.R. Bundle, *Pure and Appl. Chem.*, **61**, (1989) 1171-1180.
49. F-I. Auzanneau and D.R. Bundle, *Can. J. Chem.*, **71**, (1993) 534-548.
50. P.L. Privalov, and S.J. Gill, *Adv. Protein Chem.*, **39**, (1988) 191-195.
51. R.U. Lemieux, *Accts. Of Chemical Research*, **29**, (1996) 373-380.
52. M.C. Chervenak and E.J. Toone, *J. Am. Chem. Soc.*, **116**, (1994) 10533-10539.
53. E.J. Toone, *Current Opinion in Structural Biology*, **4**, (1994) 719-728.
54. J.D. Dunitz, *Science*, **264**, (1994) 670-672.
55. M.R. Eftink, A.C. Anusiem, and R.L. Biltman, *Biochemistry*, **22**, (1983) 3384-3396.
56. J.P. Carver, S.W. Michnick, and D.A. Cumming, in *Carbohydrate Recognition in Cellular Function*, Wiley, (1989) 6-26.
57. A. Imberty, *Adv. In Biophysical Chem.*, **3**, (1993) 71-117.
58. R.U. Lemieux, *Can. J. Chem.*, **58**, (1980) 631-640.
59. K. Bock, S. Josephson, and D.R. Bundle, *J. Chem. Soc. Perkin Trans. II*, (1982) 59-70.
60. H.P. Wessel and D.R. Bundle, *Carbohydr. Res.*, **124**, (1983) 301-311.
61. R.R. Schmidt, *Angew. Chem. Int. Ed.*, **25**, (1986) 212-235.
62. G-J. Boons, *Contemporary Organic Synthesis*, (1995) 173-200.
63. H. Paulsen, *Angew. Chem. Int. Ed.*, **21**, (1982) 155-173.
64. N.K. Kochetkov, *Carbohydr. Res.*, **16**, (1971) 17-25.
65. P. Sinaj, *Pure and Appl. Chem.*, **50**, (1978) 1437-1452.
66. W. Koenigs and E. Knorr, *Ber. Dtsch. Chem. Ges.*, **34**, (1901) 957-960.

67. R.U. Lemieux and J.I. Haymi, *Can. J. Chem.*, **43**, (1965) 2162-2173.
68. T. Norberg, *Modern Methods in Carbohydrate Synthesis*, Harwood Academic Publishing, (1996) 518-547.
69. R. Madsen and B. Fraser-Reid, *Modern Methods in Carbohydrate Synthesis*, Harwood Academic Publishing, (1996) 155-170.
70. R.R. Schmidt, *Pure and Appl. Chem.*, **61**, (1989) 1257-1270.
71. R.R. Schmidt, *Modern Methods in Carbohydrate Synthesis*, Harwood Academic Publishing, (1996) 20-54.
72. R.R. Schmidt, in *Glycosciences*, Chapman and Hall, (1997) 31-57.
73. F-I. Auzanneau and D.R. Bundle, *Carbohydr. Res.*, **247**, (1993) 195-209.
74. C. Malet and O. Hindsgaul, *J. Org. Chem.*, **61**, (1996) 4649-4659.
75. J.M. Kim and R. Roy, *Carbohydr. Res.*, **298**, (1997) 173-179.
76. J.M. Kim and R. Roy, *Angew. Chem. Int. Ed.*, **38**, (1999) 369-372.
77. R.U. Lemieux, T. Takeda, and B.Y. Chung, *A.C.S. Symposium Ser.*, **39**, (1976) 90-113.
78. J.E. Cadotte, F. Smith, and D. Spriestersbach, *J. Chem. Soc.*, (1952) 1501-1503.
79. V.B. Maddali, A.K. Ray, and N. Roy, *Carbohydr. Res.*, **208**, (1990) 59-66.
80. P.J. Garegg, J-L. Maloisel, and S. Oscarson, *Synthesis*, (1995) 409-414.
81. V. Pozsgay, *Carbohydr. Res.*, **69**, (1979) 284-286.
82. K. Fuji, K. Ichikawa, M. Node, and E. Fujita, *J. Org. Chem.*, **44**, (1979) 1661-1664.
83. H.C. Brown, Y.M. Choi, and S. Narasimhan, *Synthesis*, (1981) 605-606.
84. L. Kisfauldy and I. Schon, *Synthesis*, (1983) 325-327.

85. R-I. El-Sokkery, B.A. Silwanis, and H. Paulsen, *Carbohydr. Res.*, **203**, (1990) 319-323.
86. O. Kanie, S.C. Crawley, M.M. Palcic, and O. Hindsgaul, *Carbohydr. Res.*, **243**, (1993) 139-164.
87. A.K. Bose, B.K. Pramanik, B. Lal, and M.S. Manhas, *Tetrahedron Lett.*, (1977) 1977-1980.
88. W. Liao, Y. Liu, and D. Lu, *Carbohydr. Res.*, **260**, (1994) 151-154.
89. M. Mammen, E.I. Shakhnovich, J.M. Deutch, and G. Whitesides, *J. Org. Chem.*, **63**, (1998) 3168-3175.
90. H. Mack, *J. Enzyme Inhib.*, **9**, (1995) 73-86.
91. M. Wilstermann, J. Balogh, and G. Magnussen, *J. Org. Chem.*, **62**, (1997) 3659-3665.
92. G-J. Boons, and A.H. van Oijen, *Chem. Eur. J.*, **5**, (1999) 2281-2294.
93. N. Navarre, A.H. van Oijen, and G-J. Boons, *Tetrahedron Lett.*, **38**, (1997) 2023-2026.
94. H.C. Kolb, *Biorg. and Med. Chem. Letters*, **7**, (1997) 2629-2634.
95. R. Alibes and D.R. Bundle, *J. Org. Chem.*, **63**, (1998) 6288-6301.
96. G.H. Veeneman, S.H. van Leeuwen, H. Zuurmand, and J.H. van Boom, *J. Carb. Chem.*, **9**, (1998) 783-796.
97. V. Pozsgay and H.J. Jennings, *J. Org. Chem.*, **53**, (1988) 4042-4052.
98. N.J. Davis and S. Flitsch, *Tetrahedron Lett.*, **34**, (1993) 1181-1184.
99. M. Bessodes, D. Komiotis, and K. Antonakis, *Tetrahedron Lett.*, **27**, (1986) 579-580.
100. E.J. Corey and A. Venkateswarlu, *J. Am. Chem. Soc.*, **94**, (1972) 6190-6199.
101. R. Knorr, *Tetrahedron Lett.*, **30**, (1989) 1927-1930.

102. M.J. Sophia, *J. Org. Chem.*, **63**, (1998) 2802-2803.
103. P.J. Meikle, N.M. Young, and D.R. Bundle, *J. of Immun. Methods*, **132**, (1990) 255-261.
104. T. Wiseman, S. Williston, J. F. Brandts, and L-N. Lin, *Analytical Biochem.*, **179**, (1989) 131-137.
105. B.W. Sigurskjold, E. Altman, and D.R. Bundle, *Eur. J. Biochem.*, **197**, (1991) 239-246.
106. D.A. Rees, *J. Chem. Soc. B*, (1969) 217-226.
107. D.A. Rees, *Carbohydr. Res.*, **7**, (1968) 334-341.
108. H. Thørgerson, R.U. Lemieux, K. Bock, and B. Mayer, *Can. J. Chem.*, **60**, (1982) 44-57.
109. J.H. Noggle, and R.E. Schirmer, *The Nuclear Overhauser Effect*, Academic Press, (1971).
110. K. Bock, *Pure and Appl. Chem.*, **55**, (1983) 605-622.
111. B. Mayer, in *Topics in Current Chemistry*, **154**, (1990) 143-204.
- 112a. S.J. Weiner, P.A. Kollman, D.A. Case, U.C. Singh, C. Ghio, G. Alagona, S. Profeta Jr., and P. Weiner, *J. Am. Chem. Soc.*, **106**, (1984) 765-784.
- 112b. S.W. Homans, *Biochemistry*, **29**, (1990) 9110-9118.
112. S.N. Ha, A. Giamonna, M. Field, and J.W. Brady, *Carbohydr. Res.*, **180**, (1988) 207-221.
113. K.B. Wiberg and M.A. Murcko, *J. Am. Chem. Soc.*, **111**, (1989) 4821.
114. L. Verlet, *Phys. Rev.*, **159**, (1967) 98-103.

115. K. Wuthrick, *NMR of Proteins and Nucleic Acids*, Wiley, (1986).
116. I. Tvaroska, M. Hricovini, and E. Petrakova, *Carbohydr. Res.*, **189**, (1989) 359-362.
117. D.R. Bundle, R. Alibes, P. Zhang, M. Warwas, A. Otter, and S. Nilar, *J. Am. Chem. Soc.*, **120**, (1998) 5317-5318.
118. A.A. Bothner-by, *J. Am. Chem. Soc.*, **106**, (1984) 811-813.
119. T-L. Hwang and A.J. Shaka, *J. Am. Chem. Soc.*, **114**, (1992) 3157-3159.